Enhancement of Aircraft Cabin Design Guidelines with Special Consideration of Aircraft Turnaround and Short Range Operations

Vom Promotionsausschuss der
Technischen Universität Hamburg-Harburg
zur Erlangung des akademischen Grades

Doktor-Ingenieur (Dr.-Ing.)

genehmigte Dissertation

von

Jörg Clemens Fuchte

aus
Pinneberg

2014

Übersicht der Gutachter

1. Gutachter:	Prof. Dr.-Ing. V. Gollnick
2. Gutachter:	Prof. Dr. J. Reichmuth
Vorsitzender des Prüfungsausschusses:	Prof. Dr.-Ing. R. God
1. zusätzlicher Gutachter:	Prof. Dr.-Ing. R. God
2. zusätzlicher Gutachter:	Prof. Dr.-Ing. D. Krause

Tag der mündlichen Prüfung: 4. April 2014

Danksagung

Abstract

This work is concerned with aircraft design, in particular the influence of cabin and fuselage layout on aircraft direct operating cost under special consideration of airport turnaround times. The objective of this work is to establish a capacity limit above which a cabin with twin aisle layout is more efficient to operate than one with a single aisle layout. The main assumption is that twin aisle cabin layouts demonstrate much shorter boarding times, and hence allow operating the aircraft more frequently when average flight time is short. The traditional capacity-oriented design guidance for fuselage sizing is amended with a range dependency.

For this purpose aircraft design methods and advanced fuselage mass estimation are combined with a detailed boarding simulation. The analyzed capacity region ranges from 130 to 340 seats in a single class arrangement. Aircraft performance, component weights and aircraft turnaround times are evaluated. Results are used to estimate the direct operating cost of range and capacity.

Including the turnaround as influencing factor for daily aircraft utilization reduces the capacity limit from around 300 seats to 240-260 seats. A twin aisle can be of advantage at capacities as low as 180 seats if missions are very short. The threshold above which the twin aisle demonstrates lower cost of operation has a strong dependency to parameters and operational assumptions. Further, effects such as the particular cross section layout and different door layout (Quarter Door) have notable effect on the outcome.

Contents

List of Figures

List of Tables

Chapter 1

Introduction

This chapter explains the current developments in civil air transport which motivate the thesis. It further outlines the definite research objectives and the methodology.

1.1 Motivation

This work investigates fuselage design in the short and medium range segment for passenger aircraft. It focuses on aircraft turnaround as design driver for fuselage design decisions. This first section outlines what motivates this research and which developments make the investigation relevant.

Short Range Air Transport

The air transportation system is composed of flight distances ranging from very short to ultra-long range. Aircraft can be categorized into aircraft with a single aisle cabin and those with a twin aisle cabin. For short and medium distances the utilized aircraft are mostly single aisle aircraft. Figure 1.1 demonstrates that below a sector length of 2000nm the majority of available seat kilometers are produced by single aisles. It further underlines the contribution of this sector to the overall available seat kilometers. The figure includes all current Airbus and Boeing models and represents data from 2007 [OAG07].

When the focus is put into the short and medium range sector, the large number of short range flights becomes apparent. In figure 1.2 the number of flights from the same source is provided in the left hand plot. The right hand plot provides the number of operated aircraft over the sector length. The number is estimated from the left hand plot by assuming flight times and turnaround times. Currently there are around 10000 active single aisle aircraft with more than 120 seats worldwide [Fli11c]. According to figure 1.2(b), roughly 30% are required for ranges of 400nm and less. This corresponds to a market of 3000 aircraft. According to current market forecasts the traffic volume will increase further [Air09].

Eurocontrol defines Short Range as range of less than 1500km (800nm) [Eur04]. In the context of this work short and medium range are all flights below 3000nm, which is roughly the maximum effective range of current generation single aisle. Short ranges are considered as ranges below 800nm sticking to the definition of Eurocontrol.
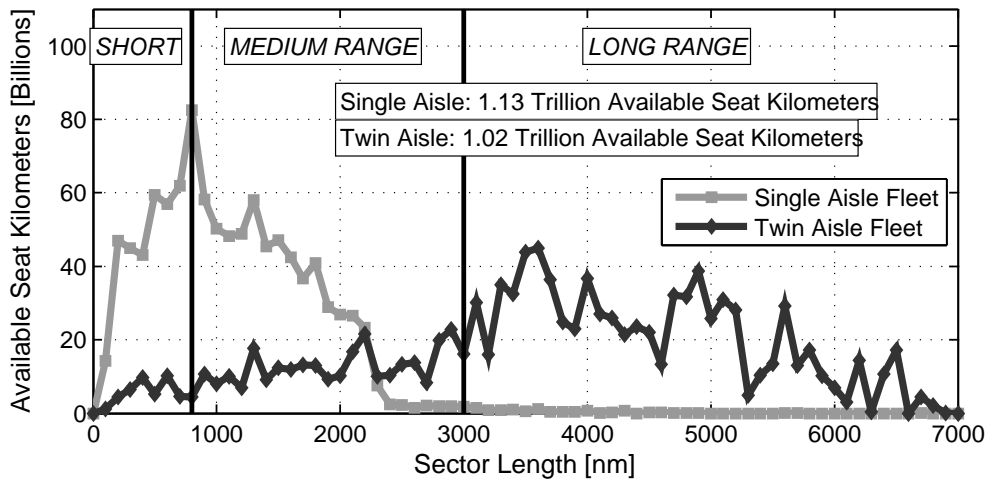
Figure 1.1 – Available seat kilometers worldwide by single aisle and twin aisle aircraft using data from [OAG07]. The separation between both types of aircraft is apparent. Range definition according to [Eur04].

(a) Flights

(b) Operated Aircraft (estimated)
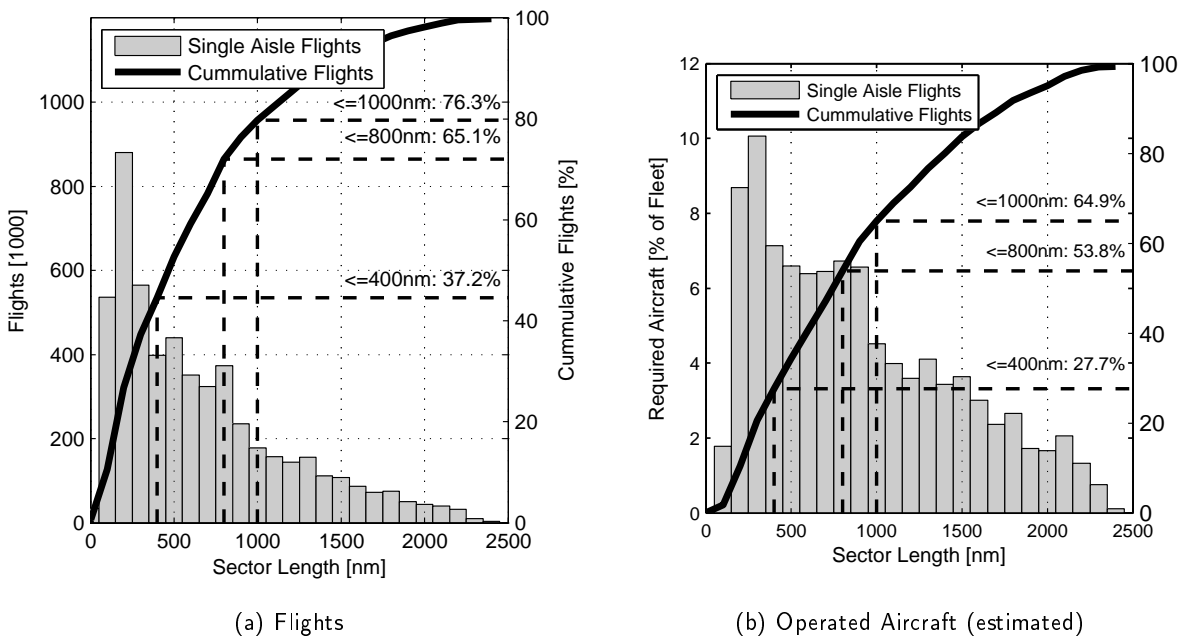
Figure 1.2 – Flights of all single aisle aircraft in 2007 [OAG07], global fleet. The right graph assumes a standard utilization (see section 2.4) for estimation of required aircraft.

The current in-service aircraft analyzed in figure 1.1 and 1.2 have capacities between 130 and 280 seats, with the majority being between 150 and 220 seats. These aircraft are operated by most airlines in the world, regardless of business model or region [Asc11b]. All these single aisle aircraft have cabins with 6-abreast seating. In figure 1.3 two trends are visible. In the left hand plot the average seat count per delivered aircraft is shown. It represents the customized seat count, means that it represents the number of seats an airline did install at delivery. The seat count demonstrates a strong growth with an approximation to a plateau below 170 seats. The increase is partly caused by the choice of larger single aisles, but also caused by the trend towards denser cabin seating. The graph was produced using the Ascend database, which lists all delivered aircraft with their seat count at time of delivery [Asc11a].

(a) Average Seats   (b) Delivered Aircraft
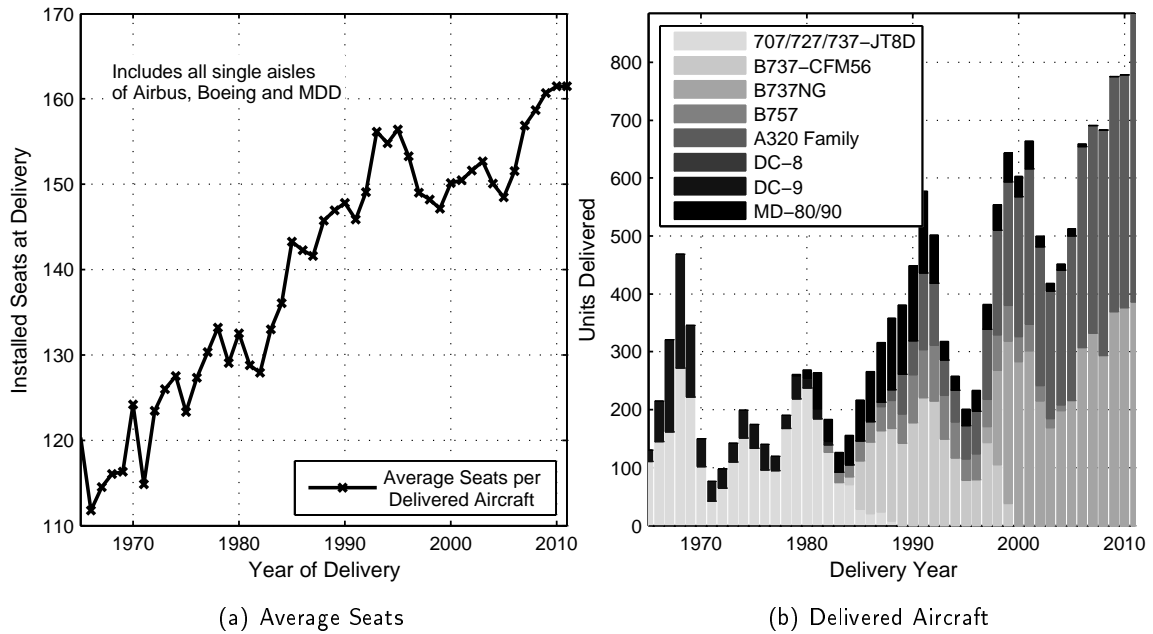
Figure 1.3 – Trends in single aisle aircraft market from mid 1960ies (excluding some minor designs). Also note major downturns in the mid 1990ies and early 2000s. The seats at delivery are that of the particular's airline layout.

If future growth of air traffic leads to increasingly congested airports, a growth in average seating capacity might be a possible relief. For non congested airports airlines may prefer additional frequency over larger aircraft, both for reasons of flexibility and marketing reasons [Cla07].

The right hand plot shows the annual deliveries of single aisle aircraft. Note that the type mix has consolidated to two families. Dedicated wide body aircraft existed for medium range routes. Today the smallest available widebody is the B767-300 with 260-290 seats in short range layouts. In near future - when the B767 ceases production - the smallest available aircraft will be the B787-8 with around 330 seats in a short range layout [Boe06]. A dedicated short and medium range variant - the B787-3 - was rejected by airlines partly because it carried the weight penalty of a long range aircraft. All widebodies available today are optimized for long range flights far beyond 4000nm. This trend clearly disagrees with the trend towards higher capacity single aisles.

Besides the trend in newly delivered aircraft, existing aircraft are refurbished with denser cabins. In order to remain competitive with low cost carriers full service network carriers are increasing the number of seats in their cabins [LH10]. New slim seats allow denser seat arrangements without loss in leg room. The change is partly caused by a diminishing number of carriers having dedicated business class offerings in their single aisle aircraft. Clark [Cla07] (p.59) shows that the share of business class passengers on short range flights has halved since 1997. Today the average seat pitch in economy class is 31.1 inch, while business class averages at 37.5 inch. The numbers were generated using data obtained from SeatGuru.com [Sea11].

Another trend is increased carry-on luggage carried during short range flights. Measurements have proven a trend towards heavier carry-on luggage [EAS09]. This is partly caused by the desire for more convenience. People are using rolling trolleys instead of bags they have to carry. But the trend is

also pushed by strict checked luggage policies. Overweight baggage has to be paid for, and checked baggage allowances have been reduced both in number and allowed weight for economy passengers. Short range travelers often try to avoid the additional time needed to check and reclaim their luggage, therefore traveling only with carry-on.
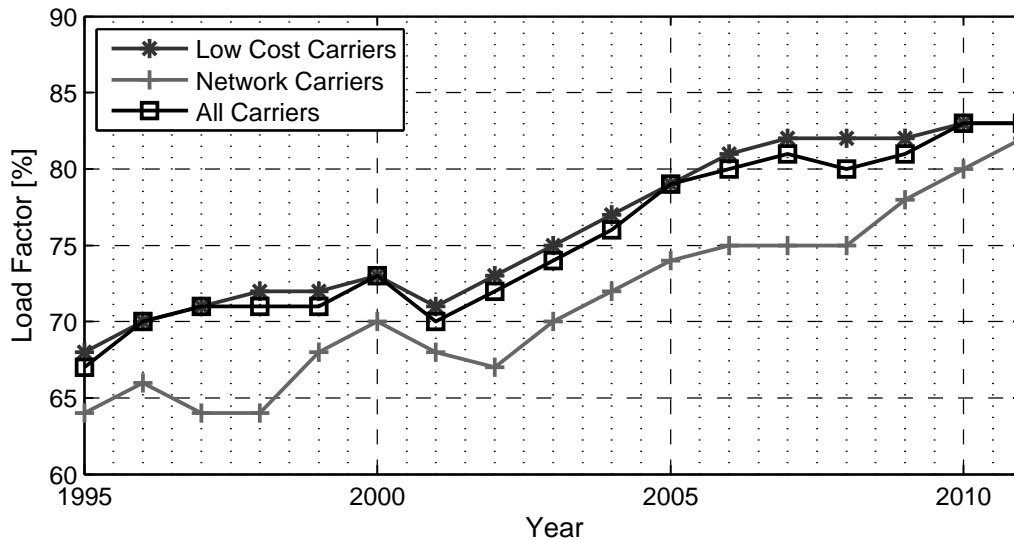
Figure 1.4 – Development of the load factor for North American carriers. Data is taken from [MIT12].

Finally, the average load factor on short range flights is increasing. While low cost carriers traditionally achieved high load factors, network carriers have followed in recent years in order to reduce cost and increase revenue [Dog10]. According to the figure load factors of 85% are the average, which means that fully booked aircraft are a common occurance.

Turnaround and Passenger Boarding

The turnaround of an aircraft is the time it spends on the ground between two flights. Wu defines it as follows:

> "Aircraft turnaround operations refer to the activities conducted to prepare an inbound aircraft at an airport for a following outbound flight that is scheduled for the same aircraft." ([Wu10] , page 63)

This definition includes all actions performed on the aircraft in the intention of readying it for the next flight. If no periods of inaction occur the turnaround time is equivalent to the gate time, the time the aircraft is parked at the gate. The turnaround time is not equivalent with the ground time. The ground time is defined as the entire time between touch down and lift-off. It consequently includes the taxi time and any waiting time before take-off, but also the pushback and engine start. The turn-around time in our context is the time the aircraft spends at the gate. This time is equivalent to the time the aircraft spends "on blocks", describing the fact that the aircraft's tires are secured with blocks to prevent inadvertent motion. The time "off blocks" is commonly known as block time [Cla07], the basic indicator for utilization. In figure 1.5 the times are displayed in a schematic way, the length of the processes do not represent any relative scale.
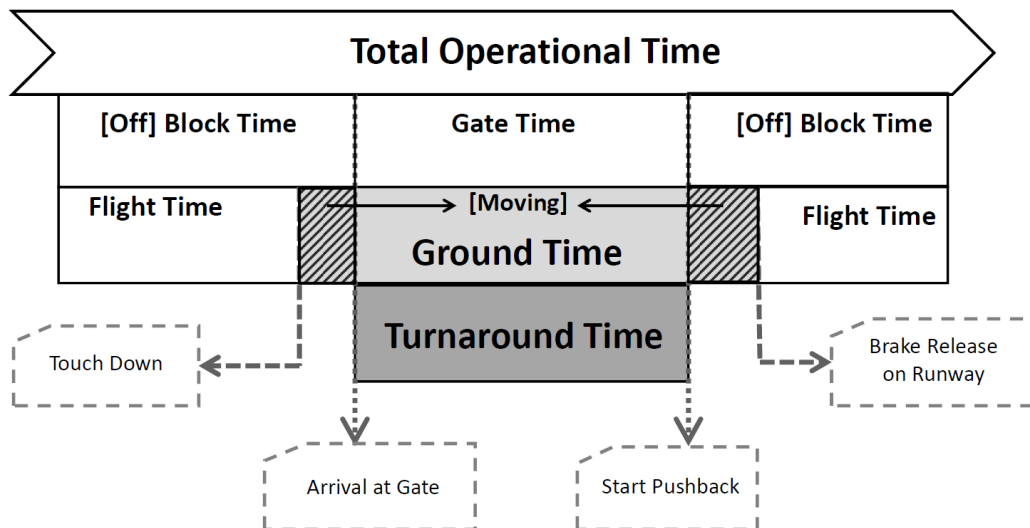
Figure 1.5 – Flight time versus ground time. The turnaround time is not the same as the ground time, which includes taxi time and potential departure delays. The moving ground time is shown hatched part of the ground time.

Understanding the different contributors to ground time is important, as reducing them requires different actions. Depending on the type of operation, the ground time might be lengthened by long taxi times or queuing for take-off at the runway. The ground time during which the aircraft is not in turnaround will be called moving ground time as shown in figure 1.5 as hatched area. The turnaround is part of the ground time. A generic turnaround chart is shown in figure 2.13. The sequence and relative length of processes are typical for a short range flight.

The chart is separated horizontally into three regions, which characterize the different entities in which actions are performed.

- **Passenger Services**: deboarding, cabin cleaning, catering and boarding.

- **Aircraft Services**: fueling, water and waste service, line maintenance and go-around check

- **Baggage and Cargo Handling**: unload containers and bulk cargo, load containers and bulk cargo

This separation between the entities can also be found in actual aircraft documents [Boe02]. In figure 1.6 a typical Gantt-chart for the turnaround process of the B757-200 - a high capacity single aisle - is shown. In between the entities processes can be parallelized. The refueling process is supposed to be finished before boarding commences. If safety measures are applied, the boarding can be started before refueling is finished (see EU-OPS 1305 in [EU08]). But cargo loading and cabin processes are running independently from each other. However, the turnaround is not completed before all of the actions are finished. The path of actions that determines the minimum time for the turnaround is called the critical path.

The critical path can be formed by all types of actions. If for example cargo loading and unloading require longer than all other actions, the critical path is formed by the cargo loading process. In practice the critical path is formed by the deboarding, cabin cleaning and passenger boarding [Fug01].

The reason is that in short and medium range operations only limited amount of cargo beyond the passengers' bags is carried. The cargo loading process can usually be accomplished within the other processes duration, especially when baggage is pre-packed in containers.[1]

PASSENGER SERVICES												
POSITION PASSENGER BRIDGES OR STAIRS	1.0											
DEPLANE PASSENGERS	10.0											
SERVICE CABIN	10.0											
SERVICE GALLEYS	20.0											
BOARD PASSENGERS	21.0											
REMOVE PASSENGER BRIDGES	1.0											
BAGGAGE/CARGO HANDLING												
FORWARD CARGO COMPARTMENT	13.0											
AFT CARGO COMPARTMENT	27.0											
AIRPLANE SERVICING												
FUEL AIRPLANE	15.0											
SERVICE LAVATORIES	14.0											
SERVICE POTABLE WATER	2.0											
PUSH BACK	----											

TIME – MINUTES

NOTES:
POSITION/REMOVE EQUIPMENT

Figure 1.6 – Turnaround chart of the B757-200 (from [Boe02]). Note that boarding is finished several minutes after all other processes, including the cargo loading. The critical path is shown along the critical processes.

The turnaround time is more relevant for the aircraft's overall utilization the shorter the average mission length is.

"An aircraft earns money in the air". While this proverb should not be taken literally, it summarizes the fact that aircraft operators are paid for a transport service. The more transport service they can offer, the higher is their theoretical total revenue potential. If an aircraft can produce more flights per day over a given distance, it can produce more total revenue. Given that the cost of operating a single flight are lower than the total revenue of that flight, any additional flight increases the operator's profit. Increasing utilization is one option of reducing cost. The so-called low cost airlines have successfully demonstrated that a reduction in ground time reduces the cost of operation per seat [Dog10]. The traditional low cost airlines like Ryanair or Southwest achieve minimum ground time by fighting both the turnaround time and the moving ground time. The first by speeding up boarding through abandonment of assigned seats and usage of dual boarding stairs. Moving ground time reduction is achieved by usage of small airports with shorter taxi times and rarely any queues at departure.

A further motivation for turnaround time reduction is the recapture of delays. Short mission ranges do not allow to catch up time with increased cruise speed. The turnaround remains the only option to make good time, and also the least costly. Shorter turnaround hence allow to increase the robustness of a rotation planning.

---

[1]The statements were verified through expert interviews with staff from Hamburg airport ground service provider.

A more detailed analysis of turnaround time is provided in section 2.4.1.

Future Short Range Configurations

In future, a general growth in passenger numbers can be expected which might lead to an increase in passenger capacity in the short range segment. Congestion at airports might deny the option of higher frequency. Populous countries like China or India have strongly growing passenger traffic, mostly between the large cities. This might be a further stimulus for short range air traffic [Air09] [Boe12].

Currently aircraft are designed and optimized primarily for best flight performance. That is, minimum fuel burn for a given distance, in order to obtain an aircraft with minimum direct operating cost. Other factors such as comfort and airport compatibility are regarded, but usually do not influence the decision whether the cabin is designed as single aisle or twin aisle layout. Mass and drag of the fuselage are important contributors to the overall aircraft's mass and drag. When capacity increases, the switch to a twin aisle layout is expedient at some particular point to achieve optimum performance. Certification requirements specify that no more than 6 passengers can be seated abreast when using a single aisle ([EAS06], CS25.817). So the step from 6-abreast to 7-abreast represents a step change due to the second aisle (see chapter 2.2, especially figure 2.7). Hence, the switch from 6- to 7-abreast is different than changing seat abreast configurations within the single aisle or twin aisle segment.

In short range operation the overall direct operating cost is influenced by the ground operations of the aircraft. This is due to cost for the ground handling itself, and loss of utilization when turnaround processes take longer (see section 5.1). At a certain point, an aircraft with inferior flight performance might be superior in direct operating cost due to these effects. The particular capacity where this happens is unknown, but most likely somewhere between 200 and 280 seats capacity [Fli11b]. Of further relevance are the parameters that influence this limit. In short range operations, the boarding and deboarding processes have large influence on the overall turnaround time (see chapter 2.4), often dictating the minimum turnaround time for an aircraft [Fug01].

Twin aisle aircraft are regarded as being faster in passenger boarding and deboarding [Fli87]. However, neither reliable numbers nor actual test data are available. In order to speed up turnaround the introduction of a second aisle might be useful at a lower capacity than that for best flight performance, in order to achieve minimum direct operating cost through higher utilization.

1.2 Research Objectives

The objective of this investigation is to establish a seat capacity limit above which a second aisle offers superior direct operating cost. It is further aimed at identifying the best cross section and seating arrangement as function of the seat capacity and range. The investigation hence aims at amending the current aircraft design philosophy by including the turnaround performance into the cost assessment. This is required for a holistic assessment of aircraft direct operating cost.

The fundamental assumption is that twin aisle cabins perform significantly better in typical aircraft

turnarounds than single aisle aircraft due to shorter times for boarding and deboarding. The difference is significant enough to influence the aircraft's utilization, and has profound influence on the overall direct operating cost of the aircraft.

(a) Current Design Practice　　　　　　　　　(b) Proposed Practice
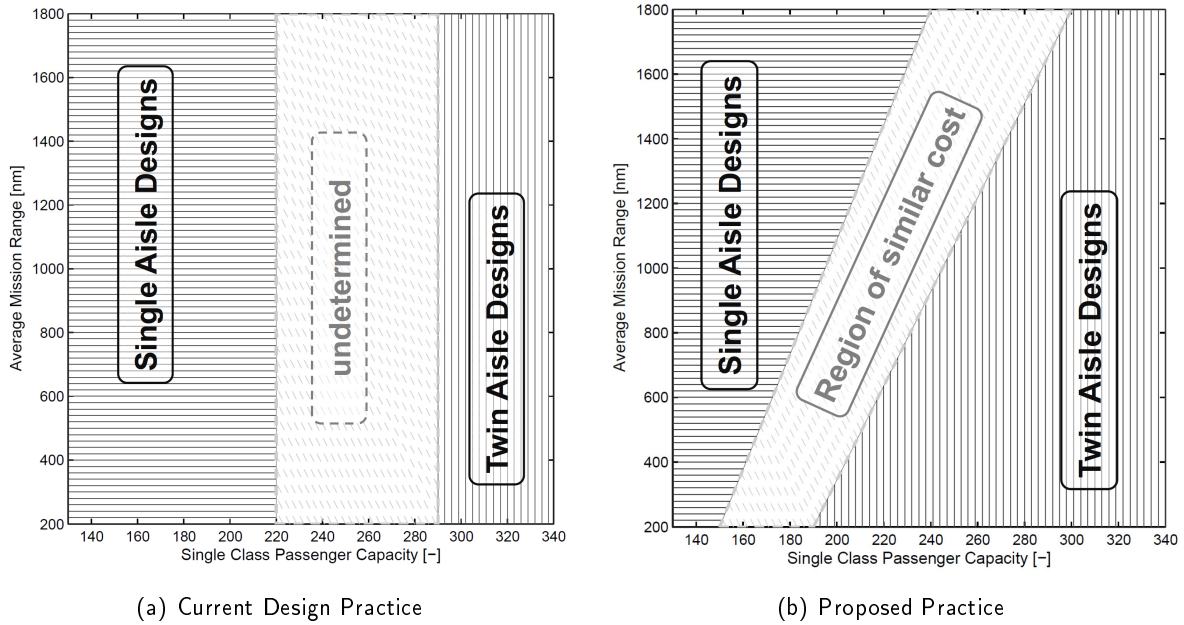
Figure 1.7 – Range-capacity areas for single and twin aisle design based on lower direct operating cost per seat. The limits are guesses at this point and determined over the course of this work. The current design practice is independent of average mission range. The inclusion of turnaround-related loss of utilization in the proposed practice leads to a range-dependency.

In figure 1.7 the fundamental objective of this work is illustrated. Current design practice shown on the left draws the line between single aisle and twin aisle solely on seat capacity (see section 2.2 for sources). There is no definitive point, but rather a region in which based on better flight performance a twin aisle has better direct operating cost than the single aisle. The boundary between single and twin aisle is hence no different than that between different single aisle (for example 5-abreast and 6-abreast) or different twin aisles.

On the right the new, proposed design practice is shown. The fundamentally different behavior in turnaround influences the utilization of the different design, causing a shift of the limit to lower capacities when mission length is short. Hence, the region of direct operating cost advantage becomes a function of the average stage length. The intermediate region is the region of similar cost. The exact location of the regions is probably depending on the nature of operation and specific characteristics of the investigated aircraft.

This work is located in the field of aircraft design. It analyzes the air transportation system at its interfaces by incorporating aircraft operation, up to a point where aircraft design decisions can be analyzed regarding their influence on turnaround time and consequently daily utilization.

This requires that the basic assumption, that twin aisles board faster than single aisles, is proven as first step using appropriate methods. Therefore, it is the objective of this work to analyze turnaround times of different designs applying realistic assumptions for the operational environment. The found results shall enhance the preliminary aircraft design process for short and medium range aircraft for any future design problem. This work should deliver useful equations for turnaround time estimation

for preliminary aircraft design. The introduced formulas should be sufficient to include them in multi-disciplinary design processes and allow these to find minimum direct operating cost. As such it allows to analyze a cabin layout not solely under the aspect of flight performance, but additionally under the aspect of operational considerations in a short range environment.

As prerequisite for the enhancement of the current design practice, the investigation needs to locate the capacity limits between different fuselage layouts. As shown in section 2.2, this can be achieved with rather simple analytical relationships. However, the task becomes more complicated if specific cabin layouts are used as basis for comparison as shown in section 4.3.2. The results show that current design guidance as given in accepted text books can lead to non-optimum layout in the relevant capacity region.

The findings of this work are strongly dependent to the assumptions concerning airline operation and air traffic management. The dominant assumption is that an airline can use any additional flight in their fleet rotation and that sufficient demand is present to fill all additionally generated flights. Further assumption is that sufficient airspace and airport capacity exists to operate additional flights. The applicability of the threshold is closely connected to these assumptions, and therefore not necessarily valid in general as soon as a different type airline operation is looked at. These assumptions are highlighted in the text, and their effect on the result is also clearly stated in the result section.

1.3 Methodology

The stated objective requires a methodology that exceeds methods usually used in aircraft preliminary design, and introduces methods that have so far not been used in an aircraft design process. Figure 1.8 shows in a simplified manner how the stated research objective is achieved. The classic approach of determining the influence of a new technology on the weight and drag (or maintenance cost if applicable) of an aircraft is amended by analysis of the turnaround time. The difference to classic approach is that the cabin layout becomes the distinctive difference between otherwise similar configurations. For this purpose a number of methods are used that are specially adapted for the research objective.
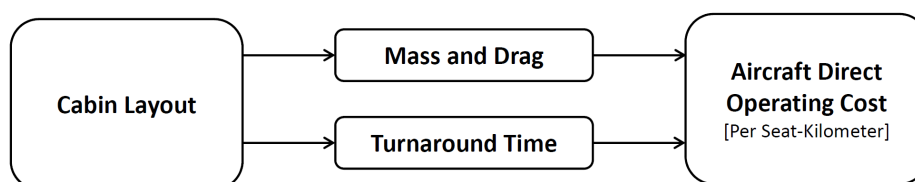
Figure 1.8 – Methodology of the work in a simplified manner. The classic mass and drag assessment is amended by the estimation of turnaround times. The chosen cabin layout becomes the point of distinction.

Fuselage and cabin design is performed using a high fidelity cabin layout process which allows the design of cabins of comparable standard. This is required as cabin layout requirements and practices cause step changes in the actual cabin layout. For example, the required addition of an emergency exit above a particular capacity will lead to a step change in fuselage length and mass.

Aircraft preliminary design relies on statistical methods for mass estimation of structure and systems. In case of the fuselage these methods have limitations in their accuracy caused by their simplistic nature (see page 19 and page 40). Further, as all methods are validated against currently existing aircraft, the investigated range of fuselages exceeds the region of validity of current statistical formulas. A more detailed method for fuselage mass estimation is introduced. The method exceeds the accuracy of current statistical methods by including physical relationships for sizing load cases. The method allows to study designs beyond the region of validity of current statistical formulas. Statistical equations for secondary weights are introduced, too, which represent a substantial enhancement of current design formulas for secondary masses.

Passenger boarding and de-boarding times and full turnaround times are determined using a boarding simulation. The usage of a boarding simulation in aircraft preliminary design is a new feature and widens the field of application of boarding simulations, which have been limited so far to boarding strategy problems (see section 2.4.3). The boarding simulation is based on a proven methodology, but introduces new features of specific importance to the research objective. These features are the effect of fuselage design decisions on the boarding time. These decisions are besides seat arrangement the door position, the overhead bin size and the aisle width.

For the assessment of aircraft performance and subsequently operating cost an aircraft design method is introduced. This method is oriented on proven methods but enhanced by a prudent calibration with current aircraft designs. The method hence offers higher fidelity in the desired region, resulting in a qualitatively and quantitatively reliable statement on aircraft flight performance. The determination of direct operating cost follows proven methods. A method for ground handling cost is introduced to better understand this important contributor of cost in a short range environment.

The inclusion of turnaround time affects the number of flights an aircraft can perform on any given day. While cost like fuel, salaries and maintenance behave proportional to number of flights, the cost for aircraft finance are spread over the number of flights. Figure 1.9 shows that the so-called cash operating cost can be calculated for each individual flight and then multiplied with the number of flights. The cost caused by financing an aircraft are in contrast divided by the number of flights.
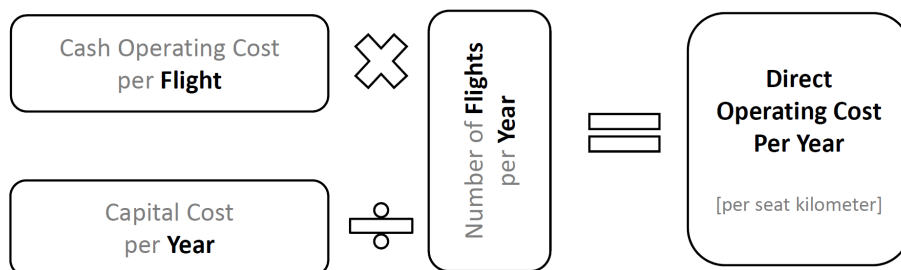
Figure 1.9 – Basic relationship between number of flights, cash operating cost, capital cost and the direct operating cost per year.

The cost assessment is performed with an accepted method that includes both flight-time and flight-number specific maintenance cost. The method is slightly changed by removing the mass-dependency in some of the regression formulas in order to prevent the method from creating virtual

disadvantages. These are for example the effect of small differences in empty mass on maintenance cost and crew cost, which distends the effect of small differences in empty mass on aircraft operating cost.

1.4 Work Overview

Following this introduction to the objectives and motivation a brief review of fuselage design is given in chapter 2. The focus is on the influence of seat capacity on fuselage design decisions. The turnaround process is then analyzed in more detail. Relevant literature and recent research is reviewed. The historic developments are shown using historical aircraft data and known industry concepts.

The third chapter describes the utilized methods. At first the fuselage and cabin design with the fuselage weight estimation is described, then the boarding simulation. The chapter closes with a description of the aircraft design method including the mission performance and cost analysis. Validation and short description of the technical background of the methods is provided in each section.

The fourth chapter introduces the analyzed cross sections and provides the disciplinary results. The results are provided for each of the three fields (fuselage & cabin design, boarding & turnaround, overall aircraft design), allowing the reader to reenact the analysis. The disciplinary results lead the way to understand the results in the analysis section.

The fifth and final chapter conducts an analysis of the found results. Several set of assumptions are used to establish different thresholds between single and twin aisle. The analysis is limited to a number of comparisons. It does only include the most relevant results of the previous chapter.

The work closes with a summary and a conclusion. The probable impact on future designs is critically reviewed, including aspects of aircraft market dynamics.

The appendix contains regressions formulas for boarding, deboarding and total turnaround time.

Chapter 2

Fuselage Design and Aircraft Turnaround

The following chapter provides an introduction to relevant aspects of fuselage design. These basic physical relationships are explained using elementary formulas. Recent literature concerning fuselage design and turnaround time reduction is reviewed.

2.1 Introduction to Fuselage Design

This section outlines which considerations influence the size and shape of the fuselage. The explanations are focused on passenger capacity, which is usually the primary driver for fuselage size selection.

2.1.1 Basic Considerations

Fuselage design is part of aircraft design and hence covered in most textbooks concerning that subject. For this work the accepted standard textbooks by Torenbeek [Tor76] and the relevant parts of Roskam's aircraft design series [Ros04a] [Ros04b] were used. Further textbooks were consulted for additional information with only little additional information being identified. Beside textbooks further sources were assessed for state-of-the-art cabin design knowledge [FPO07] [Heh01] [FPO11].

The fuselage is characterized by its cross section. The cross section is of crucial importance for the success of a design, and it further is the only item that can never be changed within the product life cycle. The Boeing737 has demonstrated how an aircraft can receive new wings, new engines, new systems and can grow considerably in size and capability. But the B737 still retains its original cross section. Fuselage design decisions are influenced by numerous fields of engineering, a choice is listed in the following enumeration.

1. Payload accommodation of both passenger and cargo: The fuselage needs to house the entire payload, and has to provide a flight deck.

2. System installation: many systems need to be integrated in the fuselage, some at particular positions. Further the fuselage needs to have volume for connections between systems (like ducts, wires).

3. Structural efficiency of the fuselage: For pressurized aircraft a circular cross section is strongly encouraged in order to achieve minimum structural mass. Crash safety and fatigue resistance over the entire lifetime are major drivers in fuselage structural design.

4. Aerodynamic efficiency: the fuselage produces both skin friction drag as function of its wetted surface and pressure drag as function of the frontal area. The front and rear end need to be tailored to improve aerodynamics.

5. Flight stability and control: The fuselage length sets the lever arm of the tail surfaces for conventional aircraft. A short lever arm requires larger surfaces and may offset drag and mass savings of the fuselage.

6. Producability: the fuselage needs to be produced in a cost efficient manner, possibly in different locations with a joined final assembly. For that purpose long constant sections are preferable.

7. Airport compatibility, safety and comfort: the fuselage has to allow a quick exchange of payload. Quick egress of passengers in case of emergency needs to be assured. The fuselage further needs to assure a comfortable environment for the passengers at any altitude or speed.

The list demonstrates that fuselage design is a field of compromise between multiple disciplines. A key parameter of the fuselage is the so called fuselage fitness ratio λ_f or slenderness, which is length divided by diameter. In case of non circular fuselages, an equivalent diameter is calculated.

$$\lambda_f = \frac{l_{Fuselage}}{d_{Fuselage}} \tag{2.1}$$

$$\lambda_f = \frac{2 \cdot l_{Fuselage}}{h_{Fuselage} + d_{Fuselage}} \tag{2.2}$$

The slenderness is important both for structural and for aerodynamic performance. On the structural side the slenderness characterizes the stiffness of the fuselage for bending loads. On the aerodynamic side it sets the relationship between frontal drag and skin friction drag. Aircraft with low slenderness have increased tail area and in extreme cases the access to the fuselage (airport compatibility) is compromised. Aircraft with high slenderness need longer landing gear for rotation at take-off and may experience structural penalties due to increased bending stress. Long and thin fuselages might be prone structural vibration problems as stiffness is insufficient.

The optimum region for the fuselage slenderness is considered between 10 and 11 [FPO07], while the ends are soft. The highest slenderness was achieved by the DC-8-71 with 14.2, the lowest by the B737-100 with 7.1. The reasons for extreme values are usually commonality and product strategy: the DC-8-71 was the maximum stretch of the basic DC-8, the B737-100 was the standard Boeing cross section from the B707 reduced to a capacity of 100 seats[1]. Most likely both would have received a different cross section if it had been of free choice at the beginning of the design process.

2.1.2 Seat Capacity

The seat capacity is one the first decisions in the aircraft specification process [[Tor76], page 5]. Together with the specified range, the seat capacity determines largely the commercial potential of an aircraft design. While the seat capacity obviously determines the maximum amount of revenue an aircraft can generate, it also influences the cost of operation for an aircraft. The seat capacity affects

---

[1]Interestingly Boeing also produced the B757-300, which trails the DC-8-71 by a small margin in slenderness ratio, using the very same cross section as the B737-100. This shows how commonality drove design to the extremes of fuselage slenderness.

the economics of an aircraft. Larger aircraft are typically more efficient for each offered seat-kilometer, which is shown using two examples from literature.

Figure 2.1 shows the direct operating cost per available seat kilometer. The data is reproduced from [Dog10] [Figure 5.2, page 104], but can also be found in an updated fashion in [Ros13]. The data is generated by evaluating the data airlines report to the US Bureau of Transport Statistics in the so called Form 41 datasheet [BTS13]. The data clearly indicates an advantage of higher capacities. However, the data is skewed for several reasons. The capacity is the actual capacity, hence it mixes single class short range cabins with long range multi-class cabins. Secondly, the character of operation is different between the short range types and long range types. Finally, especially in case of the larger aircraft, the cited aircraft types represent fleets of a single airline and are optimized for a particular market, which limits the comparability. Nevertheless, it becomes apparent that cost change with aircraft capacity. The minimum indicated by the regression is only virtual, which can be seen in the next figure.
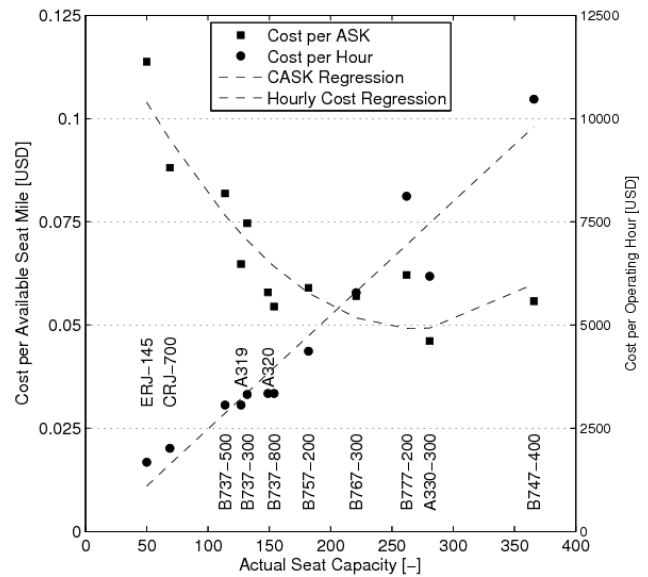
Figure 2.1 – Figure resembling figure 5.2 from [Dog10]. Shown are cost per available seat kilometer (ASK) on the left and cost per hour of operation on the right. The larger the capacity, the lower the seat-specific cost. Also see text.
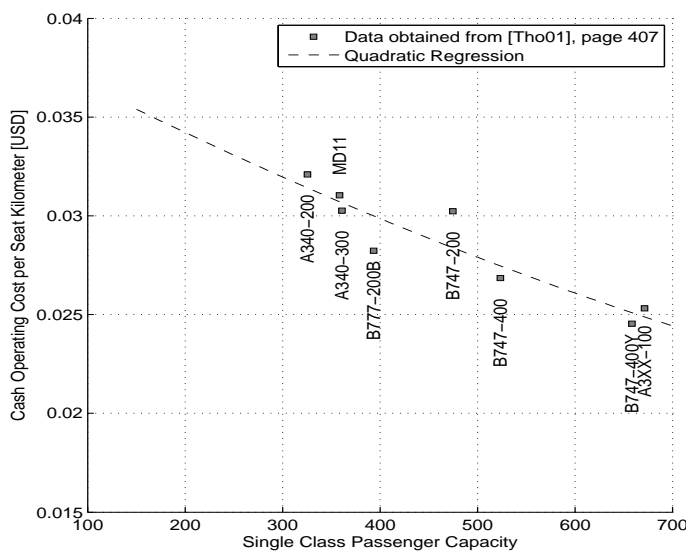
Figure 2.2 – Figure resembling one from [Tho01]. The figure compares different long range type on a 4000nm mission. The comparison is from the mid 1990ies.

Figure 2.2 shows the cash operating cost per available seat kilometer. The data is taken from a similar figure in [Tho01] [page J-8]. The data points represent long range designs configured in an all-economy layout operated by the same airline. Hence a direct comparison is possible. The data is based on designs available in the mid 1990ies. The points furthest to the right are the then projected A3XX (today A380) and the B747-400Y, which was a proposed stretch of the B747-400. The cost was estimated for a 4000nm reference mission. Although this data - like the previous example - is not universally applicable to all capacities and ranges, it demonstrates that increased capacities enjoy better cost per available seat kilometer.

The reasons are both technical and operational. Technical reasons are in theory better aerodynamics and better propulsive efficiency, while the structural mass is supposed to increase. Operational aspects are the flight crew, fees and maintenance cost. If - as done in the figures above - the cost is divided by the number of seats, the seat layout has a strong influence.

2.1.3 Seat Arrangement

Previous section shows that seat-specific cost decrease if capacity increases. The same data also shows that aircraft of comparable capacity may have different cost. This is partly caused by design differences that result in different weight and drag. One influential parameter is the number of seats abreast. In dependence of the chosen seat capacity, the number of seats abreast determines the fuselage length and the relationship between length and width of the fuselage, called the slenderness (see page 14).

4 Abreast
Surface: +29%
Length: +35%

5 Abreast
Surface: +9%
Length: +13%

6 Abreast
(Reference)

7 Abreast
Surface: +7%
Length: -12%
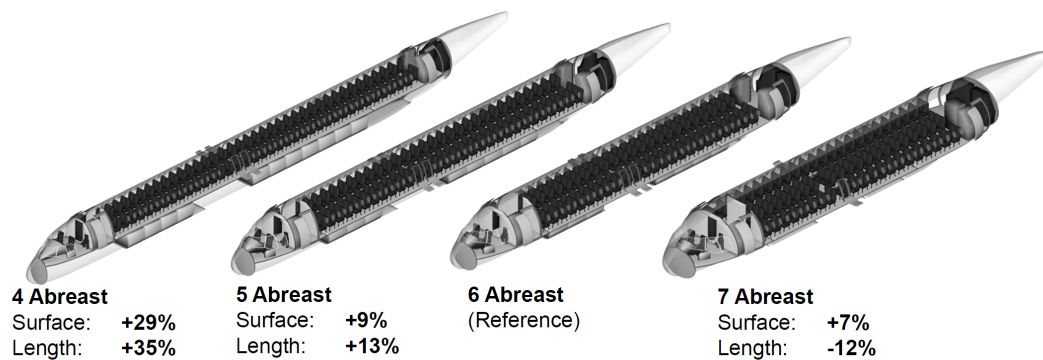
Figure 2.3 – Four different fuselage configurations for a 150-seat aircraft. The reference configuration is the 6-abreast. From [Hei07].

In figure 2.3 four different fuselage configurations are shown with 150-seats capacity. It is taken from [Hei07]. The reference configuration is the 6-abreast. It has lowest surface of all fuselages shown. While the surface is an indicator for the aerodynamic drag and fuselage mass, it does not represent the final figure of merit for a fuselage as shown in the subsequent section. Under pure technical consideration there is an optimum seat abreast configuration for each desired capacity.

2.2 Elementary Fuselage Sizing

This section attempts a basic fuselage sizing using simple formulas. These formulas are to some extent reliant on regression. That is, the factors have been determined through analysis of historical data.

In transport aircraft design the payload sizes the fuselage dimensions. This approach is called inside-out design or payload driven design. Choice of cross section is one of the first fundamental design decisions. When the cross section is set, the fuselage length becomes a function of the required amount of payload.

The most important parameters are shown in figure 2.4. The fuselage width is determined by the cabin width requirement, which directly relates to the chosen seating layout. In context of this work aircraft with passenger capacities ranging from 130 to 340 in a single class arrangement are considered. The resulting cross section always has a dedicated underfloor cargo hold (which might be omitted below 100 seats capacity) and a single deck layout. The fuselage height above floor level is determined by the cabin standing height or the headroom of the outmost seats. Its width by the sum of seats and aisles at armrest level (roughly 24inch or 0.61m above floor level). Below the floor level the required height and width of the cargo compartment sizes the outer dimensions. The cross section has to enclose all items while being as close to a circle as possible. Consequently, height and width are usually adapted to each other to achieve a circular fuselage. All pressurized civil aircraft designs with a single passenger deck have diameters and widths of 10% within each other.

Payload requires volume. In case of passengers it further requires minimum cabin floor area, and with a set cross section the problem becomes largely 2-dimensional. When the seating configuration is chosen, the cabin length is a function of the defined number of passengers plus allowances for door access areas, service installations and the flight deck. The number of exits is set through evacuation requirements ([EAS06], specifically 25.807). The number of service installations is a function of envisioned comfort level and assumed route length. Current short range aircraft have a low ratio of service facilities to installed passenger

Figure 2.4 – Typical cabin dimensions for cross section layout.

seats. The fuselage is no constant cylinder over the entire length, the forward and rear end have to be adapted to aerodynamic requirements. Especially the form of the rear fuselage has a major influence on the overall fuselage drag. If the fuselage narrows to quickly, the flow detaches and causes additional drag. That is why floor area is sacrificed in the aft fuselage to allow optimized aerodynamics.

The ratio between fuselage length and fuselage width and cabin respectively fuselage length is documented in two figures taken from Torenbeek's "Synthesis of Subsonic Aircraft Design" [Tor76]. In figure 2.5(a) the relationship between seats abreast (on the x-axis) and fuselage width (on the y-axis) is shown. Existing aircraft designs are plotted as dots. A gap between the widest single aisle and the smallest twin aisle can be noticed. Figure 2.5(b) depicts the relationship between cabin length on the y-axis and number of seat pitch times the rows (seats divided by seats abreast).

The required cabin width at armrest level of a single aisle can be estimated using seating standards

(a) Seats Abreast   (b) Seats and Cabin Length

Figure 2.5 – Aircraft data and statistics for fuselage length and width (from [Tor76]). Note that these statistics were made in the 1970ies, thus do not include many modern types. See text for further explanations.

for a current short and medium range comfort standard. Units have to be consistent. The wall clearance is a rule of thumb coming from the head room requirement as shown in figure 2.4. The wider the fuselage diameter the smaller the required additional wall clearance as the curvature of the cabin side wall decreases. All used symbols of the following calculation can be found on page 134 in the appendix.

$$w_{Cabin} = n_{Abreast} \cdot (w_{Seat} + w_{Armrest}) + 2 \cdot w_{Armrest} + 2 \cdot w_{Clearance} + w_{Aisle} \qquad (2.3)$$

A twin aisle requires an additional aisle and and an additional armrest.

$$w_{Cabin} = n_{Abreast} \cdot (w_{Seat} + w_{Armrest}) + 3 \cdot w_{Armrest} + 2 \cdot w_{Clearance} + 2 \cdot w_{Aisle} \qquad (2.4)$$

It immediately becomes clear, the lines never cross. A single aisle would always be smaller in diameter and hence more efficient as cross section than a twin aisle at a similar number of seats across. However, certification requirements prohibit any seat to be more than two seats from the aisle (CS25.817 [EAS06]), making a 6-abreast the single aisle with most seat across. The twin aisle achieves the same ratio of cabin width to seat count at a 12-abreast seating. This explains why a 6-abreast single aisle cross section is an efficient and popular solution.

With a specified number of passengers the theoretical cabin length can be estimated. Cabin length refers to the length of the pressurized part of the fuselage without the flight deck, as shown in figure 2.5(b).

$$l_{Cabin,theoretical} = \frac{n_{PAX}}{n_{Abreast}} \cdot l_{SeatPitch} \qquad (2.5)$$

As mentioned above the cabin needs to be longer than the added length of all rows. Beside service installations, further areas must be provided for door access. In figure 2.5(b) the theoretical cabin length (dashed line) and the actual cabin length are shown (solid line). Dots represent actual aircraft layouts. Although Torenbeek uses an old database, this statistic remains valid because the general layout guidelines for cabins have not changed. The figure shows a true cabin length as being about 35% longer than the theoretical one. Also the flight deck with a fixed length independent of the fuselage diameter is added.

$$l_{\mathrm{Cabin,actual}} = l_{\mathrm{Cabin,theoretical}} \cdot 1.35 + l_{\mathrm{Flightdeck}} \tag{2.6}$$

The fuselage length can be estimated by adding the diameter-dependent tail cone. In mass analysis, the fuselage in front of the cockpit is usually not accounted for, as it is relatively short and not part of the primary structure but an aerodynamic fairing. Hence it does not add any meaningful mass. The length of the tail cone can be estimated from current designs as being 1.6 of the diameter. The fuselage diameter is in a fixed relationship with the cabin width and can be estimated using the following formula. The formula is derived from existing aircraft.

$$d_{\mathrm{fus}} = 1.045 \cdot w_{\mathrm{Cabin}} + .084\mathrm{m} \tag{2.7}$$

$$l_{\mathrm{fus}} = l_{\mathrm{Cabin,actual}} + 1.6 \cdot d_{\mathrm{fus}} \tag{2.8}$$

Mass and drag increase proportional to the fuselage surface, depending on the specific design with a changing factor. Achieving minimum wetted surface for a given payload is beneficial for achieving best mass and drag. The fuselage surface can be estimated with a simple approximation, sufficiently accurate for this short example.

$$S_{\mathrm{fus}} = \pi \cdot d_{\mathrm{fus}} \cdot l_{\mathrm{fus}} \cdot \left(1 - \frac{2}{\lambda_{\mathrm{fus}}}\right)^{2/3} \cdot \left(1 + \frac{2}{\lambda_{\mathrm{fus}}^2}\right) \tag{2.9}$$

The best range of fuselage fitness ratio or slenderness is supposed to be between 10 and 11 as stated above. This ratio offers best performance, implying best compromise between mass and drag considering all relevant components, while not violating any of the stated requirements. It is the result of a multi-disciplinary optimization and is difficult to estimate using analytical means (compare to [Nit10] for an analytical approach towards optimum fuselage slenderness). The variance in existing designs shows that particular considerations may encourage a deviation from this optimum (see page 23). The optimum range further excludes operational factors such as turnaround.

Current short range cabin standards are 18 inch wide seats, a 20 inch wide aisle, 2 inch armrest and 31 inch seat pitch. Applying these values to the equations above yields wetted area and slenderness as function of required passenger capacity. The wetted area is shown in figure 2.6(b). The single aisle (solid lines) have always less surface area than the twin aisles. An important figure of merit is the structural mass of the fuselage. Its estimation in preliminary aircraft design is difficult, but several statistical formulas exist. Based on an analysis of several formulas, two formulas have been chosen for mass estimation [Ber09]. The Howe method uses geometric fuselage parameters and differential pressure [How00].

(a) Fuselage Slenderness   (b) WettedSurface
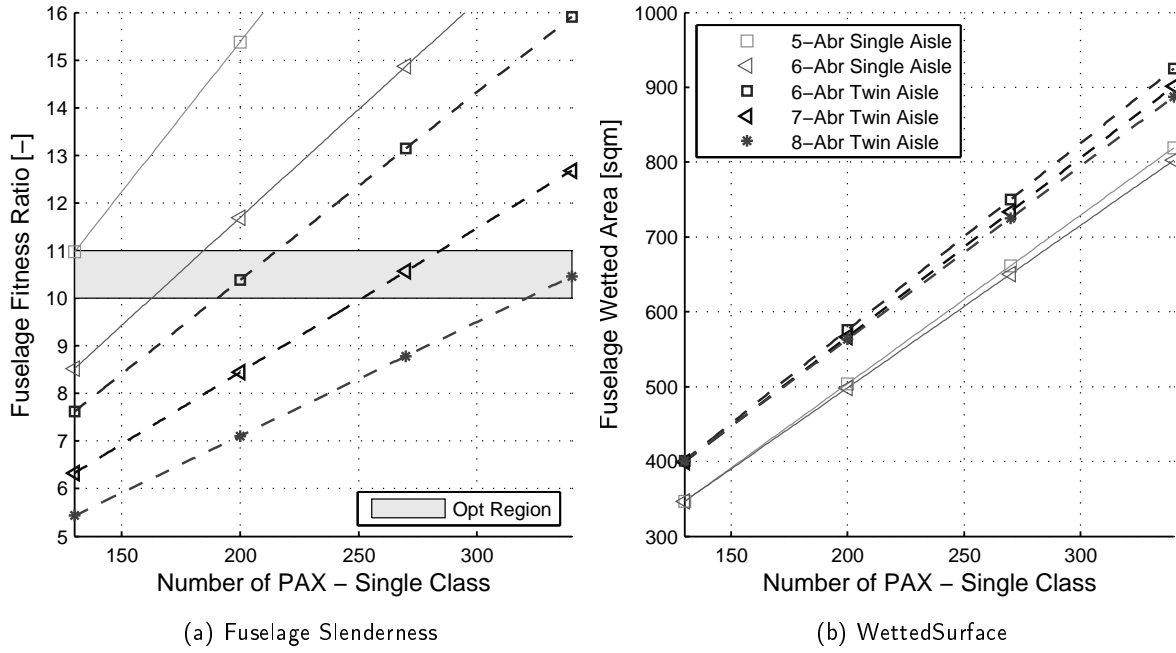
Figure 2.6 – Effect of seats abreast on basic fuselage performance indicators. The fitness ratio or slenderness indicates the structural and aerodynamic quality. The optimum region is marked. The wetted area is proportional to the zero-lift drag of the fuselage. Right plot's legend valid for both plots. Also compare to figure 2.3.

$$m_{fus} = \left[1 + \frac{(3.12 - 0.354 \cdot d_{fus}) \cdot \sigma}{1 + \sigma} \right] \left[\frac{3.56 \cdot p_{max}}{\sigma^{0.75}} \cdot d_{fus} \cdot S_{fus} \right] \tag{2.10}$$

$$\sigma = 0.8 + 0.05 \cdot (d_{fus} - 2) \tag{2.11}$$

The more recent formula from the "Luftfahrtechische Handbuch" developed by Felix Dorbath uses only geometrical parameters. [Dor11]

$$m_{fus} = 12.7 \cdot (l_{fus} \cdot d_{fus})^{1.298} \cdot \left\{ 1 - \left[-0.008 \cdot \left(\frac{l_{fus}}{d_{fus}} \right)^2 + 0.1664 \cdot \left(\frac{l_{fus}}{d_{fus}} \right) - 0.8501 \right] \right\} \tag{2.12}$$

The results are shown in figure 2.7 as mass per seat. The left figure shows the results from Howe. Although the formula achieves a good match with existing aircraft, it does not indicate any useful trend. By Howe's formula the single aisle would have the lowest mass for any capacity. The right figure shows the results of the LTH formula, which are much more educating. The optimum regions for the different configurations are clearly visible. The threshold for a switch from single aisle to twin aisle is at 290 seats, at a fitness ratio of about 15.5 of the single aisle. Note that the 7-abreast twin aisle has its best specific mass between 250 and 280 seats but is still heavier than the single aisle. The widely used formula by Torenbeek has been tried but shows even less desirable results than Howe's formula, making it virtually useless for this kind of assessment. The short analysis has shown that the single aisle appears to be the best solution from pure flight physics up to 290 seats. For a more trustworthy estimation more effects and better modeling is required. Wetted area and fuselage mass are only indicators of the resulting performance.

(a) Howe Formula (b) LTH Formula
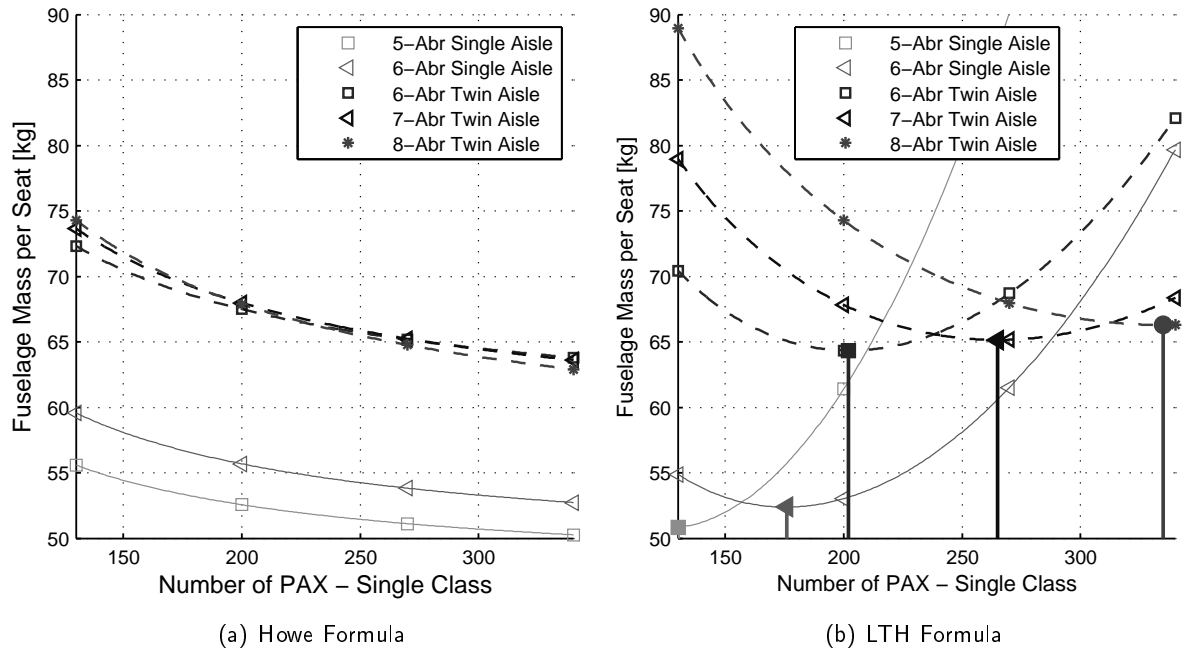
Figure 2.7 – Estimated fuselage mass per seat using accepted statistical formulas. Note that Howe's formula finds the single aisle to be the best for all capacities. The LTH formula finds a clear optimum for each seat abreast configuration.

2.3 Seats Abreast in History and Literature

The previous section provides a basic sizing for the fuselage. The results show that for each seat abreast configuration a minimum seat-specific fuselage mass exists. It needs to be stressed again that the used formula is based on regression. The approach used for cabin sizing does not incorporate step changes through added emergency exits or additional monuments. This section looks at actual and historical designs in the considered capacity range. Relevant literature is reviewed.

As shown above, the chosen number of seats abreast has a substantial impact on the overall performance of the aircraft. While the step between different single aisle layouts or different twin aisle layouts is rather continuous, there is a considerable gap between the 6-abreast and the 7-abreast. The reason is that the amount of unproductive aisles doubles. This region is in the capacity band of 200 to 300 seats in a single class layout. Below a twin aisle is disadvantaged, and above a single aisle becomes undesirable.

The number of seats abreast is consequently guided by the desire to create the most efficient enclosure around the required payload. Certification standards require a second aisle above 6 seats abreast (CS 25.817)[2]. Theoretically a 6-abreast aircraft can have a twin aisle layout. This would of course be less efficient than a single aisle. As shown in the next section, the 6-abreast twin aisle is a concept that was considered several times, however, with wider seats than assumed in the previous calculation.

---

[2]The Hawker-Siddenly Trident once had 7-abreast single aisle layout, but the 7th seat was intended for children.

2.3.1 Literature and Recent Research

There is no definitive guidance on the capacity above which a 7-abreast twin aisle layout is recommended. Many textbooks do not provide a specific limit. It is - like many other parameters in aircraft design - subject to a comparative trade study.
Torenbeek at least states a rather unspecific limit and gives no technical reasoning [Tor76].

> "If more than 150 to 200 passengers are to be accommodated the use of two aisles should be considered." [p. 67]

Advice concerning the arrangements of seats in the cabin can be found in many university lecture notes. Most rely on statistical analysis by presenting the existing designs in dependence of passenger number and fuselage slenderness, just as provided in figure 2.8.
Mentioned criteria for fuselage selection are operational considerations (like listed on page 14), but also mass and drag of the fuselage. In a design class conducted by Airbus Future Projects Office the slenderness of the fuselage is cited as key criteria for cross section selection [FPO07]. Scholz recommends a similar approach [Sch99].
Only Thorbeck clearly mentions the effect of fuselage layout on turnaround time, and its effect on direct operating cost (in [Tho01] page A-37 & A-38). He mentions turnaround as one limiting factor for fuselage length. He does not offer a directly applicable capacity limit, but a maximum of approximately 190 seats can be read from a chart.

In a conference paper Nita and Scholz of the Hamburg University of Applied Science covered the topic in depth [Nit10]. Their paper deals with the optimum slenderness ratio for passenger aircraft. The formulas used to estimate drag and mass are in majority taken from Torenbeek [Tor76]. The finding is that the optimum slenderness is situated slightly above 10, affirming the previously cited accounts that ratios between 10 and 11 represent the overall optimum [FPO07]. The analysis takes into account tail size and fuselage drag, thus includes all physically meaningful areas. Torenbeek's methods are used as sole mass estimation formula. The calculated optimum slenderness represents an optimum for minimum overall drag, including induced drag of additional mass. The work aimed at finding the fuselage with minimum drag, which is only one element of the more relevant operating cost. The work does not provide the slenderness as function of either capacity or range.
In the work a formula is presented that gives the number abreast as function of passenger capacity.

$$n_{\mathrm{Abreast}} = 0.47 \cdot \sqrt{n_{\mathrm{PAX}}} \qquad (2.13)$$

The relationship is statistical and the factor is chosen to produce the smallest error applied to existing designs. However, especially in the single aisle capacity region the factor of 0.47 can deviate depending which specific designs are being matched. With 6-abreast aircraft have spanned capacities from 100 to 280 seats, the factor could become 0.36 to 0.6 for the designs on the extreme ends (the A320 has 0.45). Consequently, the formula is only useful for very early conceptual design.

In a study by Ralf Metzger researched the optimum fuselage cross section [Met08]. The study is aimed at the methodology of finding an optimum fuselage cross section by means of optimization. The work offers extensive insight into weighting functions and optimization routines. He includes turnaround as one optimization parameter. The turnaround is simply hinged on the passenger seats per aisle. As the work aims on the methodology, no comparison in cost is given for a cost-optimized and a turnaround-optimized aircraft. The cabin layout - though advanced for a preliminary design

tool - has difficulties in estimating the cabin layout of single aisles and small twin aisles. The methods used for aircraft design are further limited in accuracy, as again, Torenbeek's mass estimation methods are used. Overall, despite the advanced algorithms introduced by Metzger, the methods used for aircraft design are insufficient to produce results with the necessary accuracy. As shown later (see section 4.3.2), already small differences in structural weight can change the outcome significantly. His methodology finds twin aisles as optimum above 170 seats capacity.

2.3.2   Existing Designs

An overlap region between single aisle and twin aisle designs exists in practice. The smallest twin aisle aircraft - the B767 - has capacities similar to the B757, which is also the largest single aisle by seating capacity. In detail the B767-200 (the basic version) has a single class seating capacity of 242 seats in dense economy layout. The B757-200 has a capacity of 238 seats[3]. Both aircraft were developed at the same time. The B767 is considerably heavier, but it was designed for longer ranges with container loading capability[4] and longer range. The B767 can further accommodate 8-seats abreast in a dense layout, while the B757 is below current standards for economy seating in terms of seat width and does not allow containerized cargo.
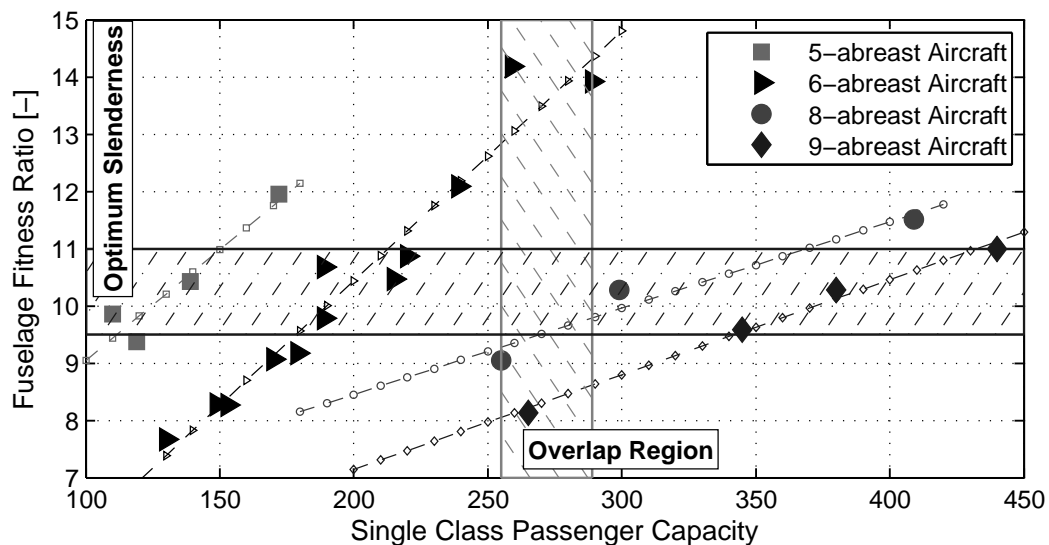
Figure 2.8 – Fuselage slenderness over single class seating capacity for existing designs. The lines represent linear fits. Note that there are no dedicated 7-abreast designs. The horizontal box marks the region of optimum fuselage slenderness, the vertical box the overlap region of largest single aisles and smallest twin aisles.

In figure 2.8 the slenderness ratio of several aircraft is plotted over their single class seating capacity. Comparable plots can be found in many textbooks and lecture notes (see for example [Tho01]) . The aircraft are grouped by their maximum number of seats abreast. There is no aircraft with a 7-abreast seating as highest number of seats abreast. The B767 and A300/330/340[5] cross sections have a standard abreast of 7 and 8, respectively. Both cross sections do allow a denser layout with 8 or

---

[3]When the aircraft is equipped with 4 full-size doors per side, otherwise exit limit is 228.

[4]Owing to this requirement the B767's cross section is higher than it is wide.

[5]The cross sections of these aircraft are similar.

respectively 9 seats abreast, which is only used by some low-cost and charter airlines (compare to [Sea11]). An overlap region exists between 240 and 280 seats. Both the single aisle (B757-300) and the twin aisle (A310, B767-200) situated in this region are out of production. The new B787-8 has a single class passenger capacity of approximately 320 seats [Boe11b]. A version optimized for shorter ranges (B787-3) was canceled before production commenced. However, the main change to the basic B787-8 was a wing of lower span for airports with restricted gates, which gave the aircraft a worse cruise performance without saving significant weight [Fli11a].

2.3.3 Concepts of Short Range Twin Aisles

On the following pages a few industry concepts are introduced. There are probably many more concepts which were never published. The intention is simply to show that the idea of a small twin aisle aircraft did not escape the attention of professional aircraft designers.

In the mid 1980ies Jan Carlzon - then CEO of the Scandinavian Airlines Services (SAS) - introduced the concept of the "Passenger Pleasing Plane", a concept possibly not invented but at least promoted by him [Car87]. The idea was to build an aircraft which offers higher comfort to the passenger which he saw compromised through the seating arrangement of the traditional 6-abreast single aisle. The arrangement was a 6-abreast twin aisle. The focus was not on turnaround but on passenger comfort. Carlzon described the 6-abreast single aisle as unacceptable in terms of passenger comfort.

In the 1980ies both McDonnel Douglas and Boeing worked on new short and medium range concepts that included a twin aisle layout with 6- or 7-abreast seating made for short ranges. Boeing included this in its B7J7 concept in the early 1990ies. The McDonnell Douglas design originated in the early 80ies as DC-11 and the aircraft stayed in public discussions well into the mid 1990ies until MDD merged with Boeing. The seating capacity was supposed to be 180 passengers in a dual class layout. The fuselage diameter of 188inch (4.75m) would have allowed a 6- or 7-abreast seating, although the latter at reduced comfort. A sketch is shown in figure 2.9 which is taken from a contemporary aviation magazine [Fli87]. The Boeing concept hinged upon usage of a prop fan, which allowed much better economics. Short boarding times and enhanced passenger comfort are specifically mentioned. The cited article reads:

Figure 2.9 – Cross section of the proposed Boeing 7J7 with 6-abreast twin aisle layout. The cross section had a diameter of 4.75m (188inch). Graphic taken from [Fli87].

"The wide body and twin aisles are the intended key to the 7J7's success. Twin aisles and 2-2-2 cross-cabin seating layout means exceptionally quick loading and unloading (aided by wider-than-standard main doors), and passenger popularity because, as Boeing points out, everyone is next to either an aisle or a window." [Fli87] [p. 78]
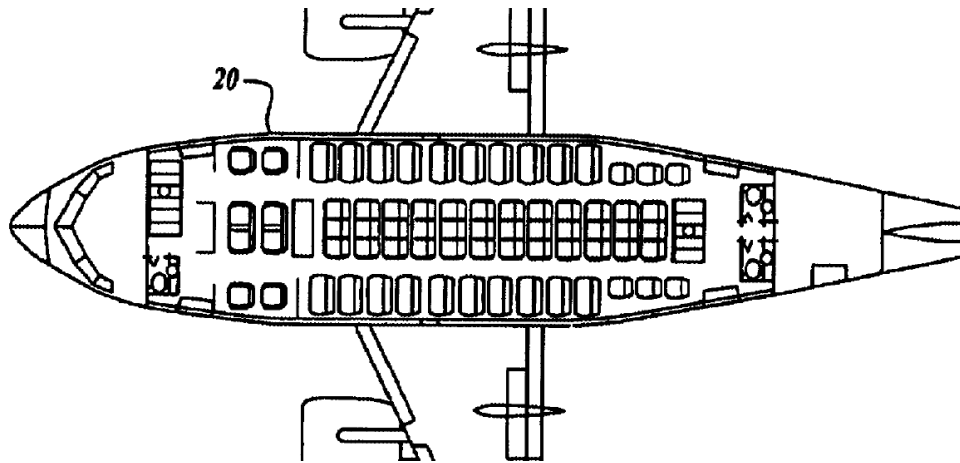
Figure 2.10 – "Twin Aisle Small Airplane" as shown in a 2004 Boeing patent (from [Boe04])

In 2004 a patent was granted for a "Twin Aisle Small Airplane" [Boe04]. Three more patents of the same author were granted which focus on structural aspects of the fuselage. The patent covers specifically twin aisle layouts for aircraft with less than 200 seats. The seat configuration as described in the text ranges from 2-2-2 to 2-4-2. Graphics in the document show two different cross sections of a 7-abreast aircraft: a circular cross section with strong resemblance to the B767 and another non-circular without lower deck cargo compartment. Both low and high wing configurations are shown. The shown cabin layout in figure 2.10 has less than 100 seats. However, patents traditionally use illustrative examples that do not represent actively pursued design projects.

A 5-abreast A320 concept is promoted by a consultant who worked with Carlzon at SAS in the 1980ies [Mue11]. The concept calls for a 1-3-1 seating with different overhead bin layout. An artist impression is shown in figure 2.11. Mentioned advantages are more comfort and quicker loading times. The changes would represent a major change to the cabin, especially as a completely new overhead bin layout is sought. Most claims made in the cited document are not backed by any identifiable investigation. The concept can probably be considered a curiosity.
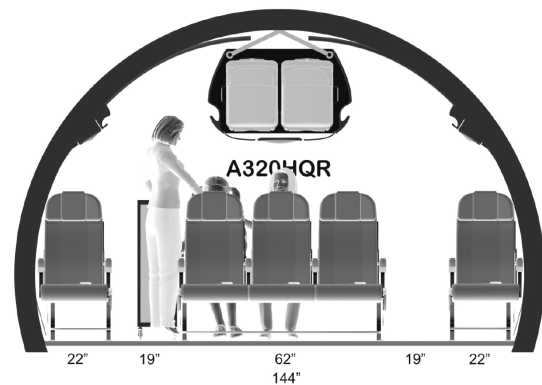
Figure 2.11 – A320 5-abreast Concepts: a concept by the airline consultant Morton Mueller. [Source: Morton Mueller [Mue11]]

2.4 Turnaround Time: Basics, Concepts for Reduction and Literature Review

The reduction of boarding times is attractive for more cost efficient operation. Consequently manufacturers and operators have tried to establish procedures to reduce boarding time. A few other options are considered for future single aisles. The motivation for reduced turnaround time is in-

creased utilization of the aircraft. Secondary motivations are the absorption of delays and reduction in ground handling cost. If shorter turnaround time results in additional utilization depends on the average mission length and the airline schedule planning. Also see section 5.2 on the actual use of saved turnaround time.

2.4.1 Turnaround Basics

When estimating time on ground, the maximum number of daily flights can be calculated under assumption of the daily time of operation. The ground time consists of taxi time, start-up time and turnaround time. The start-up time is the time required for engine start after pushback.

$$t_{\text{ground}} = t_{\text{turnaround}} + t_{\text{taxi}} + t_{\text{startup}} \tag{2.14}$$

$$t_{\text{flight}} = t_{\text{take--off}} + t_{\text{climb}} + t_{\text{cruise}} + t_{\text{descent}} \tag{2.15}$$

The daily operation time is set by the earliest time an aircraft is allowed to take-off and the latest time it is allowed to land. Night operations are not considered as noise restrictions limit the number of available airports. Additionally, most passengers do not want to arrive or depart during night time. In effect, short range aircraft operate from 6:00hrs in the morning to 22:00hrs in the evening, yielding a flight time of 16hrs. Theoretically, the aircraft can do its first take-off at 6:00hrs and can land from its final leg at 22:00hrs. The turnaround between last flight in the evening and first flight in the morning happens during airport closure[6], so that the number of turnarounds is one less than the number of flights.

$$t_{\text{daily\_ops}} = n_{\text{flight}} \cdot t_{\text{flight}} + (n_{\text{flight}} - 1) \cdot t_{\text{ground}} \tag{2.16}$$

Solving for the number of daily flights yields:

$$n_{\text{flight}} = \frac{t_{\text{daily\_ops}} + t_{\text{ground}}}{(t_{\text{flight}} + t_{\text{ground}})} \tag{2.17}$$

The flight time assumes an standard climb and descent and a cruise at optimum Mach number as described on page 81. The used performance model resembles an A320 (see page 78).

In figure 2.12(a) the resulting daily distribution of flight time, moving ground time and turnaround is shown. The graph assumes 45 minute turnaround, which is representative for a current generation single aisle with more than 160 seats except low cost airlines [Boe02]. The start-up and taxi time is assumed as 15 minutes additional ground time, resulting in a ground time of 60 minutes. At 500nm average distance the aircraft spends close to 5 hours in turnaround, has an additional 1.6 hours of moving ground time and spends the remaining 9.4 hours in flight.
The true utilization in 2008 can be seen in figure 2.12(b). The data is taken from a recent report from Eurocontrol [Eur11]. The utilization in short range operation was between 6.5hrs in winter and slightly above 8hrs in summer. It compares to figure 2.12(a), where the theoretical flight times for the first couple of ranges is printed in the figure. "Short Range" is defined by Eurocontrol as being below 1500km (800nm). In summer the practical utilization hence approaches the calculated limit. The reason why the practical is so much lower than the actual are manifold: in winter times many

---

[6]"Closure" refers to air traffic movements.

(a) Utilization

(b) Time
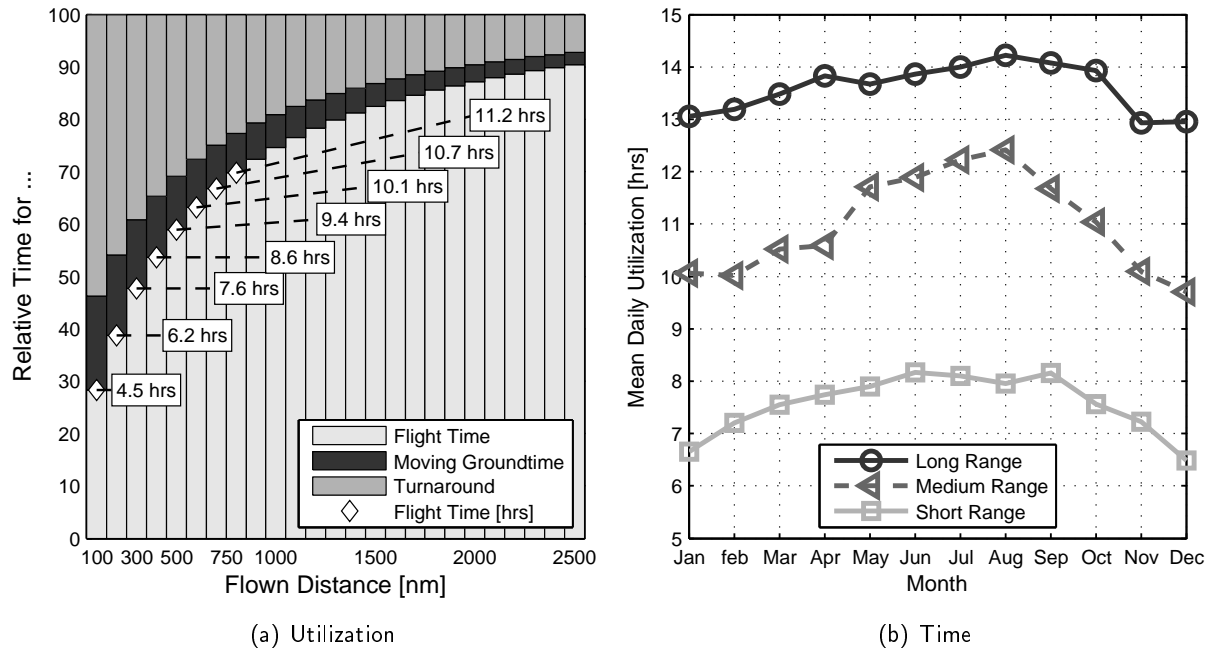
Figure 2.12 – Theoretical and practical utilization. The theoretical assumes turnaround times and a daily flight time of 16 hours. The practical values are sourced from [Eur11].

aircraft are simply not needed. Doganis provides numbers of 8.4 to 11.5 hours per day depending on operator for the A320, and 6.3 to 11.1 hours for the A319 ([Dog10] and table 6.3 and table 7.2)). No average distances are provided though.

Turnaround times can be assessed with simple means. As shown on page 4 the critical path is the sequence of processes that determines the turnaround length. The critical path is determined by a number of dependencies. For example, boarding cannot start before refueling is finished. Cargo loading cannot start before unloading is finished. The cabin cannot be boarded before the cleaning is finished, and the cleaning has to await the full deboarding of the aircraft.

These relationships are shown for two examples in figure 2.14. The example assumes a fixed rate for passengers and exiting the cabin
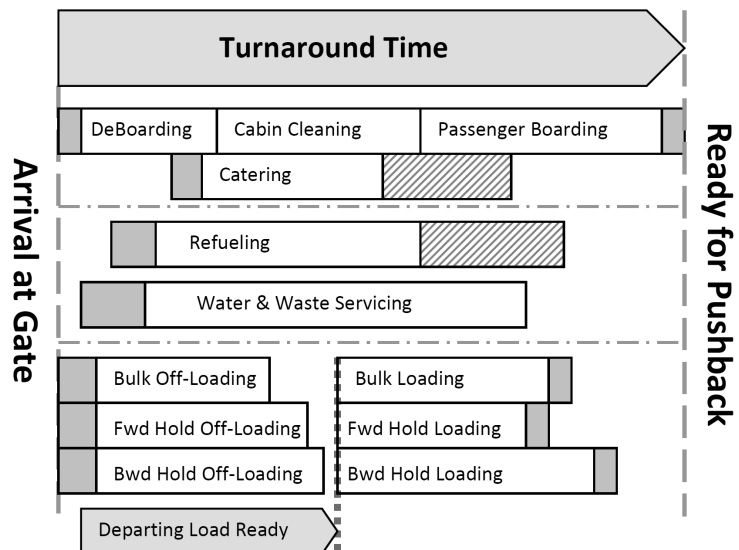
Figure 2.13 – Schematic turnaround Gantt chart. The length of the processes is typical for a short range transport. Horizontal lines depict the different entities.

per minute. The amount of fuel depends on range. 4 out of 5 passengers check luggage, which is loaded and unloaded at a rate of 12 bags per minute. The assumptions for luggage are representative

for short range and domestic operations.

(a) 180 Pax, 1400nm Range

(b) 220 Pax, 400nm Range
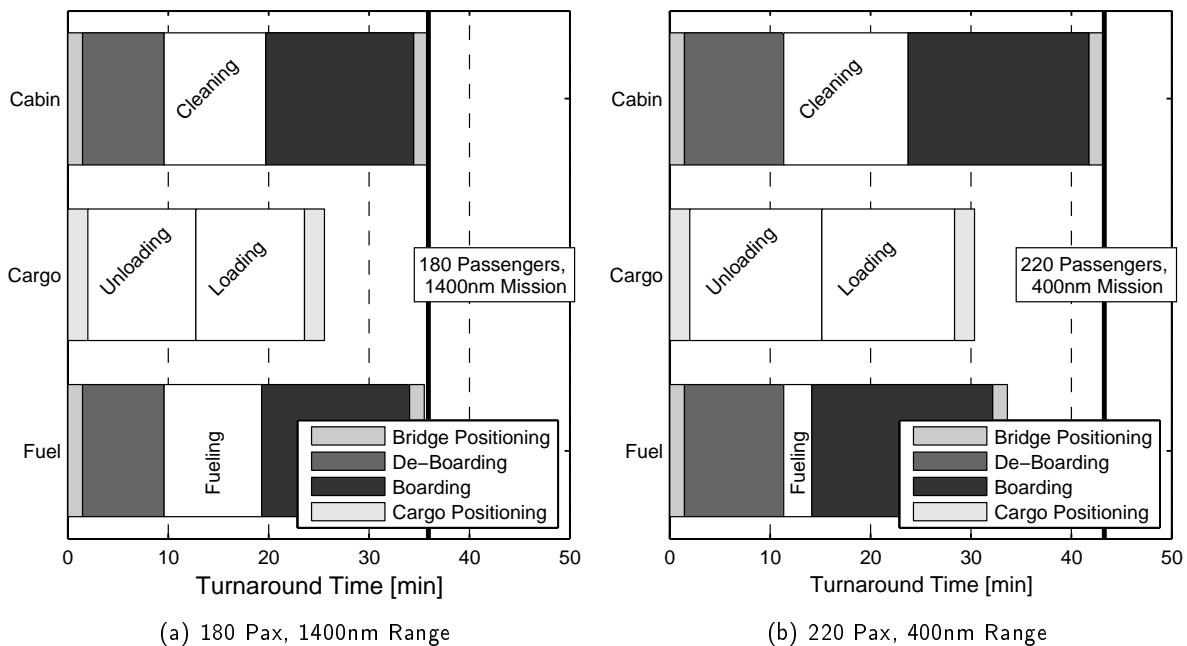
Figure 2.14 – Examples for critical path. The left example assumes a longer range and less passengers, resulting in the refueling process being of similar length as the boarding and cleaning.

The critical path can be formed by the deboarding, cleaning and boarding. Alternatively, the cargo loading can determine the critical path. Finally, the refueling may delay the cabin boarding. It becomes apparent that (under these assumptions) the boarding and deboarding is always located on the critical path.

2.4.2 Operational Concepts, Infrastructure and Changed Aircraft

The so-called low cost carriers use two methods for turnaround time reduction. First, they prefer apron positions and board passengers via stairs. This allows the usage of front and aft door and speeds up boarding and deboarding approximately by 50% (see later analysis). It also removes the need for pushback. Additionally, some do not assign seats at check-in, thus giving passengers an incentive to enter the cabin quickly to occupy an attractive seat. These methods are only partly transferable to traditional network carriers. Apron positions are not well received by passengers, both due to the exposition to weather (both coldness and rain, but also very important in many regions of the world, extreme heat) and the need to use a bus. Both increases inconvenience and problems for people with reduced mobility. Passengers moving freely on the apron is also considered a safety issue. Especially in the United States aircraft are rarely boarded via stairs. The usage of the rear door while using a boarding bridge would require a costly reconstruction of the airport gates. Figure 2.15 shows a possible solution, but retrofitting these at airports would impose considerable cost. Further, airports have little to no interest in reducing boarding or turnaround times as long as they have sufficient gate positions. The usage of the rear door with stairs and the forward with a bridge is practiced by some

airlines at some airports [7]. But at most airports it collides with infrastructure restrictions. It would require substantial changes to the gate waiting areas and the gate parking positions as was confirmed in discussions with Hamburg Airport representatives.
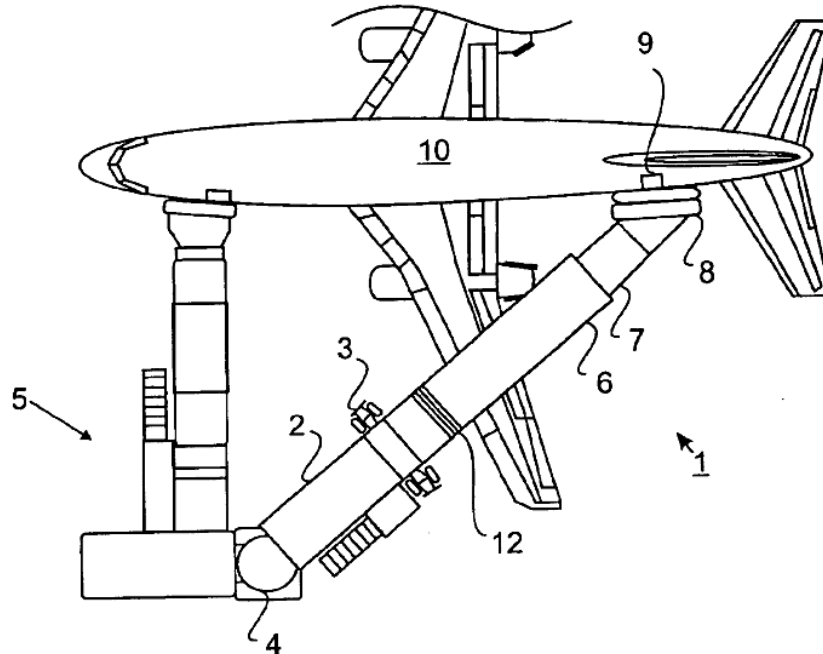
Figure 2.15 – "Flexible over the wing passenger loading bridge" as shown in a 2004 patent from DEW Engineering (from [DEW04]). Besides technical complexity, these bridges also have substantial positioning time and risk for collision with the airframe is increased.

Changes to the layout of single aisles is supposed to bring relief to boarding times. The first option is the usage of a quarter door, a door just in front of the wing root. Most current single aisle only have boarding doors at the very front and aft of the aircraft[8]. This reduces boarding times and is discussed in the result section (starting page 98). A further option is a wider aisle. Traditionally aisles are designed as small as possible. A wider aisle allows passengers to pass and reduces delays. The effects are again shown in the result section (starting page 100). Finally a wider door is proposed as mean for shorter boarding times. However, wider doors only help when the doors are the actual bottlenecks of the process, which is only the case for twin aisles. All these have consequences for the aircraft weight and performance, as discussed the result section (see part 5).

2.4.3 Boarding Strategies

Boarding strategies are sometimes proposed as possible remedy. A boarding strategy is a special sequence in which passenger groups or even individual passengers enter the cabin according to their designated seats. The objective is to reduce the boarding time by reducing the interference between passengers in the cabin. Figure 2.16 provides three examples. A number of studies have analyzed

---

[7] For example, KLM in Amsterdam and Germanwings in Cologne.

[8] The A321 has an optional boarding door in front of the wing root. If not chosen by the operator, this door just functions as emergency exit.

the effect of boarding strategies on boarding time. Their findings are relevant for this work as they identify the major bottlenecks of a boarding process.
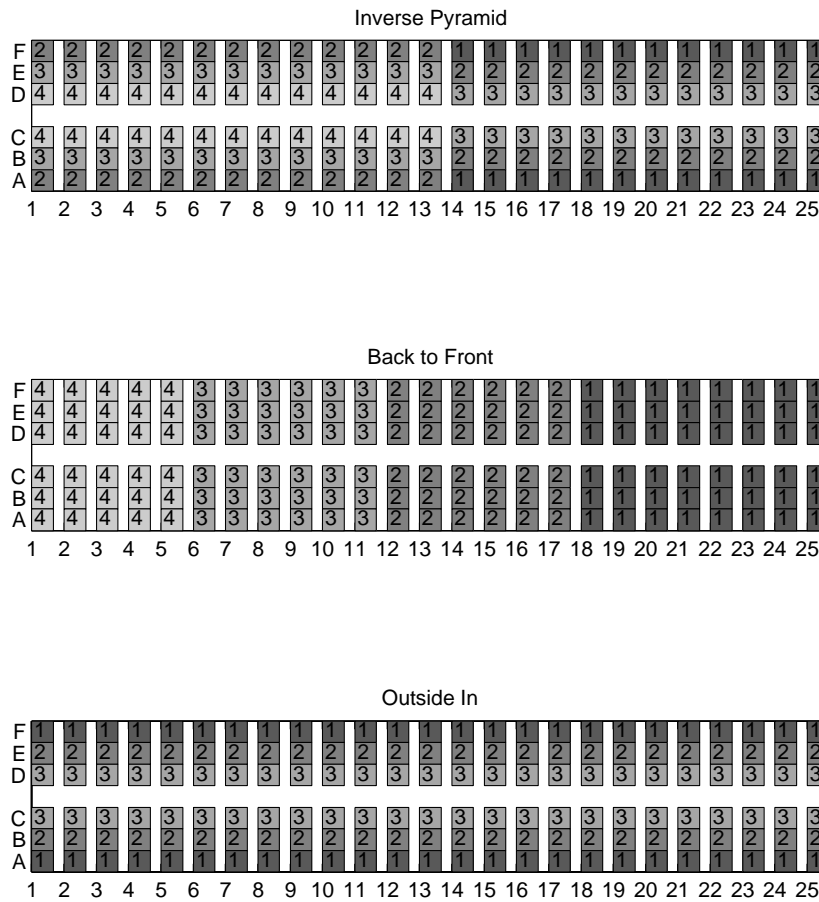
Figure 2.16 – Strategies for single aisle boarding. Note that the shown strategies are simple as only 3 or 4 different blocks are called. More complex strategies like described by Steffen [Ste11] would require all passengers to enter the cabin in exactly the right sequence.

The first known study is from Boeing and was published via the Boeing company newspaper Aero [Mar98]. The article "The Role of Computer Simulation in Turn Time Reduction" describes the attempt to create a boarding simulation. The resources available for the authors were substantial: the simulation was validated using an aircraft and a total of 600 passengers in a dedicated test. The study focused on the reduction of boarding times by usage of boarding strategies. The entire project was apparently triggered by concerns of airlines that the then new B757-300 might suffer from extended ground times. Boeing tried to calm these concerns. Still, the cited boarding times are an important indicator of the simulation performance and are used in the calibration database of this work.

The topic has attracted numerous studies into the question for the optimum boarding strategy [Lan02] [Bri03] [Fer04] [Baz07] [App10a]. Nyquist summarizes the findings of the first four studies in a journal paper [Nyq08]. The early studies focused on rather small single aisles on the lower end of the capacity spread with just 132 seats. The more recent study from the ETH Zurich [Ste10] stands out for two reasons. First the used boarding simulation was developed using filmed boarding procedures. Second, the capacity investigated was close to that of the Boeing study. The findings of the ETH study are consistent with other studies that the main reason for delay during the boarding

is carry-on luggage. Nagel [Fer04] first introduced a bin occupation model to capture the effect of decreasing space in the overhead bins on luggage stowing times.

All studies confirmed that simple boarding strategies are no improvement over the random boarding[9]. The findings are best summarized in [Nyq08]. The strategies that performed best were a boarding sequence by seat [Ste11] [Ste08]. That is, the order specifies exactly when which passenger enters the cabin. This is of course impractical in daily airline business and would be inconvenient for the passengers. A more practical strategy is either the inverse pyramid or inside-out. Some strategies are shown in figure 2.16. The practised back-to-front did not beat the random boarding in the studies (see for instance Nagel [Fer04], but also [Ste08] for a comparison of strategies to random boarding). All strategies require that passengers adhere to them and that all passengers are present at start of the boarding process. The more complicated the strategy, the less robust it is when passengers do not adhere to the sequence (see Steffen [Ste08] and Nagel [Fer04]).

A publication by Tilman Richter [Ric07] focuses on the creation of a boarding simulation using state-of-the-art modeling techniques, namely multi agent modeling and advanced path finding. His techniques are applied for the boarding simulation used in this work. He introduces important concepts such as path-finding and human factors for a boarding simulation. More detail is provided in the boarding simulation description in section 3.2.1.

2.4.4 Comparable Research Studies

The objective of reducing turnaround time sometimes opposes the drive for best cruise performance. Additional or wider doors and a wider fuselage increase mass. Only one work could be identified that performed a trade-off between turnaround time reduction and cruise performance.

The University of Applied Science investigated the reduction of turnaround cost in the project "Aircraft Design for Low Cost Ground Handling" (acronym: ALOHA) [Kra10] [Gom09]. The authors Krammer and Scholz approach is an aircraft designed for minimum ground handling cost and time. Their focus is primarily the cargo handling. Their aircraft design utilizes a continuous lower cargo hold for simultaneous loading and unloading of containers. The resulting aircraft configuration requires a high mounted wing. They further chose fuselage mounted engines for better accessibility of the fuselage by ground handling vehicles. The chosen configuration results in a weight penalty compared to the reference configuration. The aircraft design program PrADO (see [Hei01]) is used for aircraft design including performance and mass estimation. Boarding and deboarding are also considered, however, the approach is to use statistical data to model the boarding time. While this works for the deboarding, the boarding times cannot be re-enacted by regression in the study. A reduction in boarding times is assumed by the usage of different means such as folding seats and quarter door. Twin aisle configurations are not investigated. The conclusion of the project is that the reduced cost of ground handling and time do not compensate the substantial increase in aircraft mass (+15% operating empty mass).

The work offers a number of useful hints for future resarch. The concentration on cargo loading opposes expert statements concerning the driver of turnaround times (also see [Fug01]). It needs to be confirmed that cargo loading does not represent the critical path of the turnaround.

---

[9]"Random" means that passengers have assigned seats but enter the cabin in random sequence.

On the modeling side, the inability to derive any useful statistical model from 170 observed boarding events underlines the difficulty of modeling this process by regression even in the presence of substantial sets of data. Therefore this work relies on simulation rather than regression. A further conclusion is that despite the significance of turnaround time for overall cost, the negative performance impact caused by any measure needs to be small. Otherwise the savings generated through more utilization and less ground handling cost are quickly compensated by additional fuel burn and mass-related charges.

Finally, the increase in empty mass has a profoundly negative effect on the estimated direct operating cost due to the fact that most costs are modeled as functions of mass (pilot salary, maintenance, insurance, procurement, charges). The cost estimation needs to be changed in a way that small differences in size do not result in additional cost that are rather virtual (see also page 111).

2.5 Comfort Considerations

Passenger comfort is important for the product "air travel". Passenger comfort can have different definitions and scopes. In scientific research it usually includes the thermal and acoustic comfort in a cabin environment. In the field of cabin design more factors are included, especially those related to the passenger seat: seat pitch, seat width, head clearance, seat quality. Further the installed service installations per passenger are taken as indicator for passenger comfort.

Single and twin aisle layout offer vastly different cabin products, with the latter being perceived as more attractive due to larger number of attractive seats. The twin aisle offers - at least as 6 or 7-abreast - fewer or no middle seats with the effect of increased personal space for the passenger [Boe97]. This represents an advantage for the passenger, and hence a possible yield advantage for the operator.

Several works have been published that attempted not only to assess passenger comfort, but also to translate it into an equal amount of revenue. The work by Wittmann [Wit06] and Konieczny [Kon01] provide a framework for comfort assessment. It becomes apparent that many factors influence the perceived quality of the product "air travel", and that many are beyond the actual cabin product. Further, depending on the load factor and provided cabin service, the actual level of comfort can vary vastly [Bal09].

Including the factor comfort into the assessment might appear essential, but several reasons lead to the decision to exclude the passenger comfort from the assessment:

- The majority of comfort aspects of the product "air travel" are beyond the layout of the cabin. Cabin service, check-in, delays influence the perceived product quality (see Konieczny).

- Major comfort aspects such as seat width and seat pitch are the same for all researched layouts, hence no difference exists.

- The only real differences between single and twin aisles are the number of aisle seats and the overhead bin volume per passenger. The latter is considered in the boarding simulation, an advantage hence credited through the reduced turnaround time.

- The focus of this work is on short flight times below 2 hours (less than 800nm), which constitute the majority of single aisle flights (see page 1). The priority of cabin comfort when making a

booking decision is far lower than on longer duration trips. Factors such as price or frequency have higher priority.

The number of aisle seats remains the sole true advantage. Assessing this advantage and bringing it in relation to the added cost of operation proved impossible given the existing works on perceived passenger comfort. Further, recent developments in short range transport have shown little to no willingness to pay extra for increased comfort.[Lee04]

It can be stated that a twin aisle offers on average a better and more attractive cabin for the passenger. If and how much this is reflected in added revenues for the operator is not possible to say within the scope of this work.

Chapter 3

Description of Applied Methods

The analysis is performed with a number of different methods. These can be grouped in two major branches: the aircraft modeling and the turnaround modeling as shown in figure 3.1. Both utilize the results of the initial fuselage and cabin design. All tools are closely connected, sharing information and building on results of the previous ones as shown in the figure. The mission performance and the turnaround analysis each produce results that are then condensed in the final cost estimation. However, the individual results are also valuable as they answer questions raised in the motivation. In particular, which aircraft is the best in pure flight performance (mission fuel burn) and which aircraft has the best turnaround times.
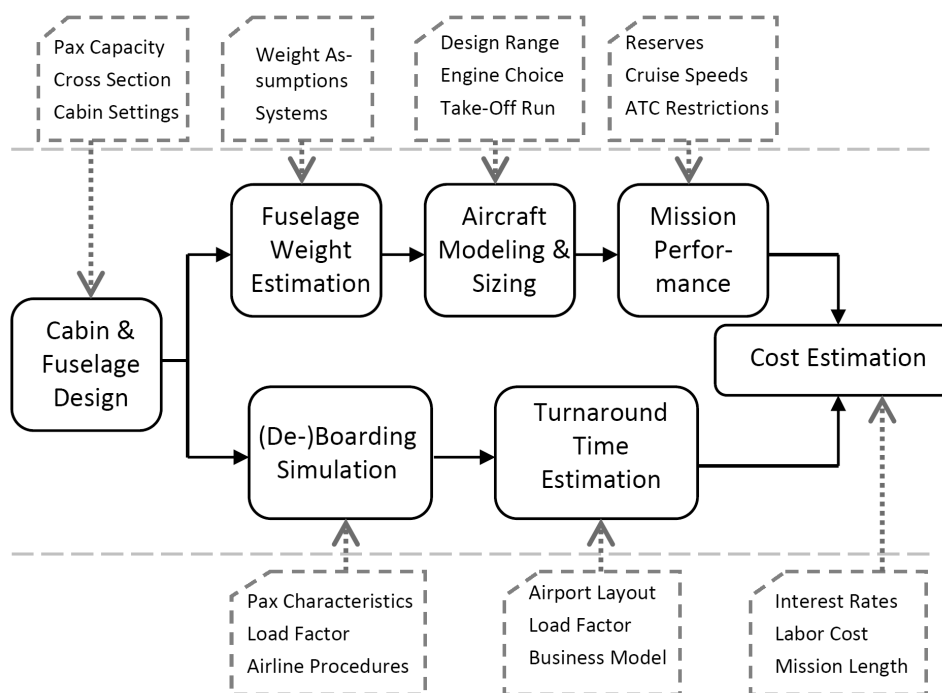
Figure 3.1 – Tool Chain Schematics

The common start for both branches is the cabin and fuselage design tool. It creates the cross section, the fuselage geometry, the cabin layout and multiple parameters connected to the fuselage and payload accommodation. On the aircraft design branch of the tool chain the fuselage mass estimation comes first. The fuselage mass estimation is essential to analyze the relative disadvantage of an aircraft utilizing a different fuselage for a similar capacity. Therefore a tool using a physics-based

model with statistical calibration was developed and is described in section 3.1. The aircraft sizing matches wing, tail and engine to the mission requirements like take-off length and reserve fuel. The process includes aerodynamic and engine modeling. The tool described in section 3.3 uses an error minimizing feedback loop to adapt the wing size to the design range requirement. Most masses are estimated using newest statistical formulas. The mission performance and cost estimation are closely linked, the only addition is the final turnaround time.

On the turnaround branch of the tool chain the boarding simulation is the dominant feature. It is described in detail in section 3.2. Its output is used to determine overall turnaround time. The critical path is either defined by the passenger process time or other items of the turnaround process. The turnaround time as function of various input parameters is passed to the cost estimation tool.

The data management is simplified by the fact that all tools run within one software environment. Data is passed from the workspace into the individual tool, with the workspace functioning as virtual data base. Interfaces are arranged in a way that data exchange is minimized. All tools are programmed in Matlab. Matlab supplies a straight-forward environment for programming and facilitates debugging. Further on, it provides a vast number of existing low level functions. The speed of execution is less than for other programming environments. However, in science the time required for tool development usually far exceeds the time actually spent for tool operation. Therefore a programming environment that trades higher performance for easy development is better suited for the challenges faced in this work. While boarding simulation and aircraft design could be coded very efficiently, the cabin and fuselage layout requires a large number of lines of code due to the large number of conditional decisions.

The process times are between 10 and 20 seconds for the initial fuselage and cabin design. The process time of the aircraft sizing depends on the number of iterations. With a reasonable starting point for the sizing, the sizing converges within 1 or 2 minutes. The mission analysis requires the creation of an performance database which takes a couple of minutes. The turnaround analysis requires longer times as different scenarios need to be investigated. For each cabin layout there are two basic scenarios plus a parameter sweep, putting the number simulations per cabin layout at approximately 150.

3.1 Fuselage and Cabin Design

The fuselage design is the starting point for both the aircraft design and the boarding and tunraround simulation (see figure 3.1). The objective of this work is to analyze the effect of different fuselage layout for similar mission requirements, so the fuselage layout is of major importance. This section describes the fuselage and cabin design process from definition to final mass estimation. The latter part is given more detailed description as it directly influences the findings of this work. Basic rules of fuselage design are already explained in 2.2.

Specific tools for cabin layout exist. However, these are merely advanced CAD solutions that offer knowledge-based features for quicker cabin design. The commercial program Pacelab Cabin offers a cabin design environment, which can be considered an enhanced CAD tool [PAC12]. It has some automation features, but on the downside requires substantial effort for definition of a new fuselage. Fully or partly automated solutions are not available as commercial product.

3.1.1 Fuselage and Cabin Design Tool

The objective of the tool is the generation of a complete fuselage layout from a basic set of inputs. These shall be limited to not substantially more than fuselage length and cross section information. The cross section is defined manually by adjusting the fuselage width, height and height of the floor. This is necessary as engineering judgment is required for the choice of a reasonable cross section. For each seat abreast configuration there are only a limited number of combinations.

The process is shown in figure 3.2. The program differentiates between normal parameter settings and global settings. The normal parameter settings are for a single type of fuselage and cabin. Fuselage length, diameter, or class standards are

Figure 3.2 – Process Chart of Fuselage and Cabin Design

defined here. The global settings control many major and minor aspects in the program, like geometric allowances. Global settings define - for example - the assumed thickness of a class divider, which is the same for each aircraft. The global parameter settings affect the entire program, and are far more numerous than the specific parameter settings. Many global settings can be overruled by user-defined parameter, for example the relative length of the constant section of the fuselage.

The different functions are run in sequence. The feedback loop is closed by the user, who has to decide whether the resulting cabin fits his expectations. Engineering judgment and experience is important to assess if a cabin design is reasonable or needs refinement. For example, it might be necessary to adjust the monument layout or shift an exit. The tool still achieves a significant

automation of the fuselage and subsequent cabin layout, but allows the user to influence at selected instances. Full automation of the cabin layout process requires a strong restriction in the complexity of the layout, or results in poor seat, door and monument layout. A simple widebody cabin with 4 exit lanes (like A330 or B787) already offers several thousand different combinations of monument locations. An approach described by Metzger [Met08] achieves respectable results, but still has issues in reasonable placement of monuments and class boundaries. Similar challenges were encountered, but could be overcome or avoided. Monument placement proved to be a particular challenge.

Fuselage Geometric Design

The fuselage external geometry is defined by the height and width of the cross section. If no specific shape of the cross section is defined, an elliptic[1] shape is assumed. This is a valid assumption if height and diameter are within 10% of each other. In the scope of this work only elliptic cross sections are used, as other cross sections would exceed the validity of the statistically calibrated mass estimation. The elliptic form with closely matching height and width result in a stress-optimal cross sectiuon layout for pressurization, which size the majority of the fuselage (see page 42 onwards). The shape in the x-y and x-z plane is defined as shape preserving spline using a number of characteristic points. The fuselage is defined by a sideline, an upper line and a lower line. The start and end of the constant section can be defined, as well as the rear fuselage upsweep and forward fuselage downsweep. Most parameters have default values that are consistent with values found on current generation aircraft, mostly in line with the A320. This also is necessary to retain consistency with the methods used for fuselage aerodynamic drag assessment. Structural items like frames, stringers and bulkheads are placed using knowledge based design rules. For the subsequent mass calculation the detailed structural layout is not required. The frame longitudinal locations are important as reference system throughout the design process. Doors and frames are shifted in order to match each other if possible. Windows are located between the frames. In figure 3.3(a) the basic structural layout of the forward fuselage of a twin aisle is shown.

(a) Fuselage Structure   (b) Monuments Placed
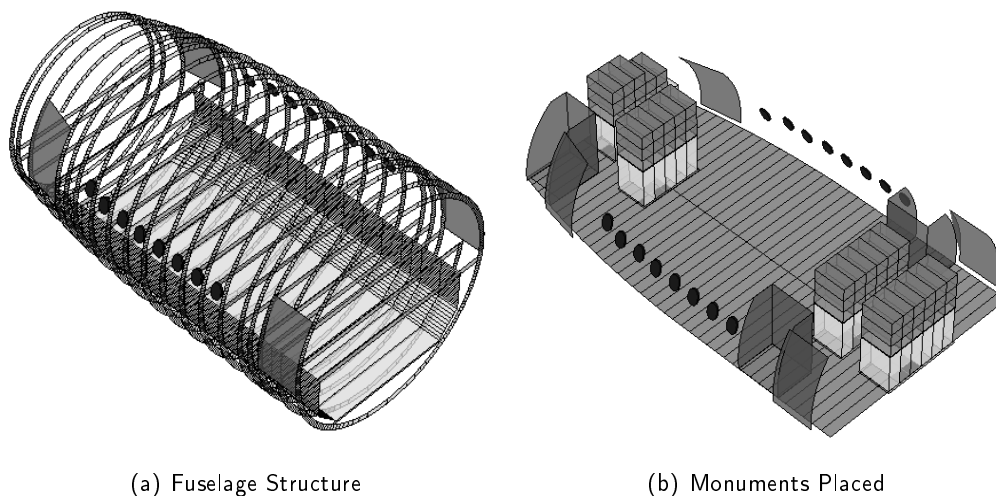
Figure 3.3 – Initial cabin design: fuselage primary structure (left) and monuments (right).

---

[1]A circle is elliptic, too.

Cabin Design

The cabin design starts with an estimation of the number of passengers based on floor area. The number is used to estimate the number of required galleys and lavatories. The galleys and lavatories are then placed in the cabin. The galleys are placed first and the location is optimized to have minimum distance between the galley and the passengers in the cabin. Monuments are exclusively positioned at exit lanes, and if possible only at lanes with service doors (in opposition to pure emergency exits). The forward and rear galley are customized in respect to the fuselage diameter, with wide bodies getting either a D-shaped or U-shaped galley arrangement. Lavatories are placed after galleys are located. The positioning is carried out along knowledge-based rules, means the locations are based on observations of actual cabin layouts. No documented rules exist where to place such monuments, but in practice they are often grouped and used to generate cabin sections. When observing actual and historic cabin layouts, it becomes apparent that current standards are equally applied at both major manufacturers, and that exotic solutions are only applied where necessary, usually in long range cabins with large first and business class. In figure 3.3(b) the cabin with monuments is shown.

(a) Seats and Monuments

(b) Entire Cross Section
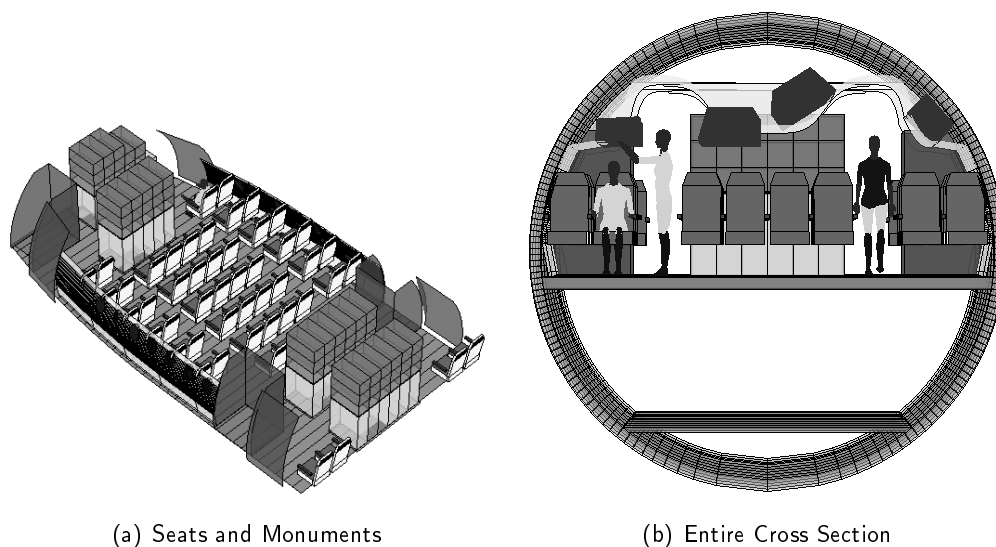
Figure 3.4 – Final cabin process: placing of seats (left) and overhead bin layout (right).

Class boundaries are located in an automated way, which is difficult and sometimes results in unreasonable layouts. Single class cabins are not affected by this. The seats are placed after all monuments are fixed in their position. The seating algorithm places seats in all available spaces within the aircraft, which are not blocked by either monuments or are reserved for exit lanes and aisles. The seat pitch is adapted if surplus space exists, at rear and forward end of the cabin the seats abreast are adapted if required, shown in figure 3.4(a). The final cross section shown in 3.4(b) contains all necessary information for further analysis. The size of the overhead bins is of importance for the later boarding simulation. They are modeled using knowledge-based design rules. Space allowances for passenger service units (which contain the reading lights and individual air outlets) are considered, the remaining volume is used to best effect for luggage bins.

3.1.2 Structural Mass Estimation

The mass estimation is very important as it has a high-ranking impact on the results of this work. The key argument against a twin aisle small capacity aircraft is the increased empty mass. Therefore an accurate way of predicting the fuselage's mass needs to be found. The mass estimation is not limited to the structural mass only. Of the entire equipped fuselage mass, only slightly more than 50% are contributed by structure. The remainder are systems, seats and monuments, and furnishing and lining. Especially the latter add considerable mass.

The structural mass estimation is done using an analytical approach calibrated with statistical data. This semi-analytical method was developed and published by NASA and adapted for this work [Ard96]. The approach was chosen after fully physics-based approach using finite element modeling did not yield the desired results. As FEM based solutions might be considered more appropriate for this work, the reasons for discontinuing the FEM are briefly explained. The semi-analytical approach is favored over pure statistical methods. The detailed fuselage layout offers a wide number of parameters that would remain unused with a statistical tool. I. e., information exists that allows a better understanding of the stresses on the fuselage.

Finite Element Modeling

Finite Element Modeling (FEM) represents the state-of-the-art in modeling of large and complicated structures. Progress in computational performance and easier interaction between different tools enable to do FEM of larger structures on desktop computers with a high level of automation, especially in modeling. A high fidelity mass estimate could theoretically be achieved using a finite element model in conjunction with a sizing algorithm [Nag06]. Figure 3.5 shows an element view (left) and a stress result view (right) of the center section of a single aisle fuselage. The spot for the center wing box and the main landing gear bay are visible. The shown models were generated using the presented tools for fuselage layout and an interface between Matlab and ANSYS, an established software for structural analysis [ANS12].

(a) Elements   (b) Stress
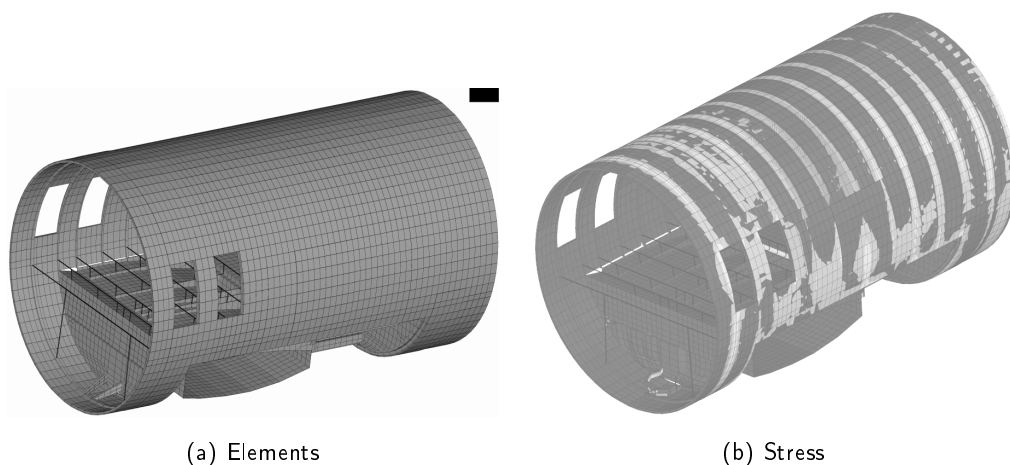
Figure 3.5 – Element and stress view of finite element model of center fuselage. This model was developed for mass estimation but discarded due to unsatisfying results.

A similar approach was executed in a work by C. Österheld [Oes03], although her focus was the entire aircraft's structure. Further, the fuselage was described in a rather generic fashion with only limited attention to detail. In scope of this work a more detailed modeling was attempted using ANSYS as solver. The implementation was similar to that described by Nagel [Nag06]. However, the execution led to major challenges, which could not be overcome in due time. While constant section barrels can be sized with relative ease, the load cases and detailed modeling required for the entire fuselage structure exceeded the complexity of the available design data. The more detailed calculation with FEM requires that the structural arrangement fits the load paths, otherwise the structure becomes far heavier than necessary, and the quality of the mass estimation is not better than with a statistical formula. Further, the calculation time for a full fuselage becomes prohibitive for a preliminary design project.

The idea of using FEM for mass estimation was consequently abandoned. However, the general concept remains valid and might yield a better result when fully validated, more information can be found in [Sch11]. For this work a different method was used, which delivers equally reliable results. Best practice in current fuselage mass estimation are methods that combine multiple entities, consisting of different methods for different mass entities of the fuselage. Such a method is FAME-F[2] of the Airbus preliminary design group [Sch97].

Statistical Methods

Statistical (or empirical) methods are the common practice for mass estimation in preliminary design. They offer good results and require limited input data. They are usually quick and robust. Statistical methods take the known masses of several aircraft designs and identify parameters that influence the design. Apart from pure geometrical parameters (length and diameter), these may include differential air pressure, design speeds and the maximum take-off mass. The fuselage mass is influenced by the overall layout of the aircraft, for example if the engines are located at the fuselage. The opposite of statistical methods are physics-based methods. Statistical methods are limited in accuracy, deviations of 10% in either direction are considered a good result. Many physical parameters are not considered, and the applicability of a statistical formula for a given problem needs to be thoroughly checked.

For this work most features of the individual aircraft remain unchanged for all different layouts, only the relationship between fuselage length and width changes. Nearly circular cross sections have been chosen. All designs have similar general configurations and major design parameters are in line with existing civil jet transport aircraft. Therefore a number of statistical formulas are applicable for mass estimation. Three formulas were considered for this work, based on an assessment of several formulas [Ber09].

1. The Torenbeek method described in [Tor76]. It is based on rather old statistical data (the book was first published in the late 1970ies). Its accuracy is limited as the mass is based primarily on the fuselage surface. The regression parameters are chosen to reflect a wider range of different designs, for example also propeller-driven aircraft.

2. The Howe method described in [How00]. This more recent method limits the inputs to dif-

---

[2]FAME-F is short for "Fast and Accurate Mass Estimation - Fuselage".

ferential pressure and some geometrical inputs. It achieves a good result especially for smaller aircraft (single aisle). But as shown on page 20, the method does not capture the physics quite well as single aisle fuselages always remain those with lowest mass.

3. The most recent method is the new LTH (Luftfahrttechnisches Handbuch) method [Dor11]. Based on a large number of commercial aircraft designs above 40t maximum take-off mass it achieves a good accuracy with pure geometrical parameters. Formula and exemplary results are given on page 20.

The methods chosen for comparison are the 2nd and the 3rd. The results for a number of theoretical designs are already presented on page 21. Although the LTH method performs on average better than the Howe method, it does not beat it for all relevant designs. The Torenbeek method comes out worst of all three with considerably higher deviations when applied to today's commercial aircraft designs. However, it was used in studies with comparable objectives [Nit10]. The mass estimation is central for this work, so that more accurate solutions were sought. A seemingly more detailed method proposed by Torenbeek called the "Mass Penalty Method" is frequently used for fuselage mass estimation (for example in [Met08]). It was implemented but did not achieve an acceptable match. Although the method appears promising, detailed design data of several aircraft designs is necessary to fully validate its calculations. Comparison to the data provided in [Bau03] (see figure 3.7) did neither achieve a particularly good match of the individual components nor of the overall mass.

Adapted Semi-Analytical Method

As outlined in the previous paragraph, the opposite of statistical methods are physics-based methods. These can be separated into numerical methods and analytical methods. FEM for instance represents a numerical method. Analytical methods are the base of any physical model, however, a structure like a fuselage is too complicated too describe it with a single physical relationship. It is possible though to describe certain characteristics with physical relationships and hence create a reduced analytical model of the fuselage. In order to obtain valid masses, the results are calibrated with data of existing aircraft. A calibration is required for most physics based methods, even those of higher complexity. This approach assumes that the difference between obtained mass and actual mass is proportional.

In a NASA technical report Ardema [Ard96] published a method that allows to calculate the fuselage mass using simple parameters and calculating the stresses for each fuselage station. The method is 1-dimensional and based on beam theory. The fuselage is divided into stations along the longitudinal axis. Each station is characterized by a radius and by local forces acting on that station, for example local masses or tail lift. Using formulas for circular shell and factors for the structural concept, the method considers three stress types:

- Axial forces primarily by fuselage mounted engines (not relevant in this case).

- Bending forces being caused by maneuver loads.

- Pressurization loads.

Each force is translated into a normal stress on the individual station. The station-wise calculation allows to take into account the length of the actually pressurized fuselage. Different load cases are

applied to generate forces on the different fuselage stations. A load case is a set of environmental parameters. The most important parameters for the fuselage are the vertical acceleration and the differential pressure between cabin and atmosphere. Two major load cases have been identified.

– Pitch-up maneuver with $2.5\mathrm{g}$ at normal cabin pressure.

– Level flight with normal pressurization and $1\mathrm{g}$.

The chosen load cases are in line with a brief overview of critical load cases given by Niu [Niu88], page 388. Lomax [Lom96] cites similar design load cases for the fuselage. Some often relevant load cases cannot be implemented into such a method, for example local damage tolerance (bird strike) or ground loads. The forces of the load case are translated into stresses in the material. With material stress limits a minimum shell thickness can be calculated.

The first load case is a static design load case and is multiplied with a safety factor of 1.5. Additional static design load cases as shown in [Lom96] did not yield additional stresses, so that they were omitted. As the method is 1-dimensional, it does not differentiate between the part of the fuselage shell where the load is acting. Lateral load cases consequently do not exceed the stress level caused by the pitch-up maneuver. The second load case is a fatigue load case. That is its stress level is relevant not for the static strength of the material but the resistance against cracking and crack propagation over the lifetime of the aircraft. A current generation short and medium range aircraft is usually certified for 50000 cycles. During this time no fatigue damage should occur on the aircraft, and if it occurs a minimum residual strength has to be be garantued. The effect of this requirement is best reflected by applying lower allowable stresses than the material can handle in a static case. The factor can be found in material-specific diagrams in dependence on the number of cycles. The statistics used to estimate this factor can be found in [Niu88], page 538ff.
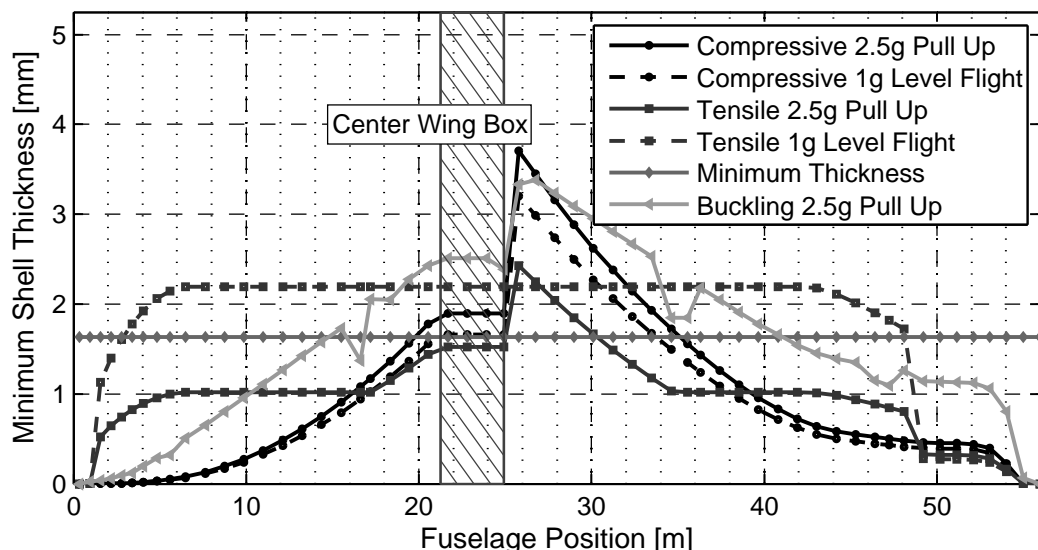
Figure 3.6 – Required shell thickness for several load cases. The straight line at 1.6mm represent the minimum gage thickness. The majority is sized by the 1g fatigue loads (Tensile 1g Level Flight) except the area behind the wing, which is sized by maneuver loads (Compressive 2.5g Pull-Up).

Each load case generates a minimum shell thickness to withstand each of the stresses. The highest thickness defines the local thickness as it represents the required amount of material to withstand

the critical load case. A minimum gage thickness is applied as the shell thickness cannot be chosen indefinitely thin. This approach binds the results to some extent to the surface area of the fuselage, similar to most statistical methods. The mass of the frames is estimated as fixed function of the shell thickness. In figure 3.6 the results are shown for a normal fuselage. The loads are partly caused by the inertia forces of the masses inside the fuselage, which requires a more detailed determination and positioning of non structural masses in the fuselage (see section 3.1.3). In order to capture the inertia effects by the structural masses itself, the process is iterative. It converges quickly after three repetitions.

As can be seen, most of the fuselage is sized by pressurization. The area behind the wing is sized by maneuver loads. This is consistent with findings by Oesterheld using more sophisticated tools [Oes03]. In a published work concerning the Airbus fuselage mass estimation tool FAME-F a similar load case distribution is shown [Kei02]. Some parts are sized by minimum shell thickness. While in some parts of the fuselage skin serves more an aerodynamic than a structural purpose, the dominance in this example is due to lack of load cases in those areas.

In order to capture the effect of additional and larger doors the door mass is modeled explicitly. The mass of doors is calculated using their surface area and multiplying it with a unitary mass taken from an LTH publication [Hie97]. The approach still strongly simplifies the complex art of installing large doors into pressurized fuselages, but offers better accuracy than a method that ignores the doors completely.

Calibration
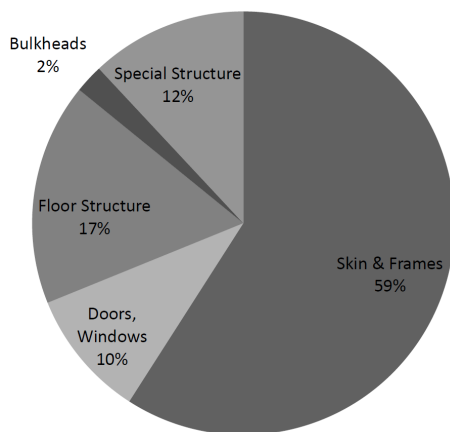
Figure 3.7 – Relative contribution to fuselage structural mass. Reproduced from an LTH paper by Baur (see [Bau03])

The calculation via the presented method results in an unrealistically low mass. This hovers around 35-40% of the actual structural mass (see figure 3.8(a)) as defined in [Air08]. This is a common problem of all methods, even the more sophisticated finite element methods [Pin82]. The method only sizes the shell of the fuselage, which carries bending and pressurization loads. However, in reality only a part of the fuselage mass is caused by these structures, usually between 55% and 70% of the structural mass. In figure 3.7 the different contributors are shown for a conventional wide-body aircraft. Source is another LTH publication [Bau03]. The presented method (and likewise some more sophisticated methods) would only calculate this mass. But even this is difficult as in reality many design requirements increase the mass from the theoretical optimum (therefore these are sometimes referred to as "non-optimum factor"). These are windows, cut-outs, joints and manufacturing considerations [Niu88]. Additionally, not all sizing load cases are captured.

However, it is assumed that the calculated mass by the method is proportional to the real struc-

tural mass by a constant factor. In order to obtain the calibration factor, the method is used for estimation of the structural fuselage masses of known aircraft. The result is compared to the known actual mass. In figure 3.8(a) the calculated masses by the tool are compared to the actual fuselage structural masses of current civil transport jets. The numbers are normalized. The calculated mass is between 30 and 45% of the actual masses.
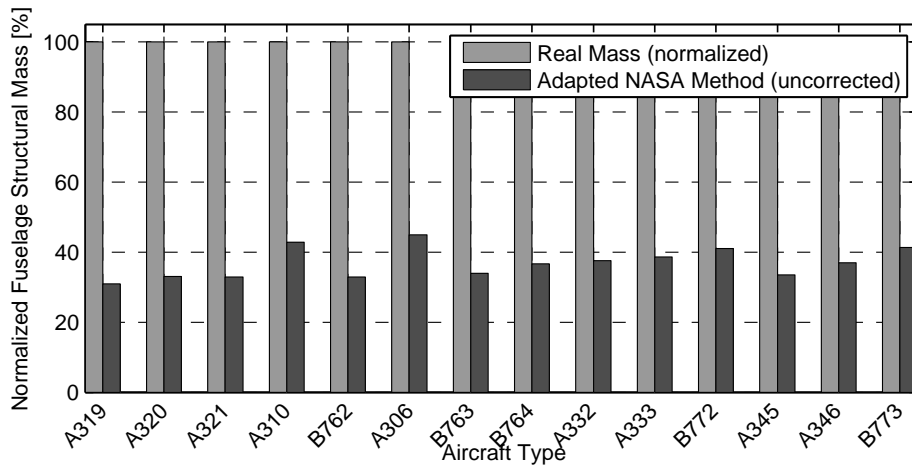
(a) Basic Result
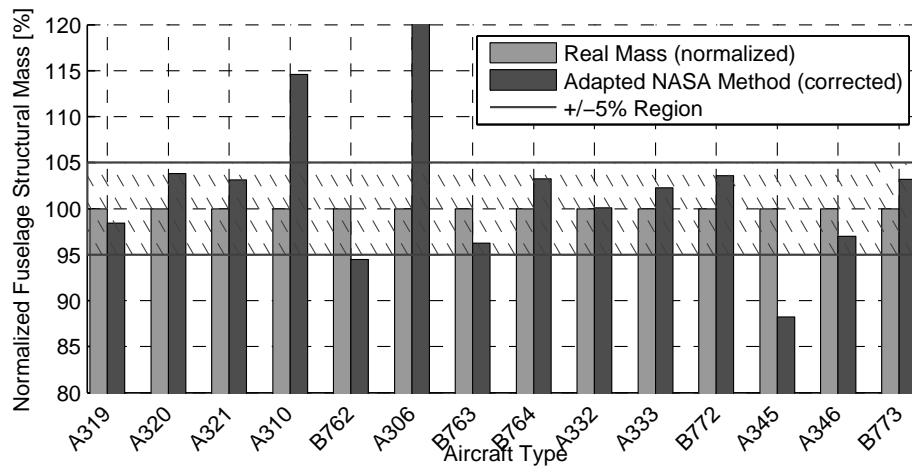
(b) Calibrated

Figure 3.8 – Result of structural mass estimation. Left the basic tool result, right the calibrated result. Only three aircraft are far outside the +/-5% region.

The author of the method used a constant correction factor. Additionally, his database is dominated by older aircraft designs with quite different fuselage layouts. Using only a single or two designs would likely lead to misleading results. The calibration gets better if a larger number (14 overall) of aircraft of similar technology level are used for calibration, and if the aircraft chosen for calibration are similar in configuration to those analyzed in this work (low wing, wing-mounted engines). For this work a number of masses of more recent aircraft were available, which greatly helped to boost the accuracy of the calibration compared to the original. Therefore a physical parameter was identified that influenced the calibration factor. The best factor found is the fuselage diameter. It was found

that the deviation increases when fuselage diameter decreases. Probable reasons are different sizing load cases and a heavier floor structure. The door mass is subtracted from the mass of the original data for the calibration to account for the number of doors separately. The final structural mass is calculated as shown in equation 3.1.

$$m_{Fuselage,structural} = m_{Fuselage,estimated} \cdot \left[f(d_{Fuselage}) + const \right] \qquad (3.1)$$

When applying the correction factor the structural fuselage mass is better matched. In figure 3.8(b) the calibrated results are shown. The method underestimates the mass for some designs, especially on the A340-500 [A345]. This particular aircraft has a fuselage with design features similar to its longer peer (the A340-600 [A346]) and hence carries a small mass penalty. The A300-600 [A306] and A310 are estimated to be heavier. This is partly explained by different mass accounting: the forward and rear main frames[3] are accounted in the wing for this aircraft models [Air08].

The motivation for adaption of this method is the desire to increase the accuracy of mass prediction over best currently available statistical formulas. Further it is intended to have at least some physical relationship between length and width of the fuselage, and the resulting structural mass, as some capacities result in very long and thin fuselages. Figure 3.9 shows the used method (Adapted NASA Method) compared to the two statistical formulas. The average offset of the adapted method is 5.7%. The LTH method has an average offset of 10.3%. The Howe method has 10.4%. Both statistical methods achieve very useful results considering the limited amount of required input data. However, the introduced method allows much better accuracy, especially when the focus is on aircraft with the ubiquitous low-wing configuration with wing-mounted engines. Most aircraft are within 5% of the original, an accuracy which is difficult to match using even more advanced methods (for example [Oes03] or [Sch97]).
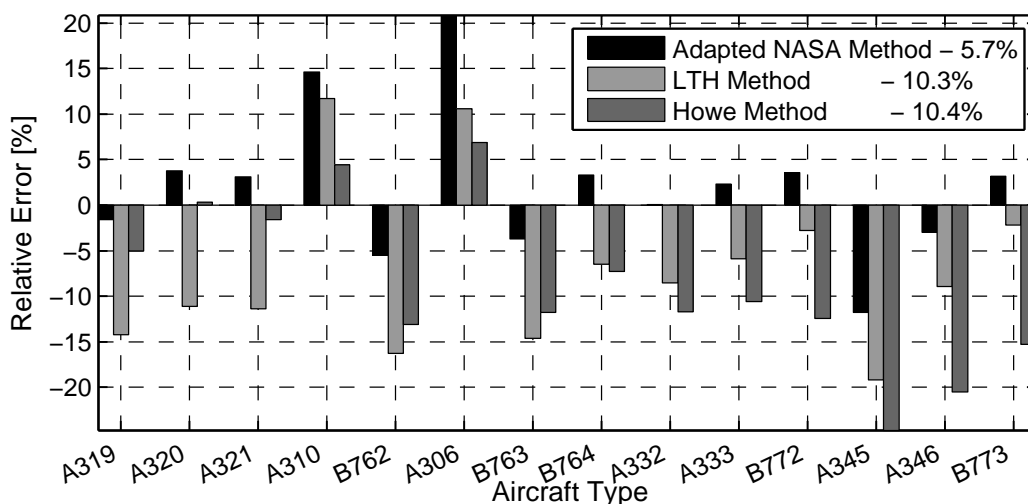
Figure 3.9 – Comparison of the relative error of different structural mass estimation methods. The percentage number gives the average absolute offset from the real structural mass.

---

[3]These frames introduce the wing loads into the fuselage and have substantial mass

3.1.3 Non-Structural Mass Estimation

The previous section dealt with the structural mass of the fuselage. However, the structural mass only contributes about 50% of the final empty equipped mass of the fuselage group. The mass of the equipped fuselage is - besides the drag contribution - one of the central drivers of a twin aisle's performance compared to a single aisle. Therefore a better understanding of the mass items apart from the pure structural mass is required. This work follows the Airbus Mass Standard as given in [Air08]. That differentiates between 5 major mass groups by functional means, not by location. The fuselage comprises elements of the mass group structures, systems, furnishings and operator items. The structures are dealt with in the previous section. About two third of the systems are located in the fuselage. The main landing gear bay, which contains many hydraulic systems, is included in the fuselage (while the landing gears itself are a separate entity). Furnishing and operator's items are nearly completely located in the fuselage. In the following the contributors from the three final mass chapters are explained separately.

Systems

All design textbooks have formulas for aircraft systems mass. Using breakdowns like provided in [Tor76] or [Hue98] an approximate separation by location can be achieved. Raymer provides formulas for system mass estimation of individual systems [Ray92]. Some systems are entirely located in the fuselage. These are the auxiliary power unit [APU], the environmental control system (often referred to as "air conditioning"), all avionics and electric generation[4]. Systems like electric distribution, hydraulic systems and fire protection are partly located in the fuselage[5]. Flight controls are located outside the fuselage. Overall about two thirds of the system mass is located inside the fuselage. Several authors have offered approaches for a detailed system mass estimation, but fuselage and cabin design does not provide sufficient data for such elaborate system analysis [Dol07] [Koe06]. Raymer's methods are often used for system mass estimation. In this context they do not yield an advantage as only few of their parameters are linked to the fuselage design. Hence, they would not produce meaningful differences between aircraft of similar capacity (and comparable mass) but dissimilar fuselage design. The formulas are apparently based on a NASA report, of which the most recent aircraft is a B747-200 [Bet77].

The LTH [Dor11] offers a formula with reasonable accuracy for system mass estimation based on recent aircraft. The average deviation is 6.7%. Although other textbooks offer formulas for individual systems, the statistical database and mean error is unknown. In this work a part of the system mass is calculated using the LTH formula. Other systems with strong connection to fuselage size are modeled separately. These are the environmental control system and electric distribution. For these systems regression formulas are used that have been developed using mass statements of several aircraft consisting of in production single and twin aisle designs. Electric system apart from the distribution is considered no function of fuselage size but rather number of passengers.
The environmental control system (including all distribution ducts) is a major contributor of mass. Furthermore, it scales both with the pressurized volume and the number of passengers. It could be found that the mass of the environmental control system correlates best with pressurized volume. However, the fitting line needs to be separated into single aisle, small twin aisle and twin aisle to account for size effects of the fuselage. The resulting relationship can be seen in figure 3.10(a).

---

[4]The Airbus mass standard allocates the generators to the power units.
[5]The main landing gear bay is not considered part of the fuselage in this context.

For electrics similar a relationship with cabin area has been found. However, the correlation is weaker than that shown for the ECS. Only some components of the electrical system scale with fuselage size, mainly the electrical connections. Main scaling parameter is the required electrical power.

The avionics do not scale with any parameter, which is understandable given that each aircraft is equipped with similar radio and navigation systems. Overall, the mass of most systems scales mostly with number of passengers and take-off weight, and is not influenced by the number of aisles.

(a) Environmental Control System

(b) Furnishings
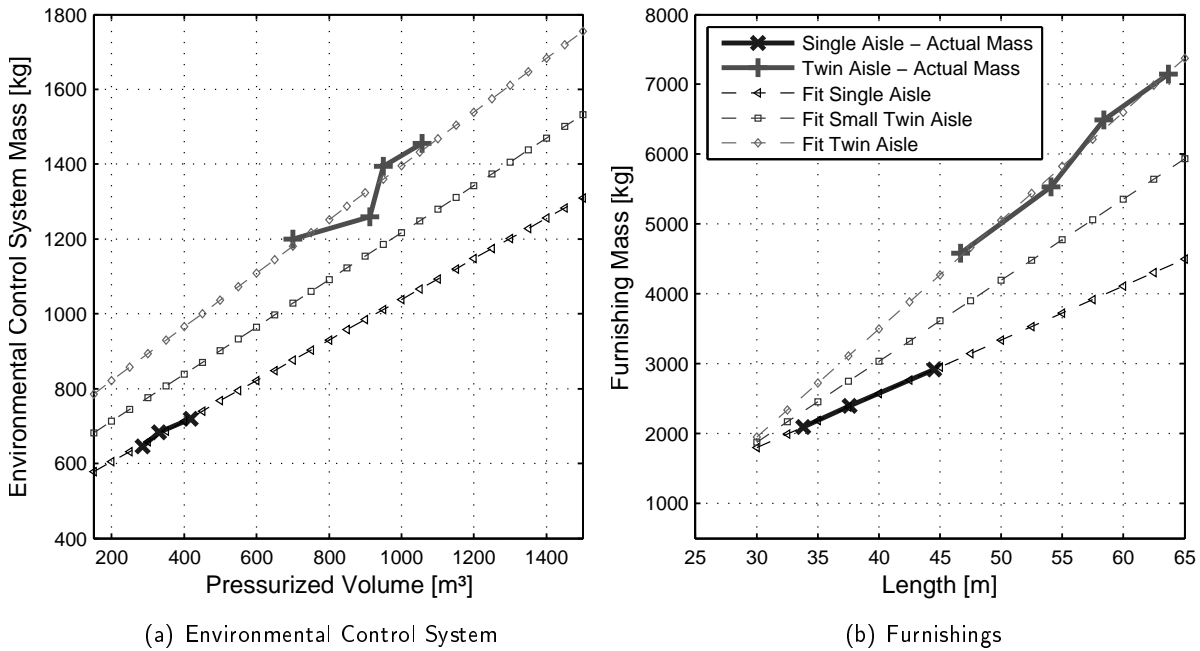
Figure 3.10 – Mass estimation of fuselage systems using regressions. The solid lines represent actual aircraft values of in-production single and twin aisle aircraft. The ECS correlates well with the fuselage pressurized volume, while the furnishings mass correlates best with the fuselage length. Right plot's legend valid for both plots.

System	Type	Equation
Electric System	Single Aisle	$m_{electrics} = 2.9 \cdot A_{cabin} + 739$
	Small Twin Aisle	$m_{electrics} = 3.9 \cdot A_{cabin} + 731$
	Large Twin Aisle	$m_{electrics} = 4.8 \cdot A_{cabin} + 668$
Air Conditioning	Single Aisle	$m_{ECS} = 0.54 \cdot V_{fus} + 496$
	Small Twin Aisle	$m_{ECS} = 0.63 \cdot V_{fus} + 587$
	Large Twin Aisle	$m_{ECS} = 0.72 \cdot V_{fus} + 678$
Cabin Systems	all	$m_{CabSys} = 4.3 \cdot A_{cabin} + 61$

Table 3.1 – Formulas for estimation of fuselage system mass (all results in kg). Cabin systems include lighting and emergency oxygen and are usually counted as part of furnishings. See appendix page 135 for list of symbols.

Furnishings

Furnishings can be defined as all non movable installations in the fuselage that are not systems. They are a major mass contributor to the equipped fuselage mass. The furnishings include amongst other things:

- Cabin insulation for sound proofing and temperature control.

- Cockpit trim panels, cockpit consoles (but without instruments), flight crew seats.

- Cabin lining and overhead bins, including their attachment structure.

- Floor covering (but not the panels) and decorative covering.

- Cargo loading system and cargo hold side lining.

The list shows that the furnishings are difficult to handle as some items do scale with the fuselage size (like the cargo loading system or the cabin lining and insulation), and some items are independent of the fuselage's size (water installation, cockpit furnishings). The mass contribution of the furnishings is too substantial to be left aside. The differentiation between structural mass and furnishings is not consistent in literature [Tor76]. Torenbeek stresses the contribution and offers a simple regression formula. He further offers detailed masses and regression formulas for particular items. However, his regression formula is based on data with unknown consistency. Manufacturers have different standards on where they register certain masses. Therefore a new regression formula is introduced. It was found that the furnishing mass correlates well with fuselage length. Twin aisles have higher furnishing mass, which is mostly due to larger cargo holds and additional overhead bins and their attachment structure. In figure 3.10(b) the relationships are shown. The shortest twin aisle is only 2m longer than the longest single aisle, yet it does have more than 1000kg of additional furnishing mass. The single aisle and twin aisle used for the regression represent the smallest and largest cross section used in this investigation (see page 87).

Type	Equation
Single Aisle	$m_{furnishings} = 77 \cdot l_{fus} - 510$
Small Twin Aisle	$m_{furnishings} = 116 \cdot l_{fus} - 1605$
Large Twin Aisle	$m_{furnishings} = 155 \cdot l_{fus} - 2700$

Table 3.2 – Formulas for estimation of furnishings mass. Note that the formulas are only applicable within the analyzed region, and are especially not suitable for much smaller aircraft or very large aircraft. See appendix page 135 for list of symbols.

Operator's Items

Operator's items include all movable equipment. However, while the entire galley installation is included in the operator's items, the lavatories are included in the furnishing. Major mass contributor are the seats, installed inflight entertainment and emergency equipment. Further the mass of the flight crew. All fluids excluding the consumable fuel is included in the operator's items. The operator's items are calculated directly using masses for each item. Emergency equipment is calculated as sum of items located at each door (like emergency slides) and items allocated to each seat (oxygen and life vest).

Seat mass data can be found in several textbooks, however, the data found there is not representative for current generation passenger seats. This was shown by an investigation of textbook seat masses and currently offered models [Kre10]. New technology has decreased the mass of economy class seats, while increased comfort expectations have increased the seat mass of business and first class seats. For this work average seat masses were determined using a current customization guide for a long range aircraft [Kre10] [Boe06]. Crew mass is established using average mass for pilots and flight attendants, which can be found in several design textbooks and which have not changed since [Tor76].

Mass Positioning
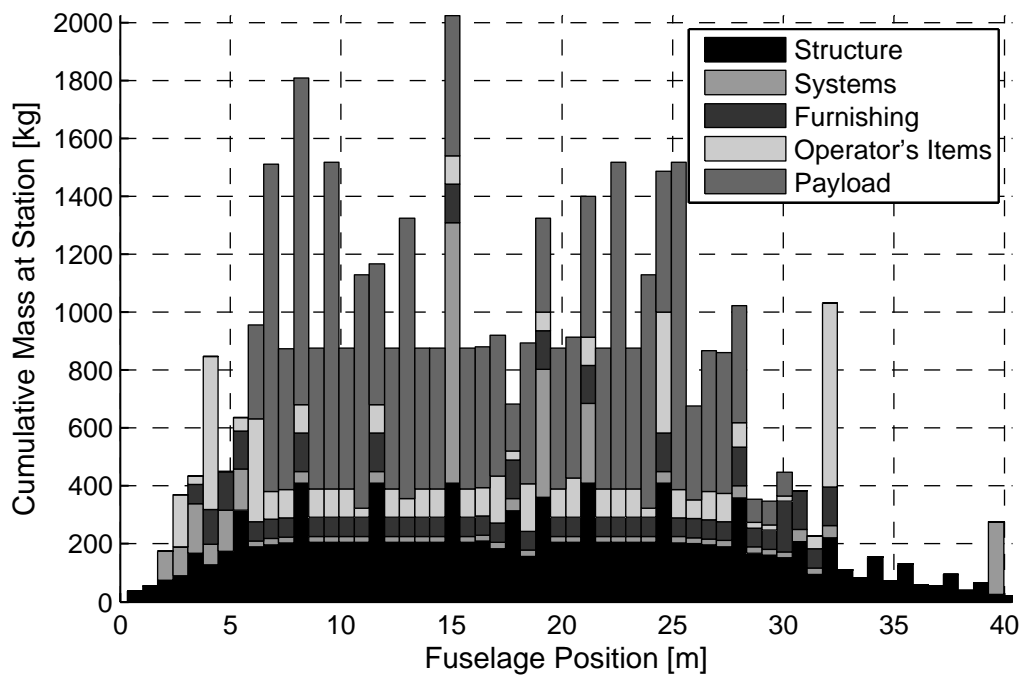
(a) Mass Distribution in Fuselage
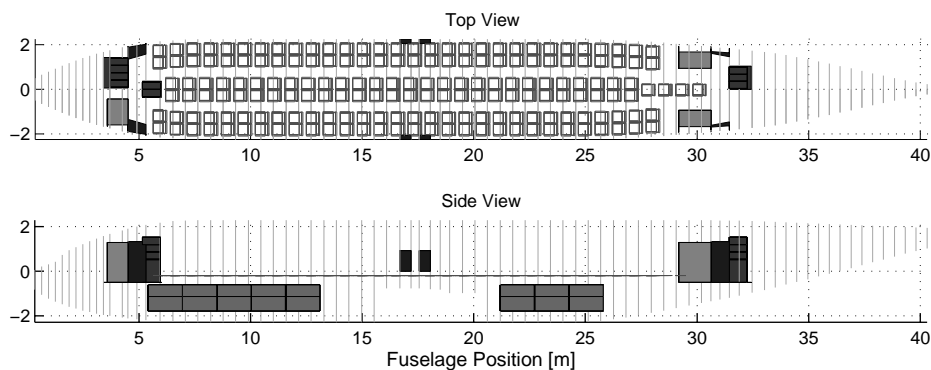
(b) Fuselage Layout

Figure 3.11 – Distribution of masses inside the fuselage, including structural mass. Note for example the position of the environmental control system packs at x=15m and the forward and aft galley. Peaks occur as some heavy items like containers are represented as point masses. Wing is excluded.

The calculated structural and non-structural masses are positioned in the fuselage. This is important as the inertia of these masses influences the structural loads. In figure 3.11(a) a mass distribution is shown. The different mass items are stacked on each other. Due to discrete location of some heavy items like loaded containers, the payload distribution may appear uneven. The effect on the structural mass estimation is neglectible. Many system masses are distributed over the entire fuselage, while other are located in a single place. The packs of the environmental control system can be identified at 15m fuselage length. The peaks in operator's item at front and back represent the galleys.

The center wing box is not part of the fuselage structure and consequently not in the figure. Further, due to the nature of the structural mass estimation, the actual distribution of structural mass is not entirely realistic. Peaks would be expected at locations which house a pressure bulkhead. As explained previously, this is a direct consequence of the used method.

3.1.4 Conclusion

The section outlined the methods and tools used for cabin layout and fuselage mass estimation. The parameters generated by these tools are the input for both the boarding and turnaround simulation and the aircraft design. Hence they are essential for the results of this work. The presented method for mass estimation halves the average offset from the best statistical methods. The method produces an average deviation of 5% in structural mass for current generation aircraft. The seperate consideration of door masses allows a higher fidelity in fuselage structural mass estimation. The methods and formulas introduced for the non-structural mass estimation allow a better understanding of these important mass contributors. The database is more recent than those used in standard textbooks. Operational items are calculated using state-of-the-art data for cabin equipment.

3.2 Boarding and Turnaround Simulation

This section describes the boarding simulation and the estimation of turnaround times. Initially a short overview of existing boarding simulation tools is given. Subsequently the basic principles of a boarding simulation are explained. The major assumptions of the boarding simulation are listed and finally the validation with existing results is described. That followed is the turnaround analysis that includes the other ground service processes.

3.2.1 Existing Tools

Boarding simulation tools have been developed by several individuals and organizations. One commercial was identified. The tools apparently differ in their level of complexity and the intended application. The works described on page 30 all have some type of boarding simulation tool as basis. As described later, the results of a boarding simulation depend strongly on the assumptions made inside the tool. The basic simulation environment is of lesser importance.

CAST Cabin - Airport Research Center

The Aachen-based company Airport Research Center markets the software suite CAST. It provides a variety of functions for airport planning [ARC11]. One module - CAST Cabin - is marketed as boarding simulation tool. It is the only known commercially available boarding tool. By description given on the website it uses an agent-based modeling approach. The described features appear comparable to MASim described in the next paragraph.
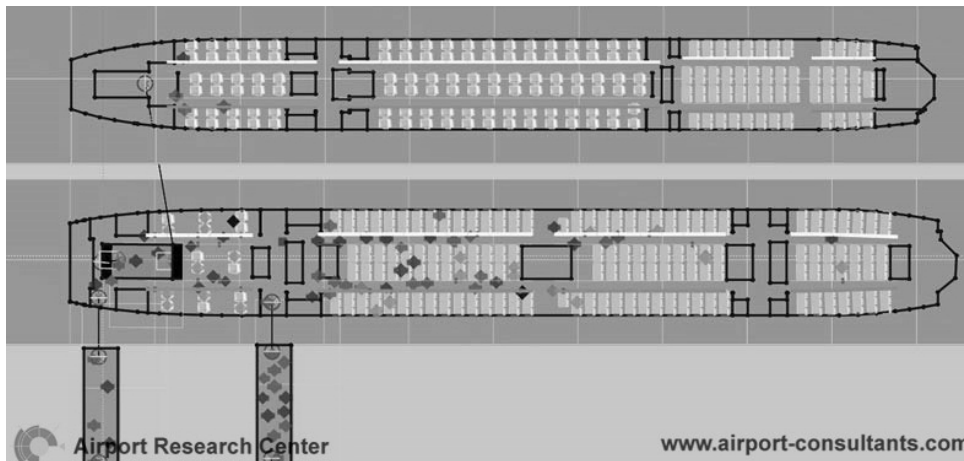
Figure 3.12 – Screenshot of the boarding simulation "CAST Cabin" marketed by Airport Research Center. (from [ARC11])

Traffic Oriented Microscopic Simulation - TOMICS

The simulation tool TOMICS (**T**raffic **O**riented **Mic**roscopic **S**imulation) was developed by the German Aerospace Center over a period of several years [DLR11]. TOMICS initial objective was the simulation of passenger flow within an airport terminal building. Over time the area of application has been widened. TOMICS has been used extensively in airport passenger analysis of different elements of the airport like the check-in area, the security check and the boarding area. The usage for aircraft boarding is an extension of the tool's area of application. TOMICS has been used both for

boarding and deboarding analysis [App10a] [App10b]. TOMICS provides an environment for simulation of passenger movement, especially provides powerful path finding algorithms. As shown later in the text, the key factors for a boarding simulation are the time allowances for actions inside the cabin (like baggage storing). Interactive path finding, one of the key features, is of lesser importance in this context. The process times for baggage storing and other actions inside the cabin need to be fed in the simulation. This complicates a close interaction with the cabin design as intended in this work.

Multi-Agent Simulation - MASim

The boarding simulation tool "Multi-Agent Simulation" was developed in the scope of a PhD-thesis at the TU München by Tilman Richter [Ric07]. As the name implies the tool uses multiple agents to simulate the passenger interaction and movements. The simulation field is sophisticated. The path finding is based on the A* (pronounce: A star) algorithm. The tool was available for this work. Although the modeling approach is fully state-of-the-art, the tool has a few disadvantages that made it impractical to use for this work. First, the simulation time for a single boarding process is in excess of 30 minutes. The structure of the program does not allow batched execution, which means each simulation has to be started manually. For this investigation several thousand different scenarios need to be simulated, so parallel or batched execution is necessary. The simulation further tended to get locked when agents blocked each other and the path finding did not find a solution. The simulation then basically froze without producing a runtime error. This problem occurred especially when many agents were simulated, so exactly at those conditions which are of key importance for this work. Despite these problems the basic simulation setup is replicated in the simulation used for this work, many features are included in a simplified manner though.
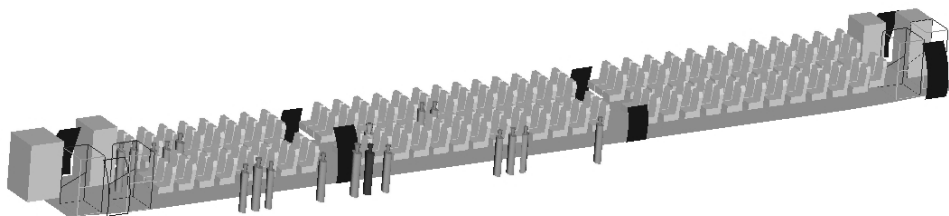
Figure 3.13 – Screenshot of the visual output of the Multi-Agent Simulation by Tilman Richter [Ric07].

3.2.2   The Boarding Simulation

A boarding simulation has the objective of simulating the process of passengers entering the aircraft cabin. The purpose is primarily the estimation of the required time. A secondary purpose can be comfort analysis. Depending on the type of simulation the results can be used to evaluate the effectiveness of procedures for boarding time reduction. Most known existing publications concerning the use of boarding simulation analyzed the effect of boarding strategies on the boarding time.

Basics and Types of Boarding Simulation

A simple and not very accurate method is the application of a constant rate of passengers entering the cabin per time. Multiplied with the number passengers, the boarding time is quickly obtained.

Although this method is no simulation, the method is efficient if reliable data concerning the boarding rate exists.

$$t_{Boarding} = \frac{n_{Passenger}}{n_{Passenger}/minute} \tag{3.2}$$

It is impossible to compare different cabins with this method. The identification of influential factors can be achieved by usage of a database of recorded boarding events. If such data exists, the boarding rate can be estimated as function of the number of passengers and other parameters recorded in the database. This method can be used for boarding time estimation (see [Kra10] and [Gom09]), however, the close to 170 recorded boarding events of the cited publications were insufficient for derivation of any useful function for the boarding rate. Even the regression analysis over the number of passengers is of limited correlation. The Airplane Characteristics For Airport Planning documents issued by the manufacturers supply such boarding rates, but these numbers are clearly stated in the document as assumed rates and not a definitive number (see also table 3.3).

The most common simulation type is the Discrete Event Simulation (DES). A discrete event simulation changes the state of a system or a part of the system whenever an event happens. As an example, if the aisle of an aircraft is separated into multiple cells, each cell has the state "occupied" or "unoccupied". When a passenger moves into the cell, it changes its state. This is called a discrete event (Passenger enters cell). The event has a preset time duration. The simulation moves forward whenever another event takes place. It only simulates a "step" when an element changes its state. Therefore the time interval between two steps is not fixed. This makes the discrete event simulation less costly in terms of computer resources. On the downside, the interactions between individual passenger agents are more difficult to implement. The Boeing program PEDS is a discrete event simulation [Mar98], as are simulations used in other published studies.

The other simulation type is the Discrete Time Simulation. The discrete time simulation proceeds at a given time interval. The state of the elements is checked at every time step. This type of simulation is more costly in terms of resources as it generally requires more time steps. MASim for example is a discrete time simulation. Different than the discrete event simulation, the discrete time simulation checks the state of each passenger agent at each time step. The number of steps is therefore linearly connected to the simulated time. The step length needs to be sufficiently short to prevent simulation errors. These occur when events end within two time steps and are artificially prolonged due to the step length. For boarding simulation purposes, where the walking speed of passengers is the dynamic element, five to ten steps per simulated time second have proven reasonable. The study published by ETH uses a discrete time simulation [Ste10].

Independent from types mentioned above is the feature "agent-based". An agent-based or multi-agent simulation uses elements with different characteristics and limited level of information. A single agent - for example a passenger in a boarding simulation - is defined by a set of characteristics that are unique or at least not common to all agents. The simulated passenger has a limited field of view, i. e. he[6] is not aware about the state of the entire system at any time. Using an agent-based simulation approach therefore makes sense for a boarding simulation as the simulated entities - individual passengers - do exactly behave in this manner. MASim is a multi agent simulation. Other studies do not mention if their simulations are agent based, however, most simulations probably use some

---

[6]For reasons of convenience, all passengers are referred to as "he" in the text.

elements of a multi agent simulation.

Functional Principle

The used approach for this work is Discrete Time Simulation. Despite its higher demand for computational resources the approach was more economic to implement. The pursued solution is oriented strongly on MASim by Tilman Richter [Ric07]. The program was available as source code. It demonstrated several disadvantages in actual use as described above. It still represents a state-of-the-art boarding simulation by the standards of other known or published simulation tools. The problem of MASsim is that some solutions are actually too sophisticated, being too costly in terms of resources without adding additional confidence in the results. Further limitation is that the program is enveloped in a graphical user interface and not handy to use with large number of different cabins. Last and most important limitation was the lack of the all-important time allowances for actions inside th cabin. Non of the original source code was used. The basic simulation consists of a loop that is executed at every time step (see figure 3.15). The standard sample time is 0.1 seconds. Each passenger is modeled as a single agent and at each time step each passenger can execute his current tasks. The tasks of a passenger are moving towards a defined target or remaining at his current location. Other tasks like storing luggage or waiting for people to get up are modeled as one of these tasks.
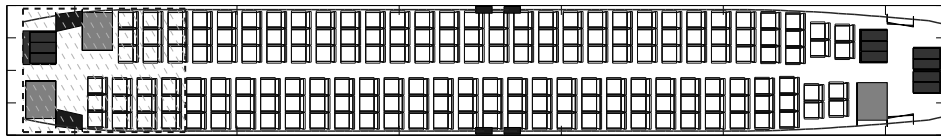
(a) Aircraft Cabin Layout
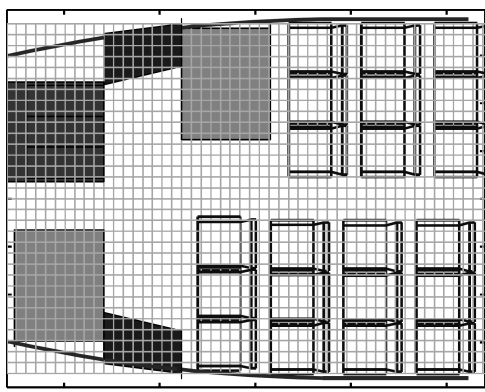
(b) Node over Layout
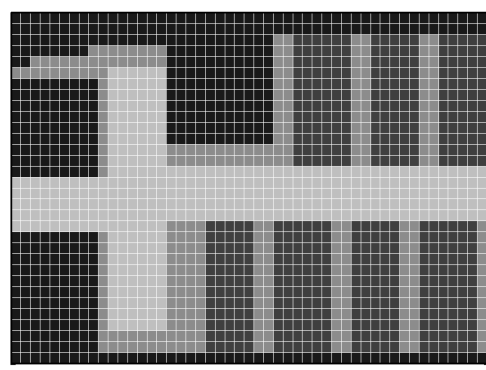
(c) Superimposed Cost

Figure 3.14 – Creation of the node field for the path finding in case of a single aisle layout. The lower plots show a zoom of the forward door area with an overlay of the simulation field nodes. Shown is the standard node size of 10cmx10cm. Dark areas represent areas of high cost.

The passenger moves along a pre-determined path. The path is created with the help of a path-finding algorithm. The used algorithm is called "A*" (pronounce: A-star). The A*-algorithm is a widely used path-finding algorithm and straight-forward to implement [Har68]. The basis for this

algorithm is the existence of a 2-dimensional field, with the individual field elements being called a node. Each node represents an area and has specific (though not unique) characteristics. The nodes are spaced equally. According to the cabin layout, each node is given a cost which the path finding algorithm uses to determine the optimum path.

In figure 3.14 the layout of a single aisle is shown. For the path finding algorithm the layout is translated into a field of cost. The individual cost of objects decides whether the path will ever cross these areas. The relative cost are decisions put into the simulation. As can be seen, the area outside from the cabin is given highest cost, as well as the monuments. Both cannot be used by passenger agents. Seats are given high cost, they can theoretically be passed but would not if any other option exists. The aisle and passage ways are given negative cost. This increases the likelihood of paths leading upon them. The advantage of this approach is that the path finding will always chose the aisle as least costly part. The solution is very robust and would also be applicable to non-straight aisles or more complicated simulation fields like a non rectangular multi-aisle cabin of a blended wing body.

The field resolution has to be chosen right. A very rough resolution increases the speed of the simulation, but small objects might disappear. On the other hand, a very fine resolution increases the computation time of the path finding algorithm. The time required for path finding increases with the number of fields. If resolution is for example halved, the number of nodes quadruples. The usage of a path finding algorithm is not strictly necessary. An aircraft cabin usually consists of straight aisles and hence no elaborate path finding is required to find the best way between entry door and seat. Additionally, in reality a passenger would not know the best way to his seat, either. But the path finding algorithm is a robust and efficient option for the boarding simulation, as suitable paths are found for all layouts. The path finding is done for each passenger agent once. The paths are not re-calculated at each step. Other agents are not regarded in the path finding. That is, the passenger will always identify the aisle as best way to his seat even if it is blocked by another passenger. This leads to queuing of

Figure 3.15 – Simplified structure chart of boarding program. See text for further explanations.

passengers and represents a major difference to the approach pursued by Richter. There, the agent recalculated his path dynamically. While this is a suitable solution for a simulation field with alternative routes, the aisle of an aircraft leaves little room to pass. The aisle passing is implemented in a different way as described later.

The work with MASim and intensive study of other boarding simulation studies lead to a set of objectives for this simulation tool. Any simulation regardless of the topic represents a simplified model of reality. A good simulation simplifies the reality as much as possible without neglecting the crucial effects. However, complexity is no advantage in itself. Thus primary objective of this boarding simulation is simplicity and speed. The complexity of the boarding simulation is chosen to be as low as possible to resemble the system. The speed of execution is result of this approach. A further objective is selected accuracy. Some parts of the cabin have to be modeled in great detail to catch effects that otherwise go unnoticed. In order to allow agents to pass each other in the aisle as function of cabin layout, the agents size, their luggage and the local aisle width has to be known. Trying to capture this with a node field like done in MASim would require an extremely small node length, which would have disadvantages for the rest of the simulation. Further, some events are not simply triggered by physical parameters, probability function represent a more suitable approach.

The basic principle of the boarding simulation is shown in figure 3.15. Some sub-processes are excluded in the chart to ease understanding. Each passenger agent can either be activated or de-activated. The latter is the case before he enters the cabin or when he has sit down. When the agent is active, he is performing tasks. These are either static or dynamic. Static tasks are luggage storing or waiting for people to clear a seat in order to reach his seat. A static task means the agent will remain in its position for a defined time. The time is function of assumptions on task durations as described later. A dynamic task requires the agent to reach a particular position using the path that is calculated once at the beginning of the task. The agent checks if the next node leading to his target is free. If so, the agent moves. Depending on the individual walking speed and node length, the agent is moving in between the nodes and is blocking both until he reaches the node. When the next node is blocked, the agent waits. Where ever an agent is positioned he is blocking the node and the neighboring nodes depending on node length. Objects in the cabin do not occupy nodes, their presence is considered via the path finding algorithm. The agent cannot change its path dynamically during the simulation.

The figure 3.16 the a normal view (left) and the node status (right) can be seen. The node size is chosen with 10cm. Each agent occupies 4 nodes in each dimension.

In essence, compared to the other described boarding simulations, the used simulation incorporates actual cabin design features into the simulation. These features are not simply the position of the seats, but the effect of the luggage capacity on baggage stowing times. Such feature represents a crucial advantage. The simulation was created with focus on quick and robust simulation. The direct link between cabin layout and boarding simulation allows a direct simulation without further need of modeling, and within a single automated process. This integrates the boarding simulation directly into the aircraft design process. The setup of the simulation may enable the inclusion of aircraft turnaround into a multi-disciplinary optimization, which is beyond the capability of the other boarding simulation tools.

3.2.3 Important Features of the Boarding Simulation

The described algorithm allows to simulate the movement of passengers. It prevents the agents from moving above each other. However, this capability does not represent the decisive part of a boarding simulation. The boarding process is characterized by individual delaying events in the aisle that pre-

(a) Normal View

(b) Blocked Nodes
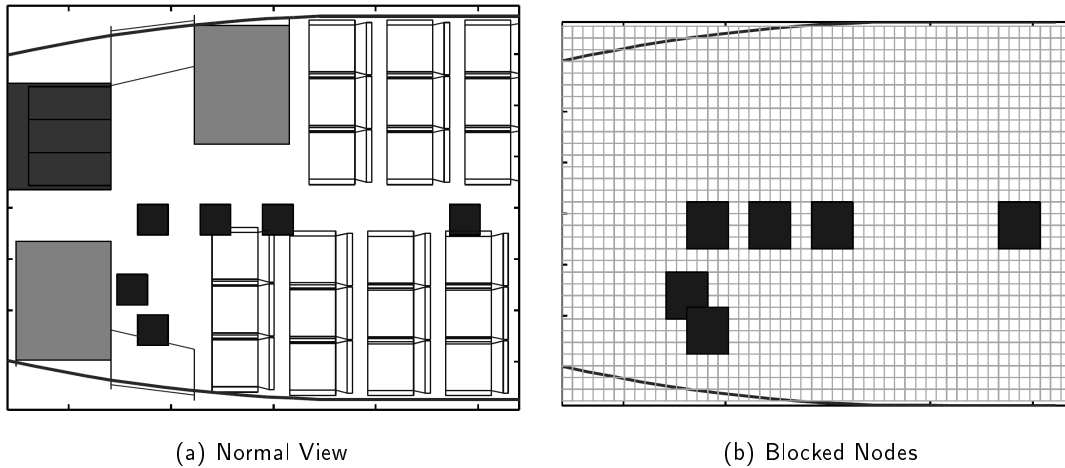
Figure 3.16 – Representation of passenger agents in the simulation field. Left a normal view of the forward door area during a boarding event. Right the corresponding status of the node field. Note that seats and monuments are considered via the path finding.

vent following passengers to reach their seat. If these events are not considered, the entire purpose of the agent-based approach becomes questionable, because simple movements along a known distance can be calculated with less effort. The two central delaying events are described in several publications like [Ste10] or [Fer04]. First type is a passenger that stores his luggage in the overhead bin. This is deemed by most publications the most important reason for blockage of the aisle. Another major delay occurs when a passenger wants to sit at a seat not directly located at the aisle. If another passenger has already occupied the seat in between, the seated passenger needs to get up to let the newly arrived passenger pass.

In figure 3.17(a) this is shown visually using a cabin modeled in the 3D environment CATIA. A CATIA-based CAD model was used to determine the available space for a passing passenger in dependency of aisle width (see page 61).

(a) Luggage Storing

(b) Seating
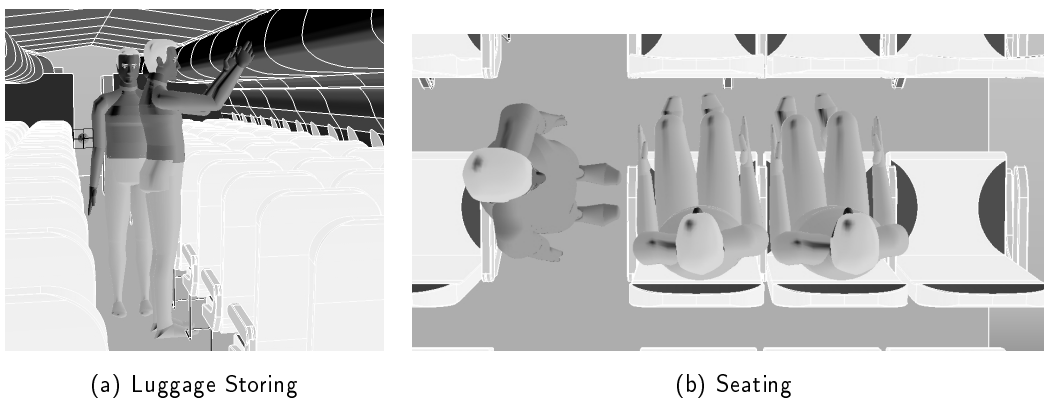
Figure 3.17 – Basic reasons for aisle blocking: left the aisle is blocked by a passenger loading luggage. Right the passengers already sitting need to get up to let the newly arrived passenger pass to his seat. (Graphics generated with CATIA)

Luggage Storing and Overhead Bin Model

The carry-on luggage represents the single most important factor in aisle blocking. And as aisle blocking is the key reason for prolonged boarding times, the luggage storing was given special attention in the simulation. In theory the storing of luggage only requires the passenger to lift his bag and store it in the overhead bin. The time required therefore might be seen as function of the bag's size and the physical strength of the passenger. However, observations in real boarding situations demonstrated far more variety. One major influence factor is the available space in the overhead bin. If the overhead bin is empty, even large pieces of luggage (given they fit into the bin at all) are quickly stored. As soon as the overhead bins start to fill with luggage, a passenger needs to look for available space or re-arrange the other luggage items in order to free up space. As described in 3.1.1 (see especially figure 3.4) the actual volume of the local overhead bins is known through detailed layout of the cabin. While other simulations considered the number of carry-on luggage items, this simulation assumes at maximum one piece of carry-on luggage, which also represents the current policy at all major airlines. But the type and size of the luggage is different. The bulkiness is assumed as key parameter for luggage storing time.

(a) Trolley (14inch width)   (b) Backpack

Figure 3.18 – Examples for bulky (left) and medium (right) carry-on luggage. All trolleys are considered as bulky item in the simulation.

Three categories were defined: small bags like hand bags that are limited in weight, can be stored easily also in small volumes and can also be stored under the seat with limited loss of comfort. These small items do not increase the passengers physical size in any meaningful way. The second type is a medium sized bag or a backpack, shown in figure 3.18(b). This item is still carried and it is flexible, but the size is increased so that the storing below the seat is not the preferred situation. The medium sized item slightly increases the passengers size and decreases his ability to pass in the cabin. Finally, the third category represents any type of trolley-like luggage as shown in figure 3.18(a). These items are rarely carried but rolled behind the passenger. They are not flexible and require significant volume inside the overhead bin. They cannot be stored below the front seat or only under severe loss of comfort. The passenger is more restricted in his movements when having a trolley.

In the simulation each overhead bin is known in actual volume. A passenger arriving at his seat will store his luggage in the adjacent overhead bin. The time required depends on the basic time for his type of luggage and on the level of occupancy in his preferred overhead bin. If the available volume

(a) Store Time per Passenger
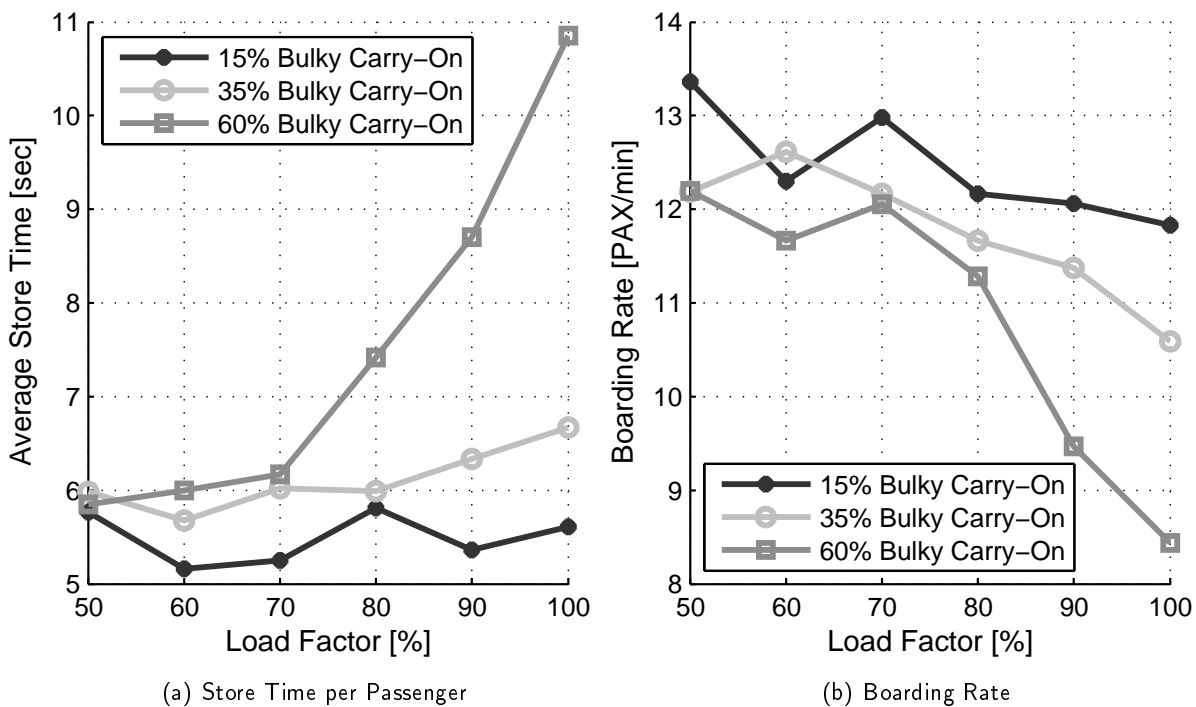
(b) Boarding Rate

Figure 3.19 – Influence of carry-on in the simulation. Left the increase in store time per passenger. Note the drastic increase for high load factor and bulky carry-on due to congested overhead bins. On the right side the decrease in boarding rate is visible.

is insufficient, the luggage is stored in either of the accompanying overhead bins with a time penalty added. If neither has enough volume, an additional time allowance is added. During the entire time the agent is blocking the aisle. The overhead bin volume represents the water volume of the bin. Any piece of luggage will cause loss of additional volume as it does not use the space with best efficiency. This is considered by addition of a loss factor. This factor is higher for trolley type luggage as these are not flexible and cannot be crammed into a free spot. This approach not only captures the actual characteristics of the cabin, but also adds a non-linear element. An example is given in figure 3.19. Three carry-on distributions (15%, 35%, 60% bulky carry-on) are simulated at different load factors in a 180 seat single aisle. The average store time per passenger increases with load factor as overhead bins are filling up. This is especially true when lots of bulky carry-on is carried into the cabin. The example with only 15% bulky carry-on and 100% load factor has no increase in store time as sufficient overhead bin volume remains. The other figure shows the boarding rate. It decays slightly for the low and medium carry-on example, but drastically for the scenario with lots of bulky carry-on.

Smartness

Behavior inside a cabin during the boarding process varies strongly between passengers. The speed usually correlates with the number of flights an individual person makes. It also correlates with the age. The differentiation between "quick" and "slow" passengers can be done via the flight's purpose: business or leisure. Business travelers are supposed to be quicker in their actions inside the cabin. Although no source exists for the difference of either type, this is considered by using a factor on the actual storing times and other important parameters. In the simulation this concept is called "Smart-

(a) Smartness (b) Aisle Passing
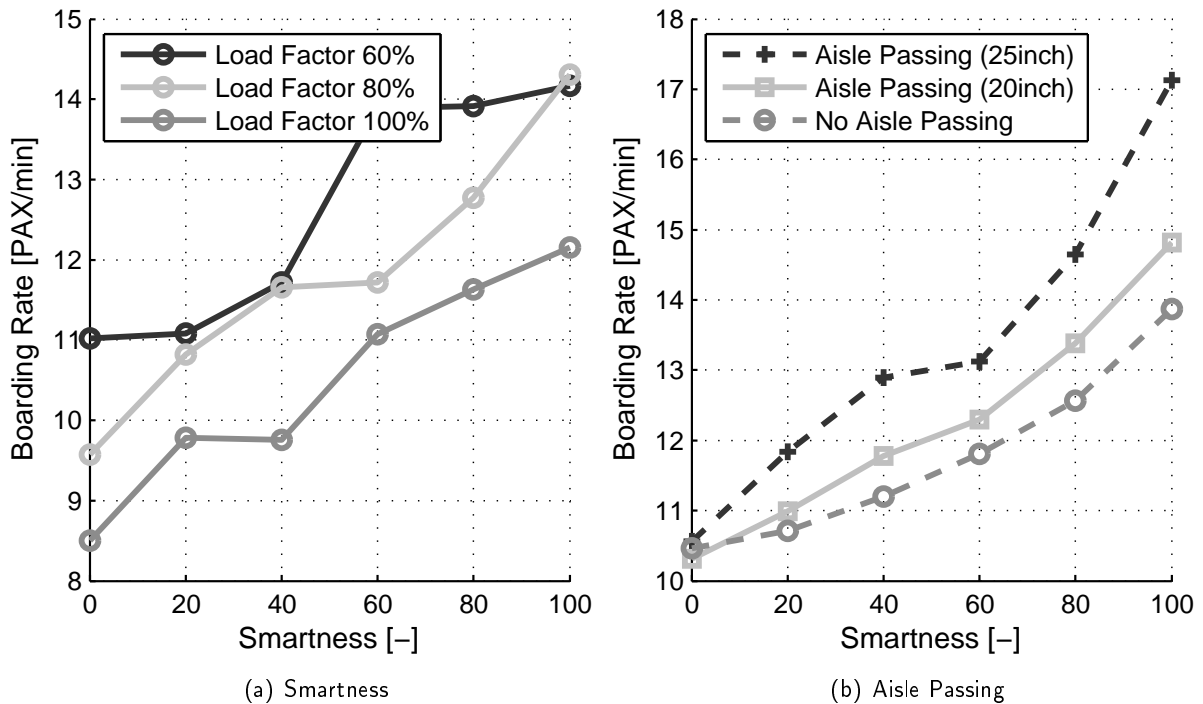
Figure 3.20 – "Smartness" as indicator of passenger behavior influences the boarding rate. On the right side the coupled influence of the aisle passing model combined with the smartness.

ness". In figure 3.20(a) the influence is simulated for three load factors. The increase in boarding rate is significant. The boarding rate increases by 50%. Real life observations indicate that the difference between different passenger populations can even be larger. Richter considered different passenger behavior through a variety of characteristics, which then affected the probability for certain actions.

Seat Interference

Seat Interference describes the fact that passengers need to get up from their seats to allow other passengers to reach their seat. This problem naturally occurs the more seats are placed per aisle. In the simulation it is assumed that other passengers always get up, also because rather low seat pitch is used throughout the investigation. The time required is depending on the number of blocked seats. When a passenger wants to reach a window seat, and both middle and aisle seat are blocked, the maximum time allowance is applied. Again, during the time assumed the passenger agent remains static in the aisle. When the time is over he disappears from the aisle. The other passenger agents are not reactivated. The actual time required decreases if passengers have high Smartness.

Aisle Passing

When one passenger blocks the aisle due to luggage storing, it may be possible that other passengers behind him are able to pass. This passing is very difficult to simulate using a strict node-based approach. If attempted it requires a very small node size, and thus slowing down the path finding substantially. The chance to pass represents a probability depending on many factors. The most important is the actual width of the aisle. Second the physical size of the blocking and the pass-

ing passenger. If two passengers are unable to pass each other without touching each other, the probability that the blocked passenger attempts a passing is very remote (though not zero). Last influential factor is the willingness of the blocked passenger to get to his seat quickly. It is important to remember that in a typical boarding situation with assigned seats, the individual passenger is not in a hurry. He has no incentive to reach his seat in the shortest possible time but can wait in the aisle until the other passenger has finished. However, when sufficient space is available he will probably pass.

In the simulation the physical size of each passenger is determined using statistical data on human sizes. By changing the continent or the male-to-female ratio the number of "wide" passengers can be changed. When one passenger blocks the aisle because he stores luggage, the effective aisle width as function of both passenger's abdominal size is calculated. If the adjacent aisle seat is empty, the standing passenger is reduced in size as he is able to move slightly into the seat row. If either passenger has trolley-type luggage the probability is reduced, if both have trolleys no passing takes place.

In figure 3.20 the resulting difference is shown for a aisle width of 20inch and 25inch. Another simulation was conducted using no aisle passing model (as standard for most known boarding simulations). The difference to the standard aisle is small, indicating that omission of an aisle model is an acceptable decision. The 25inch aisle has a quite noticeable effect on the boarding rate. However, it needs to be noted that the simulation depicted in the figure was run with very limited carry-on, greatly increasing the chance for aisle passing. When one third of the passenger are equipped with bulky carry-on, the effect diminishes quickly. It is further visible that the Smartness has a very large effect.

(a) Passing 1   (b) Passing 2
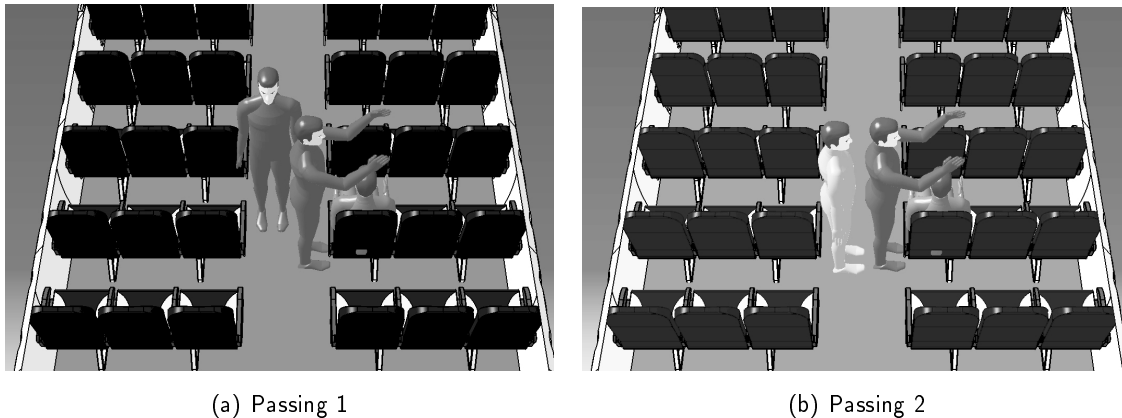
Figure 3.21 – Passing in the aisle. The shown aisle is 25inch wide. As can be seen, the passengers are coming very close. Hence passing still requires some level of cooperation by the standing passenger and willingness by the passing passenger. (Graphics generated with CATIA)

In figure 3.21 an exemplary scenario is given. The depicted cabin has a 25inch aisle, which is 5inch wider than currently found in most cabins. The decisive factor is the size of the individual passengers. Of further influence is if the static passenger can move slightly into the seat row, increasing the space for the passing passenger. In the simulation the chances for aisle passing increases when the aisle seat is empty.

The simulation thus allows to consider the effect of increased aisle size. Albeit its simple nature the method is deemed superior to a strict node-based approach because the passing probability can be adjusted in a direct manner. A key factor is the motivation of the individual passenger to push past the blocking passenger in order to reach his seat. The 25inch aisle still does not allow convenient passing. However, if other external factors are changed, for example seat assignment, the effect of a wide aisle might be more significant. Low cost carriers do not use pre-assigned seats, which motivates the individual passenger to hurry while boarding to capture a preferred seat. The consequence is that low cost carriers achieve shorter boarding times when carrying similar load factors. The statistical analysis performed by Krammer could not support the significance of the aisle width at all ([Kra10], figure 1). In a research including close to 170 boarding events, no correlation between boarding time and aisle width could be identified. The correlation factor between aisle width and boarding and deboarding time were 0.083 and 0.13, respectively[7]. Hence, the values correlate positively with time when a negative correlation would have been expected (wider aisle correlates causes reduced boarding time). The magnitude of the factor indicates no useful finding. Given the general inability to find any useful regression factor from the obtained data, the finding not necessarily disproves a possible advantage of wider aisle. In order to identify such advantage, a larger study under controlled conditions would be necessary.

Simulation Parameters

The boarding simulation has several key parameters that have substantial impact on the result. In order to capture effects of different passenger populations and operational conditions, five input parameters were defined. These are:

1. The relative number of passengers carrying bulky luggage with them. Standard is set at 45%, with edge values being 10% and 60%. From observation and measurement data (see [EAS09]) this number was chosen. As carry-on represents the major factor for delay in the aisle, the percentage of bulky luggage is very significant.

2. The load factor of the aircraft. While most boarding simulations assume 100% load factor, the actual average load factors in reality vary between 65% und 80-85% [LH11] [Dog10]. The boarding time is in first approximation proportional to the load factor, but non-linearities exist as shown in figure 3.19.

3. The passenger's ability to behave in a pro-active manner inside the cabin. This describes the often observed difference between frequent flyers and leisure travelers. Frequent flyers are observed to move faster inside the cabin, being more efficient when storing their luggage, getting seated quicker. They also allow passing more frequently. All these observations have been summarized in a factor named "Smartness". It increases the walking speed, reduces the seating and luggage storing time, and increases the passing probability. The average value is 50, with maximum values of 100 and low value of 0.

4. The number and position of boarding doors. The standard scenario is a boarding via passenger bridge through the forward left door (Door 1L). This is the usual way aircraft are boarded when parked in front of terminals. Alternative settings are boarding through the second forward door (Door 2L) if available. When parked on the tarmac and boarded via stairs, a boarding through

---

[7]The used Pearson product-moment correlation coefficient is 1 or -1 for a perfect correlation, and 0 for no correlation.

forward and rear door is common. This is the preferred solution for low cost carriers and charter operators. A boarding through two front doors is often observed at airports but usually limited to large long range aircraft. This setting speeds up boarding slightly [Mar98], but purpose is also to separate the business and first class customers from the economy class passengers.

5. The rate at which passengers enter the cabin through a single door. This rate depends on the speed at which passengers are flowing through the gate check-in in the terminal. For this work it is assumed that the rate is sufficiently high, the rate is assumed with 25 passenger per minute. In reality this number is rarely achieved, which is also due to the fact that it would not make sense as the passengers would simply queue in the passenger bridge. As only very special settings allow an average boarding rate of 25 passenger per minute, the passenger flow rate is without influence for most simulations. The rate remains a very important assumption, and also depends on pre-boarding procedures of the operator.

Using the above input parameters a variety of airline business models can be simulated. A low cost carrier would be represented by a load factor on the upper end of the scale, a large amount of bulky luggage (due to baggage fees), boarding through two doors and a medium level of Smartness. A short range domestic trip dominated by business travelers often demonstrates a lower load factor, less bulky carry-on (many travelers return in the evening) and high level of Smartness.

3.2.4   Validation of the Simulation

A simulation needs to be compared to the reality in order to prove its ability to model the system properly. The validation can be done for the individual time allowance assumptions, namely luggage storing, seat interference and aisle passing. Alternatively the total time required for a single boarding process can be compared.

A true validation would require a test under controlled conditions, preferably with different populations of passengers in a real aircraft. This was beyond the possibility of this work. Therefore, the correct functioning of the simulation is assured by comparing its results versus known results and adjusting it so it matches these. The simulation can thus be considered calibrated. For a good calibration it is necessary to use values that are not obtained from simulations themselves, which leaves only two studies for calibration.

The time allowances for the individual tasks were further checked using own observation and expert advice. All three actions (passing in the aisle, seat interference, luggage storing) are subject to wide variations. The chosen values and distributions do not cover the extreme values sometimes observed in real life.

Reference times for boarding can been extracted from the Aircraft Characteristics for Airport Planning manual each manufacturer issues for a type of aircraft. These feature turnaround charts that show the assumed boarding times. The times are listed in table 3.3. However, these times are not necessarily realistic. The spread in actual numbers for similar aircraft clearly underlines this. The boarding passenger flow spreads between 9 passengers per minute and 20 passengers per minute for single aisle aircraft. Airbus numbers are more optimistic than Boeing numbers. Both manufacturers consider twin aisles quicker in boarding. All given times for pax flow are per door.

Aircraft	PAX	Total Turn Time [min]	Boarding Pax Flow [1/min]	DeBoarding Pax Flow [1/min]	Remarks
A300-600	285	30	16	18	Door unspecified
B767-200	216	35	20	25	Door 1L
B767-300	261	40	20	25	Door 1L
A319	134	30	16	22	Door 1L
A320	164	30	14	22	Door 1L
A321	185	35	20	24	Door 1L
B737-700	140	33	12	18	Door 1L
B737-800	160	38	12	18	Door 1L
B737-900	177	40	12	18	Door 1L
B757-200	186	37	9	18	Door 1L
B757-300	243	54	9	18	Door 1L

Table 3.3 – Boarding and deboarding rates from ACAP documents. Note the wide variance between different single aisles that cannot be reasoned by any design differences. References: [Boe05a] [Boe02] [Boe05b] [Air95] [Air83]

Another source of information are actual tests or observations. Boeing conducted such a test for validation of their boarding simulation tool, as described by Boeing (Marelli et al., [Mar98]). A B757-200 with 200 seats was boarded several times, the obtained data used to validate the boarding simulation.

Further the publication by ETH (Steiner & Philip, [Ste10]) cites actual boarding times of an A321, which were taped by the authors and used to developed their boarding simulation. Surprisingly, all other publications in the field of passenger boarding do not quote any calibration or validation method. As both the observed A321 and the B757-200 are very comparable in size (198 seats versus 201 seats), they are used as reference for the results of the simulation. Table 3.4 lists the results. Several scenarios are listed for the boarding simulation, representing different sets of parameters. Each simulation is influenced by random parameters, so that a number of simulations with similar settings needs to be conducted in order to establish a mean value. The maximum and minimum value are also of interest to verify the spread.

The "Default Scenario" is close to the observed values from ETH [Ste10], as well as the single point number from Boeing [Mar98]. While the Boeing result represents an averaged value of three tests, the observed values by ETH are individual observed boarding events, therefore subject to singular events. The authors further included the check-in desk at the boarding gate and recorded several events that delayed the passenger flow into the cabin. Their rather long time recordings are partly explained by those. As can be seen, the simulation results approach those of the sources, they are more optimistic on average. When tougher scenarios are chosen, the boarding times rises but remains within times that appear reasonable given the actually observed results. The simulated results do not include any unexpected hold-ups. A systematic variation was performed of key input parameters such as stowing times, walking speed, passing probability and other. The final values produce the result shown above and are the best compromise between a good match of the known boarding times and realistic yet not too pessimistic assumptions for the individual times for actions and delays.

| Aircraft | | Attributes | | Time [min] | | | Mean Rate | Remark |
Layout	PAX	Smartness	CarryOn	Mean	Max	Min	PAX/min	
Single Aisle	200	50	35	17.5	19.5	15.8	11.5	Default
Single Aisle	200	50	60	22.0	25.4	20.0	9.1	Max Luggage
Single Aisle	200	50	10	16.7	19.3	14.3	12.0	Min Luggage
Single Aisle	200	100	35	14.6	17.3	12.4	13.8	Max Smartness
Single Aisle	200	0	35	21.4	24.7	18.4	9.4	Min Smartness
Single Aisle	200	100	10	13.6	15.7	11.6	14.8	Best Case
Single Aisle	200	0	60	25.8	28.0	22.4	7.8	Worst case
A321	194			22			8.8	ETH [Ste10]
A321	193			21			9.2	ETH [Ste10]
A321	192			25			7.7	ETH [Ste10]
A321	198			28			7.1	ETH [Ste10]
A321	197			26			7.6	ETH [Ste10]
B757-200	201			22			9.1	Boeing [Mar98]

Table 3.4 – Calibration of boarding simulation: Values from the Boeing study [Mar98] and from ETH [Ste10] are taken for calibration. The standard simulation is more optimistic than either of the sources.

3.2.5 Correlation with Actual Boarding Times

In the previous sections the boarding results were calibrated using data from other publications. The data reflected single boarding events. Boarding times are subject to wide variation in practice due to the very different possible scenarios. A flight dominated by frequent flyers with limited luggage, and a moderate load factor will demonstrate a much faster boarding rate than a fully booked aircraft with tourists with lots of carry-on. This phenomenon is known throughout the industry.

A Monte Carlo simulation was performed in order to verify that the simulation can generate both very high and very low boarding rates. That is, the three major settings (load factor, carry-on distribution, smartness) were varied using a probability distribution (also see figure 4.8 on page 95). The resulting boarding rate (passengers per minute) reflects the results the simulation is able to generate. This result is compared with actual boarding results.

The actual boarding results are from a large set of ground time recordings used in the ALLEGRO[8] project [Fri09]. Only single aisle aircraft boardings with more than 50% load factor were chosen out of the dataset. Further, results that seemed unrealistic were removed from the record. Especially very low rates may be caused by events independent from the cabin process. Missing passengers or interruptions at the boarding counter may delay the boarding process. Boarding is often started 30 minutes before scheduled time of departure, and therefore a longer time period is available than actually necessary. These events are not specifically marked, making the dataset unsuitable for calibration. Fricke shows that process times decrease when the aircraft is behind schedule [Fri09].

The result is a spread of boarding rates which represents real life boarding times. Compared to that

---

[8]The acronym stands for "**A**scending to a higher **L**evel of **E**xcellence in **Gro**und operations" [Fri09].
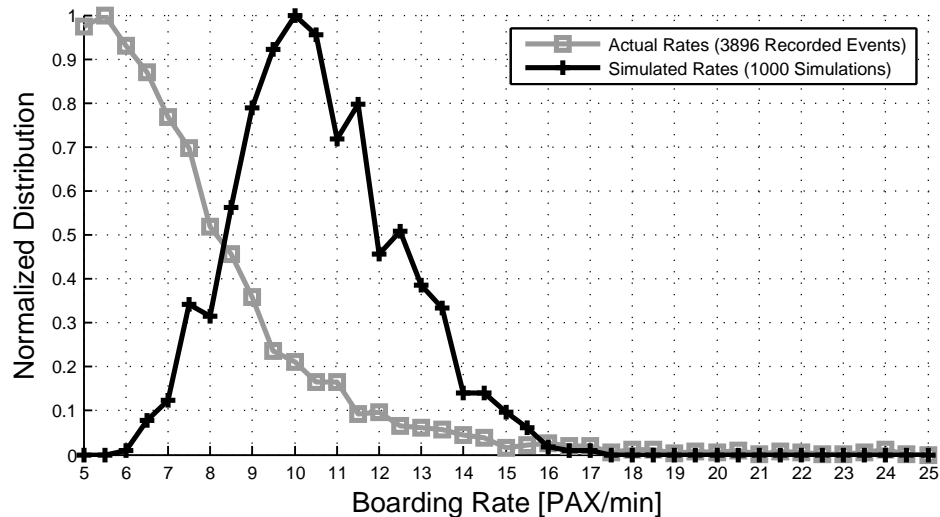
Figure 3.22 – Comparison of simulated boarding rates with recorded events [Fri09]. The spread is comparable, while the actual distribution cannot be matched due to unknown boundary conditions. Also see [Fri09].

is the spread of boarding times produced by the simulation. The significant numbers are the maximum and minimum rates, while the actual distribution is of limited importance. The result shows that the actual times reach from 5 passengers per minute (which is the lower cut-off value) to up to 25 passengers per minute (the upper cut-off value). The main region however is between 5 and 15 passengers per minute. The simulation - using single aisle layouts between 130 and 220 seats capacity - simulates boarding rates between 7 and 17 passengers per minute.

This demonstrates that the simulation is able to generate a wide variety of results while using realistic input parameters, and that this corresponds to the variety found in real life. Only apparent deviation is that the simulation is unable to generate very rapid boarding rates above 15-17 passengers per minute. However, less than 3% of the recorded events demonstrated these rates.

3.2.6 Deboarding Simulation

Deboarding is equally important for turnaround time estimation. Although the deboarding appears as inverted boarding, there are some important differences. The passenger agents start at their assigned seats and enter the aisle as soon as there is an empty spot next to their seat. The times required for taking the luggage are oriented on the storing times, assuming that extracting a bulky piece of luggage takes longer than small bag. However, the times are reduced to one third based on observations during actual deboardings. If a passenger is blocked in the aisle, he uses the time to extract his luggage. There is no passing during deboarding. The average walking speed of the passengers is increased. In a deboarding scenario the motivation of the individual passenger to leave the aircraft is high, especially if the passenger has no checked luggage and does not need to pass immigration procedures. The deboarding thus is a very simplified version of the boarding. The calibration of the deboarding is simpler as the spread in available results is much lower. In fact, most sources quote very similar numbers when the deboarding time is normalized with the number of passengers.

Only the Boeing publication considers the deboarding. A more recent study on deboarding times by Appel using TOMICS does not cite any calibration or validation [App10b]. Boeing gives a time of

10 minutes for deboarding the 201-seat B757-200 of the previously mentioned test campaign. This is in line with values mentioned in the regressional analysis of 168 deboarding processes done by Krammer and those found in the analysis of recorded data [Kra10]. The general observation from the accessible data is that 20 to 25 passengers per minute is the common deboarding rate of a single aisle. The simulation was adapted to match this time.

3.2.7 Turnaround Time Estimation

As stated on page 25 the boarding and deboarding time sets the minimum turnaround time for short range aircraft in most cases. However, if a substantially shorter boarding time is achieved, the other processes need to be considered as well. Reduced boarding times are only useful to the extent where the cabin processes (compare figure 2.14) move from the critical path. A further reduction would not yield any advantage. For this purpose the competing processes are analyzed and modeled. These processes are:

1. **Cargo Loading:** The cargo loading assumes the usage of containers. Baggage is mostly loaded into these and all cargo is available on time. Bulk luggage loading does not exceed the container loading time as only few items are considered to be loaded as bulk cargo (primarily oversize baggage). Cargo loading is done with two container vehicles. The simulation calculates the time in which cargo loading could be achieved using the current system to its full potential. Today's single aisle are often serviced by only a single cargo loading vehicle. This is a decision the airline takes. If the cabin processes will determine the turnaround time, there is no need in spending additional money on a second vehicle. In the simulation containers are simulated as individual entities with assumed speeds in the cargo hold and while loading.

2. **Cabin Cleaning:** Although it is not glamorous, cabin cleaning is element of the critical path [Fug01]. Cabin cleaning can be performed in varying intensity, and the time to service an individual seat can range from 20 seconds up to several minutes. In short range operation only limited cleaning is conducted. Further the number of cleaners is crucial. Working parties usually consist of 4 to 6 people. Again, the number of cleaners is depending on the airline's willingness to spend extra money. In the simulation the cabin cleaning time is strictly a function of the seats and number of cleaners, although one can argue that a twin aisle offers advantages in the work flow of the working party. In the simulation the number of cleaners is fixed at 4 below 180 seats and 6 for all capacities above 180 seats. The time to clean a seat is set at 20 seconds.

3. **Catering:** Catering is of limited importance on short range flights. The galley capacity is rarely used to full extent and many operators perform catering only every second or third turnaround. In the simulation a single catering vehicle is assumed, and time depends on the number of trolleys.

4. **Refueling:** A single refueling vehicle is assumed with a refueling rate of 300gal/min, equivalent to just over 900kg/min. It is assumed that refueling takes place after every flight as airlines avoid to tanker fuel and haul additional unproductive weight. However, the practice this is frequently done in short range operations. The refueling takes place between deboarding and boarding according to the applicable procedure formulated in EU-OPS Nr. 1305 [EU08].

The turnaround time is also used by the flight crew to prepare for the next flight or to do a crew change. Before each flight a go-around check by a member of the flight crew is required. Statements

made by current airline pilots indicated that turnaround times below 25 minutes make accomplishment of all tasks difficult. Consequently, 25 minutes is considered as the lowest practical gate time for continuous operation.

Vehicle size and path is simulated using a waypoint based path finding algorithm with a simple dynamics model. Speed and acceleration can be adjusted. Although many vehicles might achieve reasonable speeds, the maximum speed in proximity of an aircraft is restricted to 10 to 20km/h. Vehicles do not avoid collision, the collision avoidance is achieved by sequencing the processes. For very short aircraft (twin aisles with less than 180 seats) the positioning of all vehicles at the aircraft's fuselage becomes an issue.
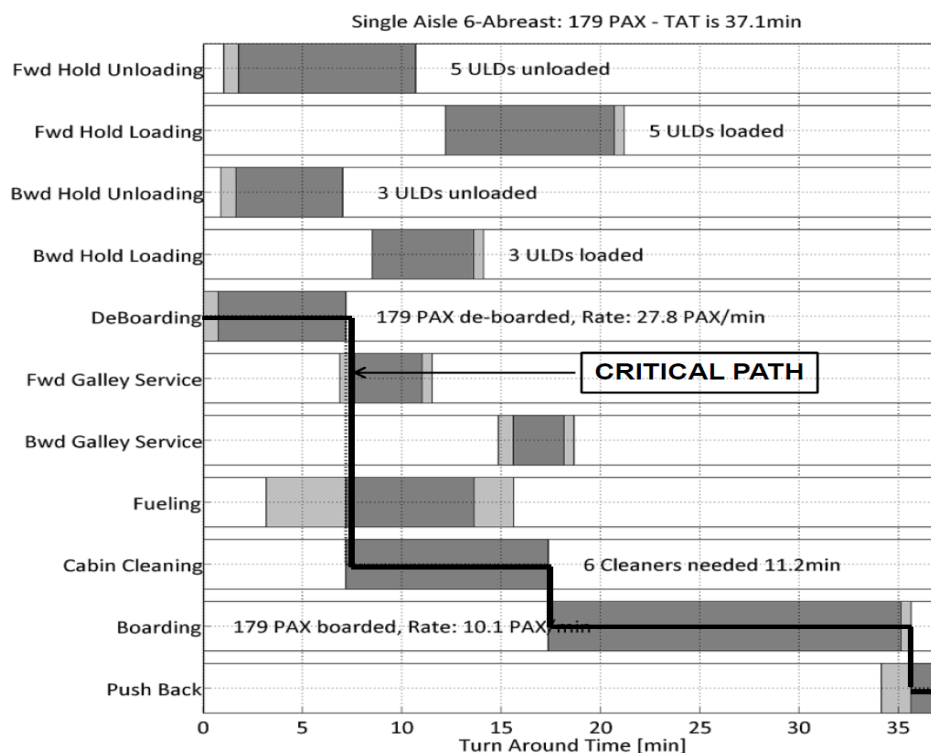
Figure 3.23 – Gantt Chart of a typical turnaround. Note the critical path. Solid grey represents the process times, light grey positioning times of vehicles.

In figure 3.23 the Gantt chart of a typical turnaround is shown. The positioning times of the vehicles are considered. The shown process chart is idealized in the sense that all processes run without problems and all vehicles and personnel are available when needed. For a typical short flight a full exchange of the cargo is unlikely as the cargo capacity far exceeds the capacity required for passenger luggage. Servicing of lavatories is not included as it usually does not interfere with any other process and can be started as soon as the aircraft is parked.

3.2.8 Conclusion

This section introduced the boarding simulation. It intended to explain the used simulation techniques and especially the special features of the implemented tool. The calibration has shown a reasonable resemblance of actual boarding results, both in the absolute length and in the spread it produces for varied input settings. The results are in tendency too optimistic, by about 20% (see table 3.4), which

is important to remember. The level of complexity is sufficient for the intended purpose. Inclusion of overhead bin model and aisle passing allows a finer differentiation between cross sections.

3.3   Aircraft Design

Aircraft design describes the process in which the various elements that constitute an aircraft are matched to become a viable flying machine. "Aircraft Design" covers the entire process from initial conceptual design up to the final detailed design down to the individual components and final production drawings.

The process elements of aircraft design are described by Torenbeek in [Tor76], especially on the pages 2ff and 16f. Torenbeek stresses that Aircraft Design is an iterative process and characterized by levels of increasing the information on the design. Figure 3.24(a) is a reproduction of a figure from Torenbeek. It stresses the iterative nature and the necessity for a convergence of the design. As stated by Torenbeek, the process applies to many disciplines and is not exclusive to aircraft design.

Raymer ([Ray92], especially page 2ff) highlights that Aircraft Design has no definitive start, but rather is a continuous wheel and the start is defined by the particular design problem or approach. Therefore, a fixed and generally suitable design process does not exist. In figure 3.24(b) his figure 2.1 is reproduced.

(a) Design Process (from [Tor76], figure 1-7) (b) Design Wheel (from [Ray92], figure 2.1)
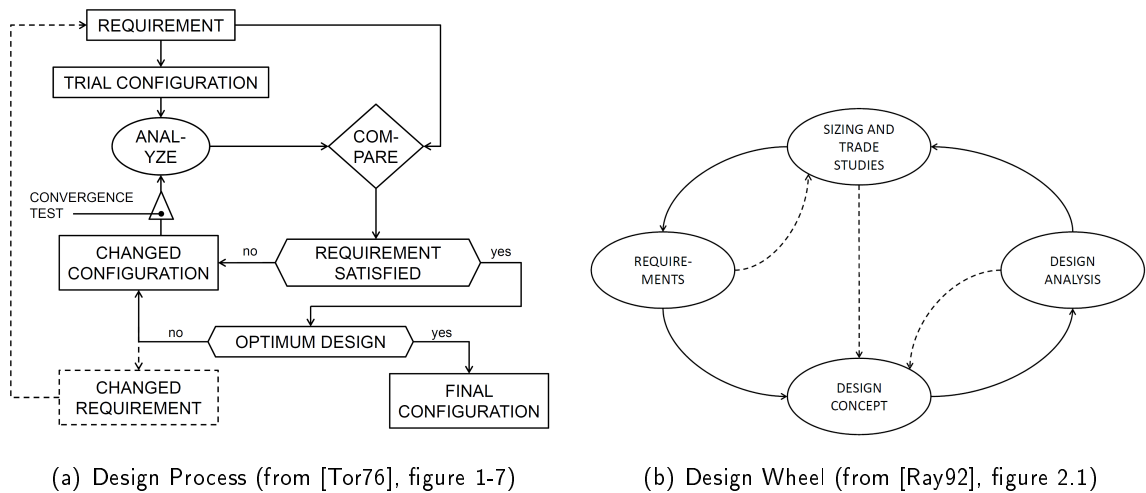
Figure 3.24 – Aircraft design process descriptions from well established textbooks. The left description by Torenbeek can be understood as general engineering process. The right concept of the "Design Wheel" by Raymer is more intended as general approach.

Both authors emphasize the different phases of a design, of which the initial one - conceptual or preliminary design - is covered in this work. In this phase the level of detail is still limited. Only a limited number of physical models are used to generate the required data. There is a stronger reliance on statistical relationships.

The starting point depends on the specific problem. In this particular case the aircraft design evolves from a fixed cabin layout. The fuselage width, number of doors, payload and other related parameters are consequently fixed. Key parameters like wing size and engine thrust need to be estimated according to the required mission range and field performance.

The workflow in this aircraft design process is hence different than traditionally used in many tools, which use the design range and the payload as starting point. Further, in this work a fixed configuration is used, in particular the classic low wing configuration with wing-mounted engines.

3.3.1 Aircraft Design Method

The developed aircraft design method in this work is matched to the required task, and uses features comparable to other aircraft design tools (PrADO [Hei01], VAMPzero [Boe11a]). The applicability is limited to the type of aircraft investigated in this study. That is, turbofan-powered subsonic aircraft with pressurized fuselage, low wing and wing-mounted engines. For this type of aircraft recent methods for mass estimation are used. Aerodynamic methods are at conceptual design level. The resulting sizing process uses take-off field length and mission range to size wing area and thrust. The method achieves a good accuracy when applied to the range of aircraft relevant in this investigation, means it matches the performance and characteristics of the reference aircraft within a few percent deviation.
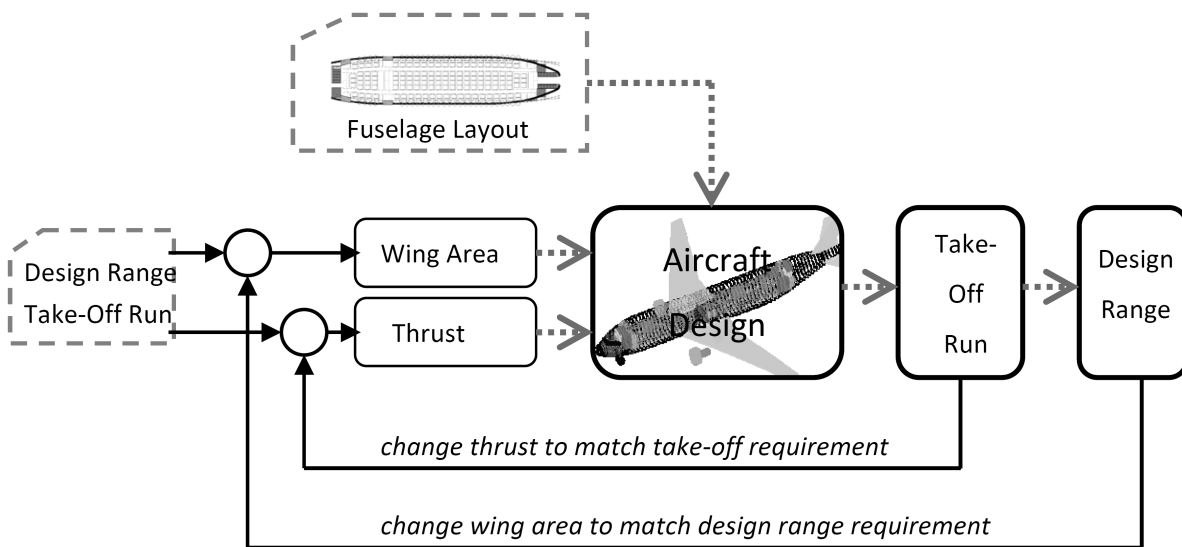
Figure 3.25 – Schematic view of the aircraft design process. The fuselage is fixed, the aircraft design adapts aerodynamic surfaces and engines to the required mission range and take-off field length.

Design Process

The tool sizes two major parameters: the wing area and the engine thrust. The basic design process is shown in figure 3.25. It illustrates the two major iteration loops for sizing the thrust and the wing area. All remaining parameters are either a direct or indirect function. The wing loading at maximum mass is fixed at a chosen value, so that the maximum take-off mass (MTOM) is a direct function of the chosen wing area. The wing's aspect ratio and sweep are fixed, so that any change in wing size leads to a geometrically scaled version.

The approach is valid for a certain set of requirements and parameters. It is no general rule of aircraft design. Parameters that size the engine thrust in cruise are not considered as they are usually no sizing criteria for twin engine aircraft. The take-off distance needs to be defined within reasonable limits, otherwise the design becomes unbalanced due to excessive thrust. The approach further requires that parameters like wing loading, high-lift system characteristics and wing geometry are fixed. This also covers indirectly the approach speed limit. When all parameters are calculated, the mission range with all necessary reserves is calculated. The wing area is changed proportionally to the difference

to the required range. If reasonable start values are chosen, the method achieves convergence within several loops. Masses and aerodynamics are re-calculated in each loop. The individual methods are explained in the following sections.

Geometry Definition

As shown in figure 3.25 the fuselage is fixed in dimensions for the entire design process. Consequently, wing and tail position are also fixed. The wing is a moderately swept and low mounted, equipped with Fowler flaps and slats. It represents the most likely choice for a short to medium range subsonic transport aircraft. The wing loading is set at $600 \ \mathrm{kg/m^2}$, which is the wing loading of the A320 with 73.5t take-off mass [Air88b]. It is important to assume a similar high-lift system to ensure validity of the assumptions for field performance.

The wing area is the iteration parameter. The tail size is changed to provide constant horizontal and vertical tail volume, which are similar to those of the A320. That is, the tail arm multiplied with the tail area is kept constant. This provides that shorter aircraft have relatively larger tail size. The method of constant tail volume is well established as preliminary design method (see for example [Ros04a], page 187f.). Tail size is normally determined by controllability at take-off, especially one engine out lateral control (vertical tail) and minimum unstick speed (horizontal tail). Additionally, static and dynamic stability sizes the tail. In case of the horizontal tail, the size strongly influences the possible operational range of the center of gravity.

The wings planform is determined from its area using a fixed sweep, taper ratio and aspect ratio. The resulting 3-dimensional geometry is relevant for the turnaround analysis, but does not influence the aircraft design process any further.

Masses

The mass estimation represents a very sensitive topic in preliminary aircraft design. Detailed physics based models cannot be used in the preliminary design process for lack of necessary detailed data and the considerable time required for processing. Hence statistical methods are used that roughly match the actual masses of the structural members. The quality of statistical mass estimation methods strongly depends on the data base used for the formula. If the new design is similar to those covered in the database, the accuracy of statistical models is satisfying (less than 10% deviation on average).
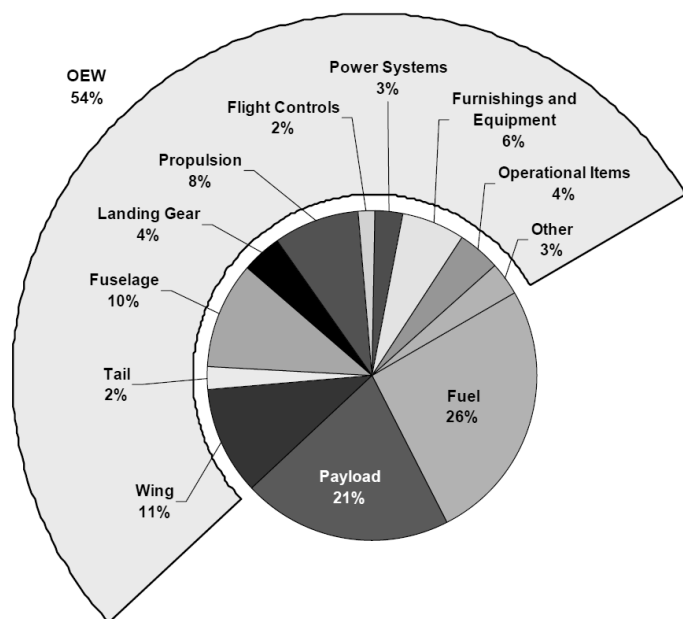

Figure 3.26 – Mass breakdown of subsonic transport aircraft (from [NAS10]). The mass distribution is representative for a current short range aircraft.

A typical operational empty mass break-down of a subsonic transport aircraft can be seen in figure 3.26. It is taken from the Boeing presentation on the Subsonic Ultra Green Aircraft Research program by NASA [NAS10]. It is more in line with state-of-the-art technology than similar breakdowns in textbooks like Torenbeek [Tor76], who uses an older database with the most recent twin jet being an Airbus A300B2[9]. The presented mass break down is for a medium range aircraft in the size of the B737-800.

The fuselage and fuselage's system mass is already described on page 40ff. Further major components are the wing and the tails, the engine, the pylons and the remaining systems (non fuselage systems). For their mass estimation latest statistical methods from the Luftfahrtechnisches Handbuch have been used [Dor11]. These formulas are based on data from all civil aircraft designs since the early 1960ies with special attention given to current aircraft technology. The formulas are listed in table 3.5.

Component	Equation
Wing	$m_{wing} = 2.2 \cdot 10^{-4} \cdot \left[401.15 \cdot A_{wing}^{1.31} + MTOM^{1.104} \right] \cdot (T/C_{rep})^{-0.5} \cdot AR^{1.5} \cdot \frac{1}{\cos(\varphi_{25})}$
Horizontal Tail	$m_{htp} = 12.908 \cdot A_{htp}^{1.1868} \cdot \left(1 + \frac{0.1 - T/C_{rep}}{T/C_{rep}} \right)$
Vertical Tail	$m_{vtp} = 25.056 \cdot A_{vtp}^{1.0033}$
Landing Gear	$m_{gear} = 1.8 \cdot 10^{-3} \cdot MLM^{1.278}$
Engine Pylon	$m_{pylon} = n_{PPT} \cdot 0.2648 \cdot SLST^{0.6517}$
Systems[10]	$m_{sys} = 0.66 \cdot 42.059 \cdot (l_{fus} \cdot d_{fus})^{0.9414}$

Table 3.5 – Formulas for component mass estimation taken from latest LTH publication. See page 134 for explanation of symbols. [Dor11]

The mean error is below 10% for both wing and tails, with all researched designs being well inside the region of applicability of the statistical formula. Systematic errors through these formulas affect all designs in a similar fashion. Structural components like the undercarriage and the engine pylons are also estimated using LTH formulas. The cited LTH paper offers a method that solely depends on aircraft maximum landing mass. A different LTH paper [Bau93] offers a method with more regression parameters, including the landing gear length. However, the landing gear length only affects the mass of the strut, but does not affect the mass of the boogie, the brakes or other components. The strut assembly represents between 40 and 50% of the landing gear mass, and it includes the boogie and the shock absorber. Hence, the landing gear length affects only about one fifth of the landing gear mass. Catching this in a statistical relationship is extremely difficult as design differences quickly obscur the effect of the strut length in the final assembly mass. Consequently, a testwise application of the more sophisticated LTH formula did not result in a particularly good match with current civil transport aircraft.

---

[9]This is the first version of the Airbus A300.

Statistical formulas do not allow to model more advanced technology in a reliable manner. Especially the effect of non-metallic materials in primary structures is not considered with the applied statistics. Hence, the found figures for structural mass are probably conservative. The beneficial effect of non-metallic materials on structural mass is supposed to increase with aircraft size, as larger aircraft require higher stressed materials [Cle70]. The heaviest design in this study has an operating empty mass of close to 90t.

Aerodynamics

For this work only the performance relevant part of the aerodynamics are considered, namely drag coefficient as function of different parameters. The drag coefficient can be expressed as:

$$C_D = C_{D0} + k \cdot C_L^2 \tag{3.3}$$

The zero lift drag coefficient can be broken down into component drag contributions.

$$C_{D0} = C_{D0,fus} + C_{D0,wng} + C_{D0,vtp} + C_{D0,htp} + C_{D0,eng} + C_{D0,res} + C_{D0,par} \tag{3.4}$$

The lift-induced drag is a quadratic function of the lift coefficient. The factor k can also be expressed as:

$$k = \frac{1}{e \cdot \pi \cdot AR} \tag{3.5}$$

with e being the Oswald efficiency factor and AR the aspect ratio. This relationship is valid as long as lift coefficients are moderate.

The aerodynamic parameters required for preliminary design are the maximum lift in the different aircraft configurations, the zero-lift drag of the aircraft, the lift induced drag of the aircraft and finally the wave drag increment at higher Mach numbers. The maximum lift coefficient is of importance for the take-off performance calculation. The value is fixed as the the assumed high-lift system is always the same. The maximum lift coefficient in cruise configuration is modeled similar to that of a current subsonic aircraft.

Component	Symbol	Wetted Surface	Reynolds Number	Friction Coefficient	Zero-Lift Drag
Unit	–	m^2	–	–	–
Fuselage	C_{D0_fus}	432.2	$2.72E+08$	0.00176	0.0067
Wing	C_{D0_wng}	238.3	$2.54E+07$	0.00246	0.0070
Horizontal Tail	C_{D0_htp}	41.4	$1.65E+07$	0.00263	0.0011
Vertical Tail	C_{D0_vtp}	38.6	$1.68E+07$	0.00262	0.0010
Engine Nacelle	C_{D0_eng}	33.2	$1.75E+07$	0.00260	0.0009
Parasitic	C_{D0_par}				0.0008
Residual	C_{D0_res}				0.0012
Total	C_{D0}				0.0186

Table 3.6 – Tool generated zero-lift drag contributions of different components at Mach 0.78 and 31000ft for a A320-sized aircraft.

The zero-lift drag or friction drag is generated by all components of the aircraft. It is proportional to the wetted area of the particular component. It further depends on so called form factors and the local Reynolds number. A brief description is provided both in Torenbeek (page 149ff) and Raymer

(page 280ff). The above described calculation of wing and tail sizes allows an exact calculation of the overall wetted surface of the individual components. The only estimated component is the wing-body fairing and flap track fairing. Both components are estimated using scaled values of an unbuilt aircraft design.

The method is the commonly accepted in preliminary aircraft design. Table 3.6 shows the zero lift drag contributions at Mach 0.78 and 31000ft altitude in standard atmosphere. The resulting drag coefficient is multiplied with a factor to address the parasitic drag. Further the upsweep drag - drag caused by the upsweep of the rear fuselage - is considered by multiplication with a factor. The values are derived from the aerodynamic database of an projected design by then Messerschmitt-Bölkow Blohm (MBB), called the MPC75. Its complete aerodynamic database was available [DAS90].

The pie chart in figure 3.27 shows the zero lift drag contributors at Mach .78 and 31000ft. The residual drag contains the upsweep drag. Fuselage and wing each contribute about one third to the overall zero-lift drag.

The zero-lift drag is a function of both altitude and Mach number. It is still relatively constant over the operational envelope of the aircraft. For Mach number above Mach 0.76 transonic drag rise (or wave drag) is modeled by a fixed drag rise. The actual transonic drag is difficult to determine with preliminary design methods. The starting point - called drag divergence - depends on the wing sweep, wing thickness, and the area distribution achieved by body fairing and flap track fairings. It further is a function of actual lift coefficient. When assuming operation below the maximum Mach number, and further assuming that each aircraft design is optimized aerodynamically for this cruise Mach number, a fixed drag rise can be used. Because at normal cruise conditions the wave drag is a neglectible contributor to the overall drag.
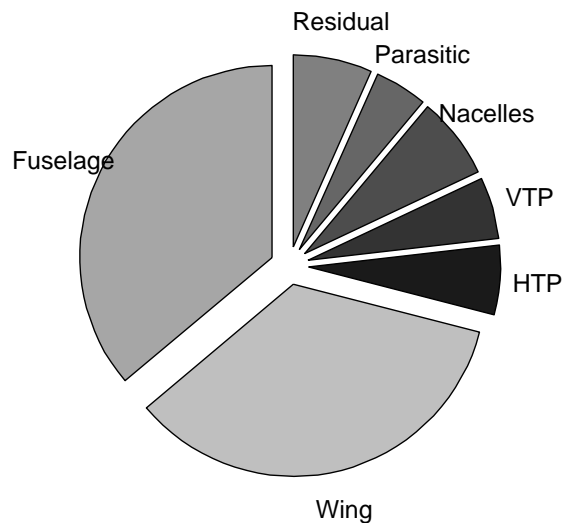
Figure 3.27 – Zero-lift drag contribution of different components.

The Oswald efficiency factor is set at 0.88. This value matches current subsonic aircraft well. The Oswald efficiency factor is a function of the Mach number as well and decreases if the Design Mach Number is approached.

Engine

The engine selected for all designs is a projected geared turbofan engine as it could be expected at the end of this decade. A geared turbofan features a gearbox between the fan and the shaft driven by the low pressure turbine. The gearbox allows to decouple the fan rotation from the low-pressure turbine rotation, and hence allows higher efficiency for both. It also yields some advantages in the

engine layout like a lighter fan shaft and less low pressure turbine stages. However, the gearbox adds mass and mechanical complexity, as well as a power loss. The first generation of the geared turbofan is supposed to deliver a 15% specific fuel consumption advantage compared to current engines (CFM56-5B). The engine is available as an engine deck with fuel flow and thrust for each combination of altitude, Mach number and throttle setting. The model was generated by engine experts using approximate parameters of the Pratt & Whitney Geared Turbofan with state-of-the-art modelling techniques [DLR12]. In figure 3.29 the thrust as function of Mach number and several altitudes is given. It is normalized with the maximum sea-level static thrust. The thrust-specific fuel consumption (TSFC) is the engine's fuel flow divided by the engine's thrust. It excludes power extraction by aircraft systems. The TSFC also depends on actual power setting, lower power settings cause higher TSFC. This is included in the engine model.
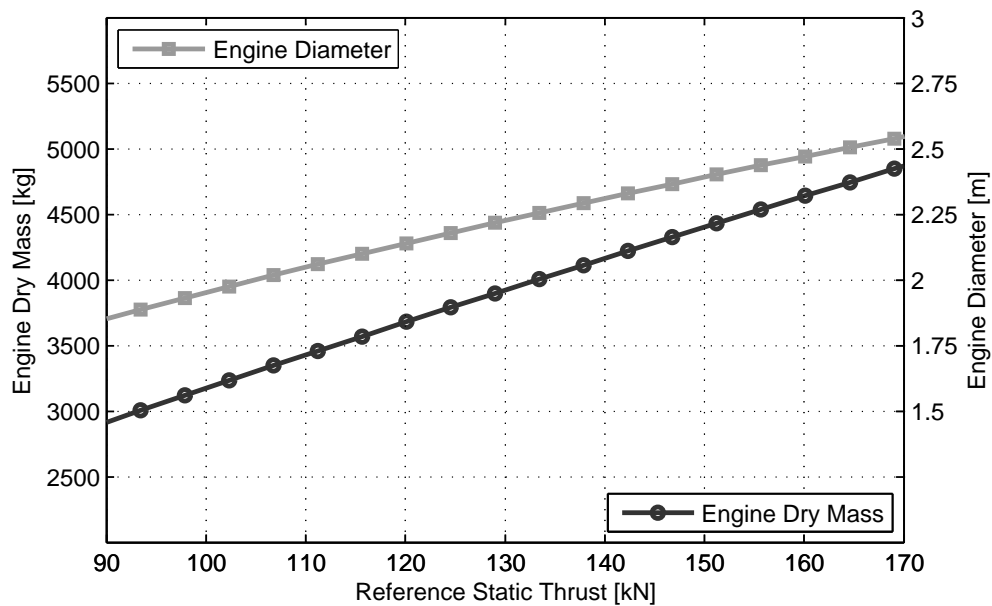
Figure 3.28 – Engine mass and drag as function of thrust. This is supposed to reflect a geared turbofan available in the year 2020. Today's A320 has engines with 120kN reference thrust.

For aircraft design purposes both the engine's physical dimensions and its mass are of importance. The mass adds to the aircraft's operating empty mass, the diameter determines the nacelle diameter and has an effect on the zero-lift drag. The mass is determined using a statistical formula from LTH [Dor11]. The formula is valid for current generation engines, the geared turbofan might be slightly heavier due to its reduction gear box. The overall effect on the aircraft is deemed small enough to neglect, especially as all aircraft designs are affected by it in a similar manner.

The engine's diameter is estimated using a scaling law from Roskam p. 256 [Ros97]. The basic value is taken from public sources about the diameter of the A320NEO engine, which is given with $81\mathrm{inch}$ $(2.06\mathrm{m})$ at a reference thrust of approximately $26000\mathrm{lbf}$ $(115.6\mathrm{kN})$.

Power offtake for aircraft systems is estimated as 5% TSFC increase. That is an approximate value as power offtake changes with flight phase. As secondary power use on the aircraft is not explicitly modeled, there is no influence on the relative flight performance. Fuel flow at idle power is set at a constant 350 kg per hour and engine regardless of the actual reference thrust. The idle fuel flow only affects a small part of the mission performance, so a more detailed analysis does not have an appreciable effect on the aircraft design.

(a) Thrust
(b) Spec. Fuel Consumption
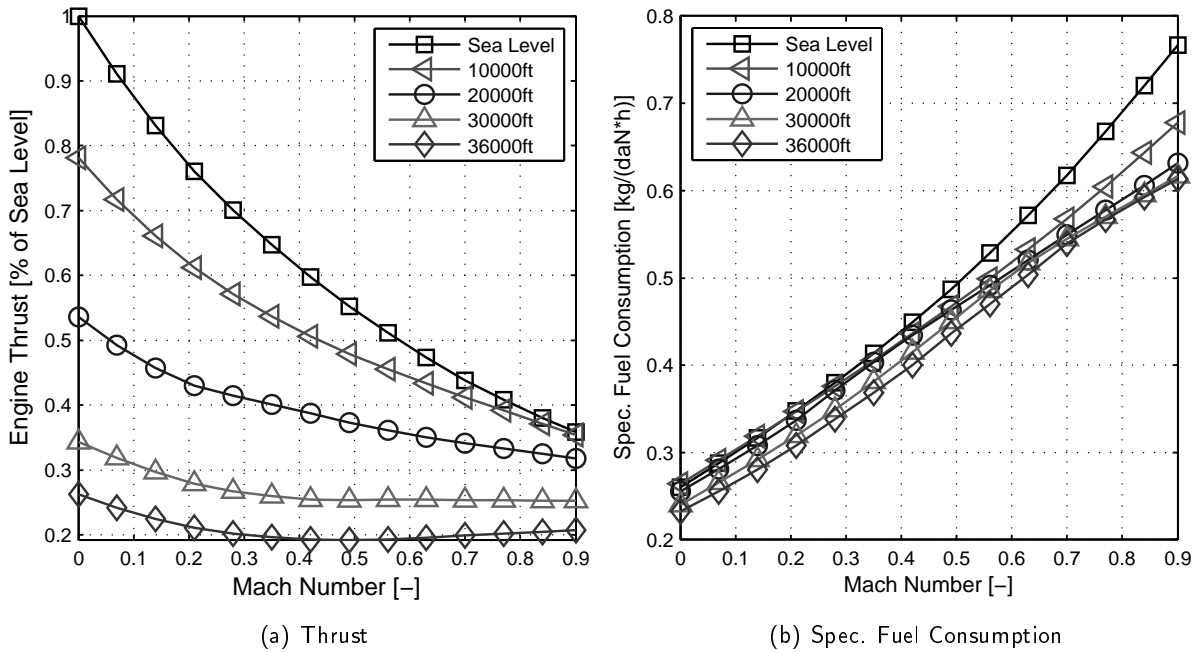
Figure 3.29 – Engine performance model with normalized thrust and specific fuel consumption (SFC). Engine deck was generated with state-of-the-art modeling techniques [DLR12].

3.3.2 Validation

In order to validate the tool an existing aircraft is re-designed. The chosen aircraft is the A320, which is used as reference for many key parameters. Although the projected aircraft for this work are often larger in capacity, they are intended as short and medium range aircraft. Hence similar design parameters apply. This is of importance as some design decisions are different on short range aircraft than on long range aircraft. One is the allowable margin of the center of gravity, having a considerable impact on the size of the horizontal tail. The field performance (take-off distance) of short range aircraft is often better, requiring more installed thrust and a moderate wing loading. That also causes a larger vertical tail volume to compensate yaw moment in case of engine failure, and to provide the sufficient control for cross wind landings.

The aircraft design starts with the fuselage definition. The basic fuselage parameters are taken from the A320, resulting in a passenger count of 167. The wing area and reference thrust is defined to be exactly the same as that of the A320. The tool calculates all remaining parameters, most importantly the mass and drag characteristics. It further adapts a generic engine to the specific thrust requirements. The resulting aircraft is provided as three-view drawing in the appendix in figure A.1.

The validation first concentrates on the mass as key factor in performance estimation. The source of the component masses of the original is the LTH ([Pau93] and [Liu98]) and the weight and balance manual [Air88a]. The original values are limited to two significant digits. As can be seen, most masses are met with satisfying accuracy. Differences are acceptable given the simple nature of the mass estimation formulas. The values for fuselage structural mass, fuselage system mass (part of system), the entire furnishing and operator's items mass are determined using the more sophisticated

methods described in section 3.1.2. The other are estimated using LTH formulas. The structural mass matches well. Operator items show deviation, which is acceptable as the masses assumed for seats and IFE in this work reflect newest technology, resulting in savings in seat mass.

Component	A320 (original)	A320 (redesigned)	Difference
	kg	kg	%
All Structure	22400	21945	-2
Engines	6700	6503	-3
Systems	5400	4959	-8
Furnishings	2900	3016	5
Operator Items	3600	3232	-10
Operating Empty Mass	40900	39655	-3

Table 3.7 – Comparison of major component masses with original masses. Original data taken from [Pau93] and [Liu98]

A detailed drag break down of the original A320 was not available. The resulting performance can still be compared in two different ways: first, the payload range diagram can be compared. The payload-range diagram provides the aircraft's range as function of the payload. This approach has the disadvantage of incorporating many assumptions into the comparison. For example, the actual empty mass used for the payload-range diagram of the original aircraft is usually unknown. The provided diagrams in publically available sources often understate the real operating empty mass. The payload range diagram is further influenced by assumptions on reserves, climb and descent profiles. If the original payload-range diagram is matched, it is still difficult to ensure that not two errors (like a lower empty mass in combination with higher fuel burn) annul each other.
A better indication of the quality of the model is the actual fuel flow for various altitudes and gross weights. This validates both the engine and the aerodynamic model of the aircraft, without having any influence from the masses (which are already validated). The cruise fuel consumption is of crucial importance for overall performance assessment.

Values for actual fuel flow of the original aircraft can be found in Flight Crew Operating Manuals (FCOM) [Air07], which are not public domain but generally obtainable. The chosen aircraft is an A320-214 with CFM56-5B4 engine. The model description "214" indicates the aircraft model in the first digit, the engine manufacturer in the second digit and the engine subtype or variant in the third digit. A specific operators empty mass is not available from the FCOM, but as fuel consumption at fixed flying masses are compared, the actual empty mass is without relevance. The relevant part of the FCOM is chapter 3.05, which has tables for climb, cruise and descent for various masses and altitudes.

In figure 3.30 the original values (taken directly from FCOM tables) and the results of the model are compared. The fuel flow is shown over the gross mass for three different altitudes. The most relevant area is between 60t and 72t gross mass. This region shows a good resemblance. Deviations in the lowest line (37000ft altitude) is caused by increasing lift coefficients. The application of a constant factor as shown in equation 3.5 is not valid for high coefficients any more.
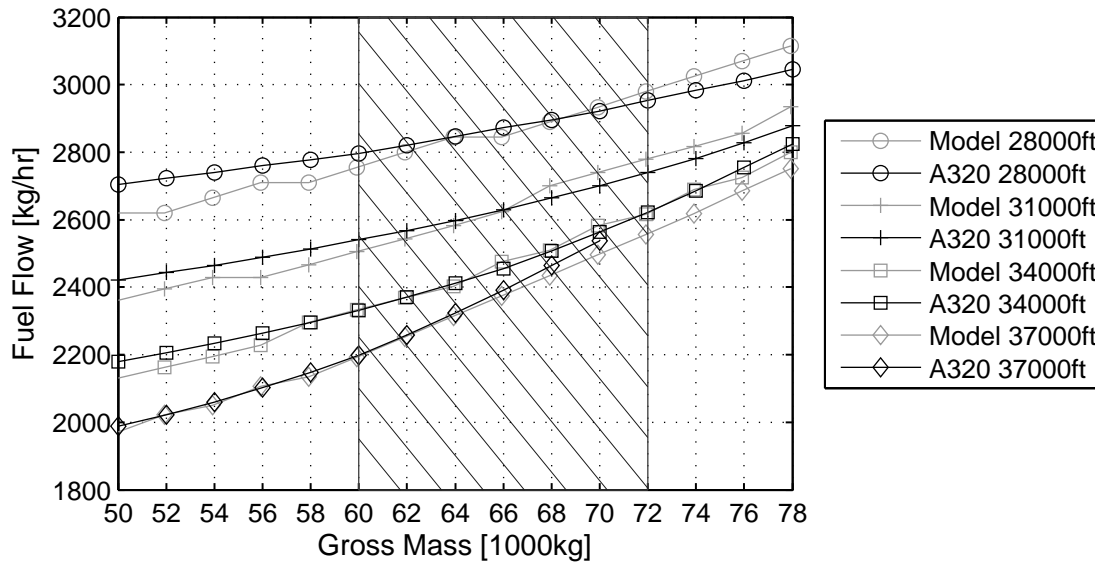
Figure 3.30 – Comparison of modeled and actual fuel flow at various altitudes and masses at cruise Mach number. With exception of high masses at high altitudes (high lift coefficients) and very low lift coefficients a good match is achieved. Hatched region marks the most relevant region.

The sizing routine is validated by generating an A320-like fuselage and defining similar mission requirements. If the sizing is successful the wing area and key parameters should be matched. The payload range diagram from the ACAP document is used as reference [Air95] for the design range. The empty mass in the document is much lower than can be realistically be assumed. Using a more realistic source the range at maximum passenger payload is given with roughly 1800nm for the 73.5t variant [Air05]. The field length is given with approximately 2000m. When sized to this design mission the resulting wing area matches the original with a 1% deviation. This is also due to the calibration of many methods with A320 data. The same is attempted with a model similar to the A330-300, with slightly increased wing loading corresponding to that of the A330-300 with 233t MTOW ($640\mathrm{kg/m^2}$), a mission range of 4800nm and 3000m field length, the wing area deviation is below 3%. Both indicates that the sizing routine - although limited in its applicability - produces very good results in the desired region.

3.3.3 Conclusion

This section introduced the methods used for aircraft design. The techniques are simple but wherever possible recent data was used to check the quality of the result. The entire process does not follow strictly to one textbook, but rather picks elements of different approaches and jumps in the detail-level of the used models. The validation using real life data at a level that allows component mass comparison (instead of overall mass) and detailed fuel burn comparison instead of the match of a payload-range diagram boosts the fidelity in the results. The focus of the tool and methods allows a very good match within the desired region. The resulting performance data, which are essential for the competitive analysis of single and twin aisle, can be given a high level of trust.
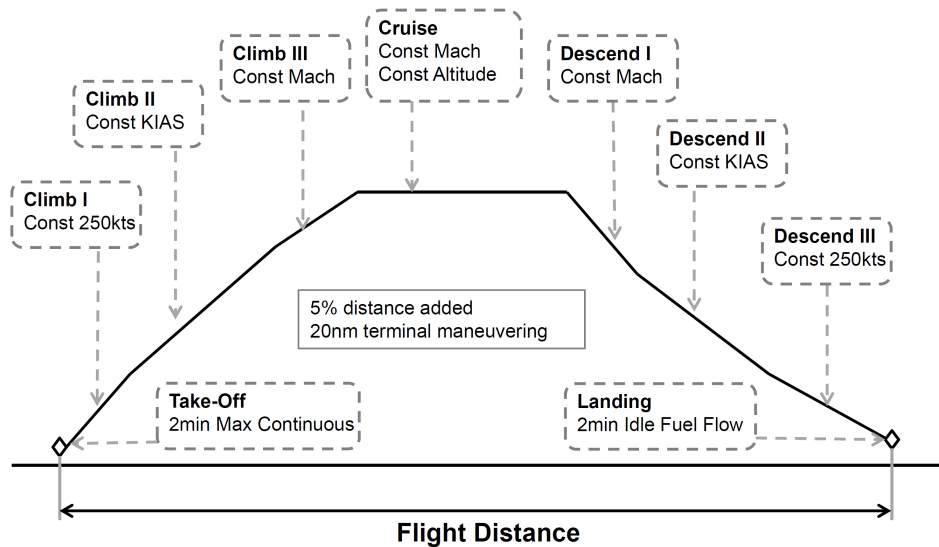
Figure 3.31 – Flight Profile for Mission Performance

3.4 Mission Performance and Cost Estimation

This chapter briefly explains the evaluation of the mission performance and the subsequent cost estimation. Both topics are well covered within several text books (see [Ros97] for step-to-step procedures) and only the key features are explained here.

3.4.1 Mission Performance

Mission performance estimation is critical to assess the fuel burn difference between the various designs. The mission assumptions are listed below and shown in figure 3.31. The techniques used for the performance estimation are taken in maority from Roskam's "Airplane Aerodynamics and Performance" [Ros97]. These are amended with further sources for current operating procedures in form of Airbus publications [Air11a] and [Air11b], which are addressed at flight crews and airline performance engineers, who are professionally estimating the fuel burn for actual aircraft missions.

- 2 minute maximum continuous thrust at take-off, no distance credited for take-off and initial climb,

- climb from 1500ft to 10000ft at 250 KIAS,

- climb from 10000ft to transition altitude[11] at 290 KIAS,

- climb from transition altitude to cruise altitude at cruise Mach,

- cruise at optimum altitude at constant Mach,

- descend down to 1500ft in a profile similar to that of the climb,

- final approach and landing modeled as 2 minutes of idle fuel flow, no distance credited for final approach.

---

[11]Transition altitude is the altitude where the desired Mach number is reached and climb is continued at constant Mach number.

Reserves are considered with a 200nm alternate airport at a maximum cruise altitude to alternate of 20000ft without consideration of the descent. Holding is set as 30 minutes at 5000ft. Fuel burn due to taxi at the airport is not considered. 5% of the given cruise distance is added as non-optimum routing and 20nm are added for terminal maneuvering (Standard Arrival Route). These settings may not entirely reflect the conditions found in short range operations, but all designs are affected in a similar way. Very short flights only consist of climb and descent. These assumptions are also used in the aircraft design process for the estimation of design mission range. The aircraft is always free to climb to its best cruise altitude, which is usually the highest achievable altitude. No step climbs are considered, as they have no particular relevance for short range operations.

3.4.2   Cost Estimation

The cost estimation covers the direct operating costs (DOC). These cost describe all expenditures connected directly to the operation of a single aircraft, usually over the period of one year. The direct operating cost can be separated into the cash operating cost (COC) and the ownership cost. In this work the potential of additional flights through reduced turnaround time is investigated, thus the full direct operating cost need to be considered. Additional flights split the cost of ownership over more flights and hence reduce the costs of a single flight, even though the cash operating cost might increase.

Methods for DOC estimation are numerous. The results can differ substantially depending on the used method. Key influential contributors of DOC are listed in Clark's "Buying the Big Jets" [Cla07], who describes the cost in a manner more closely related to actual operational conditions.

- Fuel cost, these represent between 20 and 30% on short and medium range operations with growing importance due to increasing oil prices.

- Cost for financing and depreciation. These cost items can be added to represent a leasing rate, a charge a leasing company imposes on an operator for using the aircraft. Although the leasing rates are market driven rates, the cost is ideally proportional to the cost of financing the aircraft plus a profit margin. Clark reflects in more detail on this issue (p. 186). For this study a constant rate is assumed over the assumed initial operating period of the aircraft.

- Flight crew, both cabin and flight deck.

- Maintenance expenditures, often separated in airframe and engine maintenance. These cost are often separated into flight time dependent cost, flight-cycle dependent cost and a proportional maintenance burden for the provision of maintenance facilities and personal.

- Fees for navigation, airport usage and ground handling.

Depending on route profile, region and individual airline arrangements the cost structure can vary substantially. Models exists that help to evaluate costs in a theoretical yet representative manner. It is reminded that in reality two different operators using the same aircraft over the same route may experience very different cost due to labor agreements, modes of aircraft finance and economy of scale in maintenance and training. Hence all DOC methods represent models for comparison, the absolute values cannot be compared to real life costs. Most methods use regression as mean for the cost estimation.

Two different cost models were evaluated:

1. The **Liebeck or NASA Method** introduced by Liebeck [Lie95]. The method uses regression formulas for maintenance cost, both airframe maintenance and engine maintenance. The same applies to the cabin and flight crew cost. The database is early 1990ies and is corrected to year 2007 level by applying a price escalation of 3.5%.

2. The **Thorbeck Method** as described in [Tho01]. The method uses a similar approach with different regression parameters. Its slightly more recent and stronger reflects European airlines.

The Thorbeck method includes a model for ground handling cost. The NASA Method only considers navigation charges and landing fees. In order to estimate the accuracy of both methods, a reference case is generated. An aircraft with the physical fuselage dimensions of the A320 is sized to 1800nm range at full passenger payload of 173. The resulting aircraft strongly resembles the A320 (73.5t MTOW). The cost are estimated for a 500nm mission over an entire year. Both cost models are given similar assumptions and yearly flight hours and utilization. The following table summarizes the key assumptions for the comparison (assumptions later used for actual calculations are slightly different and described separately).

Interest Rate for Finance	7%
Operating Period	12 years
Residual Value	20%
Yearly Flights	2148
Yearly Flight Hours	2828
Flight Attendants	4
Fuel Price	.69 USD/kg
Year	2007

Table 3.8 – Assumptions for DOC Calculation

The interest rate, operating period and residual value corresponds to a monthly lease rate of approximately 0.93%. The fuel price corresponds to a crude oil price of roughly 80 USD/barrel, which was the 2007 mid year price level. Thorbeck considers ground handling costs [Tho01]. To have consistent cost items, all charges are ignored for the comparison.

The two different methods demonstrate a largely similar picture. The biggest difference are the cost of the flight crew, which is about 50% higher in the Liebeck method. Liebeck uses a regression for the entire crew cost, while Thorbeck assumes a number of flight crews and multiplies these with the average salary. Thorbeck assumes 5 flight crews per aircraft. Liebeck uses salaries of US main line carriers of the early 1990ies. The used escalation factor is probably not representative for the average salary increase over the last 15-20 years. The Liebeck method is used for cost estimation in this work. It appears more applicable due to its more sophisticated maintenance module, that differentiates better between trip and flight hour dependent cost. The method for navigational charges is kept, but the methods for landing fees and ground handling cost are replaced by a separate module, as the significance of these charges is high for short range operations.
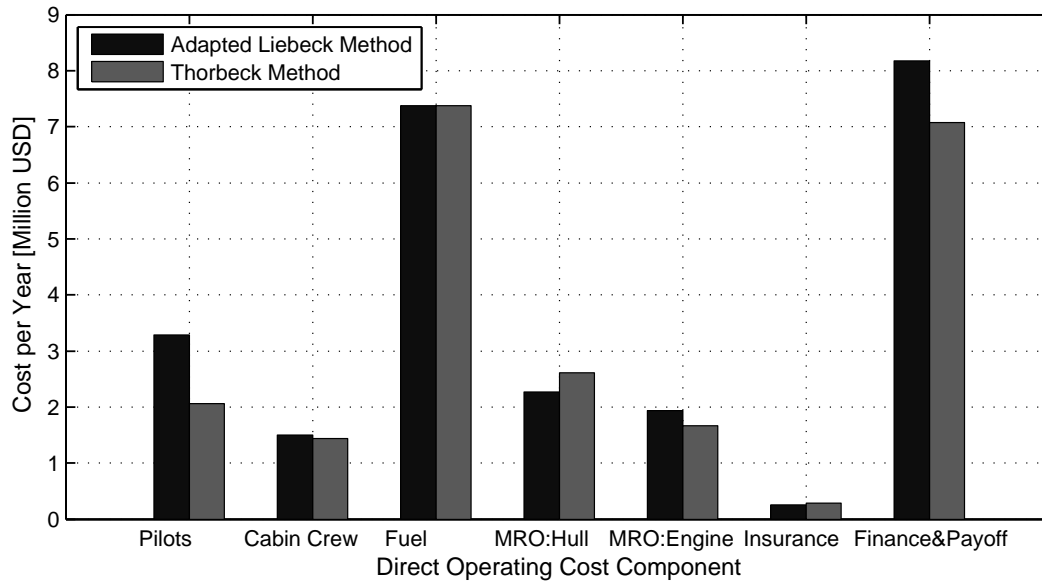
Figure 3.32 – Comparison of methods for direct operating cost calculation: Liebeck and Thorbeck method results with similar input settings.

3.4.3 Ground Handling Cost Model

Landing fees and ground handling charges usually represent a small proportion of the overall cost of operation. Landing fees depend on the official maximum take-off mass of the aircraft, regardless of the true gross weight for the particular flight. Ground handling cost are charged for loading and unloading, as well as rental for the park position, servicing, push back and ramp agent service. While landing fees are charged by the airport, ground handling is provided by independent entities. The charged prices are subject to negotiations and can vary widely. Still, in order to capture the effects of shorter turnaround a cost-based model is created. That is, the cost of the service provider is estimated and based on this the charged price to the airline is calculated. The assumption is that lower cost for the provider will result in better prices for the airline in a competitive environment with several ground handling service providers.

The ground handling cost can be estimated by assuming time-dependent costs for the vehicles and the bound man power and multiplying these with the turnaround time. However, the service provider cannot utilize his equipment and labor the entire day. He also has to keep flexibility for possible delays.

Turnaround Time ...	
... independent	... dependent
push back	bridge and gate charge
water & waste servicing	cargo loading
cabin cleaning	ramp agent
refueling	
external power	

Table 3.9 – Cost Items Ground Handling

The items in the left column are occupied for a given time, minimum 20 minutes (to allow for schedule flexibility). Cabin cleaning is depending on the number of seats and applied man power.

Again, the net period is extended by 15 minutes to provide for schedule flexibility. The turnaround depending cost are calculated as actual turnaround time plus 20% time reserve. Overhead cost and yearly utilization are included in the vehicle cost. Source for vehicle and labor cost are unpublished values for the prices of vehicles and typical hourly rates for ground handling staff. The landing fees are taken directly from the current (2012) fee system of the Hamburg Airport [HAM11]. The noise category of current A320 is assumed (Noise Chapter 4). The results for a 70t MTOM aircraft in dependence of the turnaround time can be seen in figure 3.33. Passenger service charges (security, baggage sorting, check-in counter) are not including and not considered in this work.
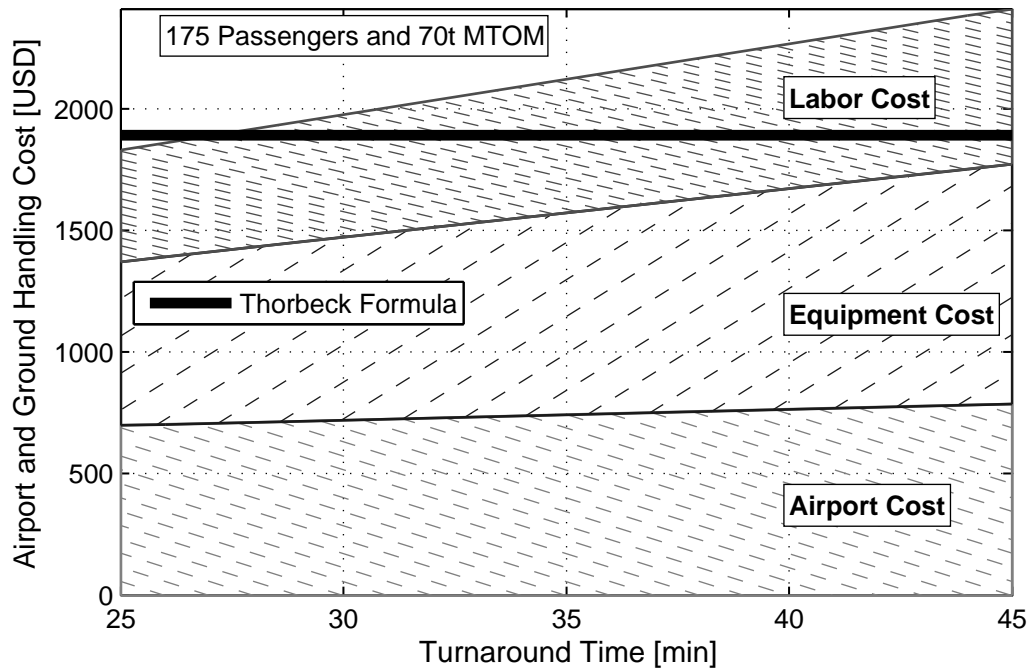
Figure 3.33 – Cost of ground handling and airport usage as function of turnaround time. The straight line represents the Thorbeck formula, which is no function of the actual turnaround time.

The airport cost (bottom) are only a weak function of the turnaround time as the majority of charges is landing fee. The gate and bridge rental is small compared to these. The ground handling cost demonstrate a stronger dependence. The overall difference between the maximum and minimum time is 600 USD. Although this might appear as small amount, the difference is sufficient to buy roughly 750kg of fuel at 0.80 USD/kg. A line in the graph shows the formula by Thorbeck, which has a mass and payload dependency. Hence, it appears as constant line in this graph. The overall pricing level of the developed method is close to Thorbeck's value. The slightly higher cost base causes it to be higher for the majority of turnaround times.

The real drivers of ground handling cost are changes that reduce the number of required personnel or equipment. In fact, in short range operations it might be more economic to stick to bulk cargo and save the cost of the container loading vehicles.

Chapter 4

Designs and Results

This chapter introduces the cross sections and cabin designs for the subsequent analysis. The analysis results are provided for each discipline, that is: the cross sections and cabins, the resulting fuselage masses, the boarding simulation results and the aircraft design results including the flight performance. An analysis is provided in the next chapter.

The chart in figure 4.1 provides an overview of the studied layouts. As stated initially, the question is not only whether a twin aisle is more efficient at a certain capacity, but the question is equally which type of twin aisle is the most suited then. Additionally, the type of single aisle for reference is important. For this purpose 5 different cross sections are analyzed. The number of passengers covers the entire capacity range of single class capacities found on 6-abreast single aisles today: 130 seats[1] to 280 seats[2], and continues up to 340 seats. The three intermediate cross sections are self-created, the smallest and the largest cross section are reproductions of actual aircraft. The following pages will further explain the cross sections and layout principles for the resulting cabins.

4.1 Cross Section and Fuselage Layouts

This section introduces the cross section layouts and fuselage designs for the later analysis. Major assumptions and design rules are explained first, that followed the 5 cross sections are briefly described.

4.1.1 Cross Sections

Figure 4.1 already provides a visual impression of the five chosen cross sections. As explained on page 16 the cross section diameter is a function of the seats abreast and the chosen size of aisle and seats. The current standard found on A320s is an 18inch (46cm) wide seat. This seat width can also be found on most long range economy class cabins. The A320 allows installation of an 19inch (measured at floor level) aisle with these seats[3]. The B737 with its cross section dating back from the B707 provides smaller 17inch seats [Boe05a]. The A320 dimensions are taken as basis. Due to demographic changes future aircraft might feature wider seats to improve comfort. However, the current seating standards are kept in this work to allow a appropriate comparison to the actual reference. Increased comfort standards would simply raise the the level without changing the relative difference

---

[1]B737-600, A318

[2]B757-300

[3]Airbus also offers smaller seats and a wider aisle [Air05]
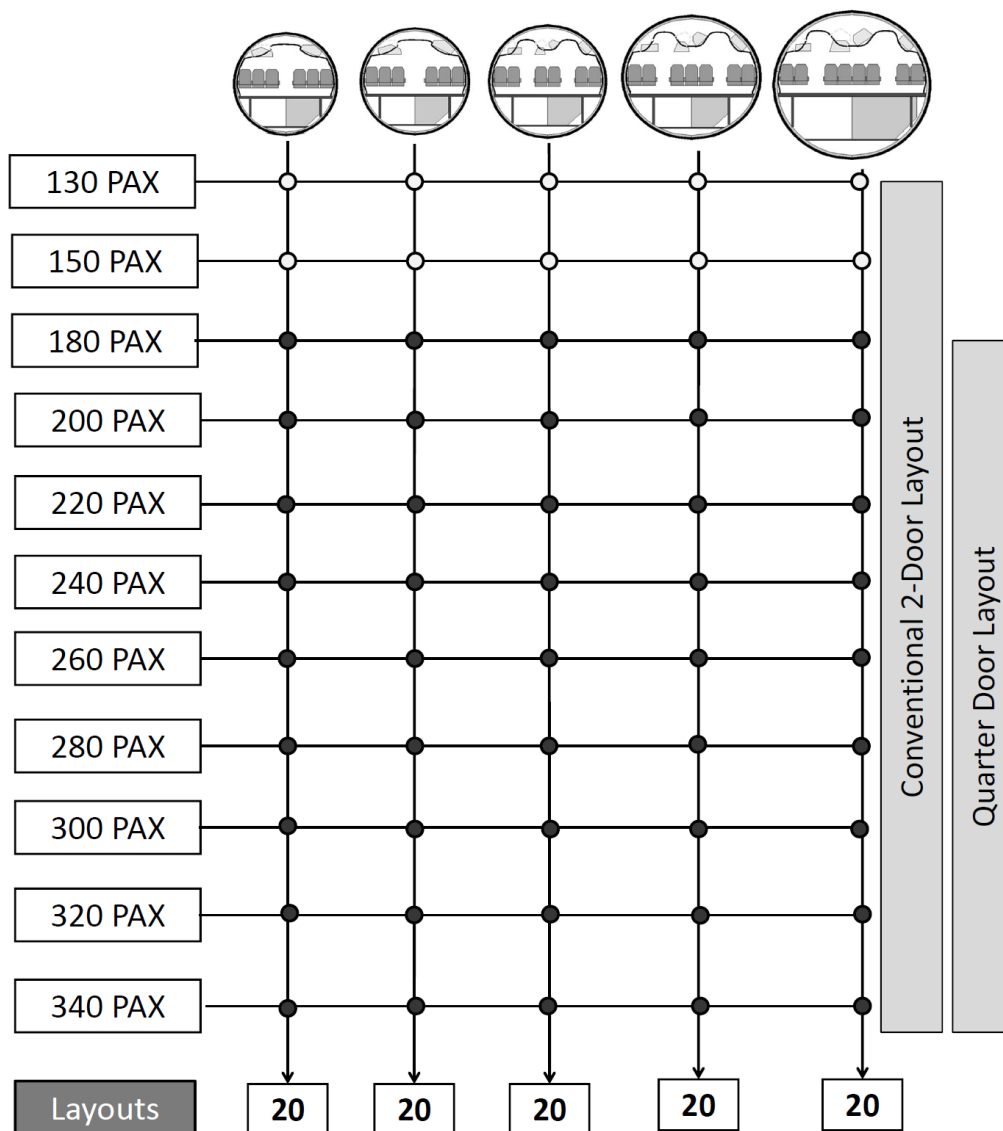
Figure 4.1 – Illustration of all studied layouts. Capacities below 180 passengers cannot support a quarter door. Beyond 280 seats all designs require a second door in front of the wing, so that 2-door and quarter door layouts are basically identical. See also page 137 for plots of the cross sections.

in a noticeable manner.

The cross section width is determined by the required width at armrest level. The height may be determined by several competing requirements (cabin height, curvature of side panel, cargo hold height), but for stress-optimal layout the height needs to be within 5-10% of the width. Otherwise substantial weight penalties occur in pressurized fuselages. The standard A320 carries a so-called LD3-45W[4] container. The "LD3" means it has the same baseplate width as the widebody LD3 container. The "45W" denotes the height of 45inch and the added width. This container size has become a standard and would also be used on newer single aisles or small twin aisles. The 8-abreast represents the original A300 cross section with capability of loading the standard widebody LD3 container. Using a smaller container would mean a significant deviation from the circular cross section, and hence would yield no mass advantage. Cross sections usually consist of several pieces of circular

---
[4]Also known as AKH.

profiles. In this work non-circular cross sections are modeled as ellipse. No detailed cross section shaping is performand as the exact cross section geometry has no influence on the mass estimation and the difference in effective cabin space is neglectible. In the following all cross sections are briefly described, plots can be found in the appendix on page 137.

The cabin lining layout is inspired by today's cabins. Figure 4.2 introduces the most important dimensions. The layout allows a standing height of at least 2.1m in the aisle and is at least 1.6m above floor level where seats are placed. The overhead bins leave sufficient room for passenger service units (like individual air outlets) and attachment structure. Overhead bins do not protrude into the aisle. They are further supposed to be pivoting bins, like found in modern cabins. For the later boarding simulation the shaping is not considered, only the volume.
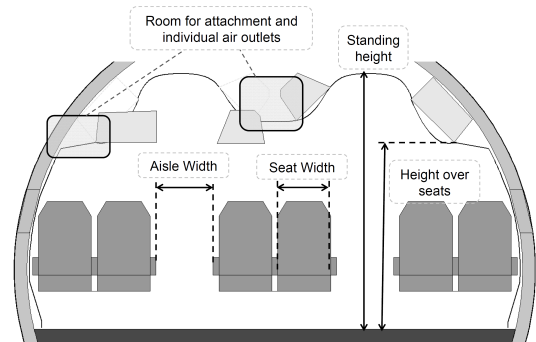

Figure 4.2 – Key cabin dimensions for cross section layout. Note the overhead bins in retracted (right) and extended position (left).

1. **6-Abreast Single Aisle - Reference Design**: This cross section resembles that of the A320 in height and diameter.

2. **6-Abreast Advanced Single Aisle - Future Single Aisle**: this cross section features a wider aisle, resulting in a fuselage width of 4.16m. As a result, overhead bins are slightly larger, too.

3. **6-Abreast Twin Aisle - Small Twin Aisle**: Compare with the concepts shown in figure 2.9 on page 24. The analyzed twin aisle aisle is restricted to 6-abreast seating, resulting in a 4.5m fuselage diameter and 4.3m fuselage height.

4. **7-abreast Twin Aisle - Intermediate Twin Aisle**: Different than the B767 the cross section is restricted to 7-abreast seating. The reduced height leads to a slight elliptic layout. The diameter is 4.95m, the height 4.65m.

5. **8-abreast Twin Aisle - Full Size Twin Aisle**: This is the actual A300/A330 cross section. Although no real alternative in the focused seat range, it allows to estimate the suitability of current twin aisles (the B787 is only slightly wider than the A330) for this type of operation.

4.1.2 Cabin Layout

As briefly described on page 39 the cabin layout starts with monument placing. The objective is to have comparable comfort standards for all different designs. Besides the seat width this includes seat pitch, number of lavatories and galleys. The seat pitch is set at 30inch (76cm). This appears small but the seats are also assumed to be very slim. The cabin standard is oriented on the Neue Europa Kabine (New Europe Cabin) of Lufthansa [LH10]. It can be expected that these standards will prevail over time in short range optimized cabins. Galley and lavatory ratios are set according to short range standards, which hardly see any meaningful meal service. There are never more than 70 passengers

for a single lavatory and at least 1.5 trays per passenger. Even without any meal service, the beverages and other consumable items require some galley volume. The galley standards are exceeded considerably in the smaller capacity aircraft as front and rear galley are always installed. The twin aisles each have a different aft galley arrangement. This is of importance as poor galley layout wastes floor area and hence increases fuselage mass.

The main exits are placed at the front and aft end of the fuselage. They are symmetric in location and type. When capacity increases overwing exits are added. If capacity increases further emergency type exits are placed in front and aft of the wing, if necessary in combination with overwing exits. The 7- and 8-abreast twin aisle utilize a full size entry door (type A), while all other use type B entry doors. For all capacities starting at 180 passengers an alternative version is created. It has an additional door placed at roughly one fourth of the fuselage length. This door is commonly called quarter door. It is not a limited size emergency exit but a fully functional boarding door. The quarter door has a beneficial effect on boarding times as shown later and also recognized in the Boeing study [Mar98]. The principle is shown in figure 4.13 on page 99. However, it increases the length and hence the mass of the fuselage below a certain capacity. Above 280 seats capacity all aircraft require an additional exit door which can be used as Quarter Door with little or no mass penalty.
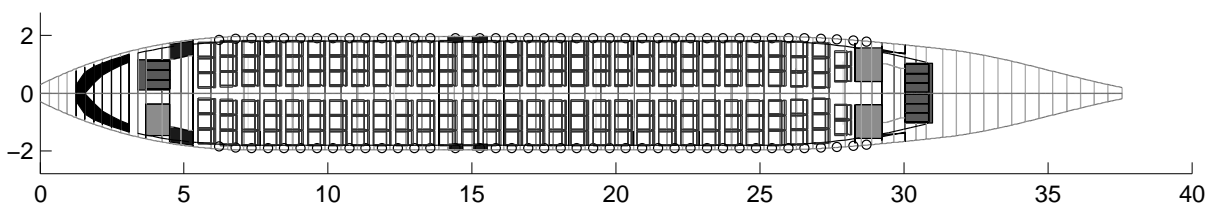
(a) Conventional Design
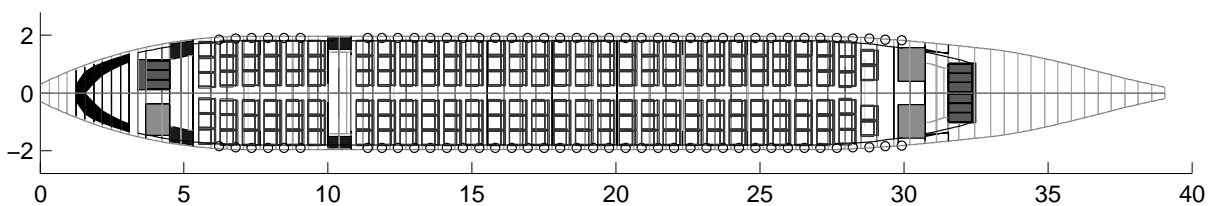
(b) Quarter Door Design

Figure 4.3 – Cabin of 180-Pax Single Aisle with and without quarter door.

4.1.3 Fuselage Layout

The fuselage is generated using similar design criteria for all models. That is, the length of the aft and front section is relative to the diameter, providing a longer constant section for designs with smaller fuselage diameter. In figure 4.4 the regular single aisle and the full size twin aisle are compared. The capacity is 180 passengers, the single aisle is hence closely comparable to the A320. The full size twin aisle has a substantially shorter cabin, but due to the required aft fuselage length the overall fuselage length remains nearly the same. The fuselage could be shortened by placing the rear bulkhead further aft. However, the much confined cabin width reduces the value of this added floor area and

the necessity for pressurization increases structural mass. Rear fuselage design is a multi-disciplinary optimization task in itself.

The lower deck compartment or cargo hold is not specified in length but depends on the cabin length. All designs have sufficient volume for the passenger's bags. Some designs have surplus capacity that allows loading of additional revenue cargo. Although this represents an advantage for the operator, no extra credit is given for surplus underfloor capacity. Cargo represents an important contributor of revenue for long range flights, but is of lesser importance on short range flights. The landing gear bay is placed behind the wing box.

(a) Regular Single Aisle

(b) Full Size Twin Aisle
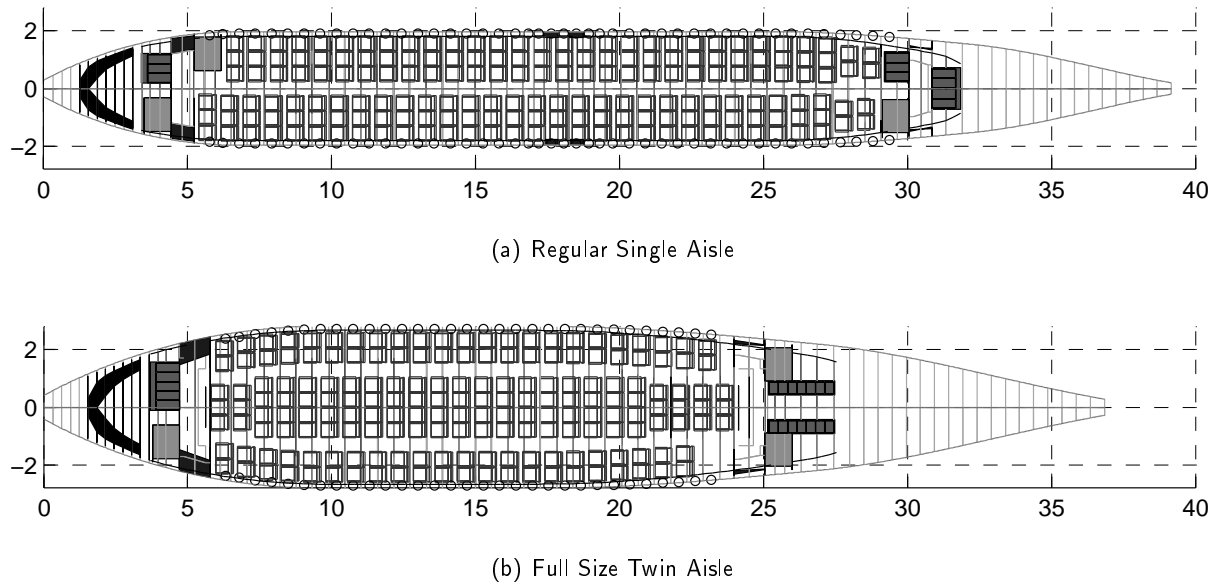
Figure 4.4 – Comparison of fuselage layout for regular single aisle and full size twin aisle, both with 180 seats capacity. Although the cabin is substantially shorter, the overall fuselage length is nearly the same due to rear fuselage layout.

4.1.4 Results

The fuselage sizing process provides a fixed length for each combination of capacity and cross section. The actual number of passengers usually deviates from the planned capacity because the capacity can only be reduced by full seat rows. In consequence the 180-seat designs have between 179 and 186 seats. Most values are given per installed seat, so such differences are not changing the relative advantage of a design. Total values are corrected with a factor that credits advantage for layouts with more than the specified seating.

$$f_{corr} = \frac{PAX_{Specified}}{PAX_{Actual}} \tag{4.1}$$

A choice of parameters is presented on the following pages. The shown parameters are deemed most relevant for later performance estimation. Different than in the initial chapter (see page 16) each layout is an individual composition. Leaps may occur as doors are added between two capacities. Some layout may experience unfavorable galley and lavatory ratio as they are just above a threshold. That explains much of the unevenness displayed in the following plots.

(a) Fuselage Length   (b) Fuselage Fitness Ratio
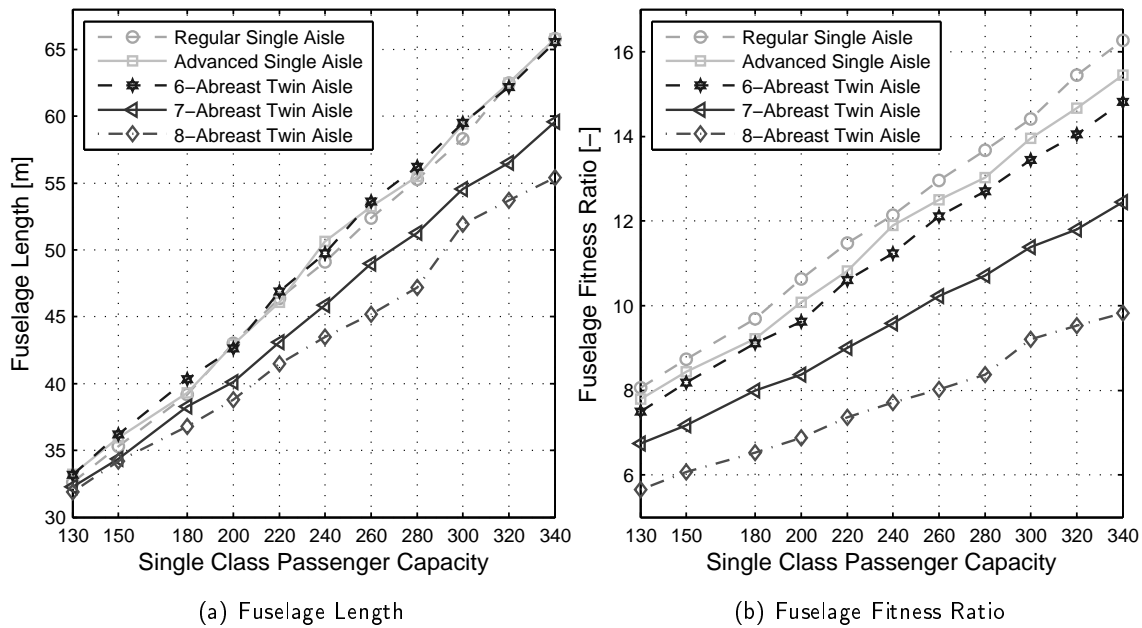
Figure 4.5 – Length and fitness ratio of designed fuselages for different cross sections and capacities. The length diverges for larger capacities. Fitness ratios reach more than 16 for the large single aisles.

The length is shown in figure 4.5(a). The length is nearly similar for the small capacity versions irrespective of the cross section, but with increasing capacity the wider aircraft are substantially shorter. The difference becomes apparent above 200 passengers. The maximum length of the single aisle is just over 65m, still leaving a comfortable gap to the maximum allowable length of 80m. An 80m single aisle would have an approximate capacity of 430 passengers. Theoretically, the fuselage length growths linearly with capacity (compare equation 3.1 and 2.8). But additional exits cause the length to grow stronger between different capacities. This effect is more pronounced for twin aisles. The 8-abreast has a very pronounced leap between 280 and 300 seats as an additional exit is added. This leap is even more visible at the structural mass.

The fuselage fitness ratio is the relation of length to fuselage diameter as explained on page 14. The fitness ratio is shown in the right hand plot. The highest fitness ratio in an actual aircraft has been 14.2 on the DC-8-61 [MDD89]. In contrast, the largest single aisle in this study achieves a fitness ratio of 16.1. On the lower side, the lowest fitness ratio in the investigation is just below 6, compared to a historical minimum of 7.1 of the Boeing B737-100.

The fuselage mass is shown in figure 4.6(a). The single aisle has the lowest fuselage mass up to roughly 310 passengers. Then the 7-abreast has lower structural mass per seat. The other plot shows the same mass divided by the cabin area and as function of the fitness ratio. Passengers require floor area, therefore the cabin area is the best indicator for passenger capacity. The plot shows that an optimum exists at a fuselage fitness ratio between 11 and 12. This is mass per cabin area. The 6-abreast twin aisle fares best as it has lowest area-specific payload. When the structural mass is shown per seat instead of cabin area, the standard single aisle is the most efficient, see figure 4.7(a). It remains the most efficient design until 300 seats, when the 7-abreast has lower mass per seat. Compare this plot to the one provided on page 21. The usage of a statistical formula puts this limit at 280 seats. This difference is not only reasoned by the different method of mass estimation, but

(a) Fuselage Structural Mass

(b) Structural Mass over Fitness Ratio
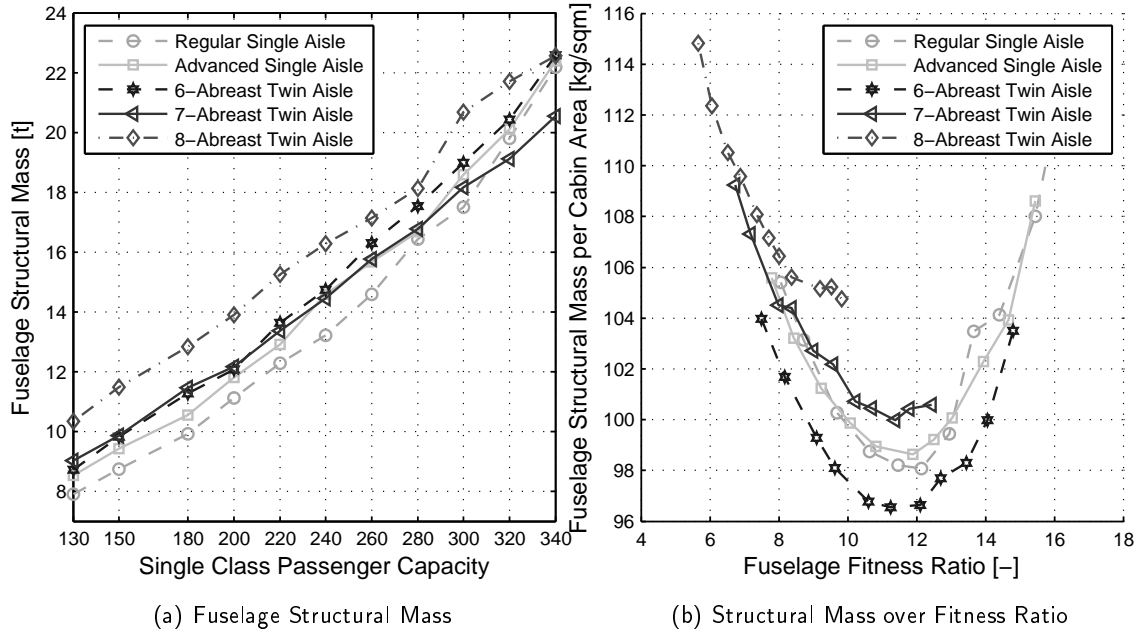
Figure 4.6 – Fuselage structural mass over passenger capacity. Left side shows mass divided by cabin area over the actual fitness ratio, clearly showing that an optimum exists in the area of 11-12 for a given cabin area.

also by the substantial differences in fuselage length when a real layout is created versus a rough estimation of the fuselage length as performed in section 2.2.

(a) Structural Mass per Seat

(b) Operating Empty Mass per Seat
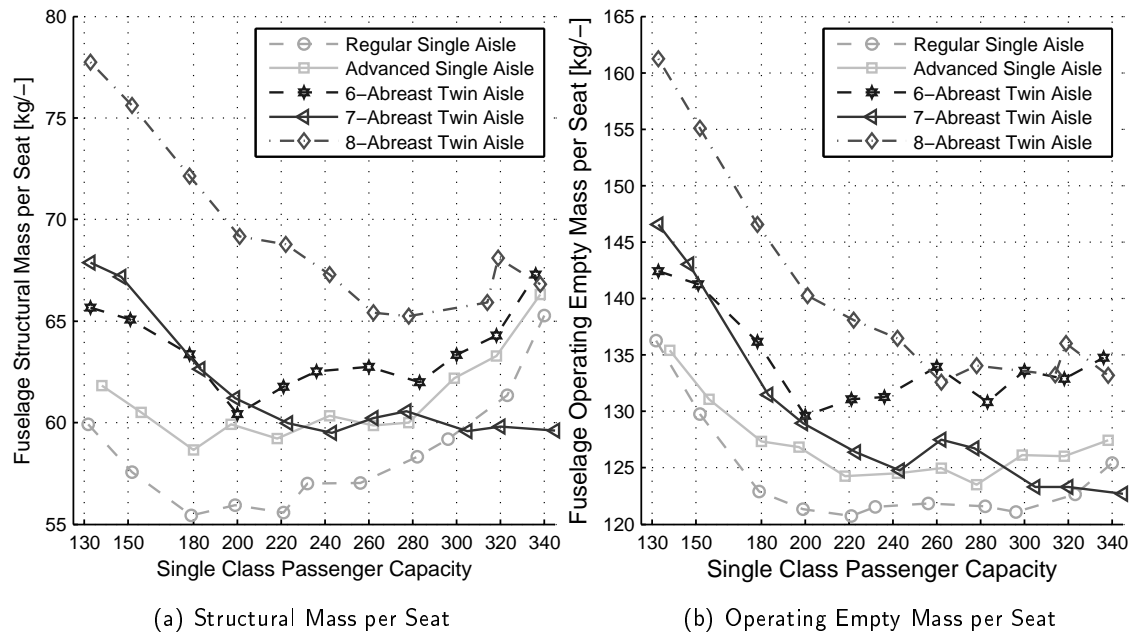
Figure 4.7 – Structural and operating empty mass per seat. Compare to figure 2.7. The operating empty mass of the fuselage includes furnishings and cabin systems.

The plots in in figure 4.7 compare the bare structural mass with the entire operating mass of the fuselage. The latter includes systems, furnishings and operational items. The twin aisle has heavier

furnishings and some systems also become heavier. The limit shifts to 320 seats. Both plots demonstrate considerable unevenness. This is reasoned by the individual layout of each capacity and cross section. For example, at 240 seats the 7-abreast twin aisle can do without additional emergency exists apart from the overwing plug-type exits. This makes the cabin layout very efficient, and hence leads to a fuselage mass very close to that of the advanced single aisle. At the next capacity it gains one exit lane, one galley and a lavatory, increasing the fuselage length disproportionally. Such effects, which occur in a similar way for the other cross section - but at different capacities - , cause the unevenness and are a direct consequence of the chosen method of cabin design.

4.2 Boarding and Turnaround Simulation Results

This section details the boarding and deboarding results of the fuselage designs introduced in the previous section. The results are separated into two different scenarios: a maximum load factor and reduced load factor scenario. The presented results are the boarding time, then the combined boarding and deboarding time (passenger time) and finally the turnaround time. Special effects such as Quarter Door, dual door boarding or wider exit door are considered in separate sections.

4.2.1 Studied Scenarios

Most boarding studies introduced on page 30 use a single scenario. That is, they consider a load factor of 100% (all seats are occupied). Boarding time correlates with load factor, the longest boarding times can be expected at maximum load factor. The load factor even has a non-linear effect on boarding time as shown in figure 3.19 (page 60) when more advanced overhead bin models are used. For a realistic assumption of the advantages of a twin aisle the load factors and luggage distributions found in normal short range traffic need to be considered. These are rarely 100%. Many short range connections actually demonstrate fairly low load factors in the 65%-region [LH11]. Load factors have increased in recent years (see figure 1.4).

The load factor is the most important and best observable parameter. It can also be used best to differentiate between different business models. The two static scenarios used in this study are simulated with 100% and with 85% load factor, respectively. The third scenario is a parameter sweep that variates load factor, carry-on luggage and smartness. That is done using randomly chosen values of each parameter along a probability distribution. This method is also commonly known as Monte-Carlo Simulation. In figure 4.8 the major parameters are listed.

4.2.2 Results of Static Scenarios

In figure 4.9 the boarding results for the two static scenarios are given. The input settings are fixed and for each layout and cross section multiple boardings are simulated to generate a mean value. This is necessary as randomized seat order and luggage distribution (albeit with constant overall distribution) means that each simulation run generates slightly different results (see also table 3.4 on page 66). The reference single aisle with 180 passengers requires 18 minutes boarding time at full load factor (left) and slightly below 14 minutes for the 85% load factor case (right). The advanced single aisle with wider aisle scores slightly better for capacities above 180 seats. The twin aisles (dark
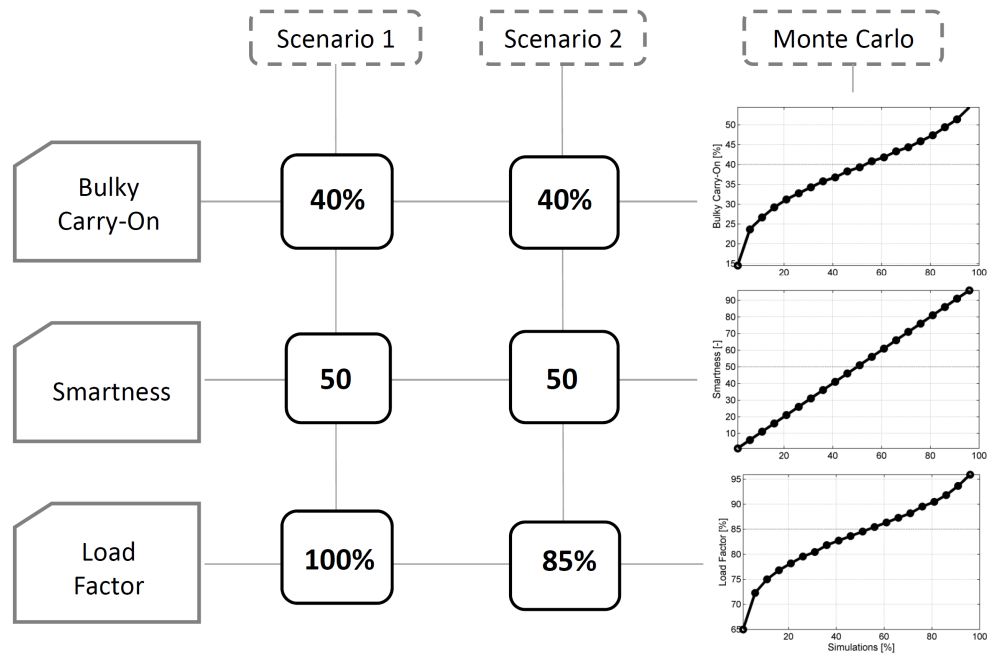
Figure 4.8 – Three boarding scenarios: the static scenario with maximum load factor and 85% load factor, respectively. And the scenario using probability distribution for the key input parameters (Monte Carlo).

lines) have substantially lower boarding times. For 180 passengers the the 7-abreast twin aisle requires roughly half the time. Overall the 7-abreast fares best in boarding, which is result of the low amount of seat interference and the added overhead bin volume compared to the 6-abreast twin. Further, the 7-abreast is shorter, slightly reducing the walking distances. The shown results are compiled from a total of 1400 boarding simulations for each of the two load factors. The deboarding was simulated with 560 simulations each.

The difference between the maximum and the reduced load factor is substantial. While the standard single aisle boards close to 4 minutes faster at 85% than at 100%, the 7-abreast twin aisle only gains about 1 minute (both at 200 seats). That shows the strong non-linear effect of load factor on boarding times, especially in case of the single aisles. In figure 4.10 the relative improvement compared to the standard single aisle is shown. The effect of reduced load factor becomes easily apparent. The advanced single aisle has no noticeable advantage. For 100% load factor the maximum advantage is 2 minutes. At 85% load factor no advantage remains. It is reminded that aisle passing is also depending on the type of carry-on luggage and the smartness. With 40% heavy carry-on and medium smartness the scenario reduces the probability of aisle passing. The fact that it demonstrates in some occasions worse boarding times than the conventional single aisle indicates that aisle passing is either not relevant or not covered in a suitable way by the simulation.

The results so far only covered the boarding process. For the turnaround the combined boarding and deboarding time is relevant. This time is referred to as total passenger time in this work. As shown in the introduction, this time directly influences the minimum turnaround time. The deboarding results are not shown in detail as spread is much lower. Each cross section has a nearly constant rate of people exiting it. The fastest is the 6-abreast twin aisle with 35 passengers per minute, the slowest is the 6-abreast single aisle with 22 passengers per minute. The wider single
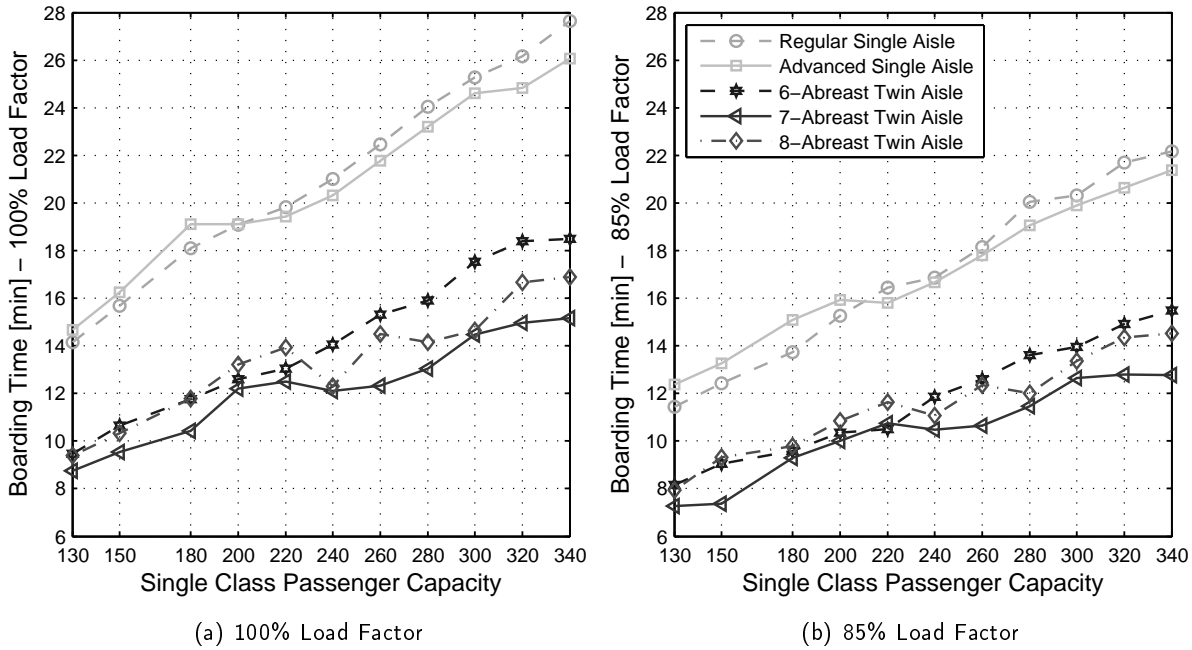
Figure 4.9 – Basic boarding time for 100% and 85% load factor. Right plot's legend valid for both plots.

Figure 4.10 – Improvement of boarding time compared to standard single aisle for 100% and 85% load factor. Right plot's legend valid for both plots.

aisle is equally fast as aisle width does not affect deboarding in the simulation. The 7- and 8-abreast twin aisles deboard slightly slower than the 6-abreast twin aisle, but still much faster than the single aisles. The results for both load factors are shown in figure 4.11. The bottleneck during deboarding for the single aisles remains the aisle: passenger get up and retrieve their luggage. While they take their luggage other passengers have to wait behind them. The twin aisle is limited by its exit door, through which only a limited number of passengers can exit. A wider exit is studied on page 100.

The relative savings are shown in figure 4.12. The scenario with 100% load factor shows significant savings in passenger time. The savings are exceeding 10 minutes even for 180 seats capacity. Larger capacities reach up to 15 minutes advantage. The 7-abreast fares best in overall time saving, while the other twin aisles are close. The advanced single aisle with the wider aisle only gains a slight advantage. As stated previously, the chosen scenario settings make aisle passing less likely.

When the load factor is reduced the advantages shrink. At 180 seats the time saving drops to slightly more than 7 minutes. The deboarding rate is less prone to load factor effects as retrieving luggage from the overhead bins is only marginally more time consuming when the bin is full. Only from 240 seats capacity onwards the twin aisles achieve more than 10 minutes overall saving.

(a) 100% Load Factor   (b) 85% Load Factor
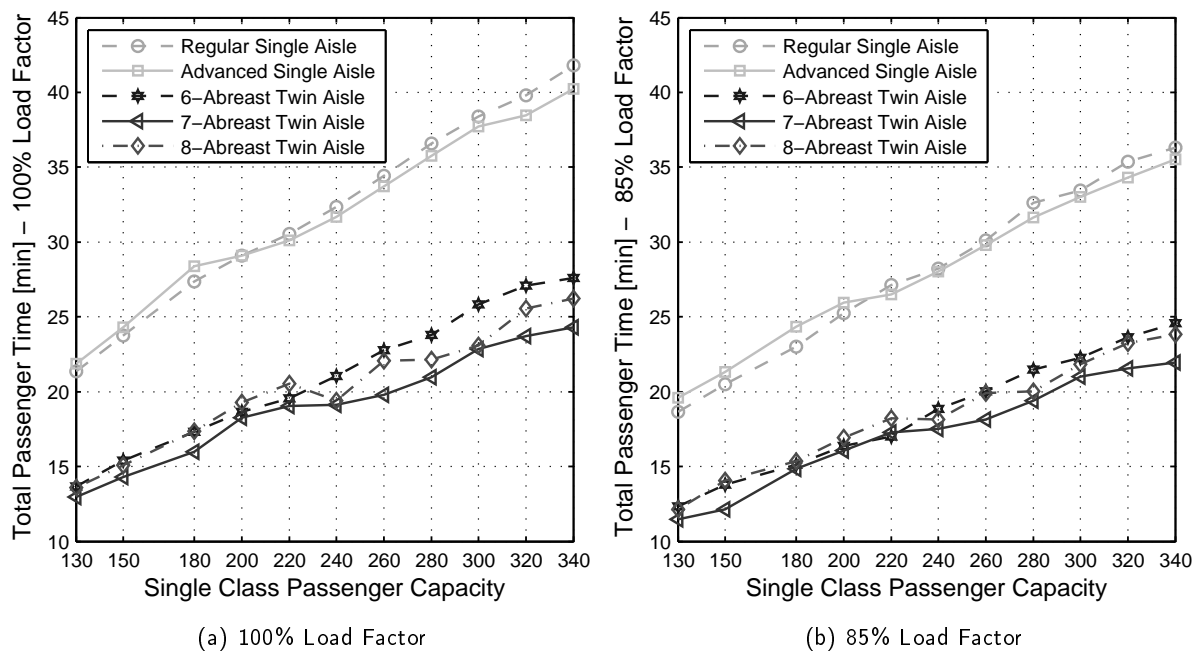
Figure 4.11 – Total passenger time (combined boarding and deboarding) for 100% and 85% load factor.

From these baseline results four relevant conclusions can be drawn:

1. All twin aisles achieve a much better boarding and deboarding time with advantages exceeding 10 minutes at capacities as low as 180 seats. The general idea that a twin aisle is faster in turnaround hence is affirmed. The dimension of the advantage further justifies a closer look at the effects of this advantage.

2. Load factor is of major importance as it increases the effective bin volume per passenger and reduces seat interference. Load factors of 100% are rare and average load factors of 85% are only achieved by some airlines on short ranges, although the average load factor is increasing industry-wide. Therefore, the airline business model is essential when analyzing the economic benefit of a twin aisle.

3. The advanced single aisle with wider aisle does not demonstrate a big advantage. This is either caused by a insufficient modeling of the aisle passing or by the aisle passing being of limited importance.

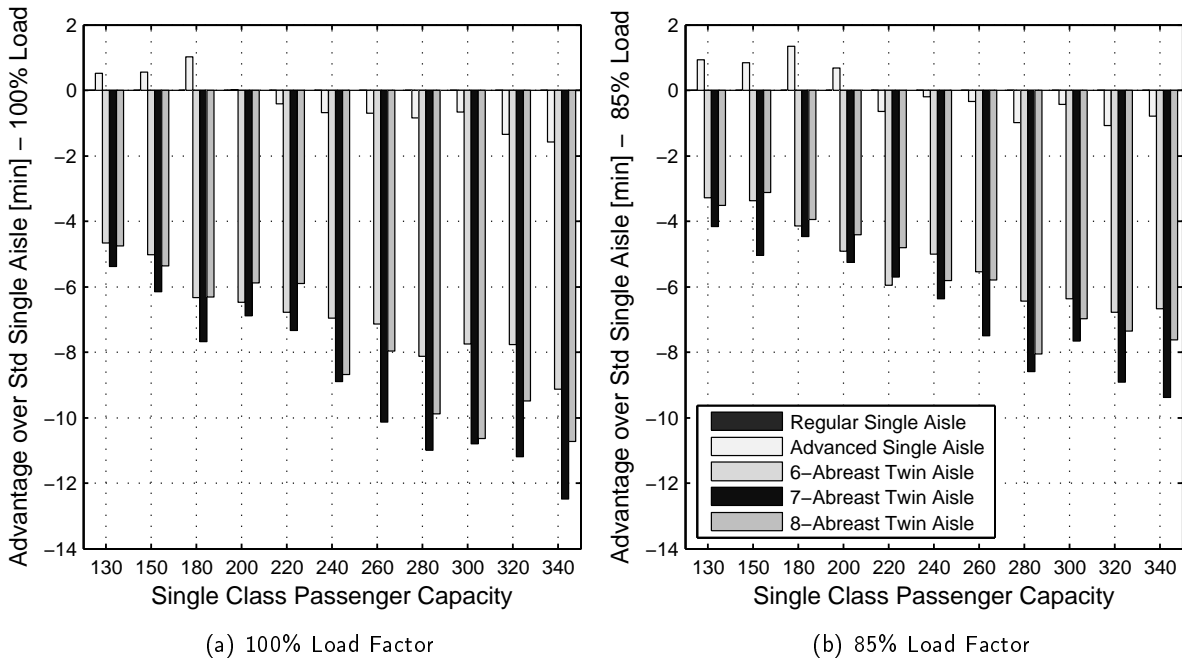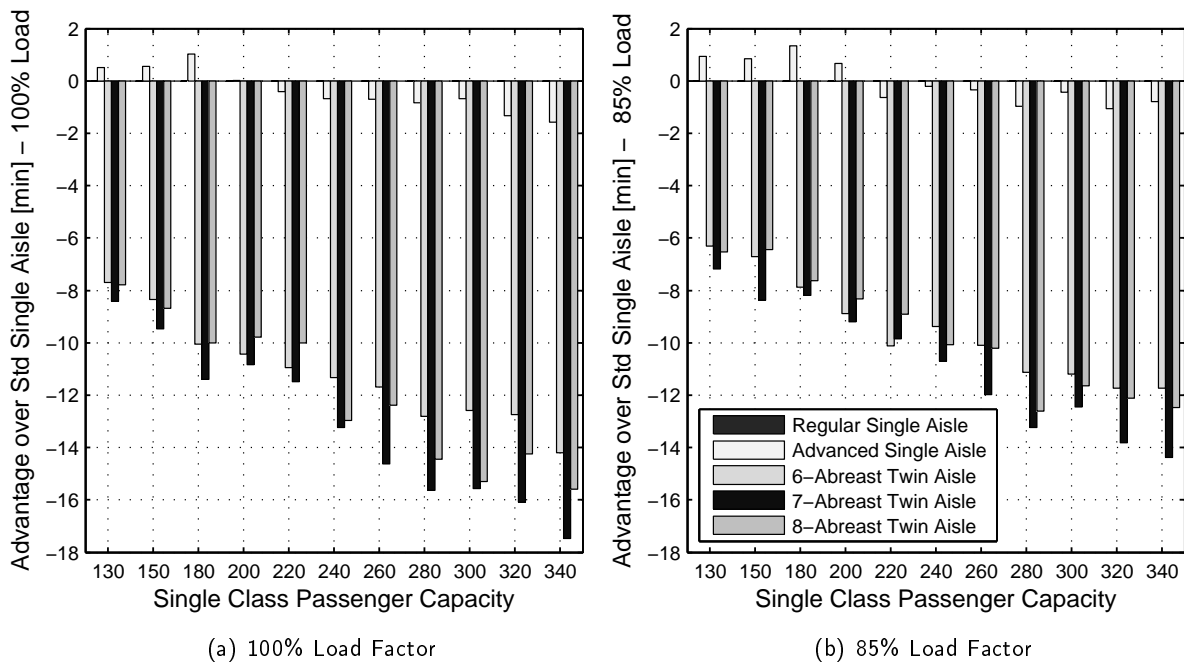**Figure 4.12** – Improvement of total passenger time (combined boarding and deboarding) compared to standard single aisle for 100% and 85% load factor. Right plot's legend valid for both plots.

4. From the overall results the 7-abreast twin aisle appears as most promising design, achieving slightly better times than his twin aisle peers. In the previous chapter the 7-abreast also fared best in basic fuselage parameters like weight and wetted surface, especially when compared to the advanced single aisle.

4.2.3 Quarter Door Effect

The quarter door has a substantial effect on boarding times. The method of action of the quarter door might not be immediately apparent. In figure 4.13 the effect is briefly explained. Through splitting of the passenger traffic the delay effect in the initial section of the aisle becomes less severe. In effect, it is like boarding two aircraft (one being the seats behind the door, the other in front of the door). From a boarding point of view it would be most beneficial to place most monuments behind the door, as this would increase the seat count of the forward compartment at cost of the rear compartment. Further displayed in the figure is the limitation of door placement: a passenger bridge needs sufficient space to access the door. In case of the A321 some operators consider the available space too small, increasing the risk of structural damage to the engine nacelle by ground service equipment.

The advantage of the quarter door is shown in figure 4.14. The graphs show the difference between quarter door boarding and normal door boarding for each layout and cross section. Capacities below 180 seats are not covered as the limited fuselage length would put quarter door and forward door too close together. First and most striking is the different level of advantage for the individual cross sections. The single aisles gain between 2 and 6 minutes. The twin aisles only gain up to 3 minutes. The comparison between the 100% and 85% load factor scenario unveils that the savings through the quarter door are only slightly affected by load factor. This means the advantage of the quarter door is not reserved to maximum load factor. Not depictable from the plots is the fact that the quarter
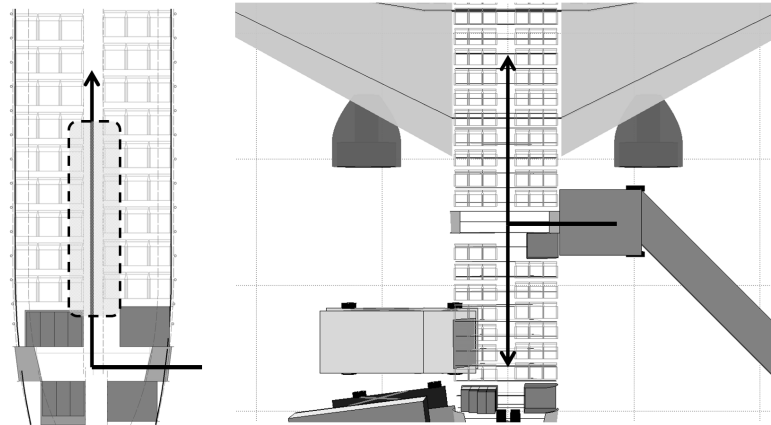
Figure 4.13 – The effect of the quarter door: passenger traffic is split. Note also the limitation of door position through the wing and engine.

(a) 100% Load Factor
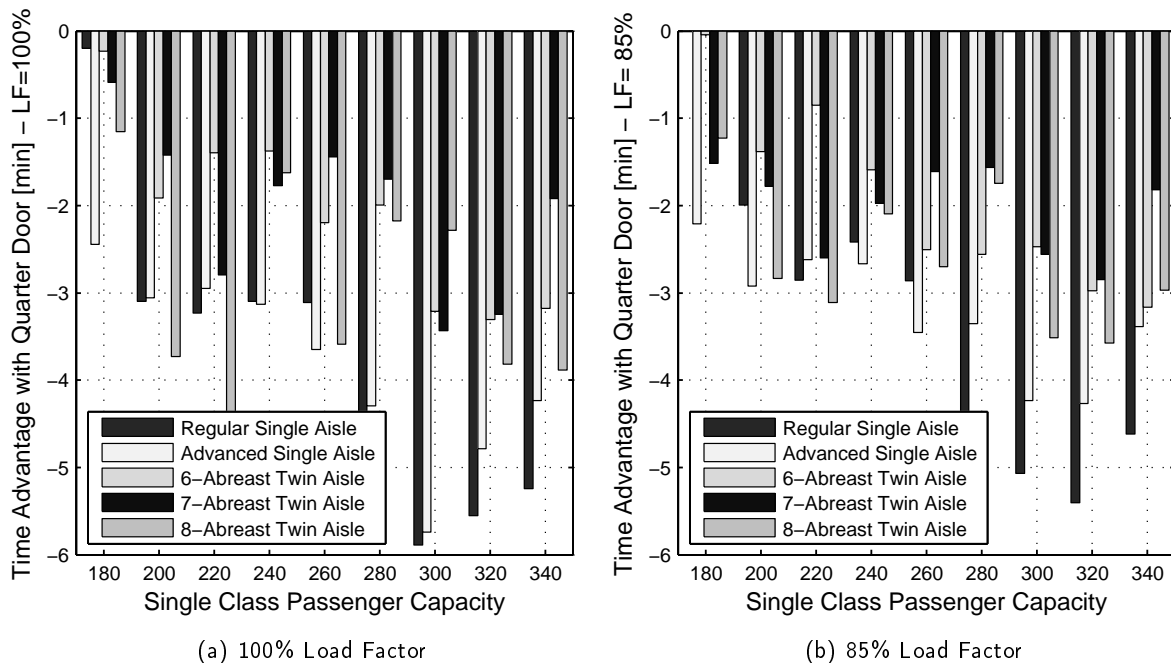
(b) 85% Load Factor

Figure 4.14 – Improvement of total passenger time (combined boarding and deboarding) with quarter door when compared to same capacity and cross section for 100% and 85% load factor.

door mainly gains in boarding. Time advantage in deboarding is small.

In conclusion the quarter door appears to be a very attractive concept for the single aisle. The twin aisle gains less. The quarter door has a substantial weight penalty when no full size exit is required between forward boarding door and wing. This is true for capacities of 220 seats and less in a single aisle. Above the quarter door has a reduced weight penalty as the exit just needs to be designed larger and a slightly more floor area needs to be reserved. The quarter door appears to be a relatively simple solution to speed up single aisle boarding. Twin aisles do not profit enough to justify the investment, only if a door is required anyways, which is the case from 255 passengers onwards[5].

---

[5]This is the maximum exit capacity with two Type A exit doors and two overwing exits.

4.2.4 Effect of Dual Door Boarding

Boarding via two doors is often performed on apron positions. Stairs are located at the front and rear door of the aircraft. This is also the preferred method of low cost carriers and charter operators. This work concentrates on the type of operation observed at larger hub-airports, where apron positions are less common. However, in order to better address the operational environment of low-cost and charter operators all designs were simulated using two doors for boarding. It is assumed, that the passengers are split evenly between forward and aft door.

(a) Total Passenger Time
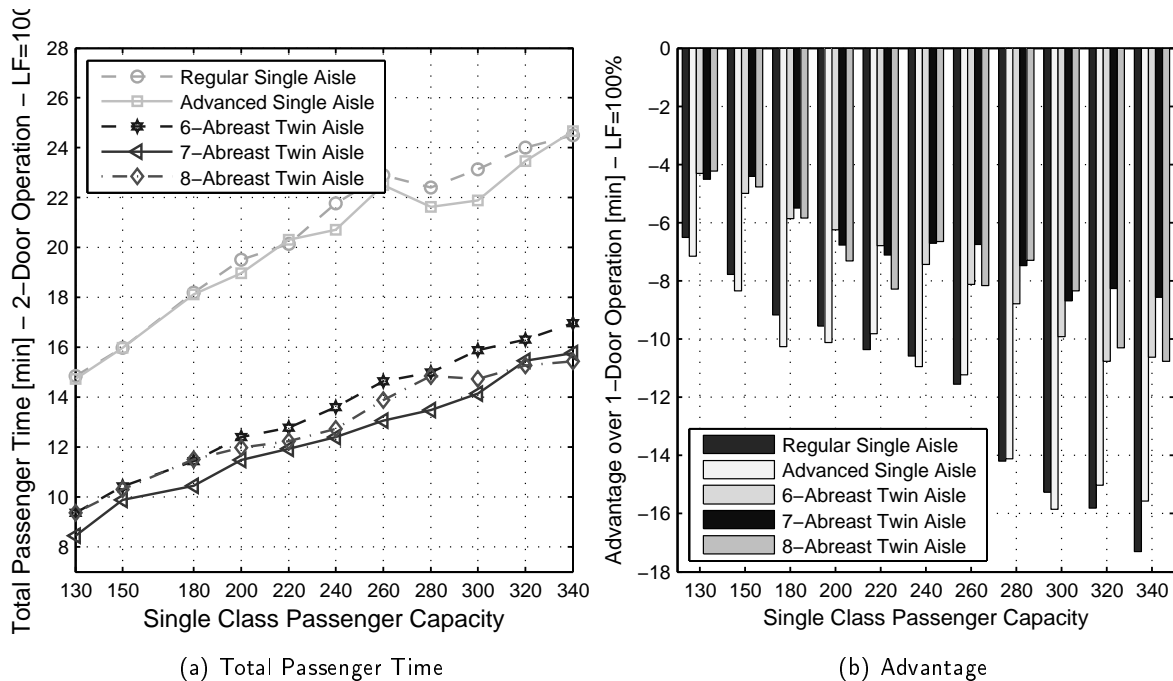
(b) Advantage

Figure 4.15 – Total passenger time (combined boarding and deboarding) with usage of a second boarding door. The times reflect usage of most forward and aft exits, passengers are evenly distributed. Maximum load factor. The time advantage is compared to boarding/deboarding via single door.

In figure 4.15 the resulting times and the difference to the single door operation are given. The boarding rates do not double but rather increase by roughly two thirds. The decrease in passenger time is still substantial. At 220 passengers, the single aisles gain approximately 10 minutes or one third of the original passenger time. When using two doors, the cabin processes (deboarding-cleaning-boarding) may leave the critical path and be replaced by the cargo loading. The plots further show that single aisles gain more advantage from the usage of a second door. The times presented here are the time until the last passenger has left the aircraft. Any additional time the passengers might spent in buses is not considered. From the passenger point of view, there is no time advantage when using two doors in connection with apron operations. In fact, rather the opposite is the case.

4.2.5 Effect of Enlarged Door

Often the door is thought to be the bottleneck for faster boarding. In order to study the effect of a larger door the effect is modeled as a door wide enough to let two passengers enter simultaneously.

That is, passengers can entry or exit the cabin parallel. This setting does not make any sense in the classical single aisle, as boarding and deboarding delays occur in the aisle and passengers simply queue up. For twin aisles and quarter door equipped aircraft the larger door does have an effect. It is assumed and implemented in the simulation that passengers using the right aisle enter in one lane, and the other passengers use the parallel lane. Such "boarding strategy" would be easy to implement without any loss of convenience to passengers. Only capacities up to 280 seats are shown, effects for larger capacities is comparable to those observed at 280 seats.

(a) Absolute Passenger Time

(b) Relative Improvement
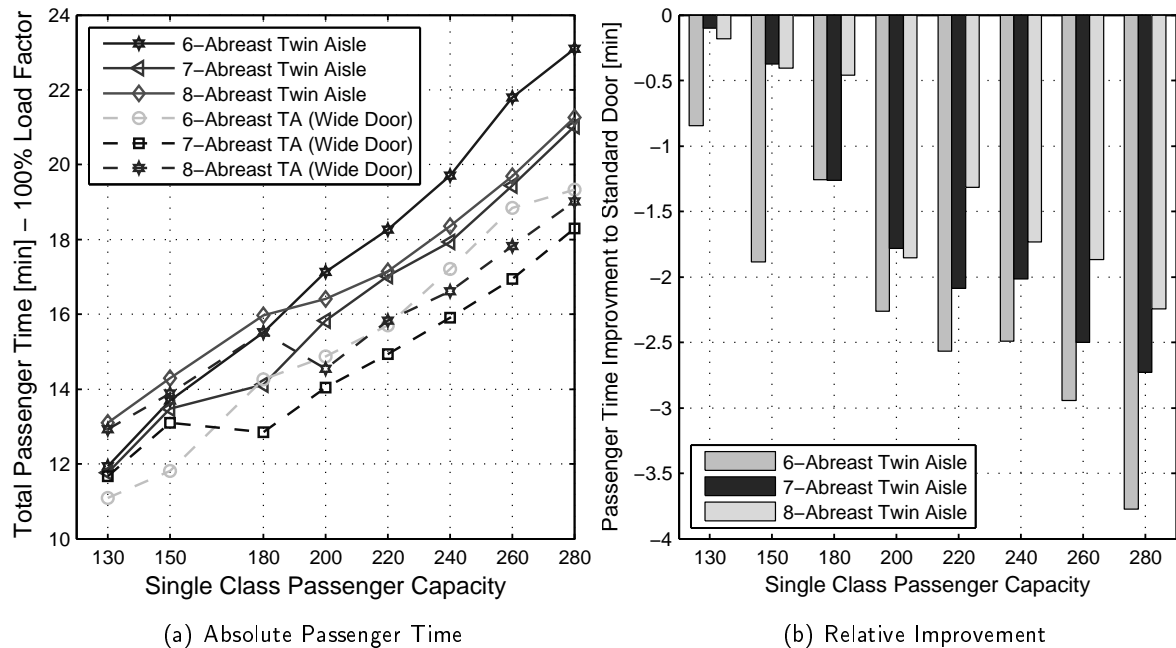
Figure 4.16 – Improvement of passenger time (boarding & deboarding) for twin aisles with wider door at 100% load factor.

The effect of a wider door is noticeable. The relative improvement is about 1.5 minutes at 200 seats capacity, and increases with passenger count. The effect on designs with quarter door (not shown) is slightly lower. The actual boarding rate is close to 23 passengers per minute, which is the highest observed rate in the entire study. It is unknown if the airport infrastructure (gate check in, passenger bridge) can handle this rate. It would be of no use if the bottleneck during boarding shifts from the aircraft into the airport. However, deboarding rates of 30 passengers and more are regular occurrence even with single aisles, so the passenger bridge should be able to accommodate this flow.

4.2.6   Results of Randomized Input Settings

The initial chart in figure 4.8 provided three scenarios, of which two have been presented so far. The first two are static scenarios with fixed input settings. Different to these the randomized input setting uses probability distributions around mean values. The mean values are similar to scenario 2 (85% load factor, 40% bulky luggage, Smartness of 50). The load factor is at least 55% and at most 100%, with a bell curve probability distribution. The percentage of people having bulky luggage can be as low as 15%, and as high as 60%, again with a bell curve probability distribution. The Smartness is lineraly distributed between 0 and 100. Different to the static simulations no multiple runs are
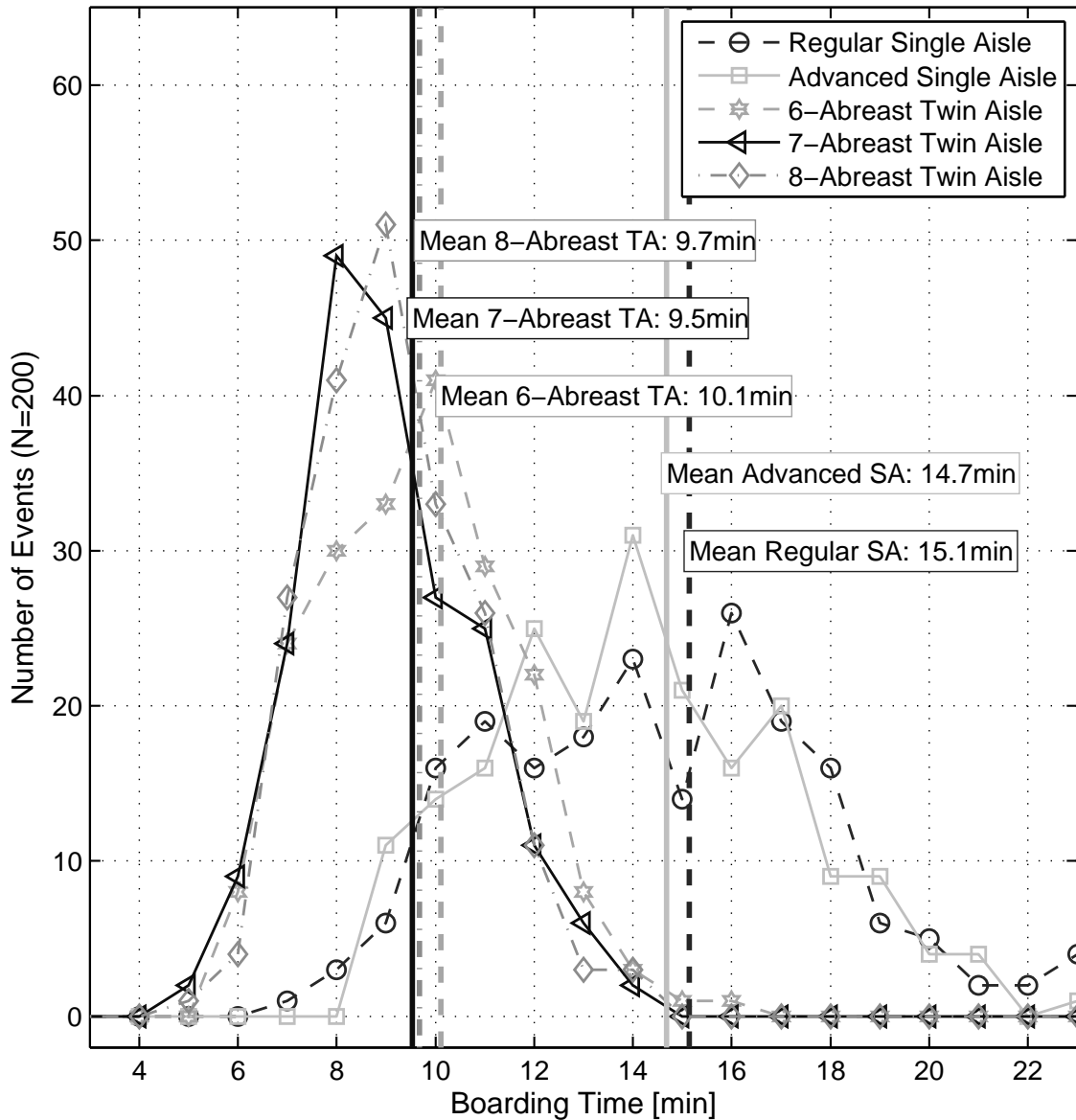
Figure 4.17 – Result for 200 simulations using randomized input settings for 220 seats capacity: the twin aisles are to the left, the single aisles to the right. The vertical lines represent the mean values, with both single aisles having nearly the same mean time.

carried out but actual inputs are diced for each simulations. For this study 200 simulations have been conducted for each layout of each cross section, resulting in a total of 14000 simulations. One simulations takes roughly 45 seconds on average, so that the entire simulation campaign takes up one week.

The intention of these input settings is an attempted simulation of an airline environment, where load factors, carry-on and passenger type is subject of wide variations. Many carriers[6] fly business travelers on domestic trips, leisure travelers on scheduled trips and charter operations into tourist destinations. The simulations hence allow to estimate the average advantage when transporting a changing passenger population. As stated above the deboarding is not prone to such wide variation so that a constant deboarding rate for each cross section type can be applied.

---

[6]For example: Air Berlin as of 2011

| | Advantage in Total Passenger Time [minutes] | | | |
| | 7-abreast twin aisle versus standard single aisle | | | |
Capacity	Static 100% Load Factor	Static 85% Load Factor	Monte Carlo Mean Time	Monte Carlo 90% of all events
130 PAX	7.6	6.2	3.7	4.8
150 PAX	8.3	6.4	4.1	5.6
180 PAX	11.3	7.7	5.5	7.8
200 PAX	11.7	9.1	5.6	8.0
220 PAX	12.0	9.2	5.6	7.4
240 PAX	13.1	11.0	6.7	9.0
260 PAX	14.5	10.9	6.8	10.0
280 PAX	14.7	11.7	7.2	10.2

Table 4.1 – Total passenger time advantage of 7-abreast twin aisle compared to 6-abreast single aisle. The left two columns list the advantage at fixed load factors of 100% and 85%. The second to the right column gives the advantage for randomized input settings, between the mean values of all simulations. The rightmost column gives the time advantage when 90% of all events are covered. Also see test for further explanations.

The resulting boarding times spread significantly. In figure 4.17 the result is shown for the 220 seat layout. Note that the x-axis is the actual boarding time, while the y-axis is the number of events out of 200 simulations. The twin aisles demonstrate on average better boarding times. The limited number of simulations results in a not entirely even distribution. The 7-abreast twin aisle achieves an advantage of just over 5 minutes on average, which is less than the 8 minutes it demonstrates for the 100% scenario but quite close to the 85% load factor scenario. All twin aisles demonstrate smaller spread of the results. Table 4.1 lists the average advantage of the 7-abreast twin aisle compared to the standard 6-abreast single aisle.

The results demonstrate that the advantage of the twin aisles decreases when boundary conditions are relaxed. As a rule of thumb, the randomized settings produce roughly half the advantage in boarding time when compared with the full load factor scenario. This will probably make the twin aisle unattractive for scenarios with less demanding boundary conditions. However, the last column of the table shows the time advantage of the twin aisle for the fastest 90% of all boarding events. That is not the mean time, but the duration which covers 90% of all turnarounds. 10% would take longer. This time could be used to make the turnaround planning. The twin aisle - due to its lower spread - wins back some advantages. In effect the twin aisle may demonstrate on average only 5 to 7 minute savings, but demonstrates less deviation for tougher scenarios.

4.2.7 Complete Turnaround Times

The turnaround times are linearly connected to the boarding results, at least when a high load factor is carried. The settings for the container loading assume a quick and hassle-free loading with two loading vehicles and the departing load ready at the begin of the turnaround. The speeds for container movement are set at 50% of the standard velocity to account for acceleration. Additionally, dead times and vehicle positioning times are accounted for. The number of cabin cleaners is set to 4 below

(a) Absolute Turnaround Time (b) Relative Improvement
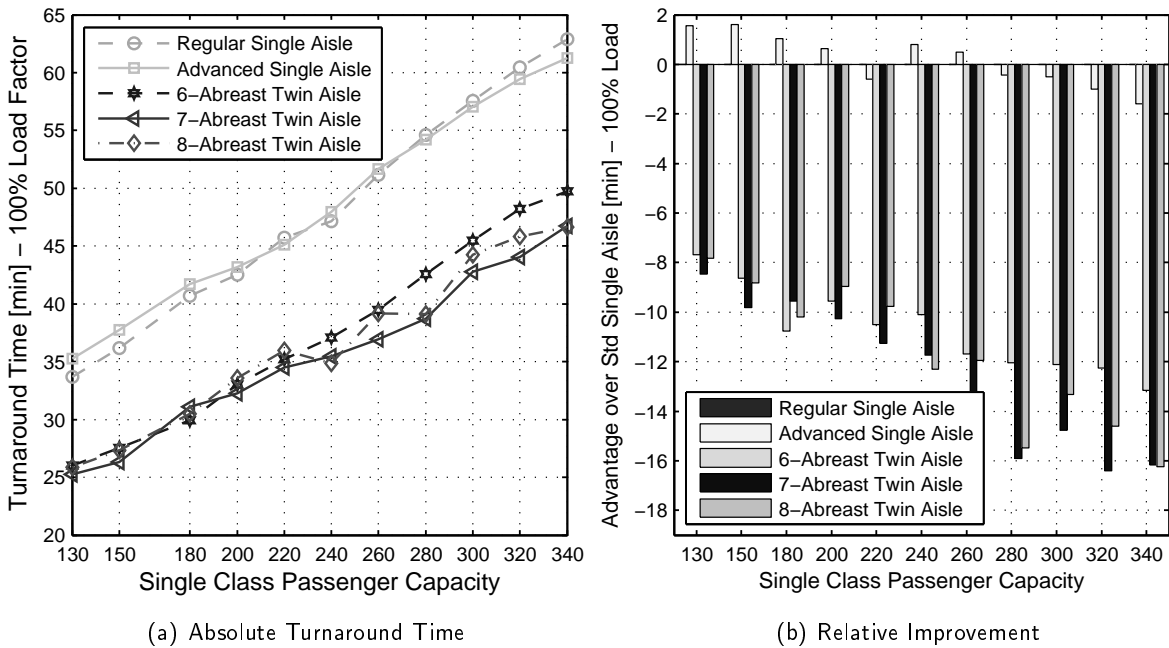
Figure 4.18 – Turnaround time including other processes at 100% load factor. Boarding via forward left door.

180 seats, and at 6 for all other capacities. Especially the larger capacity aircraft could reason a larger cleaning party. With 100% load factor the cabin processes always determine the critical path. The differences as shown in figure 4.18 are essentially the same as shown in figure 4.12. The advantage of the twin aisle is close to 10 minutes at 180 seats and approaches 15 minutes for the largest capacity. Changes to the number of the cabin cleaning crew would not change the difference. Looking ahead at the required blockfuel in figure 4.21(a), the difference between the cross sections will have no noticeable effect on refueling times. The 7-abreast twin aisle demonstrates the best boarding times from 200 seats upwards. Below it is on par with the 6-abreast twin aisle. The advanced single aisle does not show a large improvement, which may be caused by insufficient modeling of the aisle passing.

When the boarding is performed over two doors, the turnaround times are strongly reduced. The twin aisles have lower turnaround times, but do not exceed 9 minutes advantage. It is worthy to remark that except for two occasions the cabin processes remain on the critical path. One reason is that the number of cabin cleaners is limited to 6, which increases the time required for cabin cleaning linearly with increased capacity. If the number of cleaners is increased to 8 for capacities beyond 280 seats, the cargo loading becomes the critical process. However, as the cargo capacity is quite large due to the long fuselage, the total amount of loaded cargo far exceeds the amount required for passenger baggage.

As rule of thumb, the turnaround time of the single aisles using two doors approximately equals the turnaround time of the twin aisles with a single door.

(a) Absolute Turnaround Time   (b) Relative Improvement
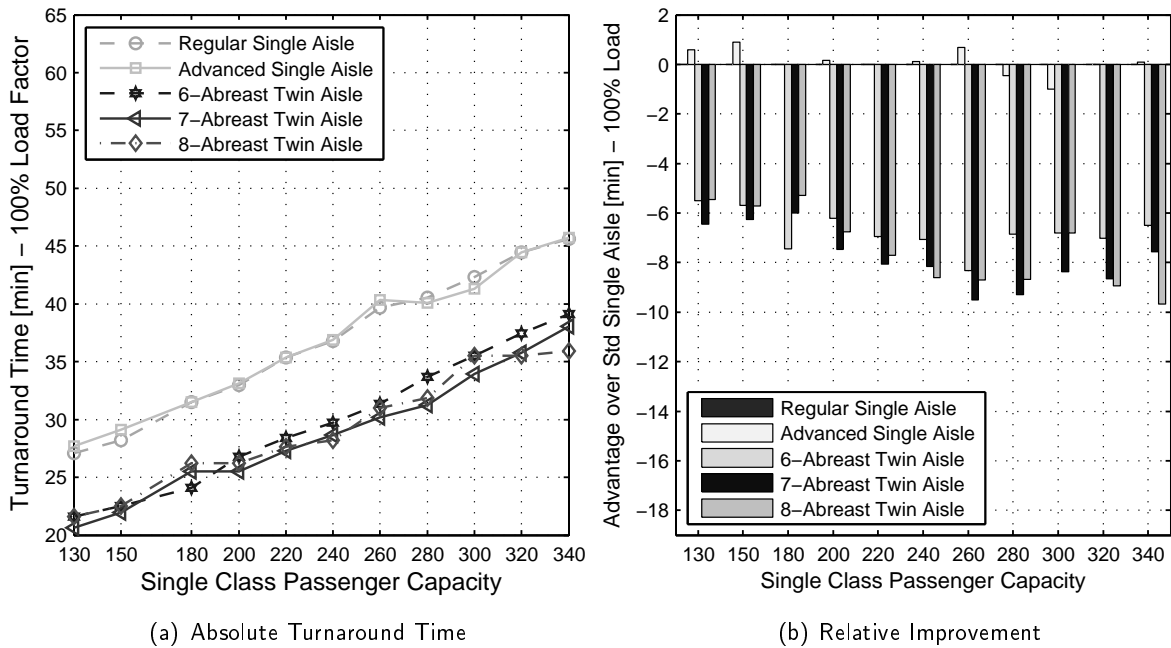
Figure 4.19 – Turnaround time under usage of two doors, including other processes at 100% load factor.

4.3 Aircraft Design Results

4.3.1 Mission Requirements

Aircraft design starts with the definition of requirements. Often called Top Level Aircraft Requirements (TLAR), these specify range and payload. Further requirements may be formulated, like initial cruise altitude. On top of these requirements are all those that are defined in the certification standards issued by the aviation authorities, like [EAS06]. The actual mission and performance requirements are shown in table 4.2. The initial cruise altitude and the approach speed are not defined. These requirements are covered by usage of a fixed wing loading. All designs use a geometrically similar wing. Tails are sized in order to fulfill tail volume requirements. Consequently, the resulting flight performance is nearly identical when it comes to climb performance and thrust loading.

Category	Requirement
Take-Off	2000m field length at ISA+10°C and 0ft elevation.
Approach Speed	*Not specified.*
Initial Cruise Altitude	*Not specified.*
Design Range	1800nm
Design Payload	Full passenger payload, no additional cargo.
Passenger Mass	100kg for passenger and luggage.
Wing Loading	604kg/m^2
Aspect Ratio	9.4
High Lift Type	Slats and single slotted Fowler flaps.

Table 4.2 – Sizing settings for the aircraft design process. The values closely resemble those of an A320 with 73.5t rated maximum take-off mass.

Many textual requirements from the certification standards need to be translated into numbers. For example, safety standards require sufficient reserve fuel for flight to an alternate airport. The actual distance is not specified as it depends on the situation at the destination airport. Reasonable translations for most specifications can be found in textbooks. It is shown in the description of the aircraft design (see page 78) that the used specifications generate a very close match to an actual aircraft. Both the masses and the fuel burn are matched well, which indicates that all relevant disciplines (masses, aerodynamics, engine) deliver reliable results.

Although not provided in this work, it can be said with high confidence that deviation from above requirements and specifications will not change the relative difference between the aircraft. That is, identified performance differences will remain even if top level aircraft requirements like the range are changed for all models.

4.3.2 Sizing Results

The sizing process determines a wing area and the necessary installed thrust for each fuselage layout. As shown previously the different fuselage layout results in different masses for the fuselage. The sizing process now covers all snowball effects.

(a) OEM per Seat   (b) MTOM per Seat
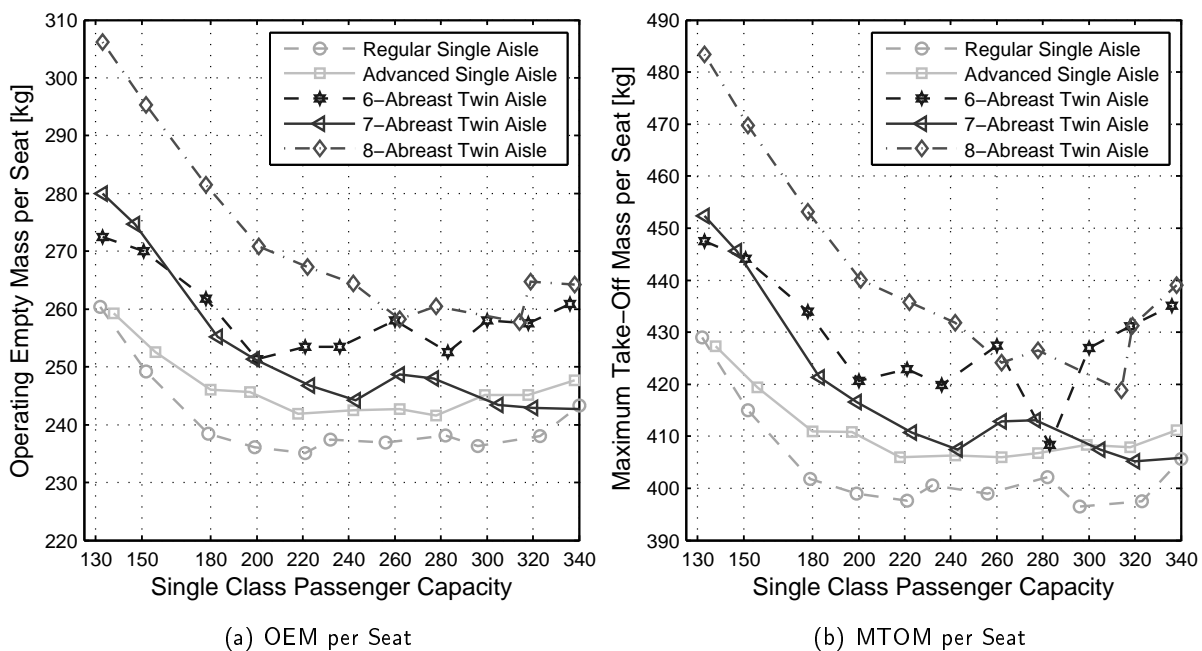
Figure 4.20 – Results of aircraft sizing. Left the operational empty mass (OEM) per available seat, right the maximum take-off mass per seat. Note that both masses correlate strongly with each other.

Most relevant for the performance estimation are the aircraft masses and the aircraft drag. In figure 4.20 the masses are given, both as mass per seat for better comparison. The operating empty mass per passenger indicates that larger aircraft are more efficient. It also shows that each cross section bottoms out above a certain capacity. The standard single aisle has its optimum empty mass per seat at 220 seats (which corresponds to a fuselage fitness ratio of 10 to 12 according to figure 4.5(b)).

Above that capacity the mass per seats slowly increases. The maximum take-off mass includes the effect of aerodynamics: aircraft with less drag per seat require less fuel and hence have lower take-off mass. While the take-off mass behaves much like the empty mass, there are slight differences. The single aisle for example achieves its best value at 300 seats. The 7-abreast twin aisle achieves similar masses at 340 seats. Previous plots have shown that the fuselage-related masses are actually lower for the 7-abreast above 290 seats (see figure 4.7 on page 93). The reason for the delay of this advantage in the overall empty mass and take-off mass is the tail, which profits from longer lever arm. Remember that landing gear mass is only modeled via take-off mass, hence the effect of longer landing gear is not covered. The masses influence the findings in two ways: first additional mass causes additional fuel burn. Second, the empty and take-off mass are used as regression parameters for cost estimation.

(a) Fuel Burn per Seat

(b) Fuel Burn Difference
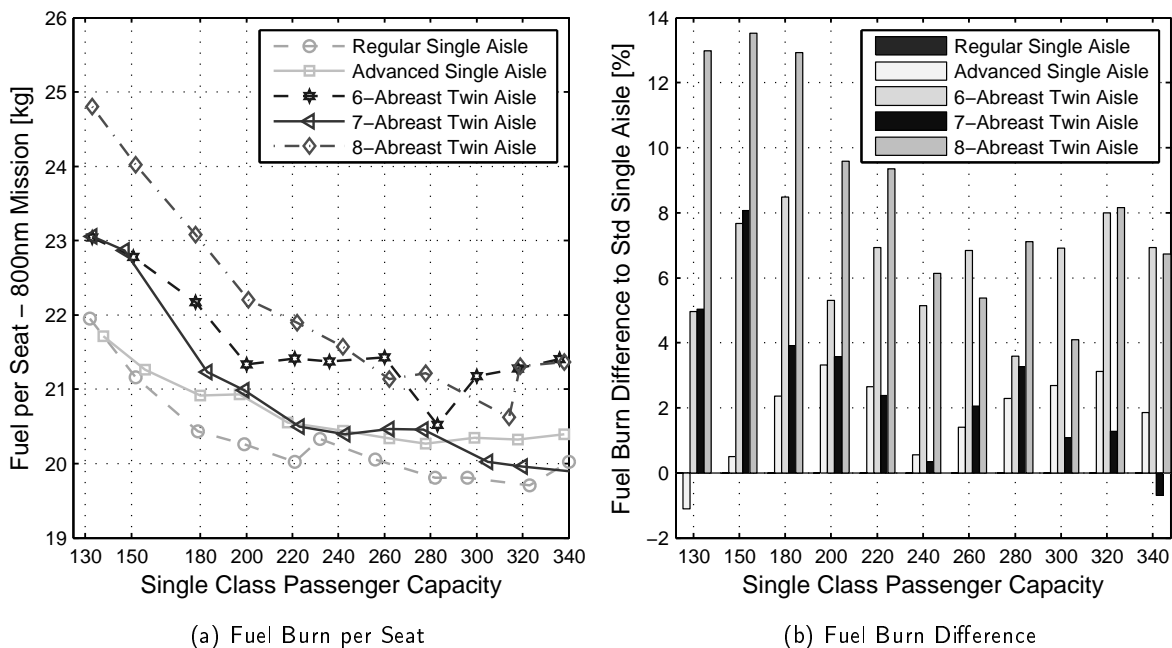
Figure 4.21 – Fuel burn per seat for a 800nm mission. Note that the fuel burn correlates strongly with the empty mass respectively take-off mass. Further note that the absolute difference is in the range of 1kg, corresponding to roughly 1 USD per seat and trip.

The seat-specific fuel burn for a 800nm mission is shown in figure 4.21. The fuel burn strongly resembles the masses shown in the previous figure. When looking at the drag (not shown) the difference between the different cross sections is very small, mostly within 1%. As the drag is normalized with the respective wing area, comparison of different aircraft delivers limited insight. The fuel burn difference is considerable in relative terms as displayed in figure 4.21(b). However, considering the absolute values, the additional fuel burned by the 7-abreast twin aisle compared to the single aisle is below 1kg per seat for most capacities. That results in added cost of 1 USD per seat and trip.

Independent from the difference it is relevant to note that the standard single aisle remains the most efficient design over the entire capacity range. That demonstrates that if minimum fuel burn is aimed for, current single aisles already represent the best of the researched designs up to 340 seats. The values for the 8-abreast full size twin aisle for capacities below 200 seats need to be taken with care, as the low aircraft fitness ratio exceeds the region of validity of some methods. The advanced single aisle has a fuel burn disadvantage of about 1-3% over the entire range with no clear identifiable trend.

The twin aisles have substantial disadvantage for capacities below 200 seats. The 7-abreast twin aisle achieves near parity to the advanced single aisle at and above 200 seats, but it does not achieve similar fuel consumption as the standard single aisle below a capacity of 340 seats. The majority of missions is below 800nm (see figure 1.2 on 2). However, the 800nm is representative of shorter missions, that is, the demonstrated relative differences remain similar for shorter missions.

It needs to be stressed that the differences are small above 240 seats, and that despite the demonstrated quality of the tools a margin of error remains.

4.3.3   Direct Operating Cost

(a) Absolute Cost per Available Seat Kilometer   (b) Difference to Std Single Aisle
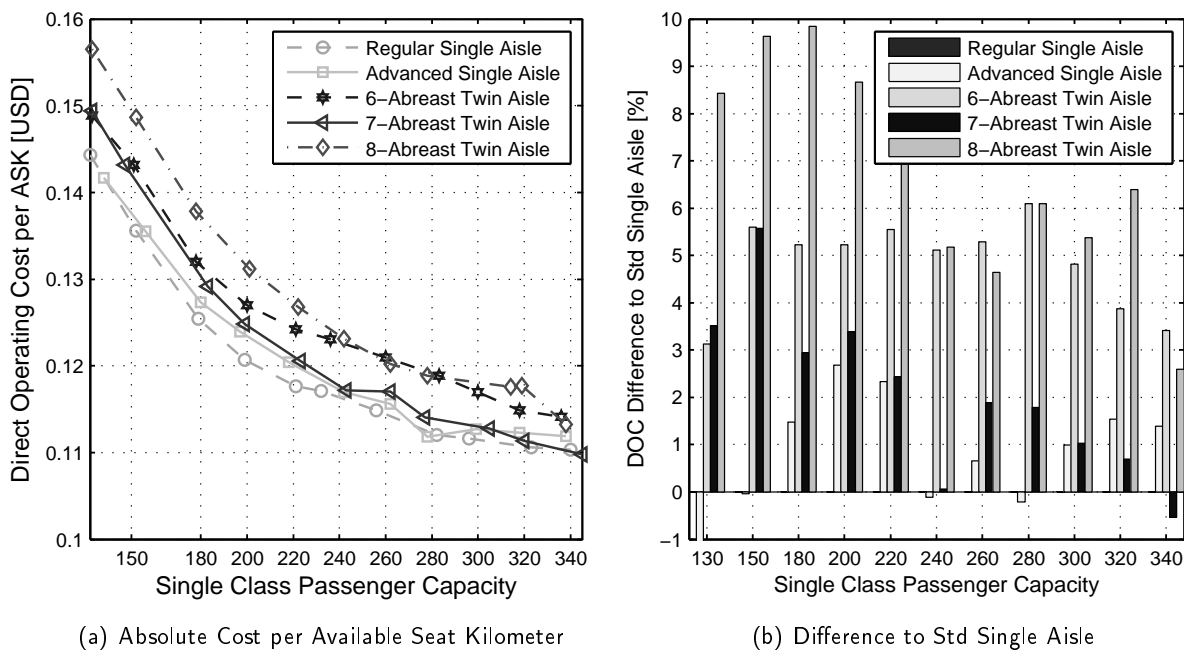
Figure 4.22 – Direct operating cost for different capacities for a 500nm reference mission.   The
turnaround time is assumed similar for all aircraft (irrespective of capacity).

The model for direct operating cost is used with a constant utilization for all aircraft. That is, the turnaround time is assumed fixed for all designs and capacities. The shown numbers are of qualitative nature. The assumed mission length is 500nm. The absolute values show the decrease with aircraft size. The design with 150 passengers have around 25% higher cost per seat than the designs with 240 seats. The lower cost per seat explains to some extent the drive towards higher capacities in the short range sector, see also figure 1.3(a). Due to the assumption of constant turnaround time, the smaller capacity aircraft are disadvantaged in this comparison. The standard single aisle loses its cost advantage only at the highest capacity to the 7-abreast twin aisle. However, the difference for capacities above 240 seats is small.

As different utilization is not considered, the difference is solely reasoned by added fuel burn and higher empty mass. Cost estimation includes financing and maintenance, and thus equals out part of the added fuel cost. The cost develop in a similar way to the fuel burn. However, the added cost items decrease the relative difference. The 8-abreast twin aisle was shown to have much higher fuel burn at capacities below 200 seats. In the cost estimation the disadvantage shrinks below 10%, the 7-abreast twin aisle demonstrates cost disadvantages between 2 and 4%. The 7-abreast achieves a

close match at 240 seats due the very advantageous fuselage layout at this capacity compared to the single aisle. This advantage is lost at the next higher capacity.

In conclusion all twin aisles are substantially disadvantaged below 200 seats capacity with significantly higher fuel burn. The current single remains the most economic aircraft due to its smaller and lighter fuselage. It is reminded that the current single aisle is sized for each mission and only at 180 seats capacity it represents a close match to the A320. The 220 seat capacity single aisle has a fuselage very similar to that of the A321, but the wing and tails are different, resulting in larger wing area due to lower required wing loading. When the current single aisle fuselage cross section represents the minimum cost alternative, it does not necessarily mean that this is true for the actually produced single aisles.

Chapter 5

Findings and Analysis

The previous chapter has provided an overview of the results obtained from the different types of analysis. In particular, the results of the boarding and turnaround analysis and the aircraft design results are presented. In essence, the analysis proves that single aisles enjoy an advantage in fuel burn per seat over nearly the entire capacity range due to lower mass per seat. However, the twin aisles demonstrate substantially shorter turnaround times. This chapter integrates those results to answer the initial research question at which range and capacity a twin aisle is more economic to operate than a single aisle. For better understanding a short section is aimed at explaining the influential factors for direct operating cost (DOC). The assessment methodology is explained thereafter.

5.1 Direct Operating Cost Assessment

A short introduction into direct operating cost (DOC) assessment is provided in section 3.4.2. The applied DOC method uses regression formulas for many cost items, especially crew, maintenance and procurement cost of the aircraft. The regressions are based on mass and flight hours. The maintenance regressions also include the number of flight cycles. Hence, if a similar mission is flown by a twin aisle instead of a single aisle the DOC distribution changes. If all design assumptions and requirements are the same, the twin aisle comes out heavier and will burn more fuel. However, it compensates by a higher number of cycles flown per year over which the cost of ownership are spread.

In figure 5.1(a) the dependencies are visualized. The DOC method uses four major aircraft parameters: the fuel burn, the empty mass, the maximum take-off mass and the yearly utilization/cycles. Maintenance cost are linked to the empty mass, while most other cost items depend on the maximum take-off mass. The fuel burn - which is also a function of the gross weight - determines the fuel cost. The utilization influences the cost of ownership, which includes interest, depreciation and insurance. The resulting DOC are shown in figure 5.1(b) over the average mission length. For 400nm (which is longer than the direct distance between Hamburg and Munich) fuel cost and ownership cost are close together. Noteworthy is the large influence of ground handling cost for short missions. Maintenance and crew cost are only weak functions of the range. The graph is produced with assumed fuel cost of 1 USD per kg kerosene, which corresponds to a crude oil price of 115 USD per barrel[1]. Kerosene is traditionally 10% more expensive than crude oil, reflecting cost for refinement and distribution [IAT12].

---

[1]A barrel is 159l and a common unit for oil products.
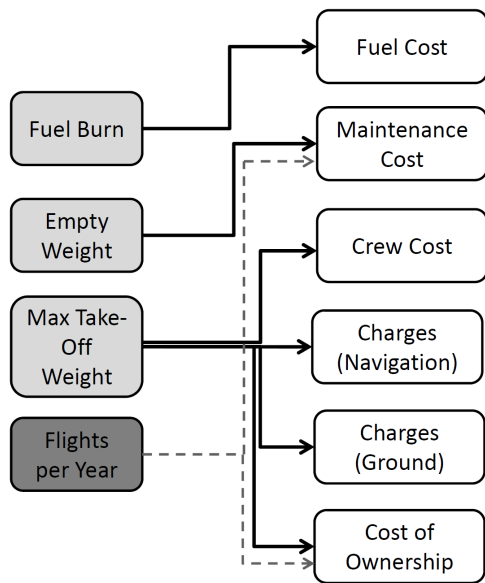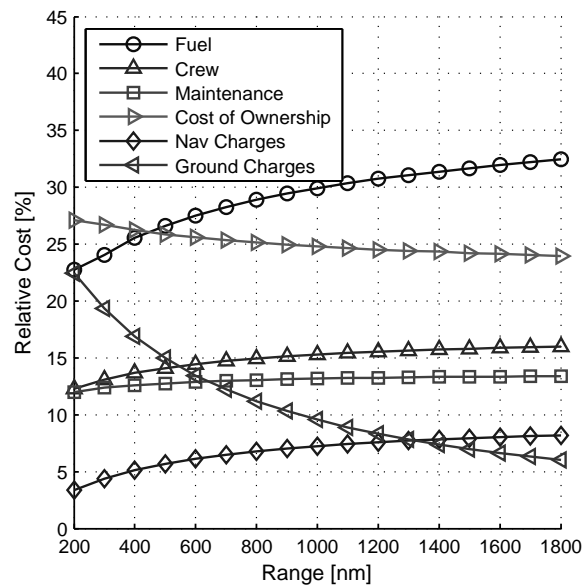
(a) DOC Dependencies   (b) Typical Distribution

Figure 5.1 – Key dependencies of direct operating cost. Left the aircraft parameters are linked to cost items. Right the development of these cost items over mission range (year-long operation) is shown.

DOC estimation is - independent of the particular cost model - always a crude simplification of reality. In reality airlines have very different operating cost. Fuel can be estimated with reasonable accuracy as airlines pay similar prices. Maintenance cost can vary significantly depending on the maintenance organization, fleet size and world region. Cost of ownership depend on the actual purchase price, and the actual interest rate an airline has to pay. Crew cost vary significantly between airlines. In this work it is assumed that the comparison happens within one airline. The comparison becomes debatable if different assumptions drastically changed the ratio between fuel cost and cost of ownership.

During the assessment it became obvious that the regression formulas for maintenance, crew and other cost items put a large disadvantage on heavier aircraft even if the actual fuel burn difference is small (see figure 4.21 on page 107). In reality two aircraft of similar technology with a small difference in empty mass would have similar maintenance cost. It is also doubtful if the crew could achieve higher wages. Therefore the cost model is modified and maintenance and crew cost are calculated by seat specific masses. That is, no matter if single aisle or twin aisle, the mass assumed for these cost items is always the same.

The weight dependency is kept for the purchase price. Finance cost are estimated using a 12 year depreciation period with a 20% resale value and 8% interest. This is a common value for high cycle aircraft ([Dog10], section 4.3.3). The seemingly low resale value compensates missing cost for a mid-life cabin overhaul. Heavy maintenance and cost for spare parts are considered via maintenance burden. The depreciation period not necessarily indicates that the aircraft is discarded after that period, but that cost of operation is estimated using this reference time frame.

5.2   Utilization

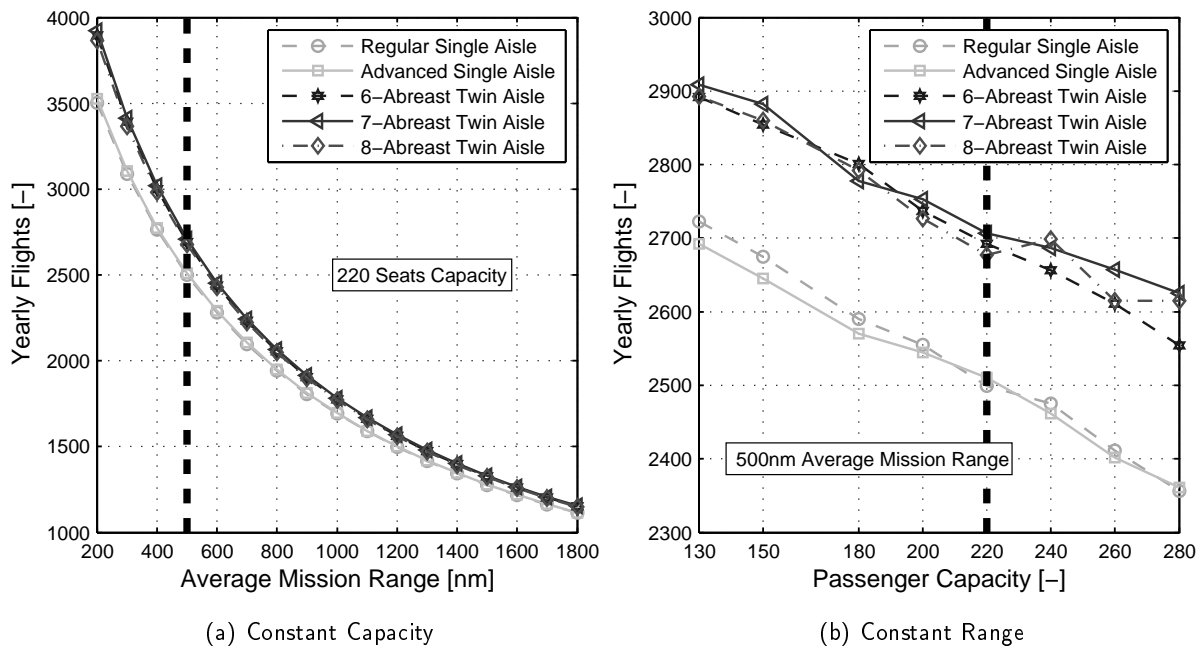(a) Constant Capacity   (b) Constant Range

Figure 5.2 – Yearly number of flights as function of capacity and range. The dashed vertical line represents the position of the other plot.

The utilization is calculated by estimation of the number of daily flights. This number is calculated using the formula provided in the introduction (see page 26). A very important simplification is that the number of flights per day is not required to be an integer. An aircraft cannot make half a flight, so the number of daily flights is an integer value by definition. But the usage of the formula will return non-integer values, which need to be rounded to the next lower integer value. As result two aircraft with different turnaround times might end up having similar number of possible flights per day when the range is fixed. A fixed mission range for a single aircraft out of an entire fleet for an entire day is extremely unlikely. An airline operating into a hub would adjust the rotation to the availability of aircraft. Therefore, all comparisons are based on non-integer number of flights. The range then needs to be understood as average mission range. This simplification or adjustment is very important for the interpretation of the results. It is remarked that with a strict integer-number of flights per day the results become largely inconclusive.

In figure 5.2 the utilization per year is shown over average mission length and capacity. The twin aisles achieve higher utilization due to shorter turnaround times. Besides the turnaround time presented in section 4.2.7, 5 minutes are assumed for taxi-in (after touch down) and 12 minutes for taxi-out. The latter includes time required for engine start. These times are the same for all cross sections and capacities, and are in accordance with observed taxi-in and taxi-out times at uncongested US airports [Dzi11]. The effect diminishes for longer ranges, but increases with capacity. For the 500nm mission (right plot) the difference in flights per year is around 200 (about 7%) for 130 seat capacity, but about 300 (about 13%) for 280 seat capacity. The utilization depends on the turnaround time and the actual time needed to perform a flight mission. All aircraft are sized to similar requirements, and the resulting flight performance is consequently the same. Consequently, the mission time is simi-
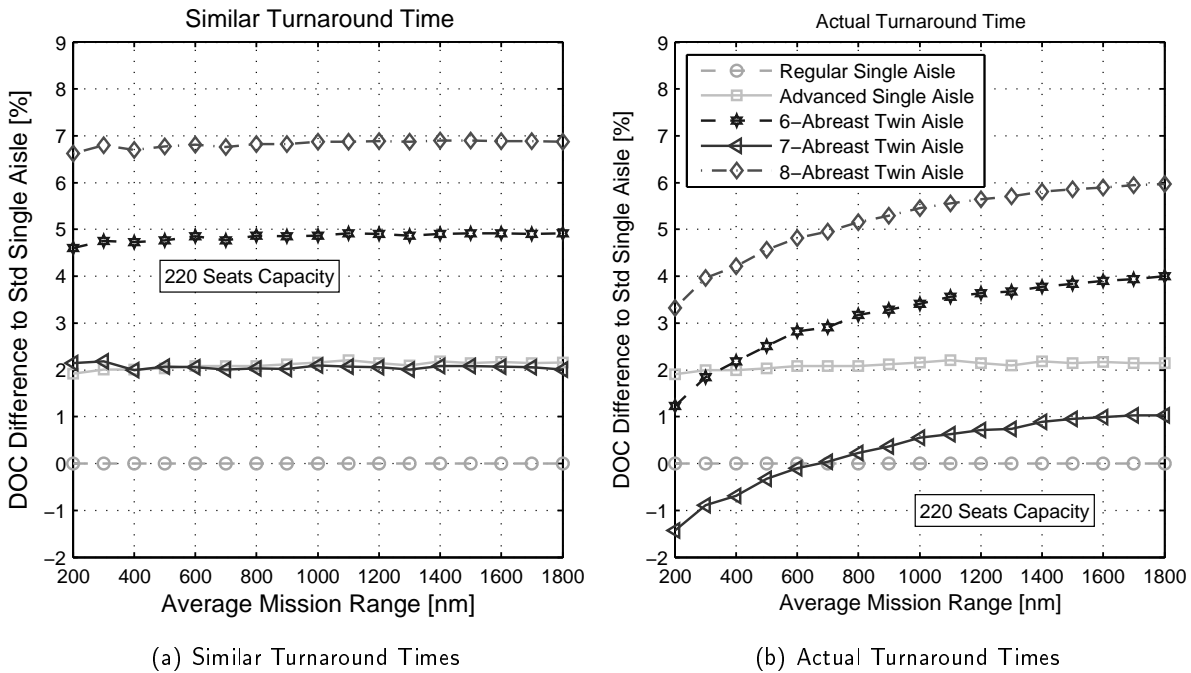
Figure 5.3 – Influence of the turnaround times on DOC. The numbers are the difference to the standard single aisle. Especially lower ranges demonstrate the influence of the turnaround times. Right plot legend also valid for left plot.

lar for all aircraft and the utilization hence depends on the turnaround time alone (when range is fixed).

Figure 5.3 the DOC difference are shown over range. The DOC are given relative to the standard single aisle. The left plot does assume a similar turnaround time depending solely on the capacity. Then the differences in DOC are no function of the average mission range. Compare this to the results shown in figure 4.22. When the true turnaround time is considered, the twin aisles have DOC differences that are changing with range. The plots are made for a fixed capacity of 220 seats. Similar plots can be generated for every capacity, and would change if assumptions change.

The previous two figures demonstrate the effect of turnaround on utilization and finally DOC. The plots are either for a fixed capacity or a fixed range. This shows that an analysis of the entire capacity and range region would result in an impractical amount of plots. Therefore, before analysis is continued, an assessment strategy is introduced.

5.3   Assessment Strategy

The difference in DOC are mostly within 10% of each other, if the more realistic options are compared the differences shrink to 2%. Therefore it makes sense to use differences to a reference instead of absolute values. Hence all values are given as difference to the standard single aisle with conventional door arrangement if not stated otherwise. The standard single aisle is not the A320. It only uses the cross section, but apart from that is sized to similar ranges and capacities as the twin aisle.

The previous plots and most results shown in chapter 3 prove that the 7-abreast twin aisle is the most promising platform of the twin aisles. The estimated turnaround time of all twin aisles is closely
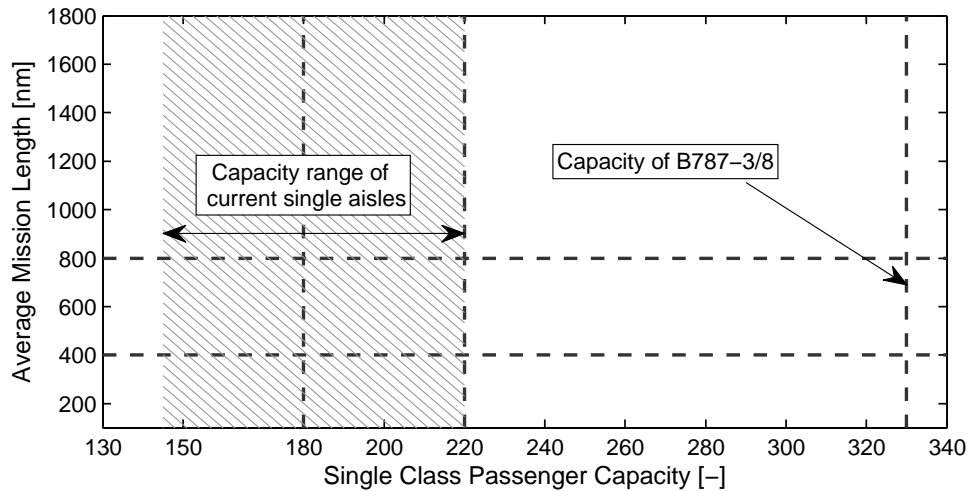
Figure 5.4 – Capacity-range region for assessment. The vertical lines and horizontal lines facilitate the orientation. Compare to figure 1.2.

spaced, still the 7-abreast is often faster than the other twin aisles by a small margin (see 4.10 and 4.12). The fuel burn and mass figures shown in figure 4.20 and 4.21 show the 7-abreast clearly in advantage over both twin aisles.

When the analysis is limited to comparing the 7-abreast against the standard single aisle, the advantage can be displayed in 2-dimensional plots like shown in figure 5.4. The capacity and range covers the entire investigated region. The currently available single aisles occupy the hatched region. The vertical lines indicate the exit capacity limit of the A320 (180 passengers) and the A321 (220 passengers). The corresponding Boeing models have comparable capacity[2]. The region right of 220 passengers is currently not covered by any available design. The next bigger aircraft is the B787-3/8 with an approximate capacity of 330 passengers in a single class layout with comparable comfort standards[3]. Aircraft like the discontinued A310, B767-200 and B757 were placed in this intermediate region between 220 and 330 seats single class capacity. For each combination of range and capacity a DOC difference between standard single aisle and 7-abreast twin aisle can be calculated. This allows to identify the capacity-range regions in which either design has an advantage.

5.4 Standard Scenario

The reference scenario is the set of assumptions most suitable to reflect the current operating environment. DOC assumptions are as listed above (1 USD/kg corresponding to a price of 115 USD/barrel for crude oil, 8% interest rate).

In figure 5.5 the results are shown. The "draw region" is defined by less than 0.5% DOC difference, positive or negative. The single aisle dominates the region with lower capacity. The twin aisle can achieve an advantage as low as 180 seats. But this is limited to average mission ranges of 200nm. A more robust advantage up to 500nm exists at 220 seats. From 260 seats onwards the twin aisle is

---

[2] The B737-800 has an exit capacity limit of 189, the B737-900ER is limited to 215.

[3] The B787-3 seats up to 375 seats in a denser 9-abreast layout, exit limit is 440 passengers [Boe11b].

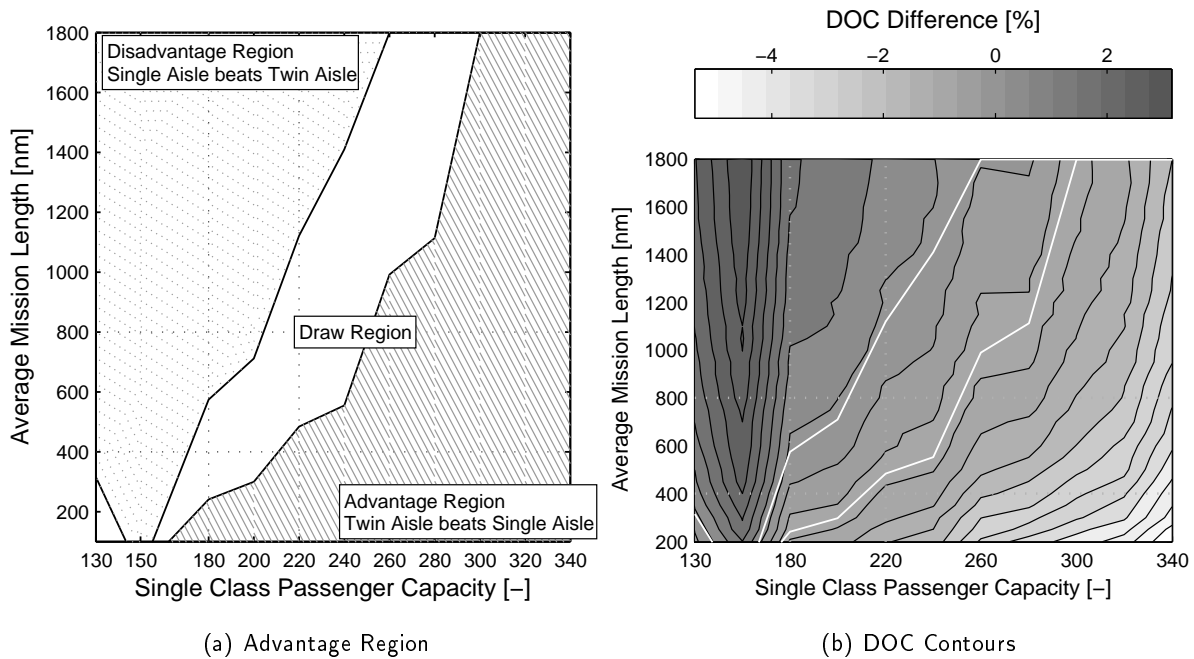(a) Advantage Region   (b) DOC Contours

Figure 5.5 – Results of DOC analysis for the standard scenario. Left plot shows the regions of advantage. On the right side a contour plot of the DOC difference is shown. The dashed line in the left plot represents the standard scenario.

generally superior and the single aisle is disadvantaged. In the region of current single aisles (150 to 220 seats) and especially in the center of the market at 180 seats, the twin aisle achieves an advtange up to 200nm distance. That corresponds to around 10% of all single aisle flights. Using the plot a few particularities can be observed. First, the boundaries between the regions are not continuous. The reason is that for each capacity a fuselage might be slightly more efficient than the other. The effect can partly be reasoned by additional emergency exit lanes being added between two capacities. Further, the lines represent the .5% DOC difference line interpolated from the dataset. The precision of the plot is to some extent virtual. That is why the draw region was added. It further becomes apparent that the disadvantage of the twin is limited to a maximum of 2%, but stays below 1% for most capacity-range combinations. Hence it can be argued that the close match in DOC allows operation of the twin aisle without huge disadvantage to the operator.

5.5 Alternative Scenarios

5.5.1 Scenario 2: Increased Fuel Price

The scenario introduced above reflects the current situation. Future developments will see an increase of the cost of fuel relative to other cost items. This is considered by raising the fuel price by 50% relative to other cost items. This corresponds to a fuel price of 1.5 USD/kg, corresponding to a crude oil price of 175 USD/barrel. Figure 5.6 shows that the increased fuel price has a negative effect, reducing the margin for the twin aisle. The fuel burn disadvantage of the twin aisle decreases with capacity (compare figure 4.21). Consequently, the larger capacities are virtually untouched by the increased fuel price. The overall effect of the fuel price is low. It causes a shift of approximately 20 seats despite a 50% increase. Still, as this scenario represents the future (2020 onwards) operating
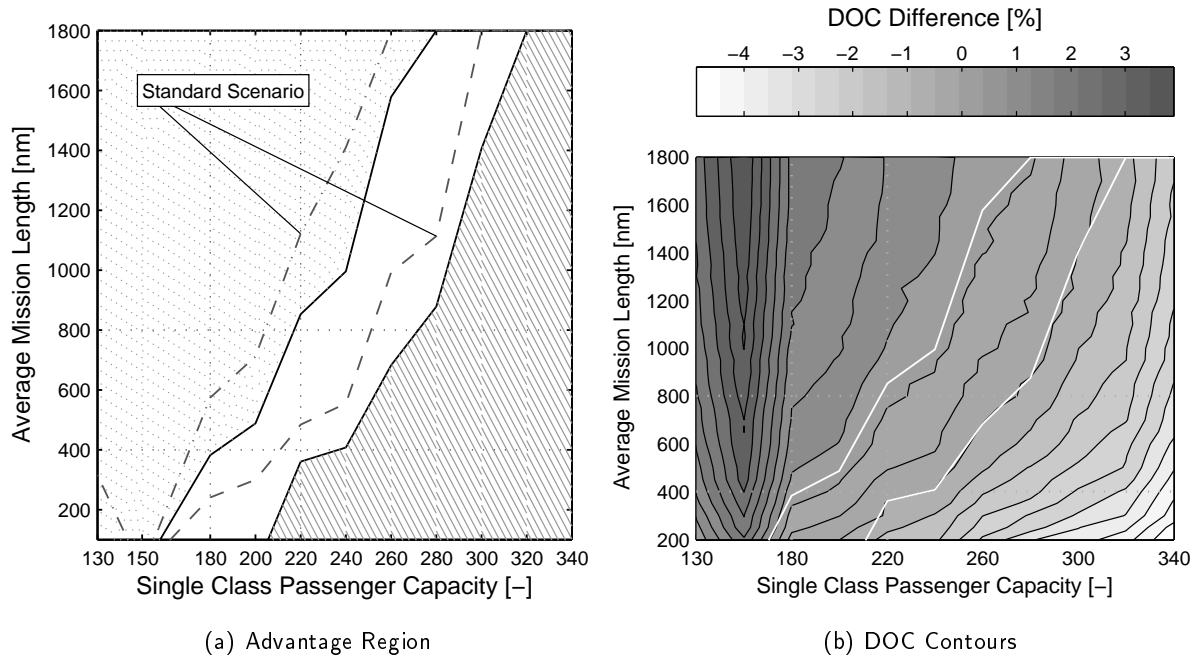
(a) Advantage Region
(b) DOC Contours

Figure 5.6 – Results of DOC analysis for increased fuel prices. The 50% increase in fuel price has only a small impact given the small difference in fuel burn above 240 seats. The dashed countours in the left plot represent the 0.5% DOC-advantage limit in the standard scenario.

environment best, it becomes obvious that a twin aisle designed to similar capacities as the current single aisle does not achieve any cost saving despite shorter turnarounds. Only capacaties above current single aisle could justify a twin aisle.

5.5.2 Scenario 3: Reduced Load Factor

The boarding results are given both for 100% and 85% load factor. As shown in figure 1.4 the average load factor on domestic flights is approaching 85%. Hence 85% initially appears to be the more appropriate assumption for the load factor. This ignores the fact that when 85% is the average, a substantial number of flights will be operated at 100% load factor. If the load factor cannot be predicted in a reliable manner the scheduling needs to consider 100% load factor for a reliable aircraft schedule. Exceptions are routes that have a strong unidirectional traffic, resulting in aircraft flying at a low load factor in one direction and at high load factor into the other. If that is not the case, full load factor needs to be assumed for each turnaround.

The influence of the load factor is provided here as it has a substantial effect on the economic attractiveness of the twin aisle. The lower load factor can also be translated into quicker boarding through other means, for example boarding strategies or restricted amount of carry-on luggage. As shown in figure 5.7, the shorter boarding time advantage reduces the attractiveness of the twin aisle. The effect is much more pronounced than the effect of the increased fuel cost. The load factor decreases the advantage of the twin aisle for all capacities, even the highest capacity models. The shift is again approximately 20 seats from the standard scenario. The effect also works the other way around: longer assumed boarding times favor the twin aisle. The assumed load factor, both average and maximum, are very important to assess the actual advantage for an operator.

(a) Advantage Region

(b) DOC Contours
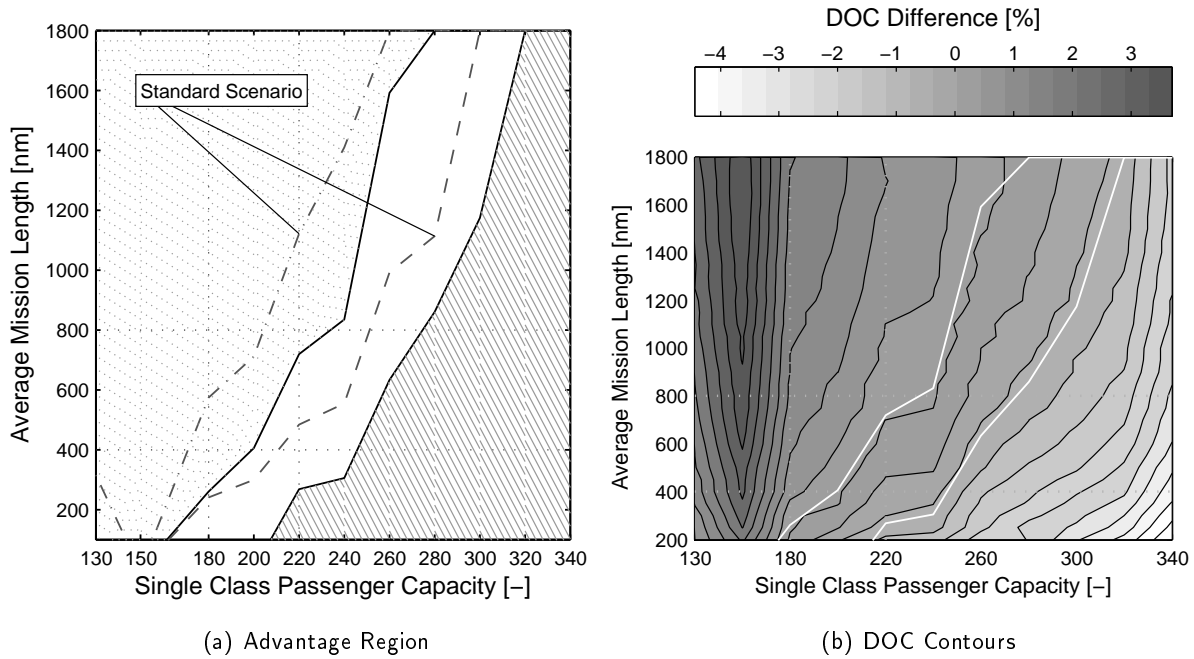
Figure 5.7 – Results of DOC analysis for reduced load factor. The advantage decreases substantially. Note that - different to the increased fuel price scenario - the single aisle achieves a much wider draw region at the top capacities.

5.5.3 Scenario 4: Dual Door Boarding

(a) Advantage Region

(b) DOC Contours
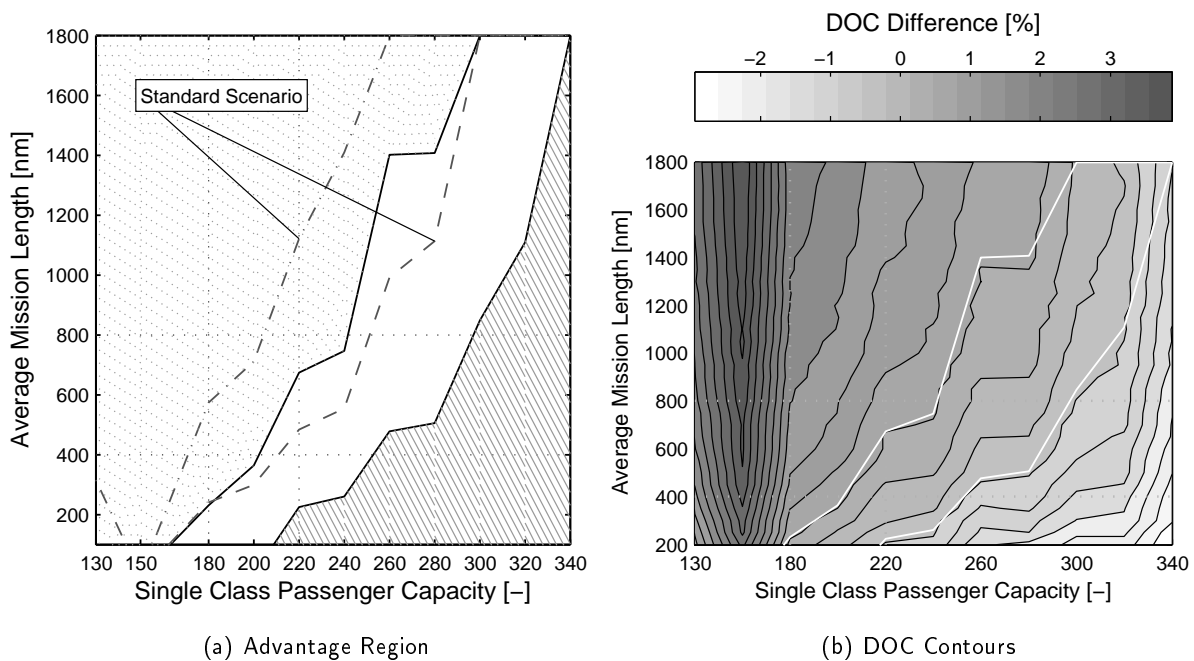
Figure 5.8 – Results of DOC analysis for dual door boarding. The twin aisle still achieves shorter boarding times, but the margin shrinks. Consequently the advantage region is restricted to the large capacities. The dashed contours in the left plot represent the 0.5% DOC-advantage limit in the standard scenario.

Dual door boarding is often performed when positions on the apron are used. Many charter and

low cost carriers nearly exclusively board passengers this way. As demonstrated in the result section, the single aisle gains more from dual door boarding. Therefore, as the look at the resulting cost comparison in figure 5.8 unveils, the twin aisle can only achieve an advantage in the top capacity region. The twin retains a small advantage for the lower ranges. This demonstrates that for charter operations a single aisle appears as more suitable solution if capacity is below 260 seats. The difference to the standard scenario is about 40 seats. It is important to note that the plot does assume dual door boarding for both the single and the twin aisle. A comparison of single door boarding twin against dual door boarded single aisle is not provided, but the twin aisle would not achieve any advantage in that case. However, boarding via stairs on the apron and via jetbridge at the terminal represents vastly different products.

5.5.4 Scenario 5: Quarter Door

(a) Advantage Region

(b) DOC Contours
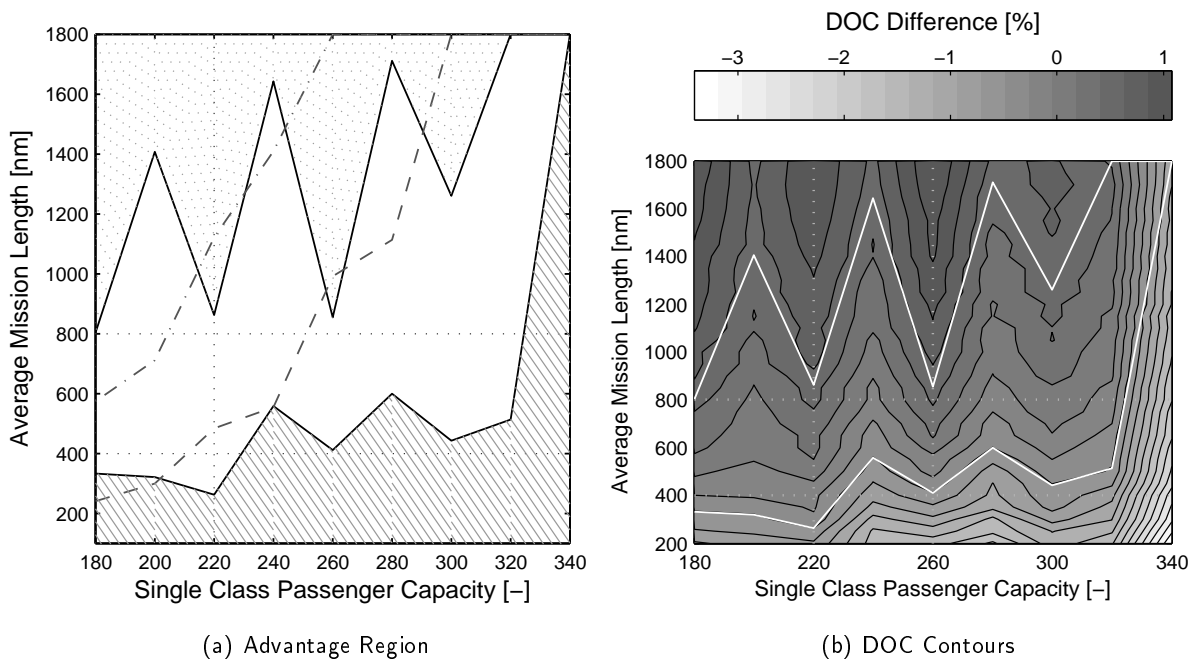
Figure 5.9 – Results of DOC analysis for when twin aisle is compared to quarter door equipped single aisle. Note that comparison starts at 180 seats. The dashed line in the left plot represents the 0.5% DOC-advantage limit in the standard scenario.

The quarter door is a simple and effective solution for faster boarding. It comes with a penalty in fuselage mass at lower capacities for the single aisle. But at and above 240 seats a door is required in front of the wing anyways. In figure 5.9 the quarter door equipped single aisle is compared to the normal twin aisle. The quarter door is specifically interesting in the 180 to 260 seat region. It is interesting to note that the quarter door causes a massive decrease in the twin aisles attractiveness. The strong spikes are caused by two facts. First, the single aisle capacities which require an emergency exit forward of the wing and hence have no large mass penalty demonstrate a solid advantage. These capacities are for example 220 seats and 260 seats. Second, the overall difference is small and the comparison exhibits a very substantial draw region. The lines are interpolated 0.5% difference lines and very sensitive to small changes. It makes sense to take a closer look at the actual DOC results at the right side, and the actual range of DOC differences. While the reduced load factor scenario in

figure 5.7 features a range from -4% to +3% DOC, the quarter door has a range from -3% to +1%. That is, the twin aisle is at no point more than 1% more expensive to operate than the single aisle with quarter door. The twin aisle requires a second emergency exit in front of the wing above 260 seats capacity. If this exit would be upgraded to a full size boarding door the twin aisle could regain an advantage.

5.5.5   Wide Aisle

No results for the wide aisle are provided here. The results have shown no particular advantage for the wide aisle. The obvious increase in mass caused by the wider fuselage would put such a single aisle in disadvantage for all but the lowest capacities. This does not necessarily disprove the usefulness of a wide aisle for quicker boarding, but the simulation failed to identify a true advantage.

5.5.6   Enlarged Door

The enlarged door profits the twin aisles only. So application of a wider door would increase the advantage of the twin aisles as the mass impact is low. Figure 4.16 shows the time savings for the 7-abreast between 1 minute at 180 passengers and 2.5 minutes for 280 passengers. If the quarter door is combined with the enlarged door, the time savings to add up to some extent. The wide door could be used to restore the advantage to some extent of the twin aisle compared to the quarter door or dual door boarding.

5.6   General Finding

Before a final conclusion is attempted a closer analysis of the results is necessary. The reference scenario demonstrates an area of advantage for the twin that steadily grows with capacity. The fuel price is of lesser importance as especially the larger capacity aircraft are very close in actual fuel burn per seat. Changes in load factor have a significant effect. The reduced load factor scenario shrinked the area of advantage for the twin aisle, prolonged turnaround time increase it. The quarter door reduces the advantage of the twin substantially, while the region with low DOC difference is large.

The DOC contour plots have shown that the disadvantage in DOC for the twin is often below 1%. One could argue that the additional comfort offered by a 7-abreast layout allows an operator to increase the yield or achieve higher load factors. The DOC plots further show "sweet spots", capacities at which a more articulated advantage exists. This is due to step changes in the fuselage design. For example if a higher capacity necessitates an additional exit lane.

In general, if aircraft of similar range capability are compared, the twin aisle retains a reliable advantage only for capacities of more than 260 seats. This finding does only slightly deviate from the pure flight performance oriented view, namely that from 260-280 seats onwards the fuel burn of both designs converges. If the single aisle is equipped with a quarter door it retains its advantage up to 300 seats and ranges above 600nm. A twin aisle as replacement for current A320-family aircraft is consequently very unlikely if turnaround is supposed to be the only justification.

It is reminded that both the 6-abreast and the 8-abreast twin aisle proved to be far less attractive than the 7-abreast twin aisle. The 7-abreast represents the best compromise of floor usage and fuse-lage diameter. The need to retain a near circular fuselage prohibits the 8-abreast, especially as the

added underfloor capacity is underused.

The results show a high sensitivity to design changes. The presented findings do not apply to all 6-abreast and 7-abreast designs. Small differences in the actual cross section, the chosen design range or the capacity may change the picture. The type of operation has a very large influence. Some airlines would be unable to use the saved turnaround time. Airlines with a strong hub often have time windows and a quicker turnaround would not produce a benefit (see [Cla07] for more on this). That is the reason why approximated linear regressions for the boarding, deboarding and turnaround time are provided in the appendix for future studies.

Shown DOC differences are for comparison of single aisle and twin aisle of similar technology level and range capability. If range capability is different, or the technology level is different, the picture changes again. Hence, there is an opportunity to replace current single aisle with a twin aisle, if the twin aisle fields better technology than the existing single aisle. However, if the single aisle is equipped with similar technology - given it is applicable - it is unlikely from this study that the twin would retain a DOC advantage below capacities of 260 seats.

The DOC analysis has unveiled that aircraft mass is critical. Charges for landing and navigation have a crucial effect. Especially the airport landing charges constitute a substantial part of the direct operating cost. Again, the benefit of the twin aisle then depends on airport specific charge structure.

Chapter 6

Summary and Conclusion

6.1 Work Summary

This works aims at amending the current design practice for cabin and fuselage layout. Currently the optimum fuselage layout is chosen solely regarding the resulting flight performance. The strong differences in both physical characteristics and turnaround times between single and twin aisles imply that the seat capacity limit for switch from single to twin aisle layout is a function of both the mission range and the seating capacity.

It is well known that boarding and deboarding are important parts of the critical path in aircraft turnaround especially in short range operations. A substantial number of aircraft are operated in short range operations. The short range sector is dominated by single aisles. Load factor, average capacity and seating density have increased in the last 20 years, and are approaching the number where twin aisles are deemed more appropriate.

For the analysis a number of methods are introduced, which have not been used in this combination before. The detailed cabin and fuselage design allows the layout of realistic cabins according to current standards, with realistic monument positions and consistent comfort parameters. An advanced fuselage mass estimation achieves a better match with current aircraft than any statistical formula. It includes physical relationships for the fuselage stress and hence allows to analyze fuselages with substantially higher fitness ratios. This approach is deemed more robust than pure numerical methods using FEM, which are not yet mature enough to be used in preliminary aircraft design. The mass estimation also includes secondary masses like furnishings and systems, which are different for single and twin aisles. Turnaround times are estimated using a boarding simulation for the all-important boarding and deboarding process. The discrete-time simulation represents the passengers as individual agents and is closely connected to the cabin layout. This allows to connect luggage storing times to the size of overhead bins. The simulation achieves a good match with published boarding times, and is able to generate a wide spread as function of input parameters. The results are integrated into a turnaround simulation that includes cargo loading processes. Aircraft design is accomplished using accepted formulas for component mass and drag estimation. The method achieves a good approximation of aircraft with entry-into-service within the next 10 years.

The result section provides the findings of the individual tools. Significant are the findings for seat-specific fuselage mass. The structural mass of the single aisle exceeds that of the twin aisle at 290 seats, but due to secondary masses the twin aisle does not achieve a lower overall operating empty

mass before approximately 330 seats. The twin aisles are shown to have significantly lower boarding and deboarding times, leading to savings in turnaround times of more than 10 minutes. It is further shown, that these savings are highly depending on the input parameters and operational setup, with the savings decreasing quickly when lower load factors are simulated. Time savings using two doors or a quarter door are provided.

In the final chapter the results are analyzed. It is shown that on a pure performance based analysis only the 7-abreast twin aisle can achieve lower direct operating cost within the analyzed capacity region. The single aisle demonstrates superior performance up to 300 seats. When turnaround times and their influence on yearly utilization are included, the twin aisle can achieve lower DOC at 220 seats for ranges below 400nm. However, tougher scenarios with higher fuel cost or lower load factors quickly reduce the advantage of the twin aisle to larger capacities. The type of operation has larger influence on the actual capacity and range than the external parameters such as fuel cost.

It needs to be kept in mind that all results are in comparison to a future single aisle, and are not in comparison to current single aisles. It is neither a comparison to near future derivatives with new engines (A320 NEO), although the assumed technology is very representative of that design.

6.2   Usage of Results and Possible Future Work

The provided results may be useful for future design campaigns. However, the established limit needs to be understood as snapshot as it is highly dependent on applied technology, actual cross sections and cabin layouts. Therefore, it is important make the trade between single aisle and twin aisle based on the actual designs. For that purpose the boarding and turnaround results are provided as linear regression in the appendix. These formulas can be included in aircraft design frameworks and enable the optimization towards minimum DOC. These relationships can also be used for fleet and network analysis that include the specific type of operation of an airline. That includes the mission length, airport operation, actual load factors and possible restrictions by air traffic management. The resulting capacity limit will hence be specific to an airline.

If new airframe or engine technology is considered, the capacity limit might shift, highly depending on the actual fuselage mass. Future aircraft might use different engine technology and hence cruise slower than current aircraft. A twin aisle might offset the reduced cruise speed and still gain compared to a single aisle. Technologies such as laminar flow will have a less observable influence. The key area for improvement of the results is the mass analysis. Despite usage of an advanced mass estimation, better methods are conceivable that consider structural dynamics, as this can be an issue with long and thin fuselages. This would then reduce the attractiveness of the single aisle. The boarding simulation has demonstrated very good performance. The representation of aisle passing possibly needs improvement as the effect of a wide aisle is nearly lost in the results. However, no data could be obtained on the real-life effect of such a wide aisle. This study did not include seating comfort as study parameter. This was motivated by the difficulty of assessing comfort in a monetary way, and by the perception that comfort does not influence booking decisions by passengers when flying short distances.

6.3 Conclusion

The study concludes that twin aisles are substantially faster in passenger boarding and deboarding, and hence in aircraft turnaround. It further concludes that by pure flight performance the single aisle retains an advantage ranging far beyond the fuselage fitness ratio usually considered the optimum region. In fact, capacities of up to 300 seats in a single class still see the single aisle in advantage, albeit the advantage is small. This advantage depends strongly on the particular cross section. The 7-abreast can outperform a single aisle with wider cross section at capacities as low as 220 seats. Seemingly small details like the required number of exits can have strong influence and cause a volatile trend (see figure 4.21 on page 107). A robust advantage of the twin aisle is observed above 300 seats when seat-specific fuselage structural mass of the single aisle increases sharply.

The inclusion of turnaround analysis reduces the capacity limit to 260 to 280 seats. Although the single aisle retains a small performance advantage, its significantly longer turnaround times have a negative effect on the daily utilization. The single aisle remains in advantage if operated over long distances and and with usage of two doors on an apron position. On the other side, when operated on short sectors and limited to passenger bridge boarding, the twin aisle establishes an advantage at capacities as low as 180 seats.

It can be definitely stated that for current single aisle capacities no twin aisle replacement appears useful. Even if short sectors and high load factors are considered, the twin aisle would only achieve an advantage at 5 to 10% of the current single aisle flights. If capacities are increased, with a stretched single aisle reaching up to 250 seats, a purpose designed twin aisle could achieve better utilization and hence operating cost on short sectors. However, an adaption of long range aircraft for short range operations does not appear promising as the disadvantage in aircraft weight would deny any cost advantage. If twin aisles are operated on such sectors today, it is usually caused by constraints in airport slots in connection with very high demand, or simply the availability of such aircraft, and not driven by aircraft operating cost.

The study shows that boarding times are a major disadvantage of current single aisles. The inclusion of a quarter door may alleviate the problem to some extent. Although it does not equal the turnaround times simulated for the twin aisles, quarter door equipped single aisles gain enough time to equal on direct operating cost. At capacities above 220 seats the quarter door causes rather little additional fuselage mass.

Bibliography

[ANS12]   ANSYS Inc. *ANSYS Mechanical Analysis*. URL: www.ansys.com/Products/Simulation+
            Technology/Structural+Mechanics/ANSYS+Mechanical. Accessed August 12th. 2012.

[ARC11]   Airport Research Center, Aachen. *CAST Cabin - Simulation of Boarding Processes*. URL:
            www.airport-consultants.com. Accessed August 10th. 2011.

[Air05]   Airbus. "A320 Family Briefing." Marketing Presentation. Airbus Marketing Division, 2005.

[Air07]   Airbus Customer Services. *A320 Flight Crew Operating Manual - Part C: Flight Operation*.
            2007.

[Air08]   Airbus Engineering - Mass Properties. *Airbus Mass Standard Reference Guide - Issue 3*.
            2008.

[Air09]   Airbus. "Flying smart, thinking big." Global Market Forecast 2009-2028. 2009.

[Air11a]   Airbus - Flight Operations Support & Line Assistance. *Getting to Grips with Aircraft
            Performance*. 2011.

[Air11b]   Airbus - Flight Operations Support & Line Assistance. *Getting to Grips with Fuel Economy*.
            2011.

[Air83]   Airbus Customer Services. *Airplane Characteristics For Airport Planning - A300-600*. 1983.

[Air88a]   Airbus Customer Services. *A320 - Weight and Balance Manual*. 1988.

[Air88b]   Airbus Industries. *Data Basis for Design - A320*. AI/ED-T431.101/88. 1988.

[Air95]   Airbus Customer Services. *Airplane Characteristics For Airport Planning - A319, A320,
            A321*. 1995.

[App10a]   H. Appel, R. Henke. "Applicability of Theoretical Approaches for Airplane Boarding." In:
            Air Transport Research Society Conference 2010 (2010).

[App10b]   H. Appel, R. Henke. "Einsetzbarkeit gezielter Aussteigevarianten beim Deboarding von
            Flugzeugen." In: *59. Deutscher Luft- und Raumfahrtkongress* (2010).

[Ard96]   M. Ardema et al. "Analytical Fuselage and Wing Weight Estimation of Transport Aircraft."
            Technical Report NASA-TM-110392. NASA - Ames Research Center, 1996.

[Asc11a]   Flightglobal Advisory Service. *Ascend Database*. URL: www.ascendworldwide.com/what-
            we-do/ascend-data/airport-data/. Accessed October 22nd. 2011.

[Asc11b]   Flightglobal. *World Airliner Census*. URL: www.flightglobal.com/airspace/media/reports_pdf
            /emptys/87145/world-airliner-census-2011.pdf. Accessed October 28th. 2011.

[BTS13]   BTS. *Bureau of Transport Statistics - Research and Innovative Technology Administration*.
            URL: www.transtats.bts.gov/. Accessed March 3rd. 2013.

[Bal09]   K. Balcombe, I. Fraser, L. Harris. "Consumer willingness to pay for in-flight service and comfort levels: a choice experiment." In: *Journal of Air Transport Management* 15 (2009), pp. 221–226.

[Bau03]   R. von Baur, H. Oltmanns. "Entwicklung der Rumpfmasse über die Zeit - A340-300." In: *Luftfahrttechnisches Handbuch* MA 508 12-51 (2003).

[Bau93]   R. von Baur, H. Oltmanns. "Hauptfahrwerk - Transporter - Statistische Massenabschätzung." In: *Luftfahrttechnisches Handbuch* MA 510 12-01 (1993).

[Baz07]   M. Bazargan. "A linear programming approach for aircraft boarding strategy." In: *European Journal of Operational Research* 183 (2007), pp. 394–411.

[Ber09]   F. Berg, T. Lammering. "Vergleich und Erweiterung verschiedener Methoden zur Massenabschätzung einzelner Komponenten im Flugzeugvorentwurf." Thesis. Rheinisch-Westphälische Technische Hochschule, Institut für Luft- und Raumfahrt, 2009.

[Bet77]   M. Beltramo, D. Trapp, B. Kimoto, D. Marsh. "Parametric Study of Transport Aircraft System Cost and Weight." Technical Report NASA-CR-151970. NASA - Ames Research Center, 1977.

[Boe02]   Boeing Commercial Airplanes. *Airplane Characteristics For Airport Planning - B757*. 2002.

[Boe04]   M. Sankrithi. "Twin Aisle Small Airplane." English. US Patent 6834833 B2. Boeing Commercial Airplanes, 2004.

[Boe05a]   Boeing Commercial Airplanes. *Airplane Characteristics For Airport Planning - B737*. 2005.

[Boe05b]   Boeing Commercial Airplanes. *Airplane Characteristics For Airport Planning - B767*. 2005.

[Boe06]   Boeing Commercial Airplanes. *B787 Airplane Description and Selections*. Revision J. 2006.

[Boe11a]   D. Böhnke, B. Nagel, V. Gollnick. "An Approach to Multi-Fidelity in Conceptual Aircraft Design in Distributed Design Environments." In: *IEEE Aerospace Conference* (2011).

[Boe11b]   Boeing Commercial Airplanes. *Airplane Characteristics For Airport Planning - B787*. 2011.

[Boe12]   Boeing Commercial Airplanes. *Current Market Outlook*. URL: www.boeing.com/commercial/cmo/index.html. Accessed February 21st. 2012.

[Boe97]   R. K. Brauer. "Optimal Airplane Passenger Seating Configurations." English. US Patent 5611503. Boeing Commercial Airplanes, 1997.

[Bri03]   M. van den Briel, R. Villalobos, G.Hogg. *The Aircraft Boarding Problem*. 2003.

[Car87]   J. Carlzon. *Moments of Truth*. Harper Perennial, 1987.

[Cla07]   P. Clark. *Buying The Big Jets - 2nd Edition*. Ashgate, 2007.

[Cle70]   F. A. Cleveland. "Size Effects in Conventional Aircraft Design." In: *Journal of Aircraft* 7 (1970), pp. 483–511.

[DAS90]   Deutsche Airbus GmbH. *MPC75 - Aerodynamic Data Base*. 1990.

[DEW04]   N. Hutton. "Flexible over the wing passenger loading bridge." English. US Patent 6820296. 2004.

[DLR11]   Deutsches Zentrum für Luft- und Raumfahrt, Institut für Flughafenwesen. *Traffic Oriented Microscopic Simulator*. URL: www.dlr.de/fw/desktopdefault.aspx/tabid-5980/9752_read-19750/. Accessed October 8th. 2011.

[DLR12]   Deutsches Zentrum für Luft- und Raumfahrt, Institut of Propulsion Technology. *Working Area Engine and Aircraft Performance Calculation*. URL: www.dlr.de/at/Desktopdefault.aspx/ tabid-1547/2182_read-3654/. Accessed September 2nd. 2012.

[Dog10]   R. Doganis. *Flying Off Course - Airline Economics and Marketing - 4th Edition*. Routledge, 2010.

[Dol07]   J. Dollmayer. *Methode zur Prognose des Einflusses von Flugzeugsystemen auf die Missionskraftstoffmasse*. Schriftenreihe Flugzeug-Systemtechnik, 2007.

[Dor11]   F. Dorbath. "Civil Jet Transport Aircraft - Statistical Mass Estimation." In: *Luftfahrttechnisches Handbuch* MA 401 12-01 (2011).

[Dzi11]   N. Dzikus, J. Fuchte. "Potential for Fuel Reduction through Electric Taxiing." In: *AIAA Aviation Technology, Integration and Operations* (2011).

[EAS06]   European Aviation Safety Agency. *Certification Specifications for Large Aeroplanes - Amendment 2*. 2006.

[EAS09]   Z. Berdowski, F.N. van den Broek-Serie, J.T. Jetten, Y.Kawabata. "Survey on standard weights of passengers and baggage." Technical Report. NEA (financed by EASA), 2009.

[EU08]   European Union. *EU-OPS: European Union Requirements for the Operation of Commercial Air Transport*. EEC No 3922/91. 2008.

[Eur04]   University of Westminster. *Evaluating the True Cost to Airlines of One Minute of Airborne or Ground Delay*. Eurocontrol, 2004.

[Eur11]   Eurocontrol - Central Office for Delay Analysis. *Study Into the Impact of the Global Economic Crisis on Airframe Utilisation*. 2011.

[FPO07]   F. Lutsch. "Preliminary Aircraft Design - Design Course at University of Stuttgart." Presentation/Lecture. Airbus Future Project Office, 2007.

[FPO11]   H. Kwik. "Payload Accommodation in Early Design Phase." Presentation/Lecture at TU Hamburg-Harburg. Airbus Future Project Office, 2011.

[Fer04]   P. Ferrari, K. Nagel. *Robustness of Efficient Passenger Boarding in Airplanes*. 2004.

[Fli11a]   Flightglobal. *ANA abandons B787-3*. URL: www.flightglobal.com/news/articles/ana-abandons-787-3-336950/. Accessed January 25th. 2011.

[Fli11b]   Flightglobal. *Boeing Weighs Narrowbody Options*. URL: www.flightglobal.com/articles/ 2011/03/21/354513/boeing-weighs-narrowbody-options.html. Accessed March 22nd. 2011.

[Fli11c]   N.N. "World Airliner Census 2011." In: *Flight International* (2011).

[Fli87]   D. Learmound. "Propfan - the price factor." In: *Flight International - 13 June 1987* (1987).

[Fri09]   H. Fricke, M. Schultz. "Delay Impacts onto Turnaround Performance." In: *8th ATM Seminar, Napa* (2009).

[Fug01]   A. Fuge, B. Höfer. "Der kritische Pfad." In: *Workshop: Flugzeugkabine / Kabinensysteme - die nächsten Schritte* (2001).

[Gom09]   F. Gomez, D. Scholz. "Improvements to Ground Handling Operations and Their Benefits to Direct Operating Cost." In: *58. Deutscher Luft- und Raumfahrtkongress* (2009).

[HAM11]   N. N. "Hamburg Airport - Flughafenentgelte -Teil I & II - 2012." Publication. Flughafen Hamburg GmbH, 2011.

[Har68]   P. Hart, N. Nilsson, B. Raphael. "A Formal Basis for the Heuristic Determination of Minimum Cost Paths." In: *IEEE Transactions on Systems Science and Cybernetics* SSC-4, No. 2 (1968), pp. 100–107.

[Heh01]   J. Hehemann. "Entwicklung von Flugzeugkabinen." In: *Workshop: Flugzeugkabine / Kabinensysteme - die nächsten Schritte* (2001).

[Hei01]   W. Heinze, C. Österheld, P. Horst. "Multidisziplinäres Flugzeugentwurfsverfahren PrADO - Programmentwurf und Anwendung im Rahmen von Flugzeug-Konzeptstudien." In: *50. Deutscher Luft- und Raumfahrtkongress* (2001). Bonn.

[Hei07]   W. Heinze. *Entwerfen von Verkehrsflugzeugen - Vorlesungsmanusskript*. Technische Universität Braunschweig, 2007.

[Hie97]   M. Hiersig, R. von Baur. "Türen Massedaten." In: *Luftfahrttechnisches Handbuch* MA 508 22-03 (1997).

[How00]   D. Howe. *Aircraft Conceptual Design Synthesis*. Professional Engineering Publishing, 2000.

[Hue98]   K. Hünecke. *Die Technik des modernen Verkehrsflugzeuges*. Motorbuchverlag, 1998.

[IAT12]   International Air Transport Association. *IATA - Jet Fuel Price Development*. URL: www.iata.org/whatwedo/economics/fuel_monitor/Pages/price_development.aspx. Accessed July 5th. 2012.

[Kei02]   T. Keilig, A. Schmidt. "Gewichtsprognose von CFK-Rümpfen für zukünftige Passagierflugzeuge." In: *51. Deutscher Luft- und Raumfahrtkongress* (2002).

[Koe06]   C. Koeppen. *Methodik zur modellbasierten Prognose von Flugzeugsystemparametern im Vorentwurf von Verkehrsflugzeugen*. Schriftenreihe Flugzeug-Systemtechnik, 2006.

[Kon01]   G. Konieczny. "Die Messung und Steigerung der Qualität von Dienstleistungen in der Flugzeugkabine." PhD Thesis. Technical University of Berlin, 2001.

[Kra10]   P. Krammer, O. Junker, D. Scholz. "Aircraft Design for Low Cost Ground Handling - The Final Results of the ALOHA Project." In: *27th International Congress of The Aeronautical Sciences* (2010).

[Kre10]   T. Kreitz, J. Fuchte. "Ermittlung aktueller Kabinenkomfortstandards und Konstruktion moderner Passagiersitze." Thesis. Technisch Universität Hamburg-Harburg, 2010.

[LH10]   Lufthansa Medienservice. "Neue Europa Kabine." In: *Lufthansa Newslink* Ausgabe 50sp (2010).

[LH11]   Lufthansa. "1. Zwischenbericht Januar-März 2011." Quarterly Report. Lufthansa Board of Directors, 2011.

[Lan02]   H. Van Landeghem, A. Beuselinck. "Reducing passenger boarding time in airplanes: A simulation based approach." In: *European Journal of Operational Research* 142 (2002), pp. 294–308.

[Lee04]   D. Lee, M. J. Luengo-Prado. "Are passengers willing to pay more for additional legroom." In: *Journal of Air Transport Management* 10 (2004), pp. 377–383.

[Lie95]   R. Liebeck et al. "Advanced Subsonic Airplane Design & Economic Studies." Technical Report NASA-CR-195443. McDonnell Douglas Aerospace, 1995.

[Liu98]   Gerdes, Liu, Quast. "Rumpfwerk - Transporter - Masserelevante Daten." In: *Luftfahrttechnisches Handbuch* MA 508 52-01 (1998).

[Lom96]   T. L. Lomax. *Structural Loads Analysis for Commercial Transport Aircraft: Theory and Practice*. AIAA Education Series, 1996.

[MDD89]   McDonnell Douglas Corporation. *Airplane Characteristics For Airport Planning - DC-8 Series*. 1989.

[MIT12]   Massachusetts Institute of Technology. *Airline Data Project*. URL: web.mit.edu/airlinedata/ www/default.html. Accessed July 9th. 2012.

[Mar98]   S. Marelli, G. Mattocks, R. Merry. "The Role of Computer Simulation in Reducing Airplane Turn Time." In: *Boeing Aeromagazine* 1 (1998).

[Met08]   R. Metzger. "Gesamtheitliche Optimierung von Rumpfquerschnitten im Flugzeugvorentwurf." PhD Thesis. Technical University of Munich, 2008.

[Mue11]   M. Mueller. "HX2QR Series SMR Feeders Study "TAO" for EADS Airbus." TwinAisle-Feeders, 2011.

[NAS10]   M. Bradley et al. "Subsonic Ultra Green Aircraft Research - Final Review." Presentation to NASA. Boeing, 2010.

[Nag06]   B. Nagel, M. Rose, H.P. Monner, R. Heinrich. "An Alternative Procedure For FEM-wing Modelling." In: *55. Deutscher Luft- und Raumfahrtkongress* (2006).

[Nit10]   M. Nita, D. Scholz. "From Preliminary Aircraft Cabin Design to Cabin Optimization." In: *59. Deutscher Luft- und Raumfahrtkongress* (2010).

[Niu88]   M. C.-Y. Niu. *Airframe Structural Design*. Conmilit Press, 1988.

[Nyq08]   D. Nyquist, K. McFadden. "A study of the airline boarding problem." In: *Journal of Air Transport Management* 14 (2008), pp. 197–204.

[OAG07]   UBM Aviation. *Official Airline Guide Data 2007*. 2007.

[Oes03]   C. Österheld. "Physikalisch begründete Analyseverfahren im integrierten multidisziplinären Flugzeugvorentwurf." PhD Thesis. TU Braunschweig, 2003.

[PAC12]   PACE. *Pace - Products - Cabin Configuration*. URL: www.pace.de/ products/ cabin-configuration/ pacelab-cabin-6.html. Accessed January 15th. 2012.

[Pau93]   Paul, Liu. "Flügel - Transporter - Masserelevante Daten." In: *Luftfahrttechnisches Handbuch* MA 501 52-01 (1993).

[Pin82]   P. Pincha. "Algorithmic Mass-Factoring of Finite Element Model Analysis." In: *SAWE Paper 1451* (1982).

[Ray92]   D. P. Raymer. *Aircraft Design - A Conceptual Approach - 2nd Edition*. AIAA Education Series, 1992.

[Ric07]   T. Richter. "Simulationsmethodik zur Effizienz- und Komfortbewertung von Menschenflussprozessen in Verkehrsflugzeugen." PhD Thesis. Technical University of Munich, 2007.

[Ros04a]   J. Roskam. *Airplane Design - Part II: Preliminary Configuration Design and Integration of the Propulsion System*. DARcorporation, 2004.

[Ros04b]   J. Roskam. *Airplane Design - Part III: Layout Design of Cockpit, Fuselage, Wing and Empennage*. DARcorporation, 2004.

[Ros13]   M. Rosskopf. "Studien zur Airline-Flottenplanung anhand eines mathematischen Optimierungsmodells." PhD Thesis. Technische Universität Hamburg Harburg, 2013.

[Ros97]   J. Roskam, C.-T. E. Lan. *Airplane Aerodynamics and Performance*. DARcorporation, 1997.

[Sch11]   J. Scherer, D. Kohlgrüber. "Koppelung der Modellgenenierung und der statischen Dimensionierung von Flugzeugrümpfen im Vorentwurf." Masterthesis. Deutsches Zentrum für Luft- und Raumfahrt, 2011.

[Sch97]   R. Kelm A. Schmidt M. Läpple. "Advanced Fuselage Weight Estimation for the New Generation of Transport Aircraft." In: *56th Annual Conference, Bellevue, Washington, May 19-21* (1997).

[Sch99]   D. Scholz. *Flugzeugentwurf - Skript zur Vorlesung*. University of Applied Sciences, 1999.

[Sea11]   SeatGuru. *Short-haul Economy Comparison Chart*. URL: www.seatguru.com/charts/ short-haul_economy.php. Accessed September 6th. 2011.

[Ste08]   J. Steffen. "Optimal boarding method for airline passengers." In: *Journal of Air Transport Management* 14 (2008), pp. 146–150.

[Ste10]   A. Steiner, M. Philipp. "Speeding Up the Airplane Boarding Process by Using Pre-Boarding Areas." In: *10th Swiss Transport Research Conference* (2010).

[Ste11]   J. Steffen, J. Hotchkiss. "Experimental test of airplane boarding methods." In: FERMILAB-PUB-11-402-AE (2011).

[Tho01]   J. Thorbeck. *Flugzeugentwurf - Manusskript zur integrierten Lehrveranstaltung*. Technische Universität Berlin, 2001.

[Tor76]   E. Torenbeek. *Synthesis of Subsonic Airplane Design*. Delft University Press, 1976.

[Wit06]   R. Wittmann. "Bewertung von Kabinenkonfigurationen." PhD Thesis. Technical University of Munich, 2006.

[Wu10]   C.-L. Wu. *Airline Management and Delay Management*. Ashgate, 2010.

Appendix A

Appendix

A.1 Abbreviations

ACAP	Airplane Characteristics for Airport Planning (document type)
ASK	Available Seat Kilometer
COC	Cash Operating Cost
DES	Discrete Event Simulation
DLR	Deutsches Zentrum für Luft- und Raumfahrt
DOC	Direct Operating Cost
DTS	Discrete Time Simulation
FCOM	Flight Crew Operating Manual
FEM	Finite Element Modeling
GTF	Geared Turbofan
HTP	Horizontal Tail Plane
KIAS	Knots Indicated Airspeed
MASim	Multi-Agent Simulation (tool name)
MTOW	Maximum Take-Off Weight
NASA	National Aeronautics and Space Administration
OHSB	Overhead Stowage Bin (common name for stowage located above the passenger seat)
PAX	Passenger(s)
SA	Single Aisle
SFC	Specific Fuel Consumption
TA	Twin Aisle
TSFC	Thrust Specific Fuel Consumption
ULD	Unit Load Device - aircraft container.
USD	United States Dollar - common currency used for cost estimation in aircraft design.
VTP	Vertical Tail Plane

A.2 List of Symbols

Table A.1 – Used symbols, page 74

Symbol	Name	Unit
m_{wing}	Wing mass	[kg]
A_{wing}	Wing area	[m^2]
MTOM	Maximum Take-Off Mass	[kg]
T/C_{rep}	(representative) Thickness to chord ratio of profile	[–]
AR	Aspect ratio of wing	[–]
φ_{25}	Sweep at 25% line	[rad]
m_{htp}	Mass of horizontal tail	[kg]
A_{htp}	Horizontal tail area	[m^2]
m_{vtp}	Mass of vertical tail	[kg]
A_{vtp}	Vertical tail area	[m^2]
m_{gear}	Mass of landing gear (group)	[kg]
MLM	Maximum Landing Mass	[kg]
m_{pylon}	Mass of pylon (group)	[kg]
SLST	Sea-Level Static Thrust	[N]
m_{sys}	Mass of systems	[kg]
l_{fus}	Length of fuselage	[m]
d_{fus}	Width of fuselage	[m]

Table A.2 – Used symbols, section 2.2

Symbol	Name	Unit
m_{fus}	Fuselage mass	[kg]
d_{fus}	Fuselage (equivalent) diameter	[m]
l_{fus}	Fuselage length	[m]
S_{fus}	Fuselage wetted surface	[m^2]
λ_{fus}	Fuselage fitness ratio (length to diameter)	[–]
p_{max}	Maximum overpressure of the fuselage	[N/m^2]
w_{Cabin}	Cabin width	[m]
$w_{Armrest}$	Armrest width	[m]
w_{Seat}	Seat width (between armrests)	[m]
$w_{Clearance}$	Head clearance	[m]
w_{Aisle}	Aisle width (between armrests)	[m]
$n_{Abreast}$	Passenger seating	[–]
n_{PAX}	Number of seats	[–]
l_{Cabin}	Length of cabin	[m]
$l_{SeatPitch}$	Seat longitudinal spacing	[m]
$l_{Flightdeck}$	Flightdeck length	[m]

Table A.3 – Used symbols, table 3.1 and table 3.2

Symbol	Name	Unit
$m_{electrics}$	Electrical system mass	[kg]
$m_{furnishings}$	Furnishings mass	[kg]
m_{ECS}	Environmental Control System mass	[kg]
m_{CabSys}	Cabin systems mass	[kg]
V_{fus}	Fuselage pressurized volume	[m]
A_{cabin}	Cabin floor area	[m^2]
l_{fus}	Fuselage length	[m]

Table A.4 – Used units (entire text)

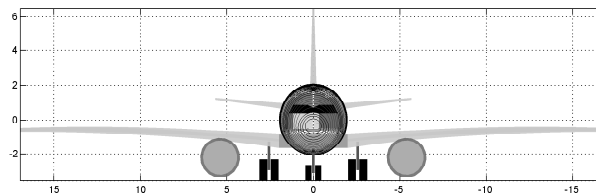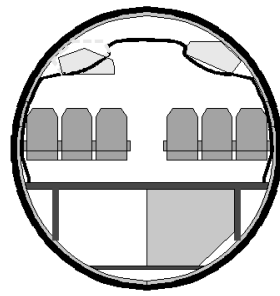| Symbol	Name	Conversion
kg	Kilogramm	
m	Meter	
N	Newton	
nm	Nautical Mile	$1nm = 1852m$
ft	Feet	$1ft = 0.3048m$
kts	Knots	$1kts = 1.852km/h$
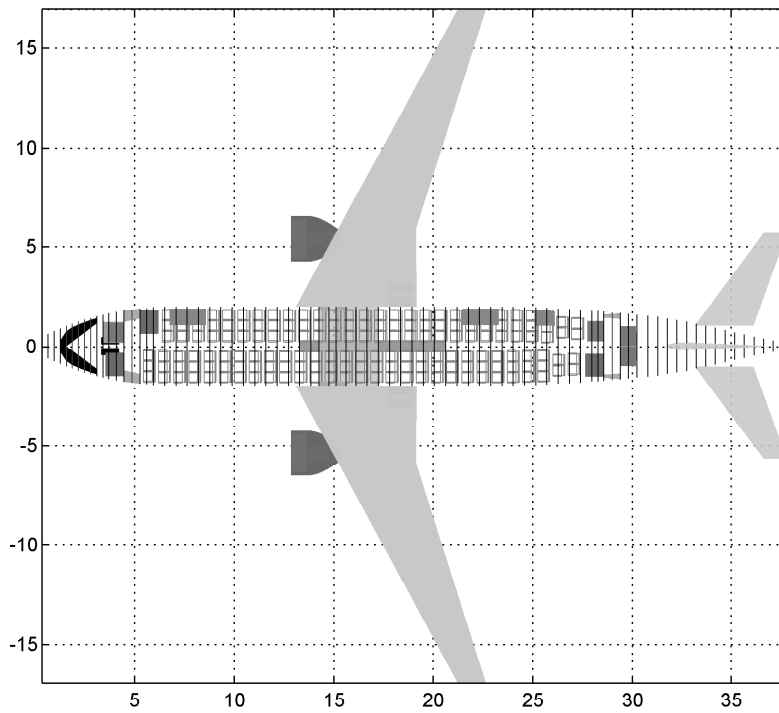
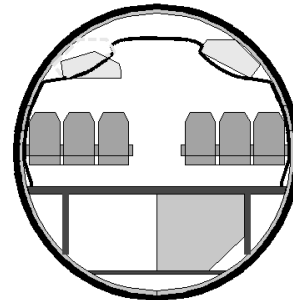(a) Top View
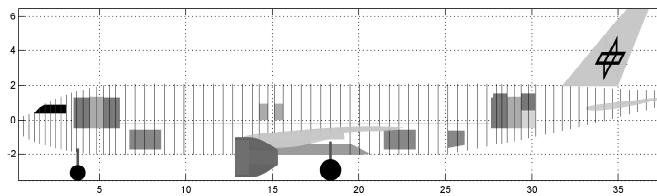
(b) Side View

(c) Front View

Figure A.1 – Three-view drawing of designed aircraft resembling the Airbus A320 in size, weight and performance.
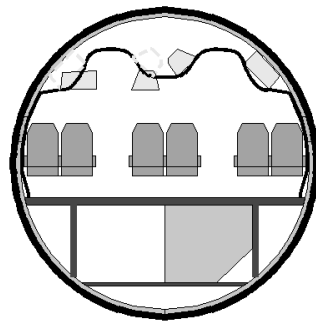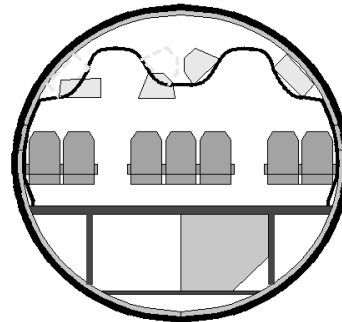
A.4 Studied Cross Sections
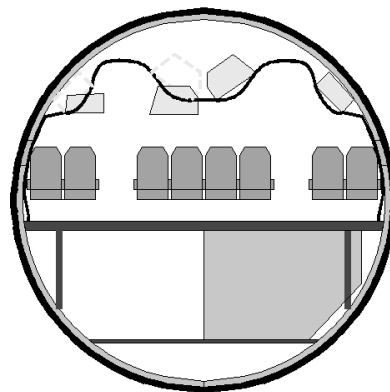

(a) Standard Single Aisle

(b) Advanced Single Aisle

(c) Small Twin Aisle

(d) Intermediate Twin Aisle

(e) Full Size Twin Aisle

Figure A.2 – The studied cross sections in correct scale.

A.5 Regression of Boarding, Deboarding, Turnaround Times

Boarding Times

The provided regressions are for 40% bulky carry-on (trolleys) and average smartness. See text at page 94 for further explanations. Regressions are valid from 130 to 340 passengers and optimized for minimum total error. The average offset (positive or negative) of the regression function to the simulated result is less than 30 seconds (or 3%). This means that the presented formulas allow a good re-enacting of the boarding simulation results.

	100% LF Door 1L	100% LF Quarter Door
Regular Single Aisle	0.063 min/PAX x PAX + 6.286 min	0.031 min/PAX x PAX + 11.462 min
Advanced Single Aisle	0.052 min/PAX x PAX + 8.507 min	0.031 min/PAX x PAX + 10.803 min
6-Abreast Twin Aisle	0.045 min/PAX x PAX + 3.680 min	0.032 min/PAX x PAX + 5.749 min
7-Abreast Twin Aisle	0.030 min/PAX x PAX + 5.274 min	0.020 min/PAX x PAX + 6.775 min
8-Abreast Twin Aisle	0.032 min/PAX x PAX + 5.700 min	0.025 min/PAX x PAX + 5.614 min

	100% LF Dual Door	85% LF Door 1L
Regular Single Aisle	0.024 min/PAX x PAX + 7.652 min	0.053 min/PAX x PAX + 4.483 min
Advanced Single Aisle	0.022 min/PAX x PAX + 7.810 min	0.042 min/PAX x PAX + 6.965 min
6-Abreast Twin Aisle	0.021 min/PAX x PAX + 4.117 min	0.036 min/PAX x PAX + 3.336 min
7-Abreast Twin Aisle	0.017 min/PAX x PAX + 3.758 min	0.027 min/PAX x PAX + 3.990 min
8-Abreast Twin Aisle	0.013 min/PAX x PAX + 5.138 min	0.029 min/PAX x PAX + 4.603 min

	85% LF Quarter Door	85% LF Dual Door
Regular Single Aisle	0.022 min/PAX x PAX + 9.994 min	0.021 min/PAX x PAX + 5.442 min
Advanced Single Aisle	0.030 min/PAX x PAX + 7.786 min	0.017 min/PAX x PAX + 6.558 min
6-Abreast Twin Aisle	0.023 min/PAX x PAX + 5.438 min	0.017 min/PAX x PAX + 3.295 min
7-Abreast Twin Aisle	0.022 min/PAX x PAX + 4.304 min	0.015 min/PAX x PAX + 3.126 min
8-Abreast Twin Aisle	0.023 min/PAX x PAX + 4.489 min	0.012 min/PAX x PAX + 4.211 min

Table A.5 – Linear regression of boarding times.

Deboarding Times

The provided regressions are for 40% bulky carry-on (trolleys) and average smartness. See text at page 94 for further explanations. Deboarding can also be approximated by using a constant rate of passengers per minute.

	100% LF Door 1L	100% LF Quarter Door
Regular Single Aisle	0.033 min/PAX x PAX + 3.272 min	0.032 min/PAX x PAX + 2.888 min
Advanced Single Aisle	0.033 min/PAX x PAX + 3.272 min	0.032 min/PAX x PAX + 2.888 min
6-Abreast Twin Aisle	0.023 min/PAX x PAX + 1.316 min	0.019 min/PAX x PAX + 1.455 min
7-Abreast Twin Aisle	0.024 min/PAX x PAX + 1.265 min	0.020 min/PAX x PAX + 1.394 min
8-Abreast Twin Aisle	0.024 min/PAX x PAX + 1.162 min	0.021 min/PAX x PAX + 1.283 min

	100% LF Dual Door	85% LF Door 1L
Regular Single Aisle	0.022 min/PAX x PAX + 2.160 min	0.033 min/PAX x PAX + 3.272 min
Advanced Single Aisle	0.022 min/PAX x PAX + 2.160 min	0.033 min/PAX x PAX + 3.272 min
6-Abreast Twin Aisle	0.015 min/PAX x PAX + 0.868 min	0.023 min/PAX x PAX + 1.316 min
7-Abreast Twin Aisle	0.016 min/PAX x PAX + 0.835 min	0.024 min/PAX x PAX + 1.265 min
8-Abreast Twin Aisle	0.016 min/PAX x PAX + 0.767 min	0.024 min/PAX x PAX + 1.162 min

	85% LF Quarter Door	85% LF Dual Door
Regular Single Aisle	0.032 min/PAX x PAX + 2.888 min	0.022 min/PAX x PAX + 2.160 min
Advanced Single Aisle	0.032 min/PAX x PAX + 2.888 min	0.022 min/PAX x PAX + 2.160 min
6-Abreast Twin Aisle	0.019 min/PAX x PAX + 1.455 min	0.015 min/PAX x PAX + 0.868 min
7-Abreast Twin Aisle	0.020 min/PAX x PAX + 1.394 min	0.016 min/PAX x PAX + 0.835 min
8-Abreast Twin Aisle	0.021 min/PAX x PAX + 1.283 min	0.016 min/PAX x PAX + 0.767 min

Table A.6 – Linear regression of deboarding times.

Complete Turnaround Times

The complete turnaround times assume full cargo exchange. Refueling does not delay passenger boarding. Cleaning is performed using a working party of 6 and short cleaning. If possible turnaround times should be estimated by using boarding and debaording times from previous tables and estimating the other processes in dependence of the actual type of operation, for example actual fuel loads and cargo carried.

	100% LF Door 1L	100% LF Quarter Door
Regular Single Aisle	0.142 min/PAX x PAX + 14.70 min	0.111 min/PAX x PAX + 19.07 min
Advanced Single Aisle	0.132 min/PAX x PAX + 17.15 min	0.115 min/PAX x PAX + 17.79 min
6-Abreast Twin Aisle	0.120 min/PAX x PAX + 9.09 min	0.104 min/PAX x PAX + 11.15 min
7-Abreast Twin Aisle	0.099 min/PAX x PAX + 12.09 min	0.091 min/PAX x PAX + 12.18 min
8-Abreast Twin Aisle	0.102 min/PAX x PAX + 12.22 min	0.096 min/PAX x PAX + 10.78 min

	100% LF Dual Door	85% LF Door 1L
Regular Single Aisle	0.092 min/PAX x PAX + 14.96 min	0.128 min/PAX x PAX + 12.41 min
Advanced Single Aisle	0.090 min/PAX x PAX + 15.27 min	0.121 min/PAX x PAX + 14.33 min
6-Abreast Twin Aisle	0.088 min/PAX x PAX + 9.14 min	0.108 min/PAX x PAX + 8.45 min
7-Abreast Twin Aisle	0.079 min/PAX x PAX + 10.11 min	0.093 min/PAX x PAX + 10.65 min
8-Abreast Twin Aisle	0.073 min/PAX x PAX + 11.89 min	0.095 min/PAX x PAX + 10.98 min

	85% LF Quarter Door	85% LF Dual Door
Regular Single Aisle	0.098 min/PAX x PAX + 16.86 min	0.093 min/PAX x PAX + 13.58 min
Advanced Single Aisle	0.108 min/PAX x PAX + 14.45 min	0.091 min/PAX x PAX + 14.58 min
6-Abreast Twin Aisle	0.094 min/PAX x PAX + 10.34 min	0.088 min/PAX x PAX + 8.81 min
7-Abreast Twin Aisle	0.091 min/PAX x PAX + 9.41 min	0.079 min/PAX x PAX + 10.01 min
8-Abreast Twin Aisle	0.090 min/PAX x PAX + 9.63 min	0.072 min/PAX x PAX + 11.95 min

Table A.7 – Linear regression of complete turnaround times. It is recommended to use these numbers with care.

Name: Fuchte

Vorname: Jörg Clemens

Geburtsdatum: 24. Februar 1980

Geburtsort, -land: Pinneberg, Deutschland

1985 – 1990	Grundschule Nord, Halstenbek
1990 – 1999	Wolfgang-Borchert Gymnasium, Halstenbek
06.1999	Erlangung der allgemeinen Hochschulreife (Abitur)
07.1999 – 04.2000	Wehrdienst bei den Heeresfliegern als Betriebsstoffwart in Celle und Itzehoe
05.2000 – 08.2000	Praktikum bei Airbus Deutschland. Lehrwerkstatt und Kabinensystementwicklung
10.2000 – 01.2007	Studium an der Technischen Universität Berlin im Studiengang Verkehrswesen, Spezialisierung Luft- und Raumfahrttechnik
02.2003	Erlangung des Vordiplom
11.2002 – 08.2004	Arbeit als studentische Hilfskraft an der TU Berlin im Bereich Prüfstandsentwicklung und Test mechanischer Verbindungen
09.2004 – 04.2005	Auslandssemester an der University of Washington, Seattle, USA, gefördert durch die Lufthansa Berlinstiftung
11.2005 – 05.2006	Praktikum bei der Airbus Central Entity, Toulouse, Frankreich, A380 Chief Engineering, Structure Ground and Flight Test
05.2006 – 11.2007	Diplomarbeit bei Airbus Deutschland, Hamburg, im Bereich Special and Dynamic Loads des Bereichs Flight Physics
01.2007	Erlangung des Diploms (Gesamturteil: Sehr Gut)
01.2007 – 05.2009	Entwicklungsingenieur bei IBK Aero, Hamburg, im Bereich Flugphysik
06.2009 – 02.2014	Wissenschaftlicher Mitarbeiter im Deutschen Zentrum für Luft- und Raumfahrt (DLR), Einrichtung Lufttransportsysteme, Hamburg. Themenbereich Flugzeugentwurf und Kabinenentwicklung.
03.2014 – heute	Verantwortlicher Ingenieur für den Bereich Cabin Innovation & Technology , Zentrum für Angewandte Luftfahrtforschung, Hamburg